KINETICS OF REDUCTION OF AQUEOUS SOLUTIONS OF CUPRIC SULPHATE AND ACETATE BY HYDROGEN.

By

Tony Frank Mason. B.Sc.(Eng.), A.R.S.M.

A Thesis submitted for the Ph.D. degree of the University of London in Metallurgy.

"The first appearance of the metallic state .....has always exerted a peculiar fascination on the metallurgist".

A quotation from E.Peters and E.A.Van Hahn.

ABSTRACT.

The kinetics of reduction of cupric sulphate and acetate solutions were studied at temperatures between 110°C and 150°C. The reactions were performed using hydrogen gas as the reducing agent, at partial pressures of 400 p.s.i., 600 p.s.i. and 650 p.s.i.

Studies were made on cupric acetate solutions containing only a small acetate concentration, where the solid reduction product was cuprous oxide; and on solutions of relatively high acetate concentration, where metallic copper powder was the product.

All kinetic studies were performed in a reaction cell which was equipped with silica windows to allow optical density measurements to be made continuously throughout the reactions. Change of hydrogen pressure over the solutions was also measured and correlation was made between these values and the changes of cupric concentration obtained by the spectrophotometric technique.

"Auto-reduction" of cupric acetate solution was observed and studied, the kinetics of this reaction were determined by the spectrophotometric method alone.

Abstract.

Powder products were analysed by X-ray powder photography to determine whether cuprous oxide or elemental copper was produced under the different conditions.

The investigations showed that during reduction of cupric solutions by hydrogen gas the reaction was controlled initially by the concentration of molecular hydrogen in the solution. After a reaction proceeded for a some time control of the reaction rate becames dependent upon the cupric concentration remaining in the solution.

The rate of the "auto-reduction" reaction was found to be constant over the period of the investigations.

An appendix containing the mechanical design of the apparatus used, and description of the preliminary work for the present investigation has been included in the thesis.

CONTENTS.

Section number.	Title.	Page number.
Section 1.	Previously proposed species structure and reduction reactions...	13
1.1.	The structure of copper species in solution.....	13
i.	The structure of the 'free' cupric ion.....	13
ii.	The effect of complexing agents upon the structure of aqueous cupric ions.....	15
iii.	The existence of a cupric acetate dimer in aqueous solution.....	17
1.2. i.	The buffer system acetic acid/ ammonia.....	24
1.3. i.	The structure of cuprous species in aqueous solutions.....	26
1.4.	Previous work on the gaseous reduction kinetics of cupric solutions.....	28
i.	Reduction of cupric sulphate solutions.	28
ii.		29
iii.	Reduction of cupric acetate solutions by gaseous hydrogen.....	32
iv.	Reduction of cupric acetate solutions by carbon monoxide.....	33

Contents.

Section number.	Title.	Page number.
Section 2.	Investigation methods employed.....	36
2.1.	Solutions used.....	36
i.	Cupric sulphate solutions.....	36
ii.	Cupric acetate solutions.....	37
iii.	pH determinations of samples and solutions.....	40
iv.	Buffer solutions and pH standards...	40
2.2.	Description of the apparatus.....	42
i.	The spectrophotometer.....	42
ii.	Reaction vessels.....	43
2.3.	Experimental procedure.....	46
i.	Use of the reaction vessels.....	46
ii.	Hydrogen consumption determination..	50
iii.	Optical density change monitoring...	51
2.4.	Analytical techniques.....	52
i.	Analyses of samples from the reaction vessels.....	52
ii.	Comparison of the acetate solutions by X-ray fluorescence.....	55
iii.	Comparison of the acetate solutions by Raman spectroscopy.....	56
iv.	Analyses of residual solutions.....	59
2.5	Observation and analyses of the solid reduction products.....	66
i.	X-ray powder photography of the reduced species.....	66

Contents.

Section number.	Title.	Page number.
2.5. ii.	Observation of the powders by laser light	68
iii.	Observation of the occurence of solid products by turbidity measurements	71
2.6. i.	Analysis of the gases remaining in the reaction vessels by gas chromatography	74
Section 3.	Results and discussion	80
3.1.	Results of cupric acetate reductions	80
i.	The methods of analysing the results of the accelerating portion of the reaction	80
ii.	The methods of analysing the results of the decaying portion of the reaction	94
3.2.	Results of cupric sulphate reductions	126
i.	The methods of analysing the results of the accelerating portion of the reaction	126
ii.	The methods of analysing the results of the decaying portion of the reaction	128

Contents.

Section number.	Title.	Page number.
3.3.	Discussion of the information determined from the results and the analysis method employed	139
i.	For cupric acetate reductions	139
ii.	For cupric sulphate reductions	151
3.4.	The precipitation of solid reduction products	153
i.	Semi-reduced species concentration at the time of precipitation	153
ii.	The proposal for the reactions occuring during the formation of copper powder	158
iii.	The effect of temperature on the hydrogenated cuprous ion concentration at precipitation	160
iv.	The proposal for the cuprous oxide formation reaction	161
Section 4.	Auto-reduction of cupric acetate solutions	163
4.1.	The investigation	163
i.	Auto-reduction monitoring using spectrophotometry	163
ii.	Autoclave auto-reduction	165
Section 5.	Conclusions	169
5.1.	Cupric acetate reduction by hydrogen	169

Contents.

Section number.	Title.	Page number.
5.2.	Cupric sulphate reduction by hydrogen.....	174
5.3.	Auto-reduction of cupric acetate....	175

APPENDICES.

Appendix 1. Design of the equipment..... 177

A.1.1. i. Design of the spectrophotometer vessel with circular chambers..... 179

ii. Design of the spectrophotometer vessel with oblate ellipsoidal chambers..... 183

iii. Heating and temperature control of the reaction vessels..... 185

iv. Stirring of the reaction vessels... 186

v. Securing of the position of the cells within the spectrophotometer. 187

vi. The cooling of the surroundings of the reaction vessels..... 187

vii. The arrangements for the gas supply to the reaction vessels..... 188

viii. Pressure measurement in the reaction vessels..... 191

ix. The sampling valve used..... 193

x. Gold plating of the oblate ellipsoidal chambered reaction cell..... 193

Contents.

Section number.	Title.	Page number.
A.1.2.	Calibration of the apparatus.....	194
i.	Calibration of the transducers.....	194
ii.	Determination of the apparent volume of the reaction vessels.....	196
iii.	Determination of the apparent volume of the gas space over the solution in the reaction cells.....	201
iv.	Determination of the value of the ' β ' factor.....	202
v.	The vapour pressure over the solution.....	203
vi.	Calibration of the spectrophotometer and the validation of Beers law.....	205
A.1.3	The dissolution of hydrogen in aqueous solutions.....	215
i.	The purpose of the determinations..	216
ii.	The dissolution of hydrogen in un-reacting sulphate solutions.....	218
iii.	The dissolution of hydrogen in un-reacting acetate solutions.....	222
iv.	A comparison of the results of the dissolution of hydrogen with previously published information...	224
A.1.4.	The apparatus used for the auto-reduction reactions.....	227

Contents.

Section number.	Title.	Page number.
A.1.5.	The design of the new apparatus....	228
i.	The design of the reaction vessel.....	228
ii.	The design of a constant pressure gas consumption measuring apparatus.....	234
iii.	Fitting of the tantalum lined reaction vessel.....	238
iv.	Stirring of the solution within the tantalum lined reaction vessel.	240
v.	Temperature measurement and control.....	241
vi.	The arrangements to avoid over-heating of the spectrophotometer...	242
vii.	Control of the gas supply to the reaction vessel.....	242
Appendix 2.	Evidence of the existence of cupric acetate dimer in aqueous solution..	243
Appendix 3.	A solid electrolyte cell to measure the activity of species in solution.....	249
A.3.1. i.	General description of the electro-lytic cell.....	249
ii.	Silver chloride pellets.....	250
iii.	Lead chloride solid electrolyte pellets.....	251

Contents.

Section number.		Title.	Page number.
A.3.1.	iv.	Mounting of the pellets to make up the solid electrolyte cell	252
	v.	Use of the solid cell	252
	vi.	The proposed operation of the cell	253
Appendix 4.		The use of the electrical conductivity properties of mica to determine water vapour activity	256
A.4.1.	i.	The proposed method to determine thermodynamic information from mica conductivity measurements	256
	ii.	Design of the equipment	257
	iii.	Measurements of conductivity	257
Appendix 5.		Tabulated results and program Alfred	261
A.5.1.	i.	Cupric acetate reduction results	261
	ii.	Hydrogen consumption data	263
	iii.	Cupric sulphate reduction results	263
A.5.2.		Program Alfred	263
Appendix 6.		Units used	312
		References used within the text	313

Section 1.

PREVIOUSLY PROPOSED SPECIES STRUCTURE AND REDUCTION REACTIONS.

1.1. The structure of copper species in solution.

1.1.i. The structure of the 'free' cupric ion.

The species of copper which may exist in aqueous solutions at normal temperatures (around 20°C) and under usual conditions of oxidation potential and pH is the hydrated cupric ion: (1)

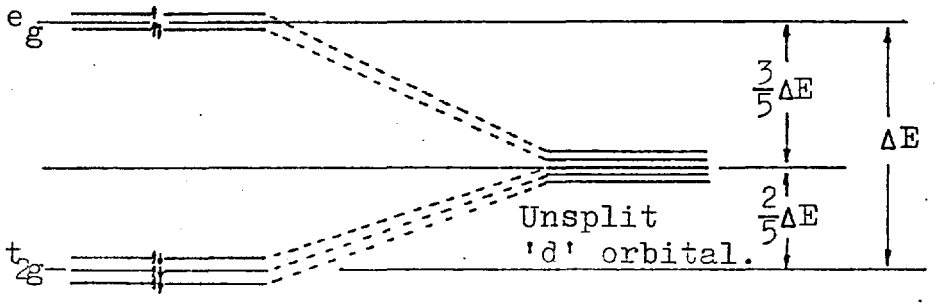
$$Cu(H_2O)_6^{2+}.$$

When an ion is surrounded by an octahedral ligand or crystal field, as the cupric ion is in the hydrated form described, the electronic configuration may be distorted from that of the truly free ion. This first degeneracy change of the 3d orbital of the copper ion under these conditions may be explained briefly as follows.

In a 'd' orbital the d_{xy}, d_{yz}, and d_{zx} electron orbitals are equivalent and may be considered to be positioned in lobes projecting between the charge effects of an octahedral ligand field, where the ligand units are positioned at the corners of the octahedron. However the d_{z^2} and $d_{x^2-y^2}$ orbitals are not equal to the others and may be considered to lie on the axes of the octahedron. The latter two orbitals, described as e_g, have, as a result of

their proximity to complexing ions or neutral polarised species exhibiting a similar charge, a higher energy than the d_{xy}, d_{yz}, and d_{zx}, or t_{2g}, electrons.

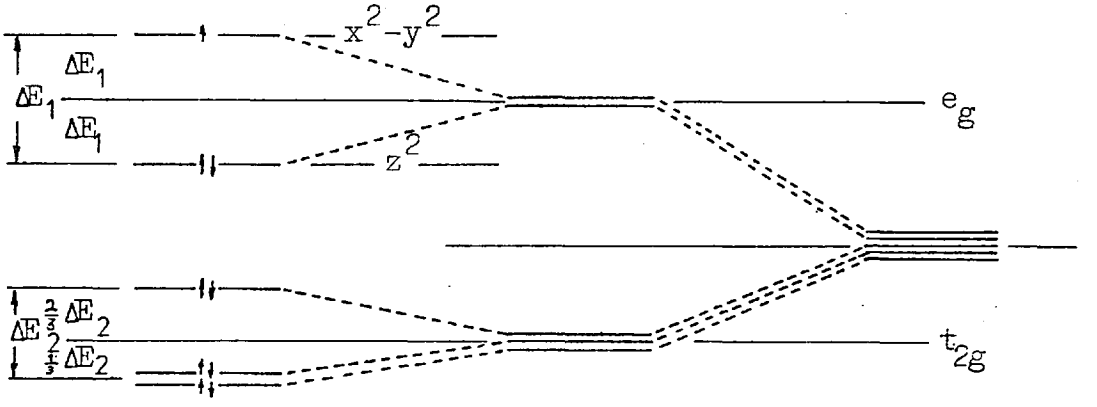
This band splitting can be pictorially shown:



This example of the illustration of band splitting by a line diagram shows the configuration of a ~~single~~ degenerate cupric species, the cupric ion being in a configuration of $3d^9$. This arrangement allows an electron 'hole' to exist and from energy considerations this 'hole' must be in the higher energy e_g orbitals.

In the case of a cupric ion the unpaired electron is situated in the x^2-y^2 orbital. The electrostatic field from the ligand units is, therefore, less screened from the nucleus by the electrons in the x/y plane than in the z axis direction of the octahedron. As a result of this difference in screening the two ligands in a 'trans' position on the Z axis have longer, weaker bonds than do the other four ligands in the square plane of X/Y.

The effect described is known as the Jahn-Teller effect. As a result of the electron energetics of the ligand field distortion, a further lowering of degeneracy of the d orbital is caused. A further energy splitting must occur due to the differing distances from electron to ligand unit which is encountered. The second degeneracy change is described by another line diagram:



1.1.ii. The effect of complexing agents upon the structure of aqueous cupric ions.

In the presence of suitable complexing species the hydration molecules are replaced in a stepwise manner. Due to the non-equivalence of the co-ordination sites it is difficult to replace more than the four short co-ordinations with complexing molecules.

In a solution which is saturated with ammonia the complex $Cu\ L_5H_2O^{2+}$ is formed; the "L" being a molecule of the complexing species, in this case ammonia. At moderate concentrations of ammonia the

most highly complexed species to exist is $Cu\ L_4(H_2O)_2^{2+}$.

In liquid ammonia the octahedral cuprammine complex is formed: $Cu\ (NH_3)_6^{2+}$.

The equilibrium constants for the series of reactions:

Eq. 1.1.i.

$$Cu(NH_3)_n(H_2O)_{6-n}^{2+} + NH_3 \longrightarrow Cu(NH_3)_{n+1}(H_2O)_{5-n}^{2+} + H_2O$$

Equilibrium constants = K_{n+1}. These are given in table 1.T.i.

TABLE 1.T.i.

Stability of cupric ammonia complexes at 18°C and 30°C (2N NH_4NO_3)

n	$\log_{10}K_{n+1}$ (18°C)	$\log_{10}K_{n+1}$ (30°C)	K_{n+1} (18°C)	K_{n+1} (30°C)	K_{n+1} conc'n corrected
0	4.31	4.15	2.04×10^4	1.41×10^4	9.77×10^3
1	3.67	3.50	4.68×10^3	3.16×10^3	2.20×10^3
2	3.04	2.89	1.10×10^3	7.76×10^2	5.37×10^2
3	2.30	2.13	1.10×10^2	1.35×10^2	9.33×10
4	-0.4 to -0.52 (20°C)		0.30×10^{-1} (20°C)		

The data composing this table is from J.Bjerrum[2] and F.Rosenblatt.[3].

The existence diagram for each complex, with ammonia activity, can be seen in figure 1.1.i.

In sulphate solutions containing copper some interaction of sulphate and bisulphate with cupric ions occurs. It appears that the major species in a cupric sulphate solution other than the hydrated cupric ion is undissociated cupric sulphate $CuSO_4$. The equilibrium constant [4] for the reaction:

$$CuSO_{4(aq)} \xrightleftharpoons{K_s} Cu^{2+} + SO_4^{2-} \qquad \text{Eq. 1.1.ii.}$$

is found to be:

$$K_s = \frac{[Cu^{2+}][SO_4^{2-}]}{[CuSO_4]} = \frac{1}{230} \text{ to } \frac{1}{250} \qquad \text{Eq. 1.1.iii.}$$

at 20°C.

Values of this equilibrium constant have, however, been found by Brown and Prue [5] to lie within a much wider range, between $\frac{1}{150}$ and $\frac{1}{300}$.

1.1.iii. The existence of cupric acetate dimer in aqueous solution.

During the present work the existence of the cupric acetate dimer was indicated by the absorption spectra in the visible and ultra-violet range of aqueous cupric solutions with a large acetate concentration. The evidence for the existence of the dimer may be seen in Appendix A.2.

The formation of the dimer at high concentration of acetate ions may be explained in the following way.

The predominent species existence diagram for cupric/ammonia complexes with ammonia concentration.

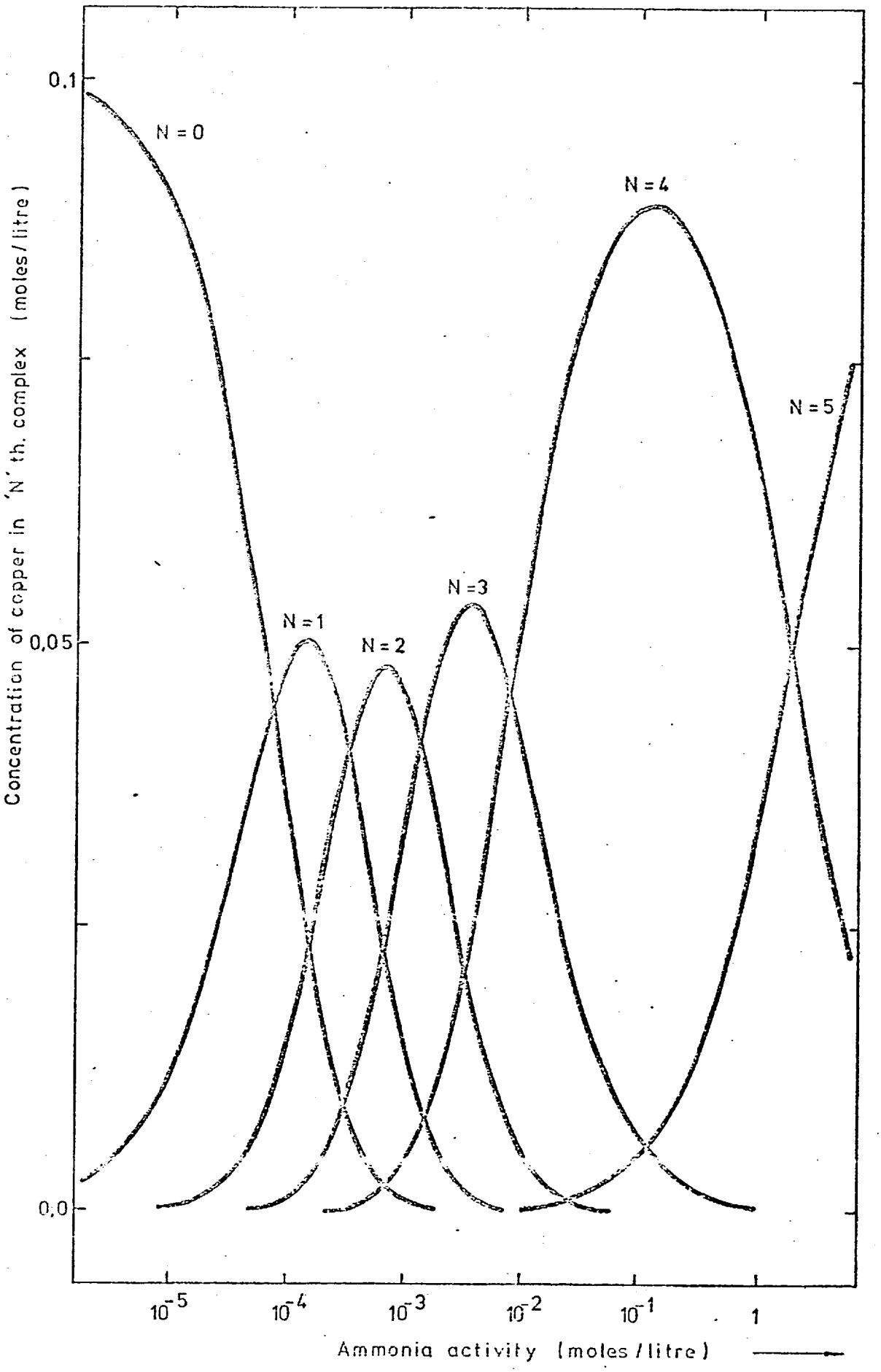


FIGURE 1.1.i.

The structure of copper species in solution.

Due to the Jahn-Teller distortion of the ligand field around the cupric ion few ligands have a sufficient dipole charge to replace hydration molecules from more than the four short co-planar co-ordinations. If a fifth or sixth replacement should begin to occur the energetics of the system would be unfavourable unless the Jahn-Teller effect were eliminated.

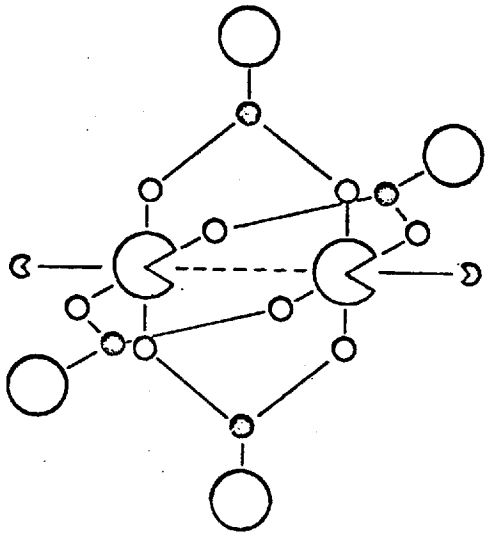
One way in which the distortion due to the existence of a singly filled orbital can be overcome would be the formation of a metal / metal bond with a shared electron from one of the 'd' orbitals of both copper atoms. By the formation of such a bond both "cupric" atoms become of an electronic configuration $3d^{10}$ and hence no ligand field distortion exists; thus the ten remaining co-ordination sites around the dimer become equivalent and a species $Cu_2(Ac)_{10}^{6-}$ could form.

The solid cupric acetate structure consists of a binuclear complex with acetate groups bridging between the copper sites. The remaining, long, weak co-ordination sites are occupied by a water molecule at each end of the complex, opposite the metal / metal bond. This structure has been studied in detail by many workers (6 to 16), and may be seen sketched, together with the proposed aqueous solution dimer structure in Figure 1.1.ii.

For the solutions examined in the present

FIGURE 1.1.ii.

a) The structure of cupric acetate dimer in the solid and in non-ionised solution.



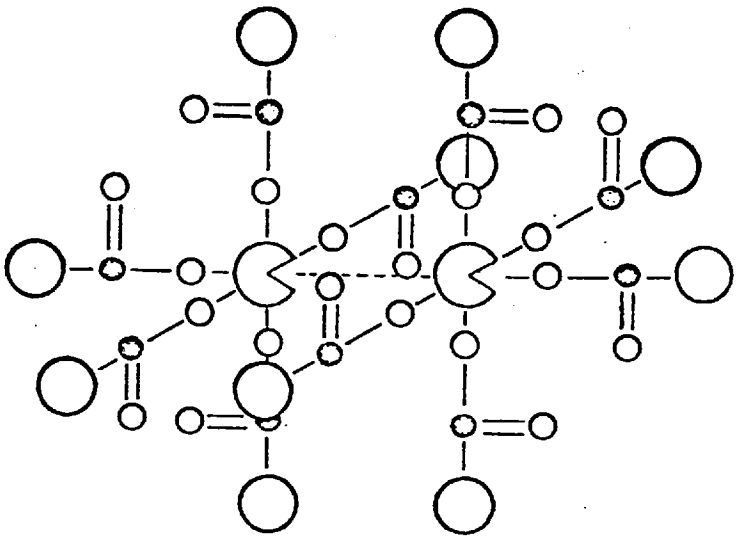
.....Hydration molecules.

....Methyl groups.

....Cupric ions.

.....Oxygen.

.....Carbon.



b) The proposed structure of the cupric acetate dimer as it may exist in aqueous solution.

work the existence of the dimer in aqueous solution may be neglected in most conditions. The dimer only becomes appreciable at an acetate concentration considerably higher than that in the solutions used. However the complexing of of acetate ions with copper (II), up to the fourth complex, in solution must be considered.

Table 1.T.ii. shows information as to the stability of the complexes:

$CuAc^{+}.5H_2O$; $CuAc_2.4H_2O$; $CuAc_3^{-}.3H_2O$; $CuAc_4^{2-}.2H_2O$;

"Ac" indicates an acetate; CH_3COO^{-}; group.

The formation reaction for this series of complexes may be simply described:

$$CuAc_n^{(2-n)+} \underset{\longleftarrow}{\xrightarrow{K_n}} CuAc_{n-1}^{(3-n)+} + Ac^{-}. \qquad \text{Eq. 1.1.iv.}$$

$$K_n = \frac{[CuAc_{n-1}^{(3-n)+}]\,[Ac^{-}]}{[\,CuAc_n^{(2-n)+}]} \qquad \text{Eq. 1.1.v.}$$

Simplification of the reaction excludes the water molecule which is replaced at each step. It must be remembered that the appropriate number of water molecules are associated with the reaction but they need not be included in the expression for K_n (equation 1.1.v.) since in aqueous solution the water activity may be considered to remain constant.

The existence diagram for the copper acetate complexes which are predominent at various acetate activities may be seen in Figure 1.1.iii. This

FIGURE 1.1.iii

The existence diagram for cupric acetate complexes.

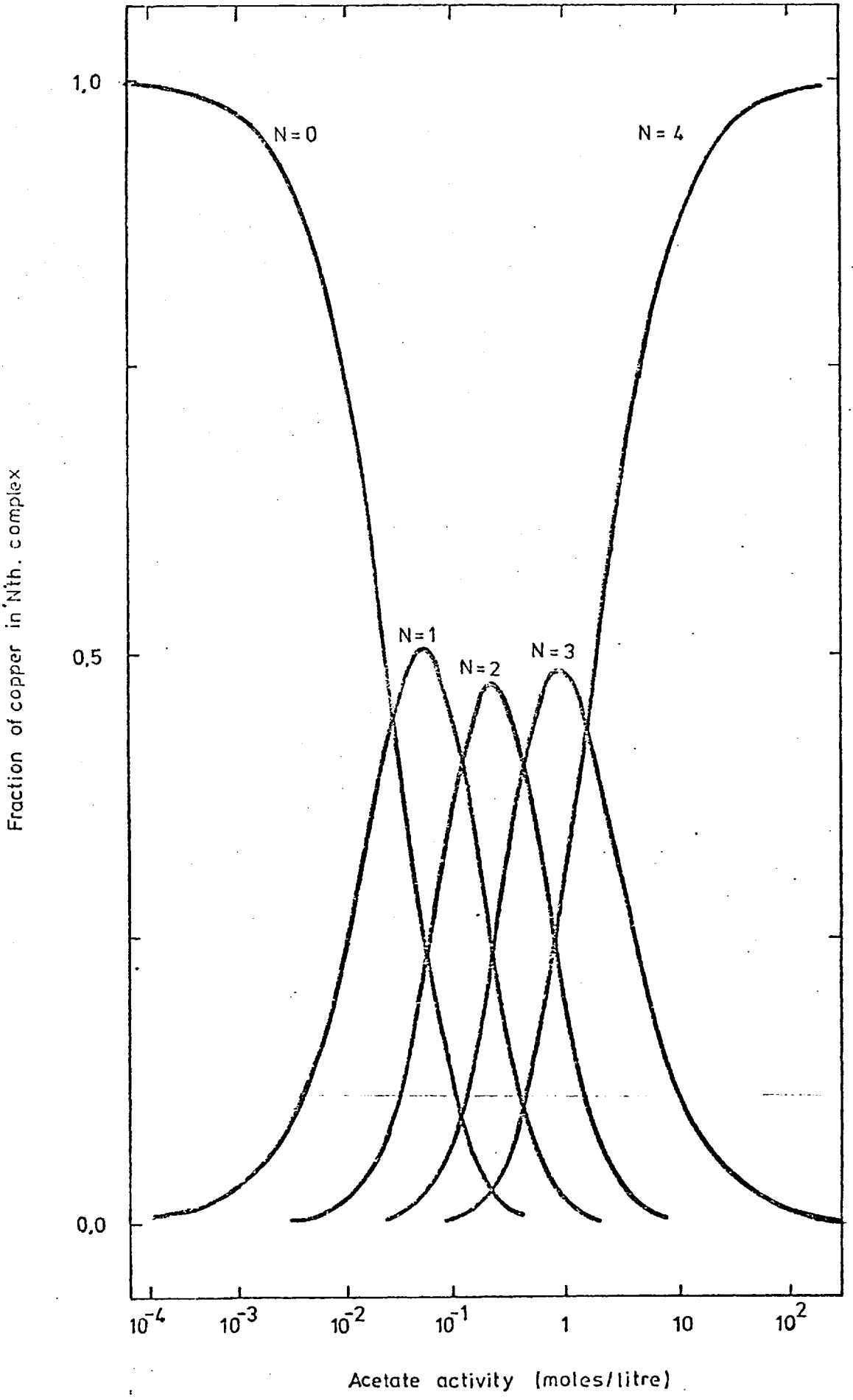


diagram was drawn using the stability data displayed in Table 1.T.ii.

TABLE 1.T.ii.

Equilibrium constants for cupric acetate complexes.

n	K_n (Fronaeus) (20°C)	K_n (Tanaka & Kato)			K_n (Lloyd) (25°C)
		15°C	25°C	35°C	
1	45 ± 2.0	41	52	69	47 ± 1.0
2	9.8 ± 1.5	4.7	1.8	1.2	10.4 ± 1.0
3	2.3 ± 1.0				2.6 ± 1.0
4	0.65				0.66 ±0.24

The data for the above table has been taken from publications by Fronaeus[17],[18], Tanaka and Kato[19],[21] and by Lloyd et al.[20]

Metal ion complex stability information may be easily found from the tabulated data prepared by the Chemical Society of London.[22]

1.2.i. The buffer system acetic acid / ammonia.

The dissociation constant K_a for acetic acid:

$$CH_3.COOH \underset{}{\overset{K_a}{\rightleftharpoons}} CH_3.COO^- + H^+ \qquad \text{Eq. 1.2.i.}$$

may be found[21] in the form of $-\log_{10}K_a$.

$$-\log_{10}K_a = pK_a = 4.69 \pm 0.9$$

By consideration of the equilibrium laws;

$$K_a \times \frac{[\text{Acid}]}{[\text{Salt}]} = [H^+] \qquad \text{Eq. 1.2.ii.}$$

assuming that activity values may be considered to be equivalent to concentration.

Thus:
$$pH = pK_a + \log_{10}\frac{[\text{Salt}]}{[\text{Acid}]} \qquad \text{Eq. 1.2.iii.}$$

In a buffer system of acetic acid and ammonia this expression becomes:

$$pH = 4.69 + \log_{10}\frac{[CH_3COONH_3]}{[CH_3COOH]} \qquad \text{Eq. 1.2.iv.}$$

However in the system which was used in control of the pH value of a copper acetate solution a component of the 'Salt' concentration is due to the acetate in the copper acetate.

Therefore:

$$pH = 4.69 + \log_{10}\frac{[\text{Ammonium acetate}] + 2 \times [\text{Copper acetate.}]}{[\text{Acetic acid.}]}$$

Eq. 1.2.v.

In this way the ammonia to acetic acid

ratio was determined so as to give a chosen pH value.

Since the major purpose in using a buffered solution for this work was to eliminate the possibility of corrosion of the reaction vessel, and to restrict the change of pH during the reaction so that it can be considered to be constant during the reaction, any more rigorous analysis of the buffer system was considered unnecessary.

The equations used in the description of the buffer, equations 1.2.ii to 1.2.v., make the assumption that the species considered have unit activity coefficients. This assumption is probably not justified absolutely, especially at the high concentrations used. However it is reasonable to use this assumption for the analysis since at the large concentration the activity coefficients will be maintained constant during a very small change in this concentration.

1.3.i. The structure of cuprous species in aqueous solution.

Since the free cuprous ion has the electronic arrangement including $3d^{10}$ then any 3d band splitting due to a ligand field does not normally leave an unpaired electron in any energy level, hence no distortion due to Jahn-Teller effect occurs. However under some conditions ligand co-ordination lengths are distorted, hybridisation in this case occurs into the 4s and $4p^3$ orbitals, giving a usual maximum co-ordination number of four.

Very little information is available as to the stability of the complexes with cuprous ions, but it is known(23.) that the free ion is thermodynamically unstable at room temperature, and under ordinary oxidation conditions, with respect to cupric ions and elemental copper:

$$2Cu^{+} \longrightarrow Cu^{o} + Cu^{2+}. \quad \text{Eq.1.3.i.}$$

However cuprous species are stable when in the presence of some complexing agents; for example, thiocyanate and cyanide. ~~and perchlorate.~~(24)(22)

It may be concluded that stabilisation of the ion is a result of the strong complexes which form under these conditions.

By comparison with other ions which have similarly completed 3d orbitals the most common

co-ordination numbers may be summarised:

Co-ordination number.	Bonding orbitals.
2	4s $4p^1$
4	4s $4p^3$

In ammoniacal conditions the dissociation constants for the first and second complexes with cuprous ions are known[25], and it is not unreasonable to suppose that the third and fourth, if not higher complexes, may exist, at least to a limited extent, but no stability information is available:

$$Cu^+ + NH_3 \overset{K_1}{\rightleftharpoons} CuNH_3^+ \qquad \log_{10} K_1 = 5.93$$

$$CuNH_3^+ + NH_3 \overset{K_2}{\rightleftharpoons} Cu(NH_3)_2^+ \qquad \log_{10} K_2 = 4.93$$

1.4. Previous work on the gaseous reduction kinetics of cupric solutions.

1.4.i. The reduction of cupric sulphate solutions.

The most significant previous investigation of the reduction of cupric sulphate solutions, using a gaseous reducing agent, is that by Van Hahn and Peters[26].

In the investigation described by Van Hahn and Peters solutions were reduced in an autoclave and samples taken at temperature by a pressure sampling technique were oxidised by dichromate solution. By colorimetric analysis at room temperature the un-reduced dichromate could be determined, and hence the cuprous concentration in the 'at temperature' sample.

The kinetics proposed by information obtained by the above technique could be expressed in the following equation, when hydrogen was used as the reducing agent:

$$-\frac{d[H_2]}{dt} = \frac{k_1[Cu^{2+}]^2[H_2]}{k_{-1}/k_2[H^+] + [Cu^{2+}]} + \frac{k_3[Cu^+][Cu^{2+}]^2[H_2]}{\left(k_{-1}/k_2[H^+] + [Cu^{2+}]\right)\left(k_{-3}/k_4[H_2] + [Cu^{2+}]\right)}$$

Eq. 1.4.i

in a mechanism described by the equations, 1.4.ii to 1.4.iv.

Previous work.

$$Cu^{2+} + H_2 \underset{k_{-1}}{\overset{k_1}{\rightleftharpoons}} CuH^+ + H^+ \qquad \text{Eq. 1.4.ii}$$

$$CuH^+ + Cu^{2+} \xrightarrow{k_2} 2Cu^+ + H^+ \qquad \text{Eq. 1.4.iii}$$

$$Cu^+ + H_2 \xrightarrow{k_3} CuH + H^+ \qquad \text{Eq. 1.4.iv}$$

$$CuH + Cu^+ \xrightarrow{k_4} 2Cu^\circ + H^+$$

The general shape of the rate curves determined by Van Hahn and Peters, figure 1.4.i., indicates by the initial accelerating portion, an autocatalytic reaction in a reduced or semi-reduced species. The mechanism above, as proposed by these workers, includes this autocatalysis.

A reaction mechanism of the type described above has also been proposed by Dunning and Potter.

By consideration of a rate of reaction against cuprous concentration plot Van Hahn and Peters were able to determine values of k_1, $\frac{k_{-1}}{k_2}$, $\frac{k_{-3}}{k_4}$, and k_3 from the slopes and intercepts of these curves, expressed in terms of $[H^+]$.

1.4.ii.

Dunning and Potter (27) followed unstirred reactions spectrophotometrically to observe the decrease in cupric ionic species concentration. They found that a long induction period existed before the reaction proceeded at a measurable rate, unless some copper metal was in contact with the

solution before the reaction was started. This was shown not to be an effect of a heterogeneous reaction site, since the long delay continued to exist when metallic platinum was in contact with the solution. This suggested to Dunning and Potter that the equalibrium:

$$Cu^{o} + Cu^{2+} \rightleftharpoons 2\,Cu^{+}$$

Eq. 1.4.v.

was established, giving an initial catalyst concentration $[Cu^{+}]$.

The rates of reaction determined from the above work were as follows:

None-catalytic rate:- r_1

$$r_1 = \frac{0.315\,[H_2][Cu^{2+}]^{2}}{[Cu^{2+}] + 0.105\,[H^{+}]} \text{ Moles. litre}^{-1}\text{.minute}^{-1}$$

Eq. 1.4.vi.

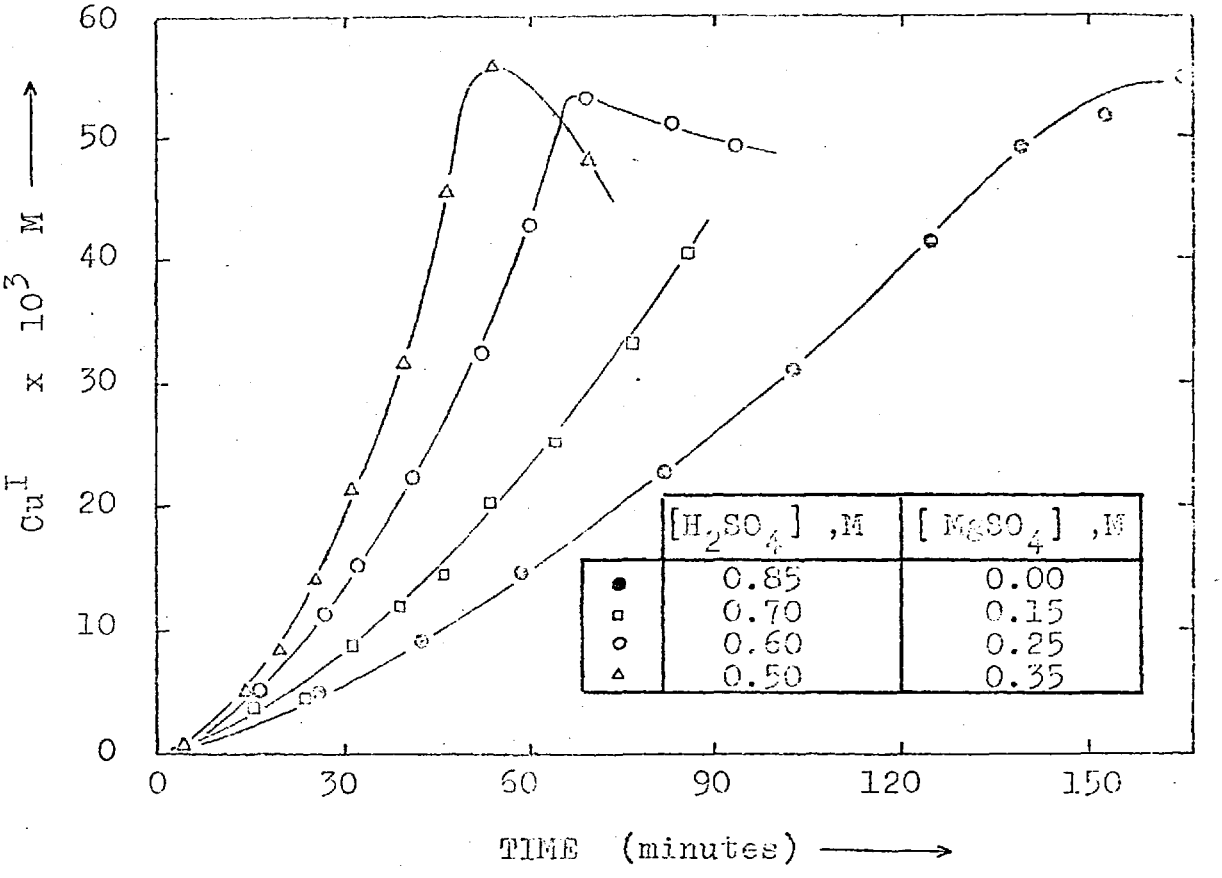
Catalytic rate:- r_2

$$r_2 = \frac{71\,[H_2]\,[Cu^{2+}]^{2}}{[Cu^{2+}] + 0.9\,[H^{+}]}$$

Eq. 1.4.vii.

The mechanism proposed was that from which Van Hahn and Peters started their proposals.

Figure 1.4.i.



The rates of 'disappearance' of cupric species from solution, in the form of the increase of cuprous ions, and the variation with sulphate concentration.

1.4.iii. The reduction of cupric acetate solutions by gaseous hydrogen

Dakers and Halpern [28] used the sampling of an autoclave product and analysis for cupric species by absorption spectrophotometry, using the cuprammine complexes, at room temperature, to determine the rate of reduction of cupric species in a solution. No indication is given in the publication of the work that any steps were taken to avoid the disproportionation of semi-reduced species as the temperature of a sample dropped. If disproportionation were allowed to occur false values for the cupric concentrations could be determined.

However under the conditions considered by these investigators cuprous oxide was always the solid reaction product, formed it was proposed by an overall reaction:

$$2Cu(Ac)_2 + H_2 + H_2O \xrightarrow{k_o} Cu_2O + 4AcH$$

cuprous acetate — cuprous oxide — acetic acid

Eq. 1.4.viii.

The rate curves resulting from this procedure showed no initiation period at the reaction start and no section of acceleration of the reaction. A non-autocatalytic reaction kinetics would thus be the expected proposal and, moreover, a first order rate dependence was shown to exist.

The work described above did indicate the homogeneous nature of the reduction product formation since it was found that the addition of suitable nucleating agents (stainless steel powder, cuprous oxide product, etc.,) made no difference to the procedure or rate of the reaction.

The overall reaction was found to have a dependence:

$$-\frac{d[Cu^{II}]}{dt} = k_D [Cu^{II}][H_2]$$

Eq. 1.4.ix.

and the mechanism proposed was:

$$(CH_3COO)_2Cu + H_2 \longrightarrow (CH_3COO)_2CuH_2$$

Eq. 1.4.x.

$$(CH_3COO)_2CuH_2 + (CH_3COO)_2Cu + H_2O \longrightarrow Cu_2O + 4CH_3COOH$$

Eq. 1.4.xi.

1.4.iv. The reduction of cupric acetate solution by carbon monoxide

The most thorough investigation of this reduction has been reported by J.J.Byerley [29][30] and E.Peters where a continuous spectrophotometric following of the cupric ion concentration was made. The solutions in this work were un-stirred and contained in a titanium reaction vessel.

The rate curves obtained for the reduction by

carbon monoxide was of the same general shape as those obtained by the present work, figures 3.1.viii. to 3.1.xxxiii, and from these reaction curves an indication of autocatalysis was given due to the accelerating first portion of the reaction.

Thus a kinetic expression:

$$\frac{d\,[Cu^{II}]}{d\,t} = k\,[Cu^{II}][Cu^{I}] \qquad \text{Eq. 1.4.xii}$$

was proposed.

To test the possibility of dependence of the rate of reaction on the product of the cupric and cuprous concentrations the differential of the concentration against time curve was plotted. Linearity was obtained. However at high cupric concentration an intercept with the rate axis was observed. This intercept indicated a further dependence upon cupric concentration.

The reaction rate was found by Byerley and Peters to be expressable by the following equation:

$$-\frac{d\,[Cu^{II}]}{d\,t} = \frac{k_1K_1[Cu^{II}]\,[Cu(CO)^{+}]}{[H^{+}]} + \frac{k_2K_2[Cu^{II}]^2\,P_{CO}}{[H^{+}]} \qquad \text{Eq. 1.4.xiii}$$

together with a reaction of the following equations:

Previous work.

$$Cu^{II} + CO + H_2O \underset{\leftarrow}{\overset{K_2}{\rightarrow}} (Cu\text{-}\overset{O}{\overset{\|}{C}}\text{-}OH)^+ + H^+$$

Eq. 1.4.xiv.

$$(Cu\text{-}\overset{O}{\overset{\|}{C}}\text{-}OH)^+ + Cu^{II} \underset{\leftarrow}{\overset{k_2}{\rightarrow}} 2(Cu^I) + CO_2 + H^+$$

Eq. 1.4.xv.

$$2Cu^I + 2CO \xrightarrow{fast.} 2Cu(CO)^+$$

Eq. 1.4.xvi.

$$Cu(CO)^+ + H_2O \underset{\leftarrow}{\overset{K_1}{\rightarrow}} Cu\text{-}\overset{O}{\overset{\|}{C}}\text{-}OH + H^+$$

Eq. 1.4.xvii.

$$Cu\text{-}\overset{O}{\overset{\|}{C}}\text{-}OH + Cu^{II} \xrightarrow{k_1} Cu^I + CuH^+ + CO_2$$

Eq. 1.4.xviii.

$$CuH^+ + Cu^{II} \xrightarrow{fast.} 2Cu^I + H^+$$

Eq. 1.4.xix.

The cuprous species described in the above reaction equations as " Cu^I " must be the cuprous oxide product.

Further work, in the form of reviews and bibliographies, covering the field of the reduction of metal ions by gaseous reducing agents has been produced by The Metallurgical Society[30], by A.R.Burkin[31], and by Warren Spring Laboratory[32].

Section 2.

INVESTIGATION METHODS EMPLOYED.

2.1. Solutions used.

2.1.i. Cupric sulphate solutions.

All reductions of cupric ions in sulphate systems were performed in un-buffered solutions made up from Hopkins and Williams reagent grade (G.P.R.) cupric sulphate hydrate. The bulk solution used was of concentration 0.393 molar, (approximately 25 grms. Cu. litre^{-1}).

The solutions for reduction investigations were made up to the required pH value and cupric concentration prior to introduction to the reaction vessel. The pH adjustment was made approximately by diluting the bulk solution to the required copper concentration using sulphuric acid of the pH required as the diluent.

Solutions for introduction to the reaction vessel were made up in volumetric flasks, the correct, required, volume was then transfered to the vessel using a pipette.

The exact pH value of the solution was determined by using a pH meter with a sample of the solution. The pH meter was calibrated against a buffer solution. The buffer solution employed was potassium tetraoxalate at a concentration of 0.05 molar.

It was considered that this type of solution was a reasonable example of a pure version of an industrial aqueous copper solution which may be encountered as a purified leach liquor for example.

2.1.ii. Cupric acetate solutions.

a). Hopkins and Williams solutions.

The first examinations of acetate solutions of cupric species was performed on solutions made up by dissolving Hopkins and Williams General Purpose Reagent grade cupric acetate dihydrate in distilled water. The solution produced in this manner was filtered through fine filter paper to remove the solid insoluble components of the Hopkins and Williams cupric acetate. This insoluble material was assumed to be basic cupric acetate. The concentration of the bulk solution made in the above manner was 0.318 molar (approximately 20.2 grams of copper. litre^{-1}).

The bulk solution was diluted for examination in the reaction vessel. Dilution included the addition of the appropriate proportions of ammonium acetate and acetic acid to buffer the reaction solution at a pH of approximately 4.0 at room temperature.

The diluted solutions, ready for introduction to the reaction vessel, were made up in volumetric

flasks and were measured into the reaction vessel by the use of a graduated cylinder.

The concentrations of components in the solutions which were investigated are stated in conjunction with the plotted results for each reduction .

In later examination of cupric acetate solutions made by the dissolution of cupric acetate dihydrate, solutions were not diluted and buffered in volumetric flasks and then transfered to the reaction vessel, as described above. Instead of diluting the bulk solution outside the reaction vessel, the required volumes of bulk solution, of Hopkins and Williams 'Reagent Grade' glacial acetic acid and of "0.88" ammonia solution were measured directly into the vessel, using pipettes, to give the appropriate cupric concentration and ammonia to acetic acid proportions.

2.1.ii.b). Copper dissolved in acetic acid.

Some investigations were also made on cupric acetate solutions made by dissolving high purity metallic copper powder in 80% (by volume) glacial acetic acid in water. The volume of the 80% acetic acid was 500 mls. during the dissolution. After filtration the solution was diluted to 1.0 litres, hence the final acetate concentration

was equivalent to 40% acetic acid.

The copper powder was poured into the acetic acid in a flask fitted with a cone ground stopper and then shaken. The stopper was then replaced by a reflux apparatus and the solution was heated to about 90°C and held at that temperature for two days the flask was shaken occasionally during this time. The solution was then filtered to remove excess copper powder and made up to 1.0 litre with distilled water.

The bulk "copper + acetic acid" solution was found to have a concentration of 0.0534 molar (approximately 3.4 grams of copper. litre^{-1}). This was the approximate copper concentration which was required to be examined, thus the solution was used from the bulk with appropriate addition of "0.88" Hopkins and Williams' ammonia solution. Five millilitres of ammonia solution were required to buffer the solution at a pH of approximately 4.0 , when added to 55.0 mls. of bulk "copper + acetic acid" solution.

The addition of the "0.88" (approx. 35%) ammonia solution was made directly,and carefully, into the reaction vessel.

The pH of the solution was initially determined by sampling from the vessel and using a pH meter. The measured value of the pH was found

to be very nearly the same over several examinations of solutions from different experiments. Therefore, for solutions made in the same way, the pH value was thereafter assumed to be the same.

Samples taken from the vessel for initial pH determination were returned to the vessel in order that a known solution volume was contained by the vessel.

2.1.iii. pH determinations of samples and solutions.

Determination of the pH value of solutions and of samples from the reaction vessels was made using a Pye model 290 pH meter in conjunction with a Pye 405/M5.E07 combined pH electrode.

2.1.iv. Buffer solutions and pH standards.

The cupric sulphate solutions, and also the samples taken from the reaction vessels during the reduction of cupric sulphate solutions, were determined for their pH by standardising the pH meter used against 0.05 molar potassium tetraoxalate ($KH_2(C_2O_4)_2.2H_2O$.) solution. This solution has a pH value of 1.68 at 25°C and a change of pH with temperature of approximately +0.001 $^{o}C^{-1}$ over the range 20°C to 30°C. Thus a pH value of 1.68 for the standard was assumed at room temperature.

Solutions used.

Buffered cupric acetate solutions were arranged to have pH values of about 4.0 by appropriate concentrations of ammonia and acetate ions being present in the solution, as described in section 2.1.ii. Because of its suitability for the pH range required the standard solution used was 0.05 molar potassium hydrogen phthalate ($KHC_8O_4H_4$.).

This solution has a pH of 4.008 at 25°C and a change of pH with temperature of approximately +0.002 $^{o}C^{-1}$. over the range 20°C to 30°C.

2.2. Description of the Apparatus.

2.2.i. The spectrophotometer.

The basis of the determination of the kinetics of reduction of cupric species in solutions was a continuous monitoring of the cupric complex concentration by a colorimetric method.

The reactions were allowed to proceed in a reaction vessel which was fitted with precisely made quartz windows. The windows of the reaction vessel were accurately aligned in the optical path of a Pye Unicam S.P. 800 recording spectrophotometer. A similar reaction vessel was aligned in the reference beam of the instrument to contain an unreacting 'blank' solution kept under the same temperature conditions as the reacting solution.

The spectrophotometer was fitted with adjuncts (Pye Unicam S.P. 820 and S.P. 850) to allow continuous following of the optical density at a preset wavelength and to give an output from the spectrophotometer suitable for recording, using a potentiometric recorder. The recorder used was a Leeds and Northrup 'Speedomax' "G" series instrument.

The spectrophotometer was also arranged to

measure and plot absorption spectra of samples over the wavelength range of 190 nm. to 750 nm., and over the optical density range up to 2.00 .

Later in the series of experiments it was found that the optical density records made by the spectrophotometer were incorrect for all values included in the range :

>600 nm., >2.00 O.D. to >750 nm., >0.00 O.D.

In consequence of the error in the instrument, modifications were made by the manufacturers to increase the wavelength range of the instrument to 190 nm. to 850 nm.

The adjunct Pye Unicam model S.P. 850 was connected to the spectrophotometer to facilitate ease of use of an external "slave" recorder as well as allowing scale expansion and 'back-off' of the recorder.

2.2.ii. Reaction vessels.

During the course of the investigations two designs of reaction vessels were employed. The basic design of both was very similar, but the total volume of the vessels, and the optical path length in the solution were both larger in the equipment used for investigation of cupric sulphate reduction, than that used for the cupric acetate investigation.

Description of the apparatus.

Detail of the design of the reaction vessels and connected equipment can be found in appendix A.1.1.

The general configuration of the reaction vessels, or spectrophotometer cells, was of two chambers machined in a block of stainless steel. Quartz windows were arranged in each chamber so that when the block was fitted into the sample compartment of the spectrophotometer each beam of the instrument had a light path through the windows of one of the chambers.

Sealed lids were fitted to the reaction vessels in order that high pressures could be used, and one chamber of each of the cell blocks was equipped with a stirrer to allow agitation of the solution in the chamber.

The cell blocks were also arranged to be heated and their temperature controlled accurately.

The lids of the chambers were fitted with unions to allow the connection of tubes to be made for flushing of the chambers, sampling of the solutions and induction of hydrogen as the reducing agent in the reactions. A pressure transducer could also be attached to the reaction vessel in which the reduction reactions took place in order that the amount of gas consumed during the reaction could be determined

by the pressure drop over the period of the reaction.

2.3 Experimental Procedure

2.3.i Use of the reaction vessel

The procedures used in the investigations varied and were developed over the series of experiments, the changes depended upon the measurements to be made. However the filling and flushing of the vessel remained the same throughout the series.

a) Filling and Flushing

Solutions were introduced to the cleaned and dried reaction vessel through the stirrer drive union in the lid. When previously made up solutions were used, the volume to be used was measured in a graduated cylinder and then poured into the vessel with the aid of a funnel. When solutions were prepared in the reaction vessel the required volumes of the 'bulk' solutions were measured into the vessel using appropriate pipettes.

After introduction of the solution the stirrer was replaced, sealed and bolted in position. A reasonable pressure of nitrogen was then put into the vessel (approximately the same pressure as the conditions of the reduction reaction, that is 400 to 700 p.s.i.) and the system was closed. The equipment was then tested for leakage by evidence of a pressure drop. If no leak-

age was apparent the nitrogen was allowed to escape from the vessel by means of the flushing valve. Some nitrogen was also allowed to escape from the upper end of the magnetic stirrer coupling to ensure that this tube was flushed of any air it may have contained.

After pressurising to about 300 p.s.i. with nitrogen, and flushing out three times, the cells were vacuum pumped for a short period (approximately one minute) then resealed and nitrogen filled again. This procedure was to ensure complete purging of all oxygen out of the vessels.

b) Absorbance spectra

The absorption spectrum of the solution in the cell, or reaction vessel, was made by scanning the spectrophotometer between the instruments highest sensitive wavelength, initially 750 nm., later 850 nm., and 450 nm. at room temperature.

The block of the reaction vessel was then heated, as described in the appendix A.1.1.iii until the temperature at which the reaction was to be investigated was attained. When a steady optical density at the absorption peak, at raised temperature, was obtained, an absorption spectra at this temperature was made.

c) Induction of Hydrogen

Two different techniques of induction were used depending upon whether the rate of hydrogen use was being monitored or if the reaction was being performed at constant pressure.

When the pressure drop in the reaction vessel was to be followed, the nitrogen pressure over the solution was released to a convenient value which was just above the water vapour pressure at the temperature. For convenience a pressure of about 100 p.s.i. was used for all temperatures. After the pressure in the vessel had become steady at about 100 p.s.i. hydrogen was inducted until the pressure in the vessel was the required hydrogen pressure plus the residual nitrogen and water vapour pressure (approximately 100 p.s.i.). The most convenient method of induction was found to be by presetting the required total pressure using the coupled mechanical and pneumatic gas pressure controllers. Induction could then be made to the correct pressure by opening the induction valve. By this means very rapid induction was obtained.

When constant pressure reduction reactions were investigated use of the flushing valve, which is shown in the cell and equipment design

details in appendix A.1.1.vii., was made. The nitrogen in the vessel was released by the flush valve until the pressure was the same as the water vapour pressure. The induction valve was then opened allowing hydrogen at a preset pressure of that required plus the vapour pressure to enter the reaction vessel. The flushing valve was kept open for about 10 to 20 seconds after the induction valve was opened so that hydrogen flowing through the gas space above the solution would purge most of the remaining nitrogen from the vessel. The flushing valve was then closed.

In the constant pressure induction technique, the induction valve remained open for the duration of the reaction. The pressure controlling equipment maintained a very nearly constant pressure in the apparatus. It was assumed under this method, since the gas space was flushed with hydrogen, that only hydrogen and water vapour occupied that space.

d) Sampling method.

When no hydrogen gas consumption was to be measured it was possible to remove several samples from the reaction vessel. This was done by means of a sampling valve equipped with a cooling jacket, surrounding the sample tube, through which cooled water was circulated. This arrangement

allowed samples of up to 5 mls. to be taken from the vessel very rapidly without risk of "flash boiling" occuring.

The sampling tube and valve had a 'dead volume' of 1.25 mls.. This volume was removed before each sample was taken. Samples taken were of 1.3 mls. to 1.5 mls. in volume. Both 'dead volume' removal, and samples taken were measured into a graduated cylinder of 2.25 mls. capacity, graduated in 0.25 mls. divisions. Samples were transferred from the graduated cylinder to sample bottles to await pH value measurement and total copper determination.

When it was found that a small amount of iron, nickel and chromium were being dissolved from the stainless steel the samples taken were also analysed for these metals.

2.3.ii. Hydrogen consumption determination.

Hydrogen consumption during the reaction was measured for some reactions by following the pressure drop during the reduction. No samples could be taken under these circumstances since removal of solution was an external effect upon the pressure drop.

As described in the previous section, the constant pressure regulator was used only as a presetting method for induction of hydrogen at

the required pressure. After induction the induction valve was closed and the pressure drop was recorded, by use of an S.E.L. pressure transducer, a transducer converter and a pen recorder.

Details of the calibration and use of the pressure transducers are included in appendix A.1.2.i.

2.3.iii. Optical density change monitoring during a reaction

After procedures of filling, flushing, plotting of absorption spectra and heating of the apparatus had been carried out, the reaction was initiated as described in section 2.3.i. c) by the induction of hydrogen. The optical density at any chosen, fixed wavelength was then recorded on a pen recorder. The spectrophotometer facilities S.P. 820 and S.P. 850 were made use of to allow fixed wavelength recording, scale expansion and back-off of the external recorder used.

The wavelength at which the optical density was monitored was between 775 nm. and 800 nm. This depended upon the most sensitive point for cupric species determination in solution being examined. Hence from the optical density change with time the rate of reduction of cupric species could be easily determined.

2.4. Analytical Techniques

2.4.i. Analysis of samples from the reaction vessel.

During several of the spectrophotometric studies of the reduction of cupric sulphate solutions samples of the solution in the reaction vessel were taken.

These samples were allowed to cool and the pH values measured. They were then diluted and analysed by atomic absorption spectrophotometry for copper. Later in the course of experiments the samples of solution were also analysed to determine the concentration of iron, nickel and chromium.

Analysis for iron, nickel and chromium was done on diluted sample solutions by atomic absorption spectrophotometry.

Due to the reaction:

$$2Cu^{+} \longrightarrow Cu^{o} + Cu^{2+} \qquad \text{eq.1.3.i.}$$

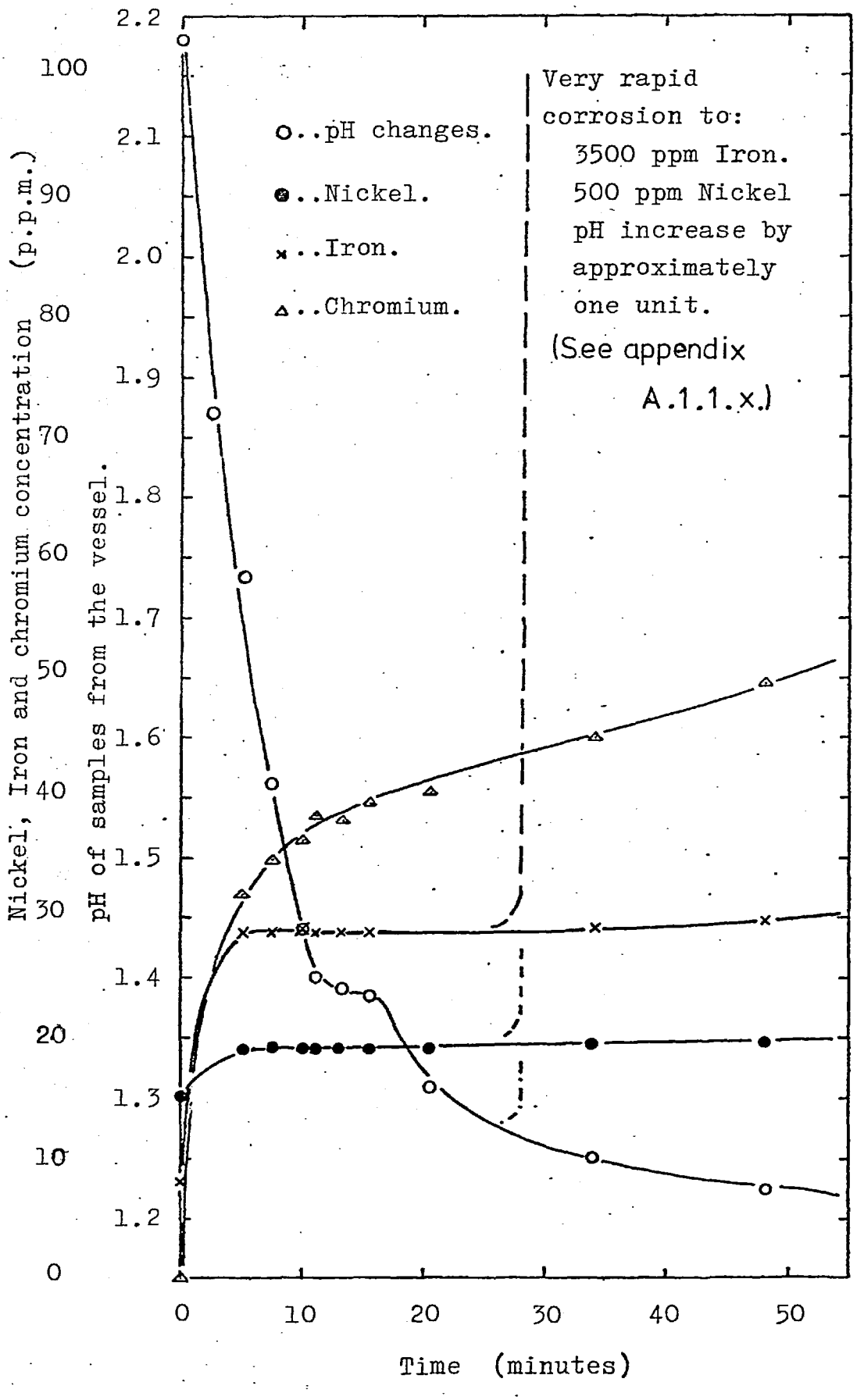
the change in copper concentration in the samples was not representative of the species which existed in the 'at temperature' solution. This reaction occured when solutions containing stable cuprous ions at raised temperature were allowed to cool, if the solution did not also contain a suitable stabilising complexing agent for the cuprous ions. Thus measurements of concentration of copper by

this technique was not significantly relevant to the kinetics of the reactions being studied. However the rate of chemical corrosion of the reaction vessel determined by this method was an important influence in making the decision to change the investigations from the un-buffered sulphate system to study of cupric species reduction in buffered solutions.

An example of the curves obtained for the changes of pH values of the cooled solutions, together with the iron, nickel and chromium concentration changes with time, determined by the above technique are shown in figure 2.4.i.

The atomic absorption spectrophotometer used in the analysis of samples was a Perkin Elmer model 290B single beam instrument. Distilled water was used as the zero standard solution for all analysis. Calibration standards were made up from accurate bulk solutions of 1000 p.p.m. of the appropriate metal in perchloric acid, supplied by Hopkins and Williams, for copper, nickel and iron analyses. Chromium standards were made from a bulk solution of concentration 86.66 p.p.m. chromium, which was made from a wieghed amount of dried potassium dichromate dissolved in distilled water.

FIGURE 2.4.i.



The variation of pH during a reduction reaction and the corrosion rates for nickel, chromium and iron.

The absorption peaks used for the analyses were as follows:

Table 2.T.i.

Metal	Peak Absorption Wavelength (nm.)	Approximate Sensitivity (p.p.m. mV^{-1})
Copper	324.75	0.5
Nickel	232.00	1.5
Iron	248.30	1.0
Chromium	357.90	4.00 to 5.00

2.4.ii Comparison of the bulk acetate solutions by X-ray fluorescence

A marked difference was observed in the behaviour upon reduction by hydrogen of:

(a) cupric acetate solution at low acetate concentration, produced as described in section 2.1.ii., from cupric acetate dihydrate crystals; and

(b) cupric acetate solution, at high acetate concentration, as described in section 2.1.iii., by dissolution of metallic copper in acetic acid.

Due to this difference in behaviour, an analysis of the solutions was considered necessary.

The analysis of the solutions was performed by X-ray fluorescence in an attempt to find a significant difference in the composition of the two types of solution.

The analysis was performed using a tungsten target X-ray tube in order to give sensitivity for transition metals. The results of the X-ray fluorescence did not indicate any conclusive difference between the trace element concentrations in the bulk solutions made in the two different ways.

Table 2.T.ii. shows the results of this analysis.

2.4.iii. Comparison of the bulk acetate solutions by Raman spectroscopy

In a further attempt to distinguish a structural or composition difference between the two types of cupric acetate solution, Raman spectroscopy was employed. This technique should have been able to indicate any marked structural difference.

Again the results obtained were inconclusive; in this case because of very large similar signals received from the acetic acid structure which "swamped" any significant spectral response from any difference of cupric acetate structure.

The solutions used for comparison were as follows:

8.75M(approx. 50% volume) acetic acid in water.
0.0535 M Cu^{2+} in 8.75 M acetate species in water.
(By dissolution of copper in acetic acid)

0.0535 M copper (Cu^{2+}) in 8.857 M acetate in water.
(By dissolution of cupric acetate dihydrate)
0.0535 M copper (Cu^{2+}) in 0.307 M acetate in water.

The Raman spectra obtained from the copper solutions, which all contained some acetic acid, were indistinguishable from the spectra of the acetic acid solution as regards the emission peak positions. However, expectedly, the peak heights were found to be approximately proportional to the acetate concentration.

From these observations it was concluded that structural characteristics of the acetate groups was the only factor which was in sufficient strength to give a measurable response by Raman spectroscopy over the wavelength range observed.

The irradiating or exciting wavelength used was 482.5 n.m.

The range of frequences of emission detected was from 100 cm^{-1} to 2000 cm^{-1}.

TABLE 2.T.ii.

Element.		Approximate concentration or the relative size of the traces in the bulk copper acetate solutions	
		"Copper + acetic acid"	"Hopkins & Williams"
Chloride		100 to 500ppm.	50 to 100ppm
Zinc.		100 to 300ppm.	100 ppm.
Tin.		50 to 100 ppm.	30 to 50 ppm
Iron.	A trace only.	=	=
Nickel.		=	=
Lead.		=	=
Aluminium.		-	+
Silicon.		-	+
Chromium.		=	=
Phosphorus		+	-
Sulphur.		+	-
Calcium.		=	=
Antimony.		+	-

2.4.iv. Analyses of residual solutions.

a). By gas / liquid chromatography.

As described in section 4. the phenomen of "Auto-reduction" was observed to occur when cupric acetate solutions, in high concentrations of acetate ions, were held at elevated temperature for a long period.

In order that an understanding of the reactions occuring during "auto-reduction" could be ~~deemed,~~ gleaned it was decided that determination of of the constituents of the residual solutions should be attempted. The first method employed for this determination was Gas/Liquid Chromatography.

One proposed reaction which involves the reduction of cupric species in acetic acid gave oxalic acid as a product. Thus acetic acid/oxalic acid mixtures, in aqueous solution, were used for comparison with residual solutions from an 'auto-reduction' reaction.

The proposed reaction was:

$$CH_3COOH + 2H_2O \longrightarrow \tfrac{1}{2}(COOH)_2 + CO_2 + \tfrac{7}{2}H_2 \ .$$

Acetic acid Oxalic acid Eq. 2.4.i.

The hydrogen produced would be in solution and available for the reduction of cupric species.

Analytical Technique.

The following solutions were used in the comparison by gas/liquid chromatography.

A sample of the residual solution from an auto-reduction of cupric acetate solution.

0.226 grams. litre^{-1}. oxalic acid solution.

0.226 grams. litre^{-1}. oxalic acid in a 8.857 molar acetic acid solution.

8.857 molar acetic acid solution.

Since oxalic acid decomposes at a temperature of above about 189^{o}C, without melting, but sublimes at about 157^{o}C an attempt was made to separate oxalic acid from other constituents of the solution in the vapour phase.

The stationary phases used to do this separation were:

1) Apiezon L on Chromosorb P (60 to 80 mesh.) (10:90)

2) Carbowax 6000 on Chromosorb W (60 to 80 mesh.) (10:90)

3) Silicone fluid MS 550 and Bentone 34 on Chromosorb W (80 to 100 mesh.) (11.5:11.5:77.0)

4) Polyoxyethylene sorbitan monostearate on Chromosorb W (80 to 100 mesh.) (20:80)

5) Silicone grease on Chromosorb P (80 to 100 mesh.) (15:85)

For each stationary phase used a range of temperatures was employed from 150°C to 250°C, in combination with a range of carrier gas flow rates from 10 to 60 mls. minutes^{-1}. The carrier gas used was high purity argon.

In the sample solution from the auto-reduction no separate peak for oxalic acid could be distinguished under any of the conditions used. The lack of response for oxalic acid may have been due to the very similar retention time of acetic acid and oxalic acid under all conditions. Therefore any response of the detector to oxalic acid would have been 'swamped' by the broad peak of acetic acid.

However at temperatures above about 189°C the decomposition products, carbon dioxide and carbon monoxide, of oxalic acid were observed.

The observation of the products from the reaction:

$$(COOH)_2 \longrightarrow CO_2 + CO + H_2O. \qquad \text{Eq. 2.4.ii.}$$

Oxalic acid.

cannot be considered to be unequivocal identification of the presence of oxalic acid in the sample solution, but it did indicate that oxalic acid may have been present.

b) Paper chromatography.

In order to verify the existence of components other than acetic acid in the final solution, after 'auto-reduction' of cupric acetate solution, paper chromatography was employed.

Chromatograph paper was cut to form strips of approximately 2 cms. wide and 20 cms. long. The ends of strips were 'spotted' with a drop of sample solution at a point approximately 1 cm from one end. Development of the chromatographs was done by suspending the paper strips in a sealed vessel, with the edge next to the sample spot just immersed in a 35% ethanol solution in water.

Two techniques were employed to try to show the existence of acids in the developed chromatographs. After drying the paper for a short period at about 130°C, a standard universal pH indicator was used to detect any acid component on the chromatograph. Acetic acid would not be indicated in this way since, at the temperature of drying, it would be evaporated.

The indicator solution was applied as a fine spray. This technique was found to have very limited success.

Heating the developed chromatographs to about 190°C was found to be a suitable indicator of the position of the components of the sample solutions.

Heating the papers had the effect of "charring" the areas containing any low organic acids, thus showing them up as dark brown spots.

The technique used was to heat the chromatograph for about 30 to 45 minutes, until the charring was easily visible, and then to wash the paper in ammonia solution in order to remove any copper powder from the paper. The very fine copper powder product of auto-reduction was found to develop on the chromatograph to a limited extent and it was found to be easily removed in ammonia solution. Having the copper powder present in the samples during development had the disadvantage that as the colloidal powder moved on the paper the porosity was changed. Thus the rates of development were also changed by the presence of the powder in the sample.

An example of the results of this analysis is shown in Figure 2.4.ii. These examples are of

short development chromatographs, the development time was about 45 minutes.

A table of the R_d : R_s ratio, that is the rate of movement of the developing solution compared to the rate of movement of the component of the solution, may be seen in table 2.T.iii.

The Figure 2.4.ii. and Table 2.T.iii. show that the paper chromatographs did not give definite evidence of the existence of the oxalic acid or of copper oxalate in the solution.

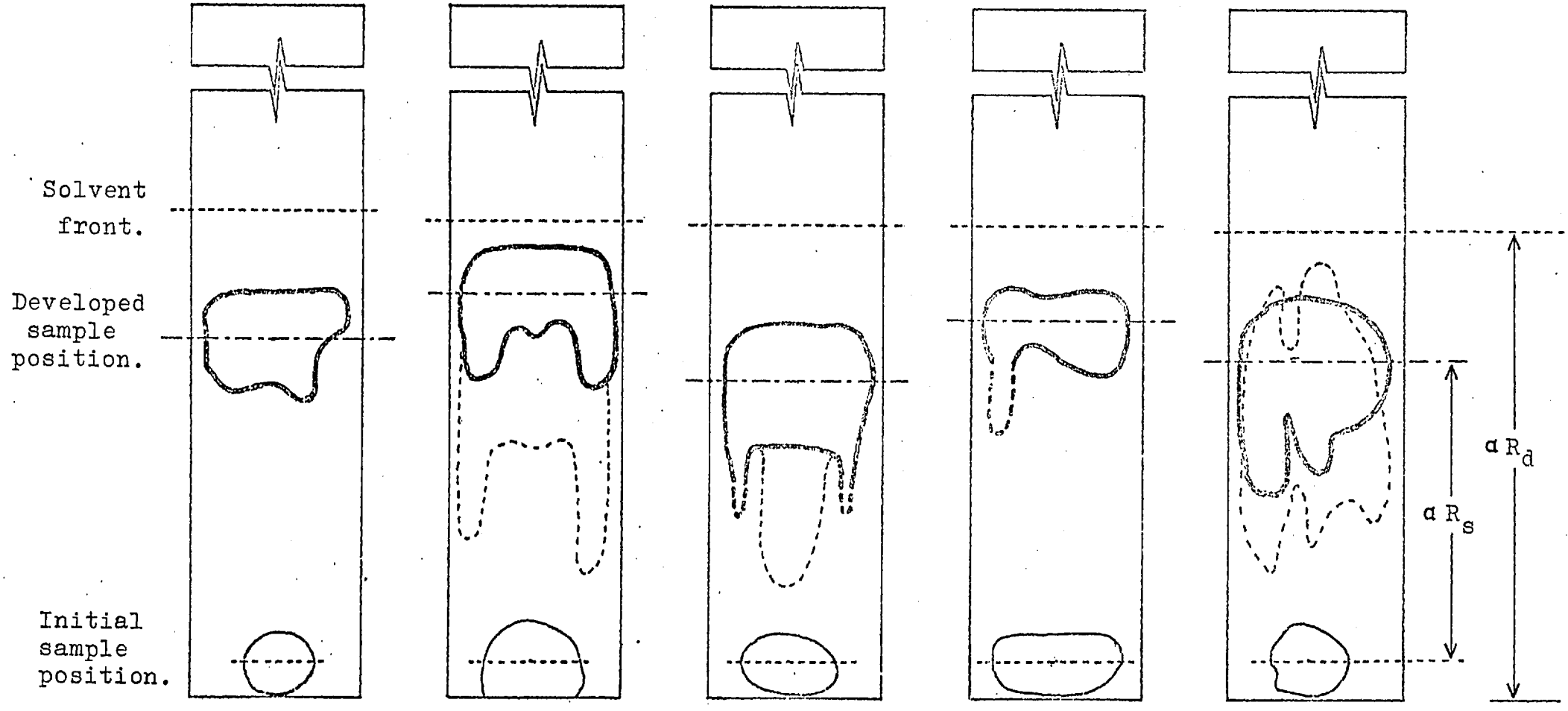
TABLE 2.T.iii.

The ratio of the solvent movement rate to the solute movement rate for several paper chromatographs.

Sample.	R_d : R_s ratio.
Copper acetate and acetic acid.	1.3954
Copper oxalate and oxalic acid.	1.1953 ; 1.3909
Copper formate and formic acid.	1.5510
Oxalic acid.	1.2781
Sample of the solution after auto-reduction. (and suspended copper)	1.4423 ; 1.4011

Figure 2.4.ii.

Examples of the paper chromatographs used to attempt to determine the constituents of auto-reduction residual solutions.



2.5. Observation and Analyses of the Solid Reduction Products.

2.5.i. X-Ray powder photographs of the reduced species.

Samples of solid reduction products were removed from the reaction vessels after a reduction was completed. These samples were washed, dried and mounted on transparent adhesive tape on a Guinier camera mounting slip. The sample mounting slips for the Guinier camera accommodated four samples. For most photographs a sample from the reaction vessel was exposed at the same time as a sample of high purity copper powder, some cuprous oxide or copper powder which contained a large proportion of cuprous oxide and one sample frame was left empty so that an X-ray 'powder' photograph would be obtained of the adhesive tape. On some occasions petroleum grease was used, mixed into a paste with the sample of the fine powder reduction product so that the possibility of oxidation of the powder was reduced. When petroleum grease was employed the 'blank' frame of the mounting slip contained the grease on adhensive tape.

No accurate measurement of the resultant powder photographs, after exposure and development,

were made since the pattern of lines from a sample and that from a standard powder were formed on the same film so that direct comparison could be easily made.

An example of Guinier camera powder X-ray photographs may be seen in Figure 2.5.i.

The conditions used were as follows:

X-ray tube current	20 mA.
X-ray tube potential	30 Kvolts.
Using an X-ray tube target of copper:	
Exposure time	1.25 to 2.0 hours.
Using an X-ray tube target of cobalt:	
Exposure time	1.5 to 2.5 hours.

By the use of X-ray powder pattern photographs the composition of the solid reduction products could be easily determined. Analysis of the product was often found to be necessary since visual observation of the product in an extremely finely divided form was easily misleading.

It was found by the above technique that copper metal powder was produced under all conditions investigated from the reduction of cupric sulphate solutions. The same technique showed that the product of the reduction of cupric acetate solutions appeared to depend

upon the total acetate concentration in the solution. At low acetate ion concentration, up to about 1.0 molar, cuprous oxide was formed as a fine powder. The colour of the cuprous oxide product varied from red to dark purple depending on the particular size.

At high total acetate concentration metallic copper was always the only solid reduction product.

The auto-reduction of cupric acetate solution in the presence of a large concentration of acetic acid was also shown by X-ray powder photography on the product, to give finely divided metallic copper.

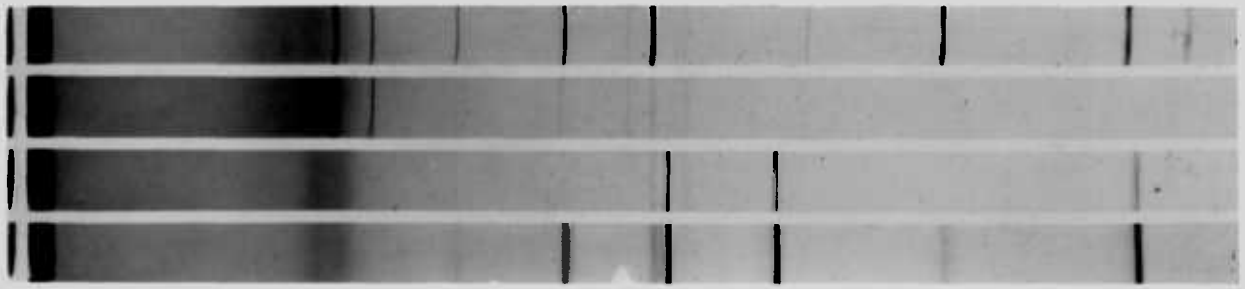
2.5.ii. Observation of powders by laser light.

When solid reduction products were formed by reduction with hydrogen gas from copper sulphate or acetate solution the resultant powder was always of sufficiently large particle size to ensure settling. However when auto-reduction of cupric acetate solution was allowed to occur the copper powder formed was of very small particle size, causing this solid to be inseparable from residual solution by physical means.

Since the high concentration of copper particles in suspension in the solution gave the appearance of a brown and very highly absorbing solution, visual examination was made using a laser beam to exhibit diffusion in the suspension.

FIGURE 2.5.i.

1.25 hours exposure time from a copper target X-ray tube:



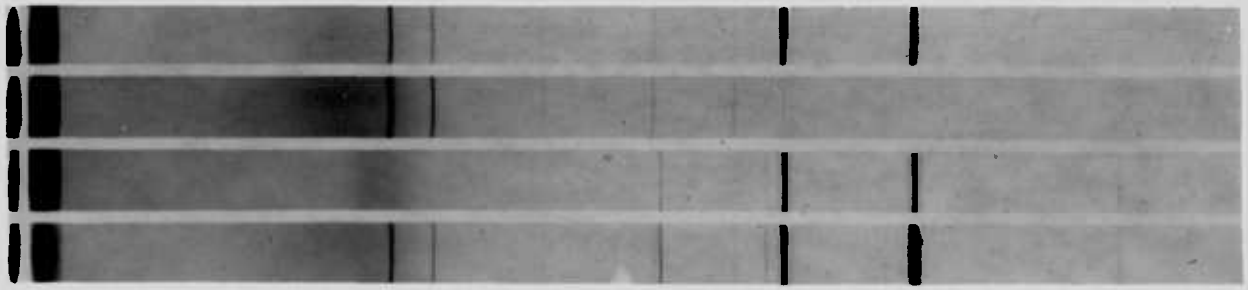
A

Petroleum grease.

Pure copper filings.

Copper powder with a small amount of cuprous oxide.

1.50 hours exposure time from a cobalt target X-ray tube:



B

Petroleum grease.

Copper powder with a very small amount of cuprous oxide.

Copper powder and petroleum grease.

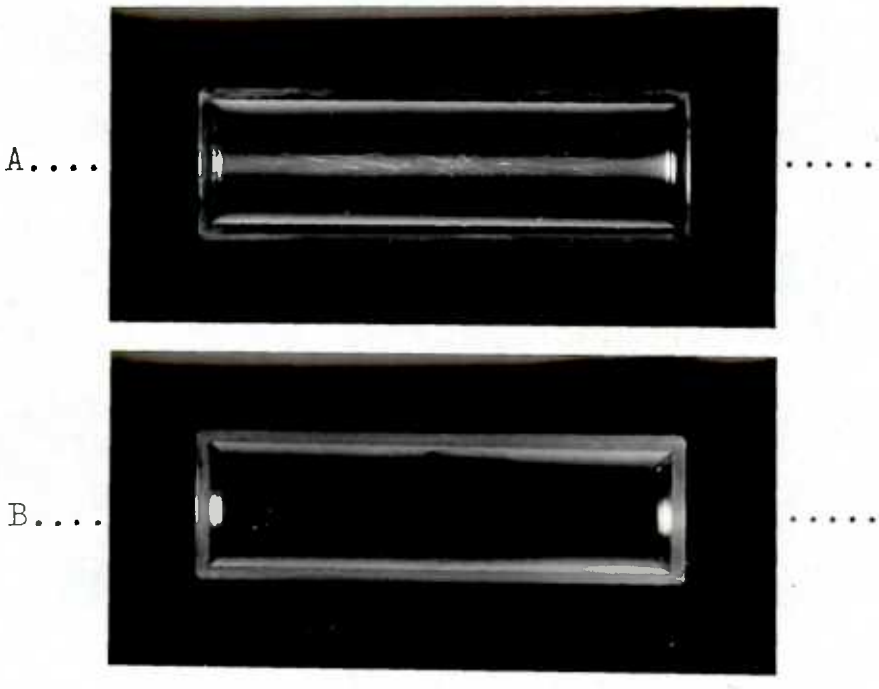
Frame A : A sample of the product of reduction of low acetate concentration cupric acetate solution.

Frame B : A sample of the product of reduction of a large acetate concentration cupric acetate solution.

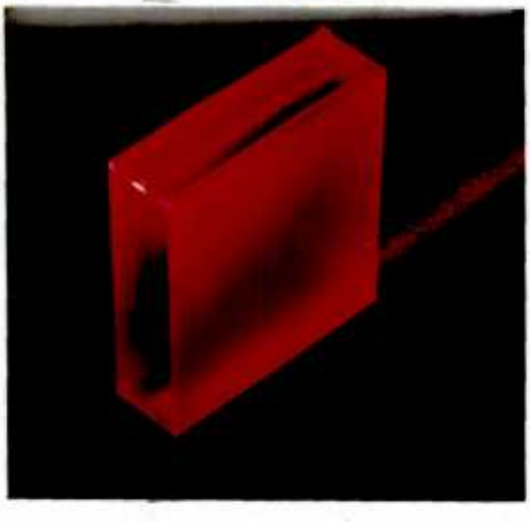
Examples of the X-Ray Powder Photographs of Solid Reduction Products.

FIGURE 2.5.ii.

A photograph showing a comparison between the visibility of a laser beam through A) a solution containing suspended copper powder and B) a similar cell containing water only.



A photograph giving evidence of the visibility of red laser light when a beam was passed through a cell containing suspended powder in a solution.



When laser light observation was employed a very obvious visible beam could be seen in the cell containing the suspension. The visibility of the beam of light in the cell is evidence of the existence of a suspension. Figure 2.5.ii. shows a photograph of the observable laser beam in the solution in a cell. Of further interest was that the reflecting faces of 'micro-crystals' of copper powder in suspension were seen to scintillate as movement occured through the laser beam.

2.5.iii. Observation of the occurrence of solid products in solutions by turbidity measurements.

In conjunction with optical density measurements made during reduction of cupric solutions, several measurements of the turbidity change during a reaction were made.

Measurement of the turbidity of solution was done by following the change in 'absorbance' at a 'trough' in the cupric species absorption spectra in solution. At this wavelength absorption was due to 'shuttering' by particles in the solution only, the ionic absorption being negligable.

Turbidity is identical in definition to absorbance or optical density:

$$T \text{ (turbidity)} = \log_{10} \frac{I_o}{I_t}$$

Where : I_o = the incident intensity

I_t = the transmitted intensity

It is assumed that turbidity is due to particles of sufficiently large size to give I_o/I_t ratios which should be independent of the wavelength of the incident radiation. If the particles are of much smaller size independence of turbidity on wavelength does not exist since Rayleighan scattering occurs, giving a variation of I_o/I_t with wavelength.

By monitoring of turbidity change during a reaction the time at which a solid reduction product begins to appear can be determined. The rate of formation of solid particles in the solution could not be accurately determined, since different particular size caused variation of the turbidity when the quantity of solid was the same. This variation was due to the proportion of the powders which settled when a powder of large size was produced, and due to the change in projected area of particles compared to their mass as the size changed.

A sketch example of a turbidity monitoring is shown in figure 2.5.iii.

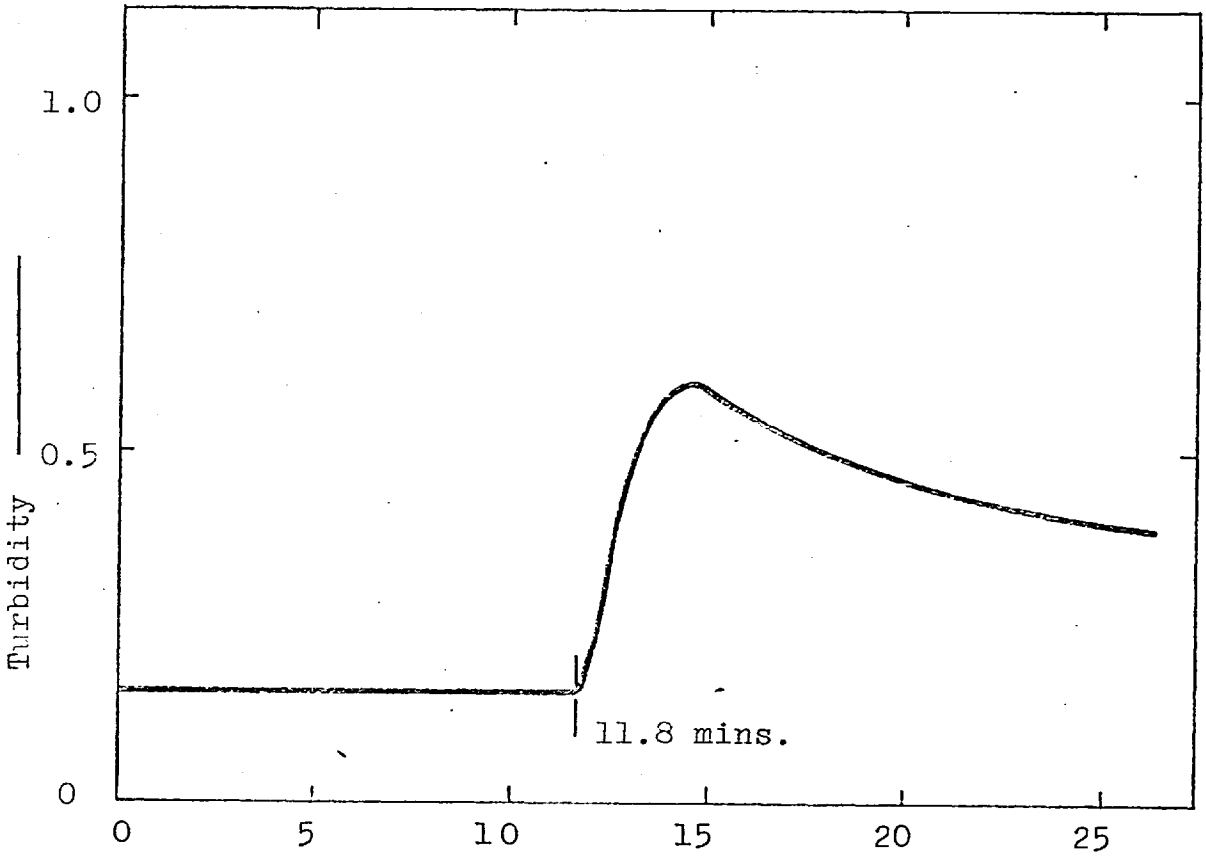


Figure 2.5.iii.

An example of turbidity monitoring. (This curve was obtained when the single cupric sulphate reduction hydrogen consumption determination was made).

2.6 Analysis of the gases remaining in the reaction vessels after reactions: by gas chromatography.

To determine the constitution of the gaseous reaction products of reduction reactions gas chromatography was employed.

The instrument used for this analysis was a very modified Fisher Instruments Gas Partitioner.

The modifications to the instrument were intended to allow the use of a single chromatograph column. The column was made from aluminium tube using Porapak 'T' as the stationary phase. The length of the tube was 3.66 metres and the inside diameter was 3.175 mm. The column replaced the two in the original instrument, which were of silica gel and of a molecular sieve material, which were arranged in tandem. In order to use the single column the gas circuits were modified appropriately. The gas sampler valve on the Fisher instrument was also modified to allow 1 ml. sampling to be made.

Carrier gases used in the investigation were dependent upon the known major constituent of the gas sample. Samples taken from the spectrophotometer reaction vessel when hydrogen gas had been introducedused high quality dried hydrogen at a flow rate of between 20 mls. and 90 mls.

min^{-1}. as the carrier. Dried oxygen free nitrogen was used on analysis of the auto-reduction gases, in order that hydrogen could be easily determined. When nitrogen was used flow rates of between 15 mls. $mins^{-1}$. and 30 mls. $mins^{-1}$. were employed.

Carrier gas flow rates were measured using a ' MeTeRaTe "A" ' rotameter connected in the gas stream, down-stream of the gas partitioner.

All gas analyses were performed at room temperature.

By measurement of the magnitude of the detector response a semi-quantitative estimate of the gases in a sample could be made.

Some examples of chart recorded responses from the gas chromatograph are shown in figure 2.6.i.

The residence times in the column for standard gas samples are shown in Table 2.T.iv.

This analytical technique gave conclusive evidence of the existence of carbon dioxide and hydrogen over the solution in a reaction vessel after auto-reduction of cupric acetate had taken place. This conclusion may be drawn from the very good agreement between residence times found for carbon dioxide and for hydrogen, and the residence times found for the constituents of the remaining gas samples.

From measurement of the relative size of

the peaks of the recorded chromatograph output an approximation of the proportions of carbon dioxide and hydrogen was made:

Carbon dioxide	:	Hydrogen
2.8	:	1.0

Table 2.T.iv

Carrier Gas & Flow Rate	Sample Injected	Times of Response (Mins)							
Hydrogen 9.5cms on MeTeRaTe 'A' Approx 85mls/min	CO_2	4.96	4.90						
	Air (O_2,N_2)	1.03	1.04	1.04	1.02				
	Cell Gas	1.02;5.02	1.025;5.05	1.005;5.10					
Hydrogen 4.2 cms on MeTeRaTe 'A' Approx 20 mls/min	N_2	2.80	2.80						
	Air	3.00							
	O_2	3.00	2.90	2.90	2.95				
	Cell Gas	3.025;15.75							
Nitrogen 8.5cms on MeTeRaTe 'A' Approx 20 mls/min	H_2	2.10	2.09	2.05					
	O_2	2.29	2.29	2.29					
	CO_2	11.08	11.50						
	Cell Gas	2.10;10.5	2.08;11.16						
Nitrogen 7.5cms on MeTeRaTe 'A' (drifting) Approx 15 mls/min	Air	1.85	1.88	1.86	1.84	1.87	1.94	1.90	1.97
	H_2				1.65		1.85	1.84	1.76
	CO_2	9.45	10.0	9.80	9.58				
	Cell Gas	1.62;9.3	1.76;9.8	1.67;9.58	1.73;9.0				

Table 2.T.iv (Cont)

Carrier Gas & Flow Rate	Sample Injected	Times of Response (Mins)				
Nitrogen 10 p.s.i. at Inlet	Ethane	6.10	6.33			
	Cell Gas	1.5;9.3	1.49;9.3	1.51;9.20	1.52;9.2	
	Town Gas (H_2+CO)	1.55;2.32				
	CO_2	9.20	9.12	9.10	9.00	
	H_2	1.52	1.56	1.50	1.50	1.51
	Cell Gas (First peak only)			1.50	1.50	1.50
Hydrogen 8.5cms on MeTeRaTe 'A' Approx 70mls/min	Town Gas	1.2;1.4	1.2;1.4			
	CO_2 : N_2 mixture 100:1	1.3;5.20	1.3;5.20			
	Cell Gas	1.2;5.55 Four times	1.2;5.50	1.15;5.6	1.15;5.65 Two times	1.17;5.70 Two times
Slightly decreased Carrier Flow Rate	CO_2 : N_2 Trace N_2 only	1.35;6.0	1.35;5.9	1.3;6.00		

EXAMPLES OF GAS CHROMATOGRAPHS SHOWING TIME OF RESPONSE

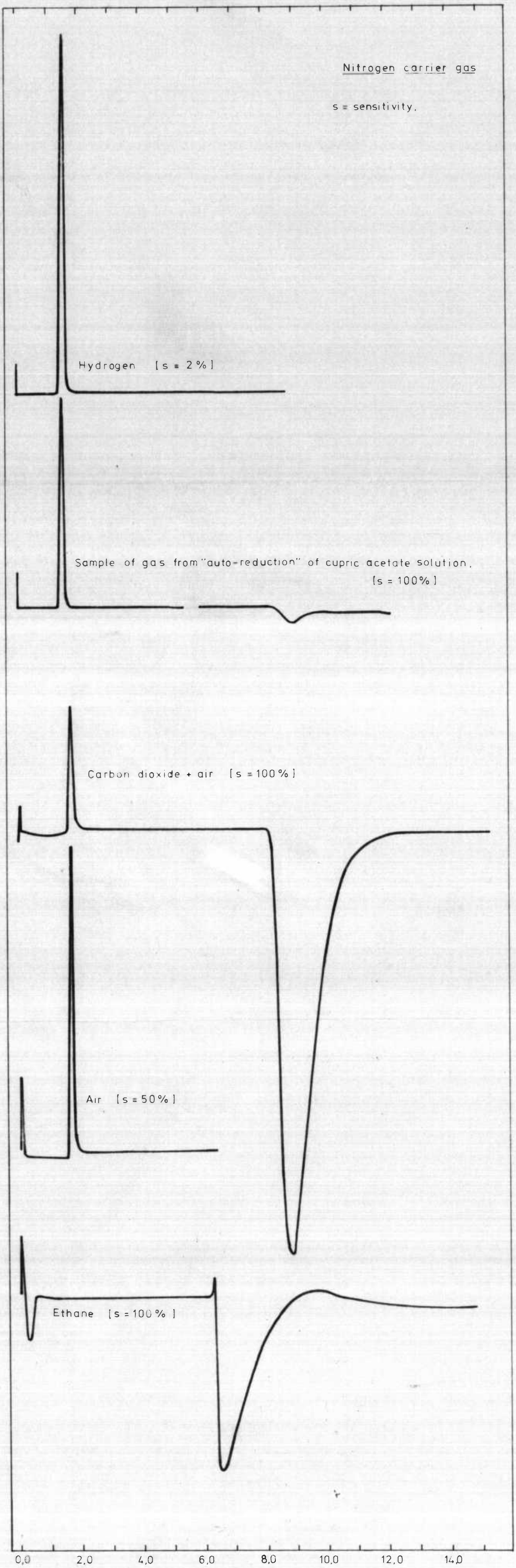


FIGURE 2.6.1.

Section 3.

RESULTS AND DISCUSSION OF OBTAINED DATA

3.1. Results and discussion of the experimental investigation of cupric acetate reduction

Chart records produced from optical density measurements, as described in section 2.3.iii., were measured in order that the optical density, or absorbance, values may be determined, tabulated and used for equal time intervals after the initiation of the reactions.

The tabulated data which was determined in this manner is exhibited in the appendices in Tables A.5.T.i. to A.5.T.xxxii.

This data at equal time intervals for each examination was treated in the following ways, so that proposals as to the mechanism of the reduction reactions could be made.

3.1.i. The methods of analysing the results of the accelerating portion of the reaction.

The accelerating section of the reduction reaction of cupric acetate in solution by hydrogen gas was studied in detail for three investigations only. The technique required the measurement of the rate of use of hydrogen during reaction, in conjunction with measurements of the rate of reduction of cupric species.

These measurements were made in the way described in sections 2.3.ii., and 2.3.iii.

As shown in figures 3.1.i., to 3.1.iii., the rate of use of reducing agent was found to have a non—continuous form, but to be exponential in three stages.

It was supposed that initially the reaction may be controlled by the concentration of reducing agent, dissolved molecular hydrogen, in the solution.

The concentration of hydrogen in the solution at any time after induction of hydrogen gas to the vessel could be calculated from the rate of change of hydrogen pressure over the solution in the following way.

Figures 3.1.i. to 3.1.iii. show that over the first part of the reaction, after steady conditions were obtained, the change of hydrogen pressure is an exponential function:

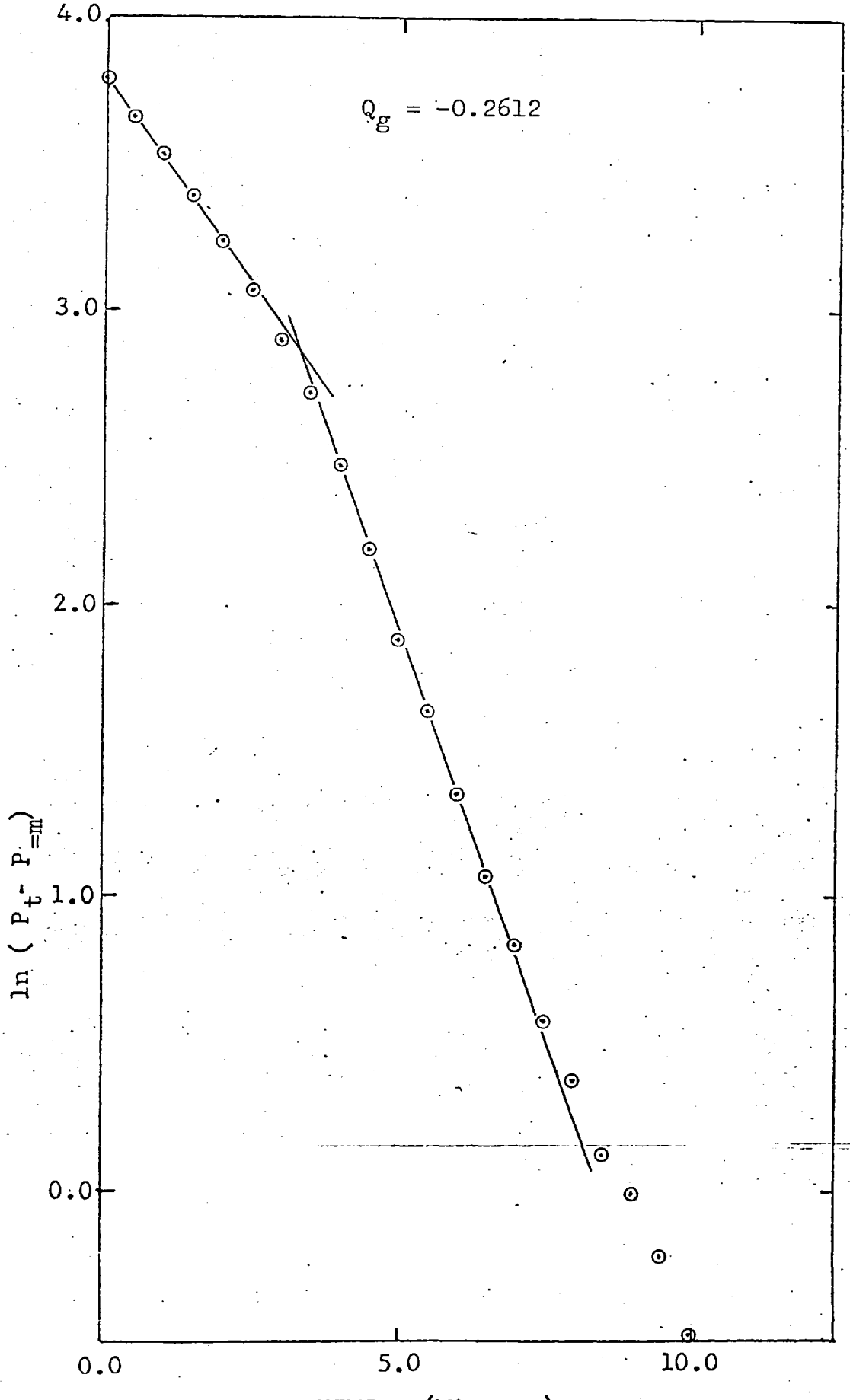
$$\log_e (P_t - P_{=m}) = Q_g t. \qquad \text{Eq. 3.1.i.}$$

where: P_t is the pressure at time t after the reaction begins. (In pounds. inches^{-2})

$P_{=m}$ is the pressure after a long time when equilibrium between gas and solution was attained. (pounds. inches^{-2})

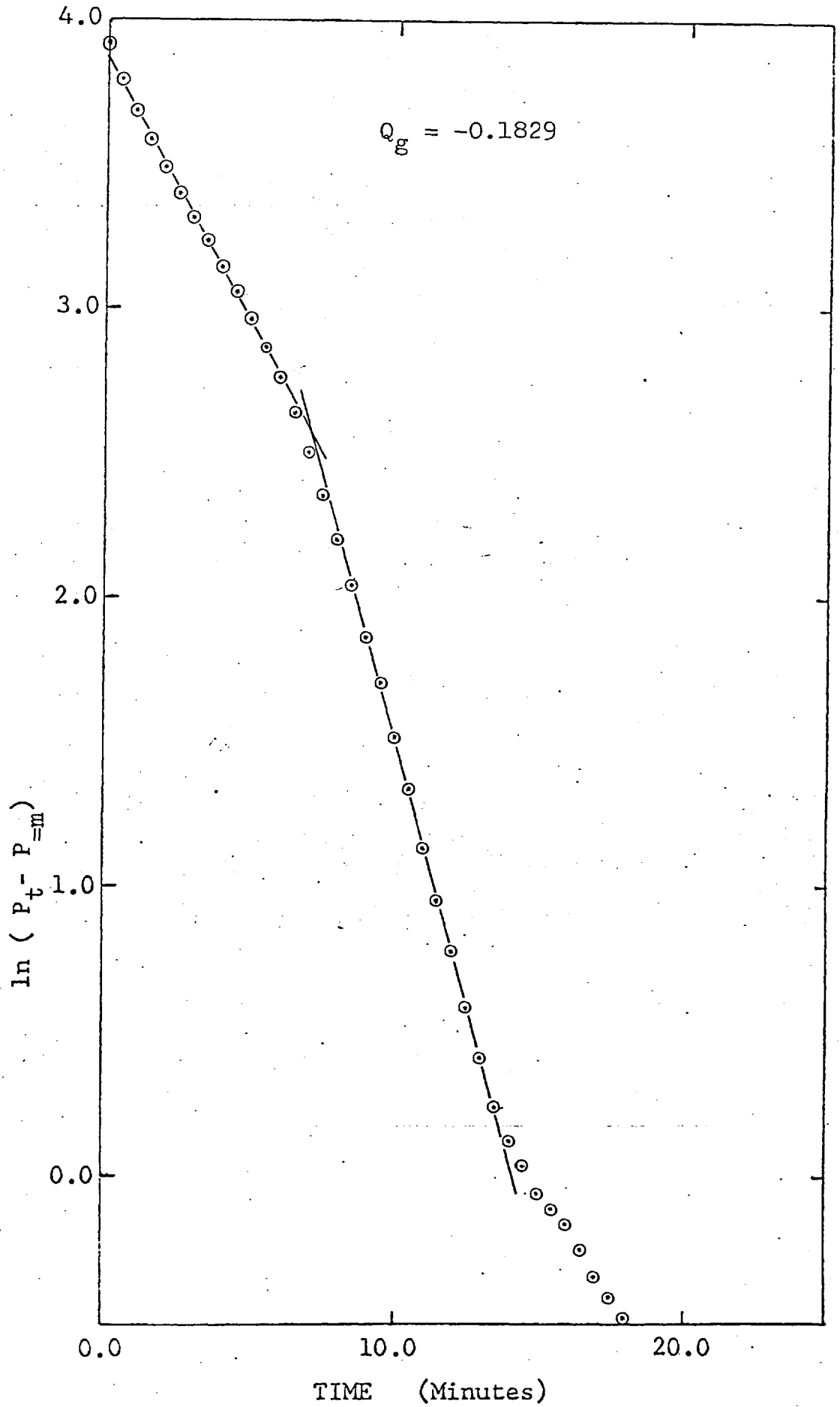
Q_g is the constant for the dissolution

Figure 3.1.i.



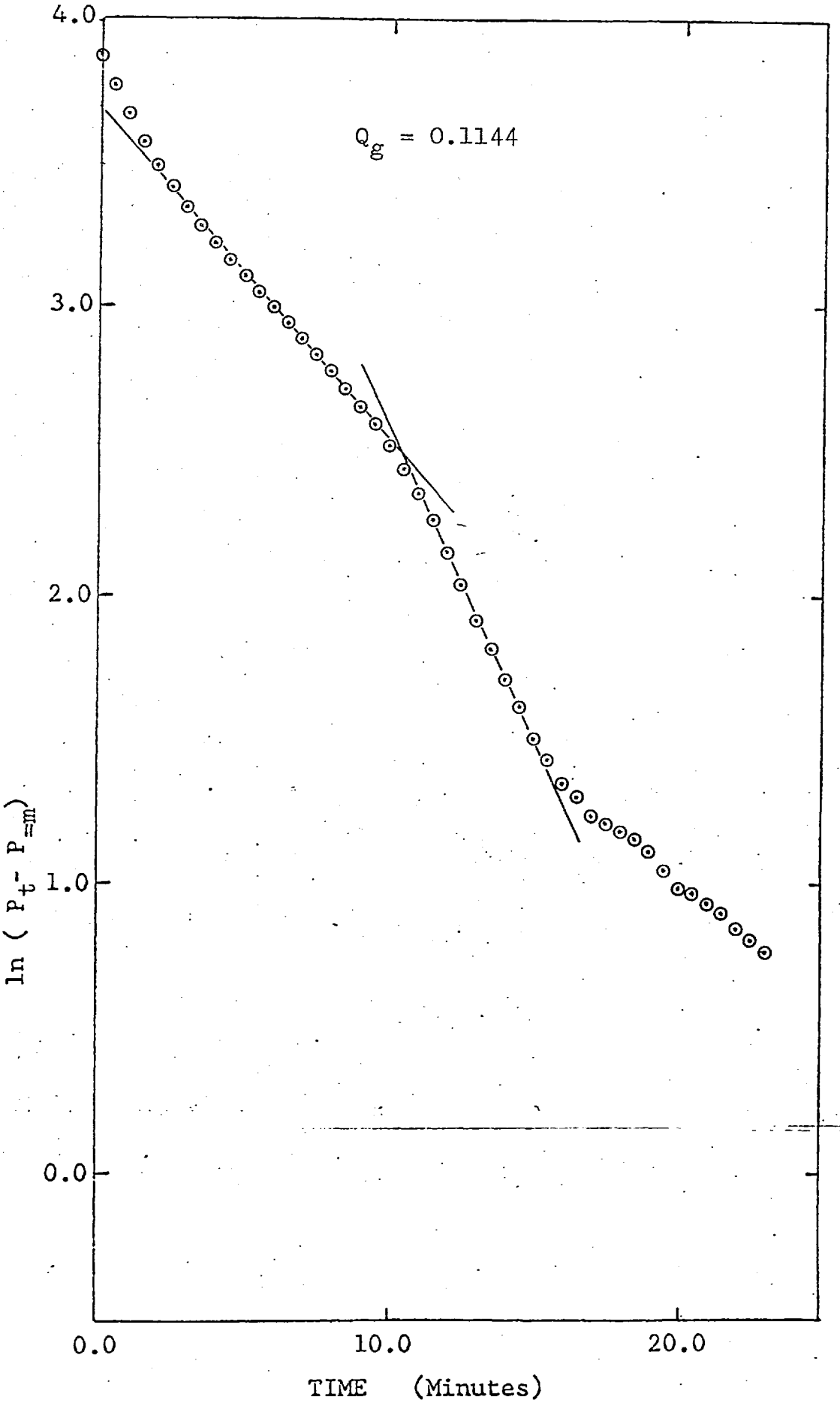
The change of hydrogen pressure with time during a reaction at 150°C

Figure 3.1.ii.



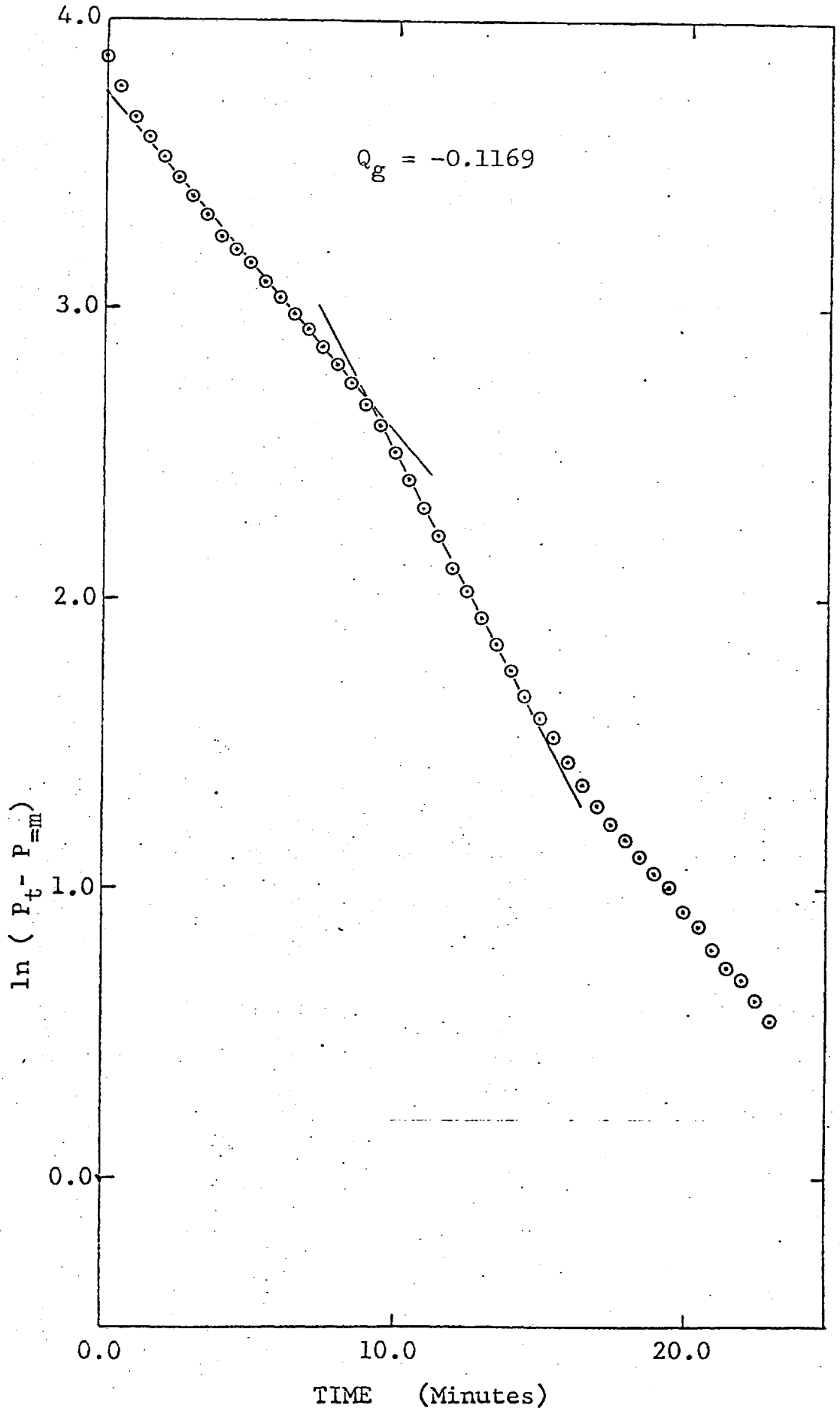
The change of hydrogen pressure with time during a reaction at 140°C

Figure 3.1.iii.



The change of hydrogen pressure with time during a reaction at 130°C (While turbidity monitoring was performed).

Figure 3.1.iv.



The change of hydrogen pressure with time during a reaction at 130°C (While cupric species in solution monitoring)

rate. (minutes^{-1})

t is the time after the start of the dissolution. (minutes.)

From the plotted data in these graphs the values of Q_g could be determined, from the gradients. Having a knowledge of the volume of the solution and of the volume of the gas space at any temperature, the change of concentration of hydrogen in solution may be obtained. The apparent volume of the gas space in the vessel was determined by a method described in appendix A.1.2

Since the volume of the solution was assumed to remain unchanged during the reaction the loss of hydrogen from the gas phase must be proportional to the increase in total hydrogen concentration in the solution.

Thus:

$$\log_e (m_{=m} - m_t) = Q_s t \qquad \text{Eq. 3.1.ii.}$$

Where: $m_{=m}$ is the total hydrogen concentration in the solution if equilibrium were attained.

m_t is the total hydrogen concentration in the solution after time t.

Q_s is the rate constant for the increase in hydrogen concentration in solution.

t is the time after initiation of the dissolution.

But:

$$m_{=m} = \beta (P_I - P_{=m})$$

P_I is the original pressure over the solution.

β is a convertion constant from p.s.i. in a known gas volume to molar concentration in a known solution volume.

Also:

$$m_t = \beta (P_I - P_t)$$

Or:

$$-P_m = \frac{m_{=m}}{\beta} - P_I \qquad \text{Eq. 3.1.iii.}$$

And :

$$-P_t = \frac{m_t}{\beta} - P_I \qquad \text{Eq. 3.1.iv.}$$

Thus:

$$\log_e(P_t - P_{=m}) = \log_e\left(\left(\frac{m_{=m}}{\beta} - P_I\right) - \left(\frac{m_t}{\beta} - P_I\right)\right)$$

$$= \log_e\left(\frac{m_{=m} - m_t}{\beta}\right)$$

Therefore, substituting from Eq. 3.1.i.:

$$\log_e(m_{=m} - m_t) = Q_g t + \log_e \beta$$

Or:

$$m_{=m} - m_t = \beta e^{Q_g t} \qquad \text{Eq. 3.1.v.}$$

Also it was possible to calculate the concentration of molecular hydrogen in the solution since:

$$m_t = m_{Dt} + m_{Rt} \qquad \text{Eq. 3.1.vi.}$$

Where: m_{Dt} is the molar concentration of molecular hydrogen in solution

m_{Rt} is the molar concentration of hydrogen which has reacted with cupric species in the solution.

Now it was proposed that for each hydrogen molecule which reacts the reaction must occur with two cupric ion species:

$$Cu^{2+}_{spec.} + \tfrac{1}{2} H_2 \longrightarrow Cu^{+}_{spec.} + H^{+} \qquad \text{Eq. 3.1.vii.}$$

So:

$$m_{Rt} = \tfrac{1}{2}\Delta [Cu^{2+}] \qquad \text{Eq. 3.1.viii.}$$

$\Delta [Cu^{2+}]$ is the difference between the initial cupric concentration and the cupric concentration after a time t minutes.

Thus:

$$m_{Dt} = m_t - \tfrac{1}{2}\Delta [Cu^{2+}] \qquad \text{Eq. 3.1.ix.}$$

But the value of m_t is known from equation (3.1.vi.) so m_{Dt} after time t can be given by:

$$m_{Dt} = m_t - \beta e^{Q_g t} - \tfrac{1}{2}\Delta [Cu^{2+}] \qquad \text{Eq. 3.1.x.}$$

If the reaction was dependent upon the hydrogen concentration in the solution:

$$-\frac{d[Cu^{2+}]}{dt} = k_o [H_2] = k_o m_{Dt}. \qquad \text{Eq. 3.1.xi.}$$

Or:

$$-\frac{d[Cu^{2+}]}{dt} = k_o (m_{=m} - \beta e^{Q_g t} - \tfrac{1}{2}\Delta [Cu^{2+}]) \qquad \text{Eq. 3.1.xii.}$$

From the data available in the form of chart records the values of $d[Cu^{2+}]/dt$ may be approximated to $\delta[Cu^{2+}]/\delta t$, small differences in cupric concentration over small time intervals. The time t being the mean over the time interval δt, now called t_m. Similarly the cupric concentration change from the original is to be refered to as $\Delta_m [Cu^{2+}]$, being the difference to the mean value over which $\delta [Cu^{2+}]$ was measured.

By plotting:

$$\frac{\delta [Cu^{2+}]}{\delta t} \text{ versus } \beta e^{Q_g t_m} + \tfrac{1}{2}\Delta_m [Cu^{2+}]$$

the value of the rate constant k_o for the accelerating portion of the reaction can be obtained by measuring the gradient of the appropriate section of the plot.

Results

For reduction kinetics followed at 130°C, 140°C and 150°C, for 0.04905 molar (at 20°C) cupric species in the initial solution, and 6.41132 molar in acetate, the plots for the data obtained of the function above can be seen in figures 3.1.v. to 3.1.vii. The three reductions investigated and analysed in this manner were performed under an initial hydrogen pressure of 400 p.s.i.

By comparison of the curves obtained for this function with the hydrogen pressure drop plots, figures 3.1.i. to 3.1.iii., and with the cupric concentration change with time curve the following points may be noticed.

The first discontinuity in the hydrogen pressure drop curve corresponds to the beginning of the none-linear section of the rate of reaction against hydrogen concentration plot. This point can also be seen to correspond to the end of the accelerating section of the original rate curve, as should have been expected.

The tabulated information, Table 3.T.i., gives the times at which a steady condition is obtained, the time when a decaying rate of cupric species 'disappearance' starts, and the time of appearance of metallic copper. This data is compared in the table to the times at which discontinuities occur in the hydrogen pressure drop curve.

Figure 3.1.v.

The plot of the rate equation for the accelerating portion of the reduction reaction at 150°C

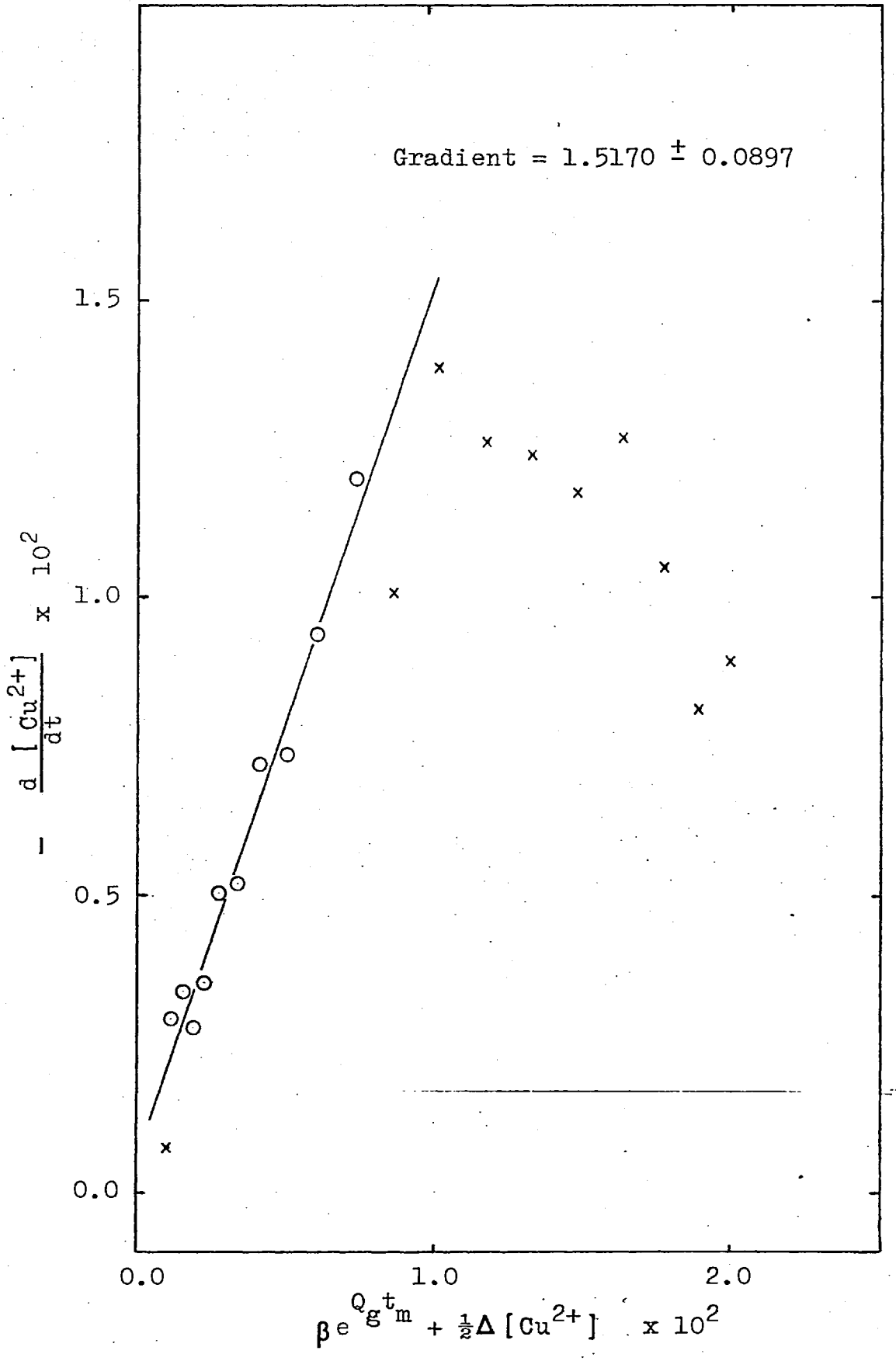


Figure 3.1.vi

The plot of the rate equation for the accelerating portion of the reduction reaction at 140°C.

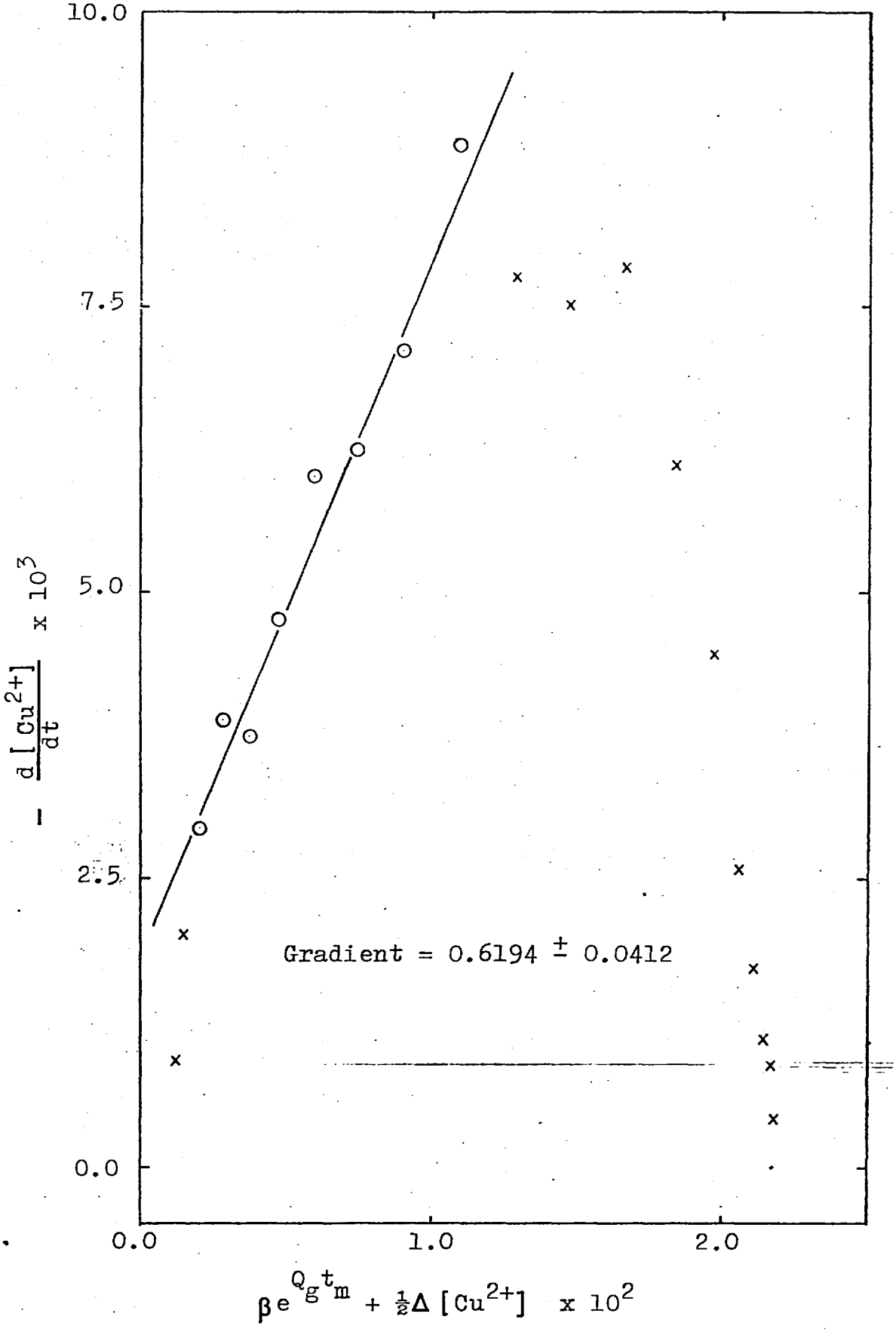
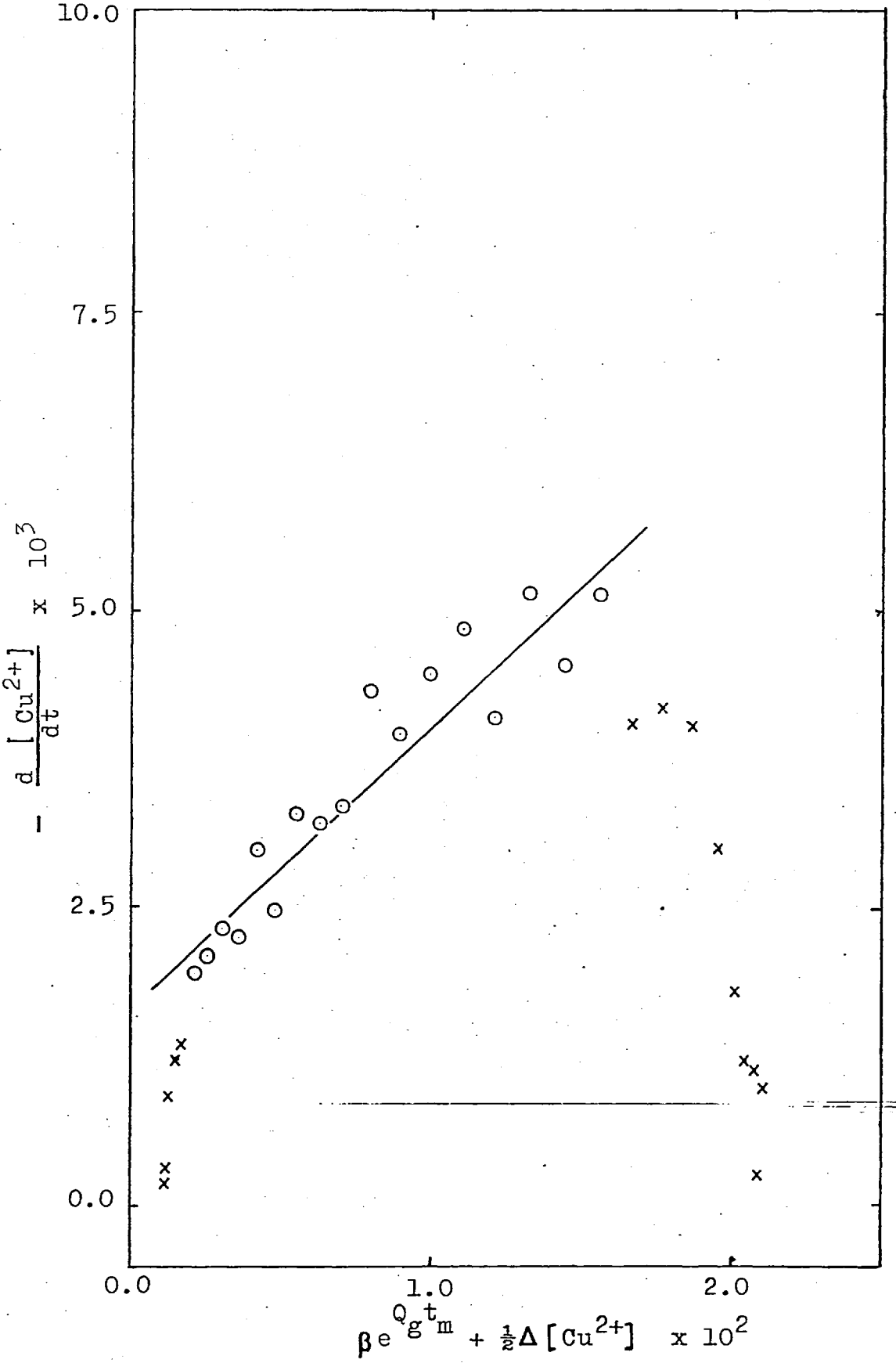


Figure 3.1.vii.

The plot of the rate equation for the accelerating portion of the reduction reaction at 130°C.



3.1.ii. The methods of analysing the results of the decaying portion of the rate curve of reduction of cupric acetate

The optical density data, derived as explained above, was treated in the following way using the Imperial College Computer Centre C.D.C. 6400 computer. Program ALFRED was developed for the purpose of operating on the decaying portion of the reaction rate curve. A copy of a listing of program Alfred is included in Appendix A.5.i.

Analyses of results was hampered due to the inability to make zero adjustments of the spectrophotometer other than before filling, flushing, heating etc. of the reaction cell has been performed.

During examination, drift from the preset zero was obvious especially during the heating of the apparatus, thus the previously set zero optical density was invalidated before the reaction to be studied was initiated. No method of determining the true optical density zero during the course of the reaction existed, hence the following approximations were made.

It was assumed, due to the favourable thermodynamics of the reduction of cupric species under the conditions used, that the reduction from cupric ions to a semi-reduced, cuprous or hydride, species would, if no further reactions took place,

continue to completion.

If this assumption was true, and if the reaction was dependent only upon the concentration of cupric species in the solution, as preliminary examinations of the data had indicated, then the equation:

$$\frac{d\,[Cu^{2+}]}{dt} = -k_h\,[Cu^{2+}] \qquad \text{Eq. 3.1.xiii.}$$

would apply.

But since Beer's Law is known to be valid for solutions being examined:

$$[Cu^{2+}] = k'\,(O.D. + C_{corr.}) \qquad \text{Eq. 3.1.xiv.}$$

Where: k' is the calibration constant for the spectrophotometer.

O.D. is the optical density value which was read from the chart-pen recording.

$C_{corr.}$ is zero correction which is unknown due to inability of the instrument to be zeroed before an investigation.

Hence:

$$\frac{d(k'(O.D. + C_{corr})}{dt} = k_h k' O.D. + k_h k' C_{corr.} \qquad \text{Eq. 3.1.xv.}$$

$C_{corr.}$ is constant for any time value, thus:

$$- k' \frac{d\ O.D.}{dt} = k'(k_h O.D. + k_h C_{corr})$$

Eq. 3.1.xvi.

Thus if $\frac{\delta\ O.D.}{\delta t}$ is plotted against O.D. the following information is available:

k_h = the gradient of the straight line

$k_h C_{corr}$ = the intercept of the line with the differential axis.

$$C_{corr.} = \frac{\text{Intercept}}{\text{Gradient}}$$

With a knowledge of the value of $C_{corr.}$ the true optical density of the solution, due to the presence of cupric species, can be easily ascertained. Hence the true cupric concentration was determinable for any time after the start of the reaction, since the initial cupric concentration was accurately known and the true initial optical density. An obeyance of Beer's law and the initial optical density and concentration was sufficient information to obtain the calibration constant (k') on each occasion. The true values of the cupric concentration at various times after the start of the reaction were then used to attempt to show that the rate of reaction was truly dependent upon cupric concentration.

The accurate determination of the dependence of the rate of reaction was obtained by plotting $\log_e [Cu^{2+}]$ against t., the time from the start of the reaction, since:

$$-\frac{d[Cu^{2+}]}{dt} = k_h [Cu^{2+}]$$

$$\log_e [Cu^{2+}] = -k_h t + A$$

Eq. 3.1.xiii

A being a constant.

Thus the gradient of such a plotted line would accurately determine the value of the rate constant k_h for the decaying section of the reduction.

Unfortunately, due to the existence of the initial accelerating portion of the reaction and the precipitation of solid product on some occasions, the analysis described cannot be used over the whole time range. An appropriate range between the end of the accelerating portion and precipitation was chosen and used by program Alfred.

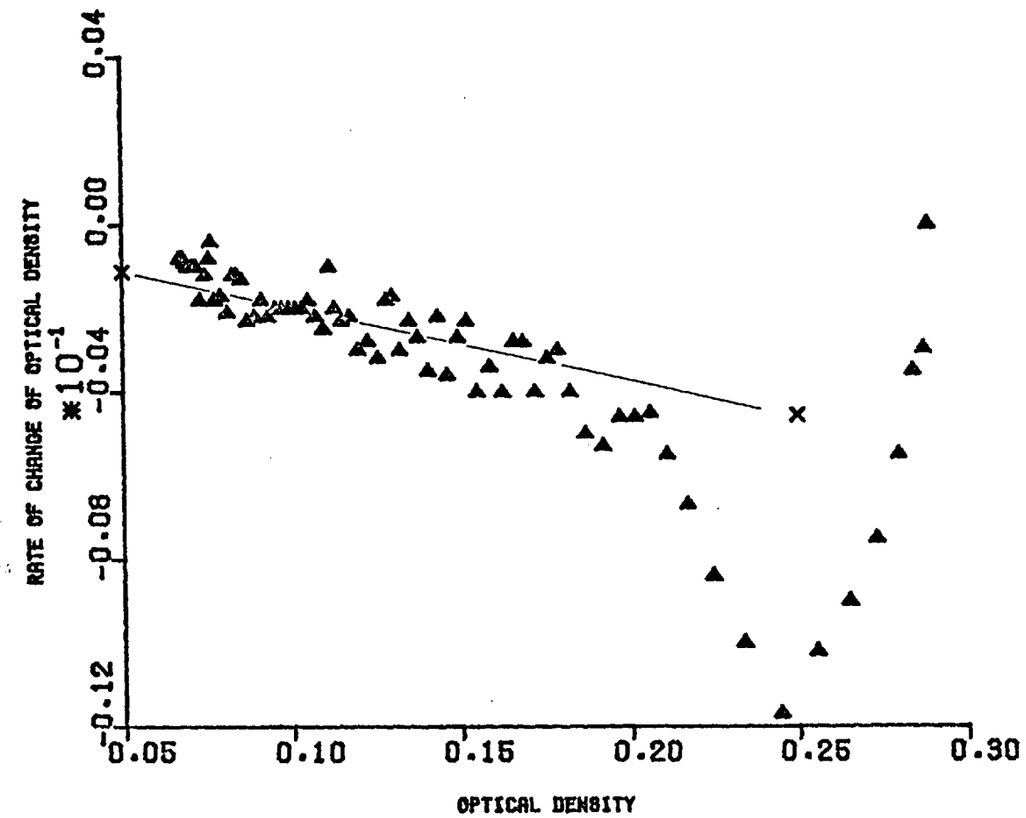
Program Alfred was also arranged to perform linear regressions on the data making up the two straight lines which were used in the analysis. (Eqs. 3.1.xvi. and 3.1.xiii) Hence, as an indication of the significance of

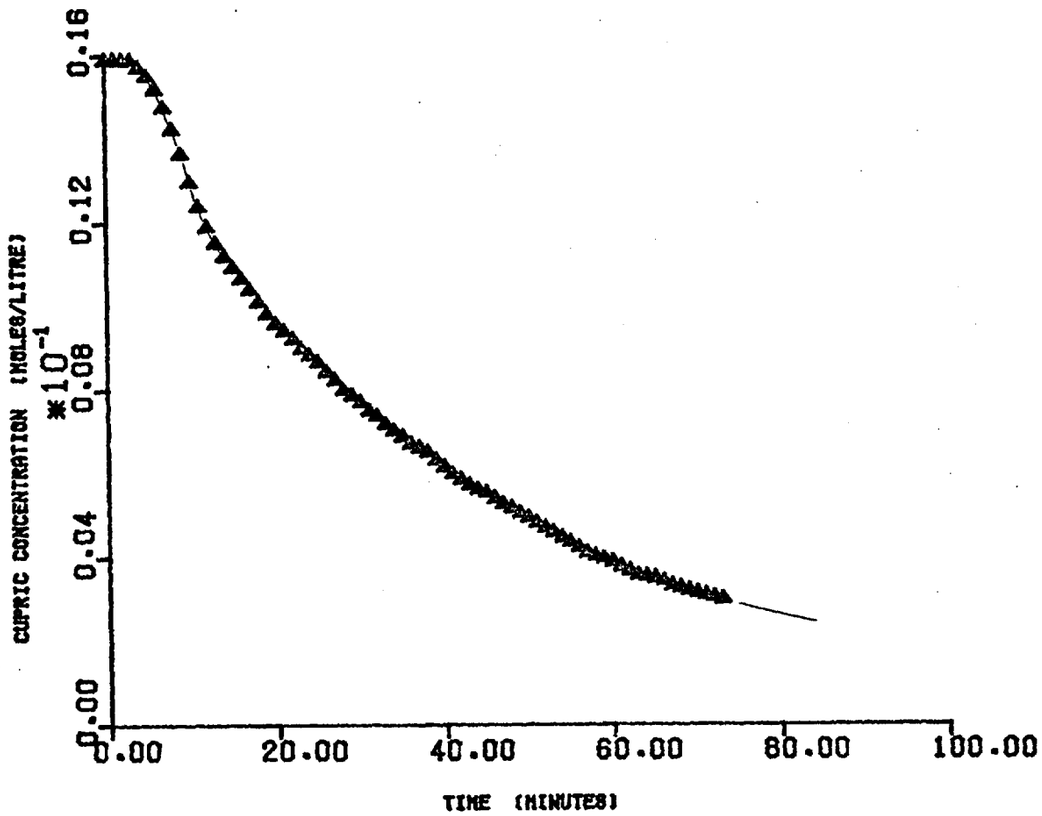
the rate constant determined and of the calibration constant, the values quoted for these pieces of information were accompanied by an error. These errors quoted, which are also calculated by program Alfred, are statistical values and are one standard deviation of the gradients of the lines through the population of points of which the points used were a sample.[33],[34]

The data used for each analysis by program Alfred is tabulated, in tables A.5.T.i. to A.5.T.xxxii., in the form of an array of apparent optical densities, headed 'Optical Density', at time intervals, in minutes, which is indicated at the head of each page of data. The number of points in the array, and the range of points over which the linear regressions were to be done are also tabulated at the top of each page.

Program Alfred also included plotting of the data used as described. The plotted results of the reduction of cupric acetate solutions are shown in Figures 3.1.viii to 3.1.xxxiii. The conditions under which the reactions were allowed to occur, together with the form of solid reaction product and the time after which precipitation occured, if at all, are also included in Figures 3.1.viii. to 3.1.xxxiii.

FIGURE 3.1.viii.





CONDITIONS OF REACTION :

Constant pressure controlled at : 670 p.s.i. ± 5.0 p.s.i. total
650 p.s.i. ± 5.0 p.s.i. hydrogen
Temperature : 110°C ± 1.0°C
Initial cupric concentration : 0.0159 molar
Total acetate concentration : 0.2418 molar

PRODUCT OF THE REDUCTION REACTION :

No insoluble reduced species were observed at the reaction conditions.
Cuprous oxide precipitated upon cooling to room temperature.

RATE CONSTANT :

The rate constant was found to be :

$$k_h = 0.022126 \pm 0.00018$$

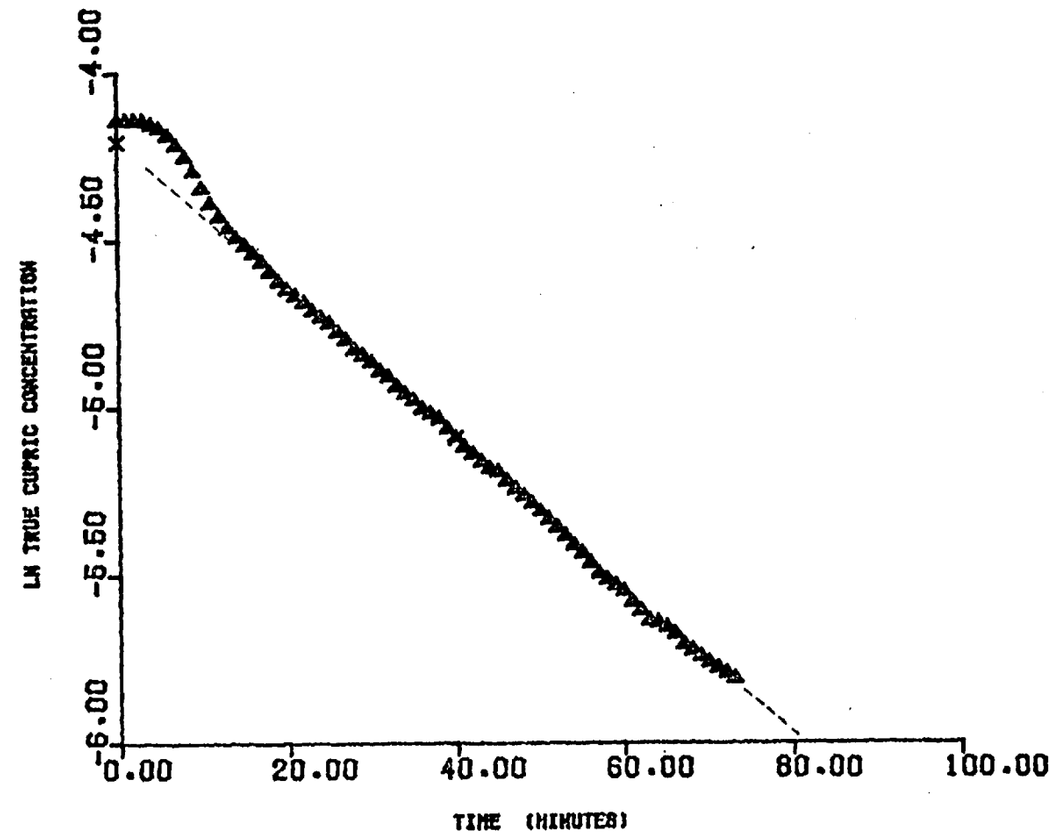
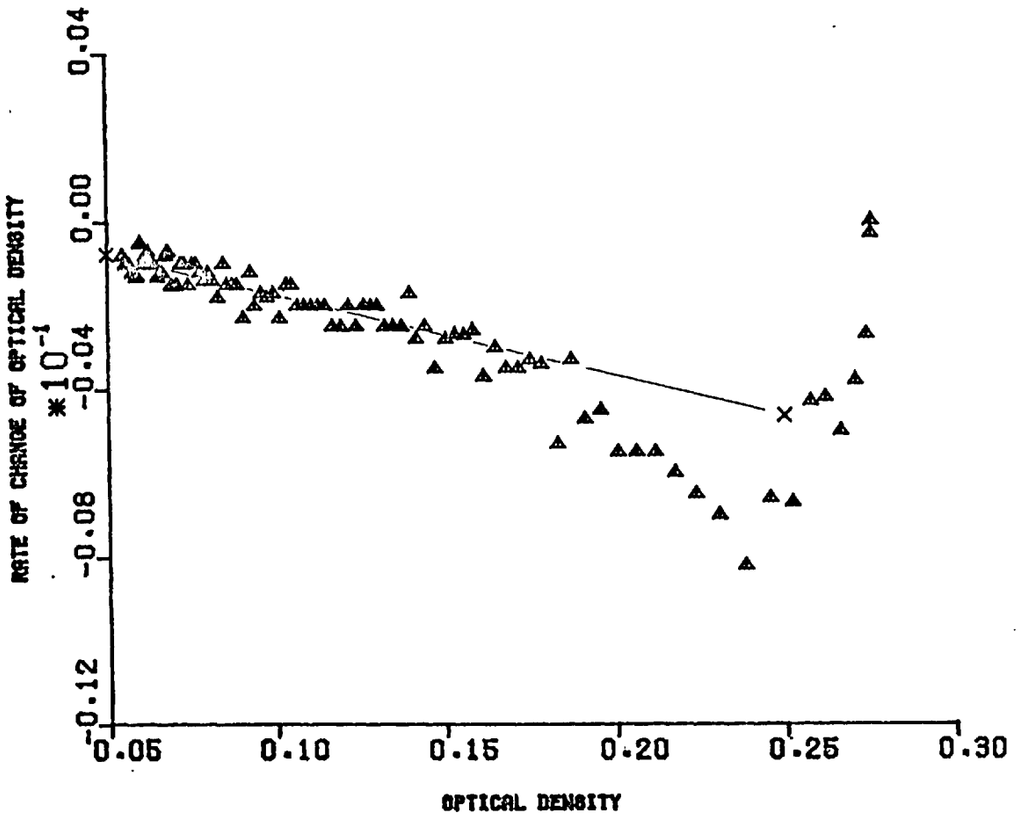
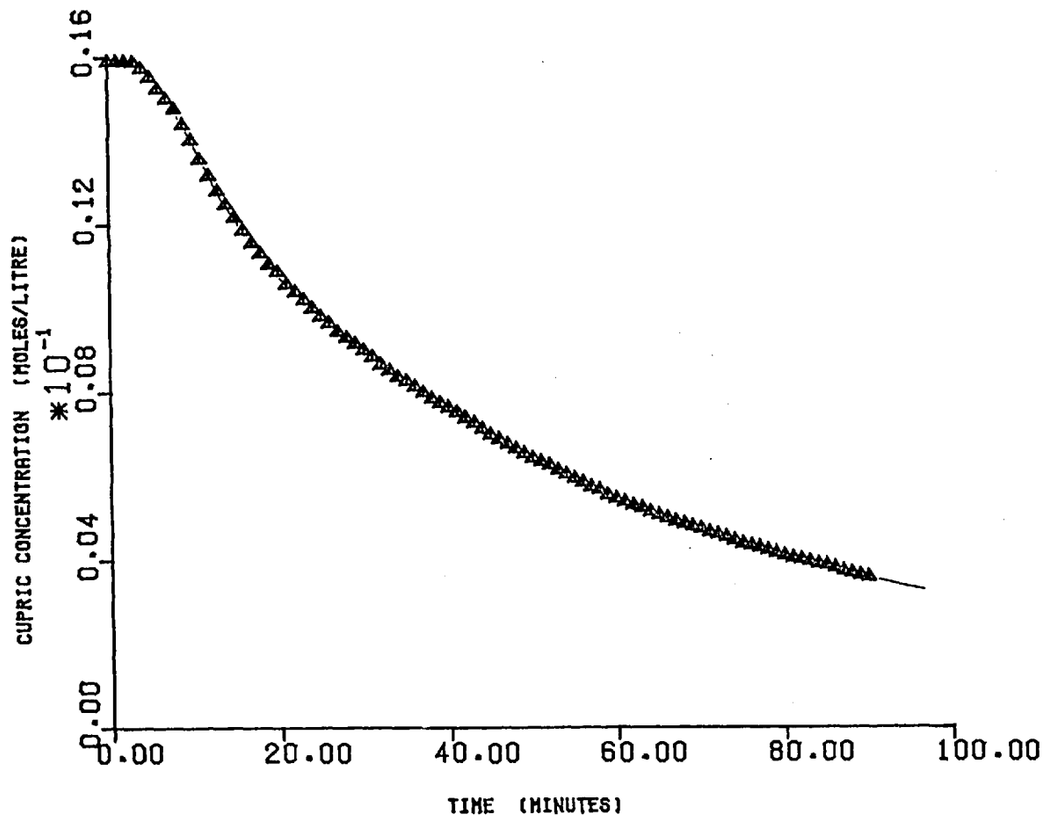


FIGURE 3.1.ix.





CONDITIONS OF REACTION :

Constant pressure controlled at : 670 p.s.i. ± 5.0 p.s.i. total
650 p.s.i. ± 5.0 p.s.i. hydrogen

Temperature : 110°C ± 1.0°C

Initial cupric concentration : 0.0159 molar

Total acetate concentration : 0.2418 molar

PRODUCT OF THE REDUCTION REACTION :

No insoluble reduced species were observed at the reaction conditions.
Cuprous oxide precipitated upon cooling to room temperature.

RATE CONSTANT :

The rate constant was found to be :

$$k_h = 0.015729 \pm 0.00008$$

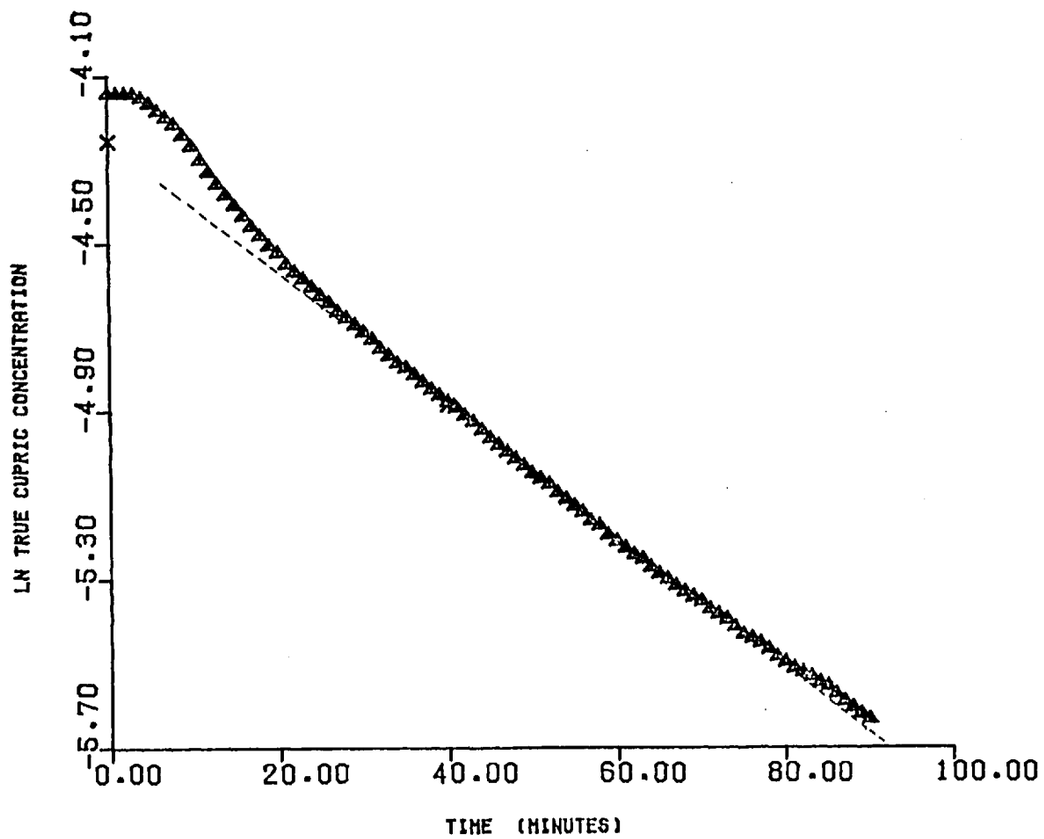
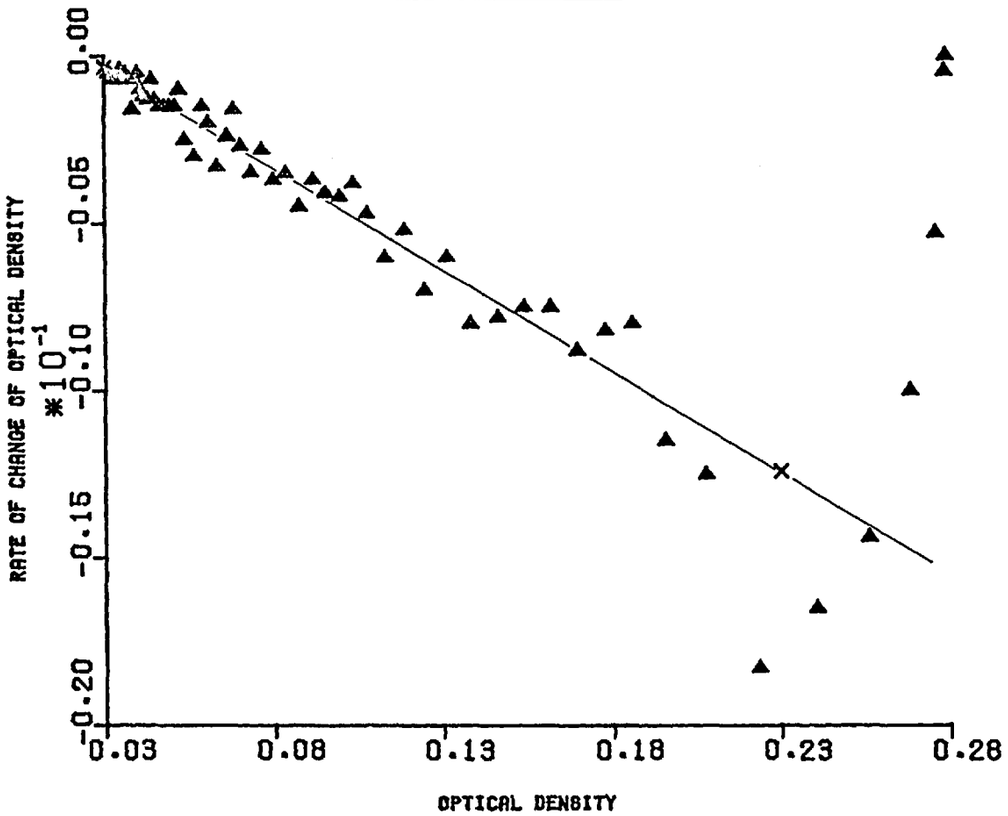
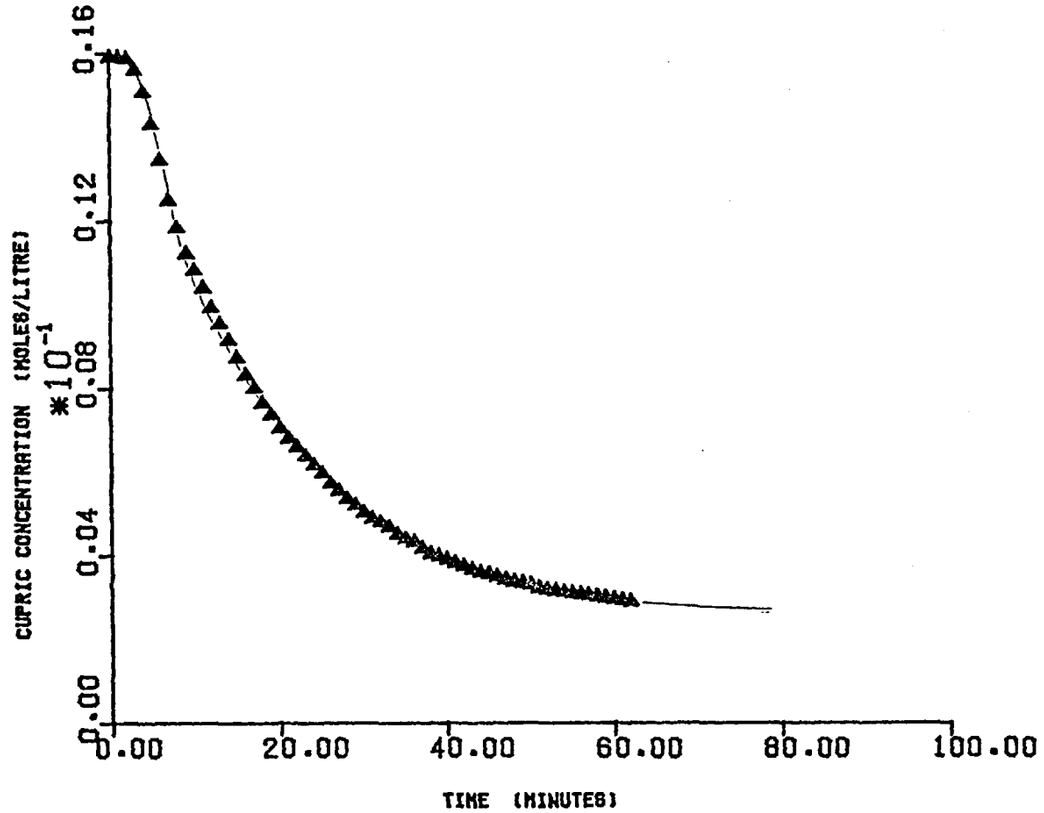


FIGURE 3.1.x.





CONDITIONS OF REACTION :

Constant pressure controlled at : 680 p.s.i. ± 5.0 p.s.i. total
650 p.s.i. ± 5.0 p.s.i. hydrogen
Temperature : 120°C ± 1.0°C
Initial cupric concentration : 0.0159 molar
Total acetate concentration : 0.2418 molar

PRODUCT OF THE REDUCTION REACTION :

No insoluble reduced species were observed at the reaction conditions.
Cuprous oxide precipitated upon cooling to room temperature.

RATE CONSTANT :

The rate constant was found to be :

$$k_h = 0.036187 \pm 0.000611$$

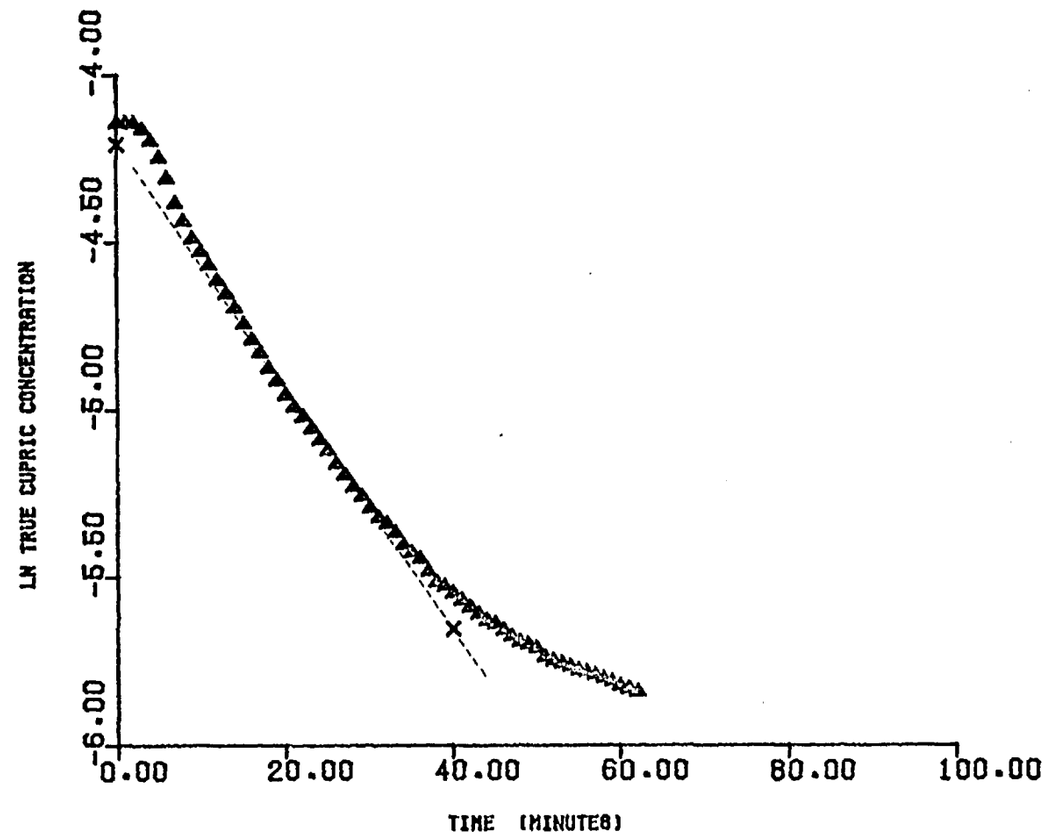
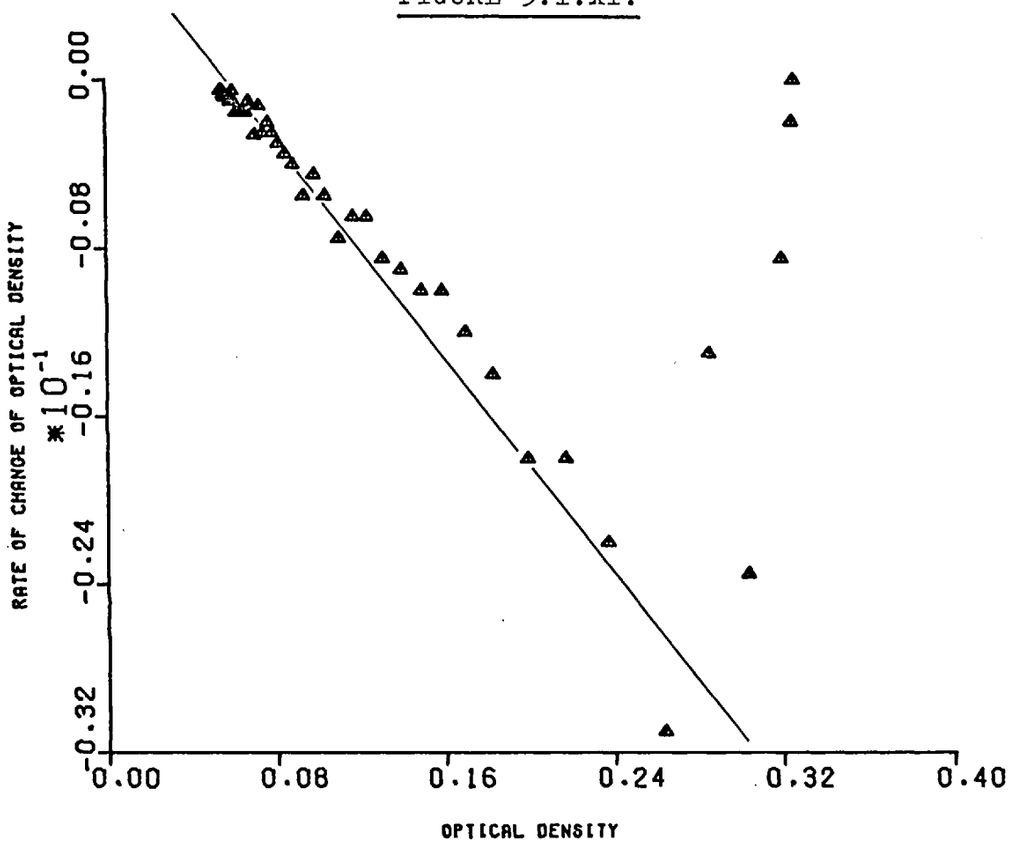
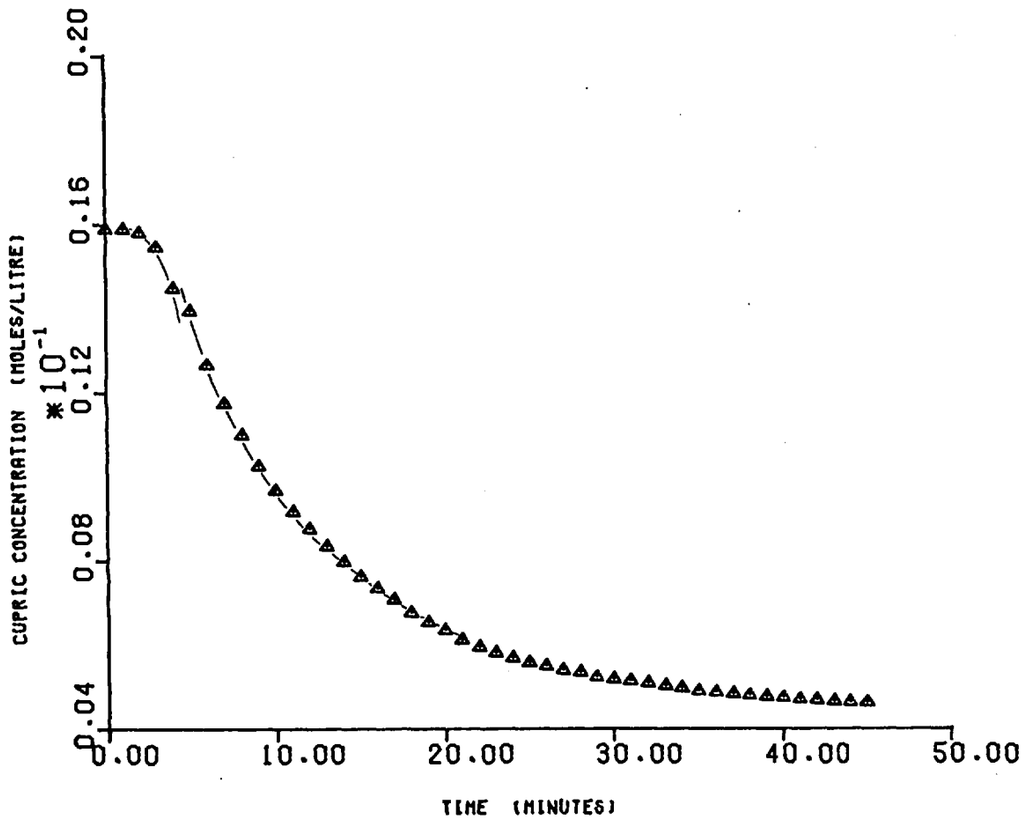


FIGURE 3.1.xi.





CONDITIONS OF REACTION :

Constant pressure controlled at : 690 p.s.i. ± 5.0 p.s.i. total
650 p.s.i. ± 5.0 p.s.i. hydrogen

Temperature : 130°C ± 1.0°C

Initial cupric concentration : 0.0159 molar

Total acetate concentration : 0.2418 molar

PRODUCT OF THE REDUCTION REACTION :

No insoluble reduced species were observed at the reaction conditions.
Cuprous oxide precipitated upon cooling to room temperature.

RATE CONSTANT :

The rate constant was found to be :

$$k_h = 0.021177 \pm 0.001226$$

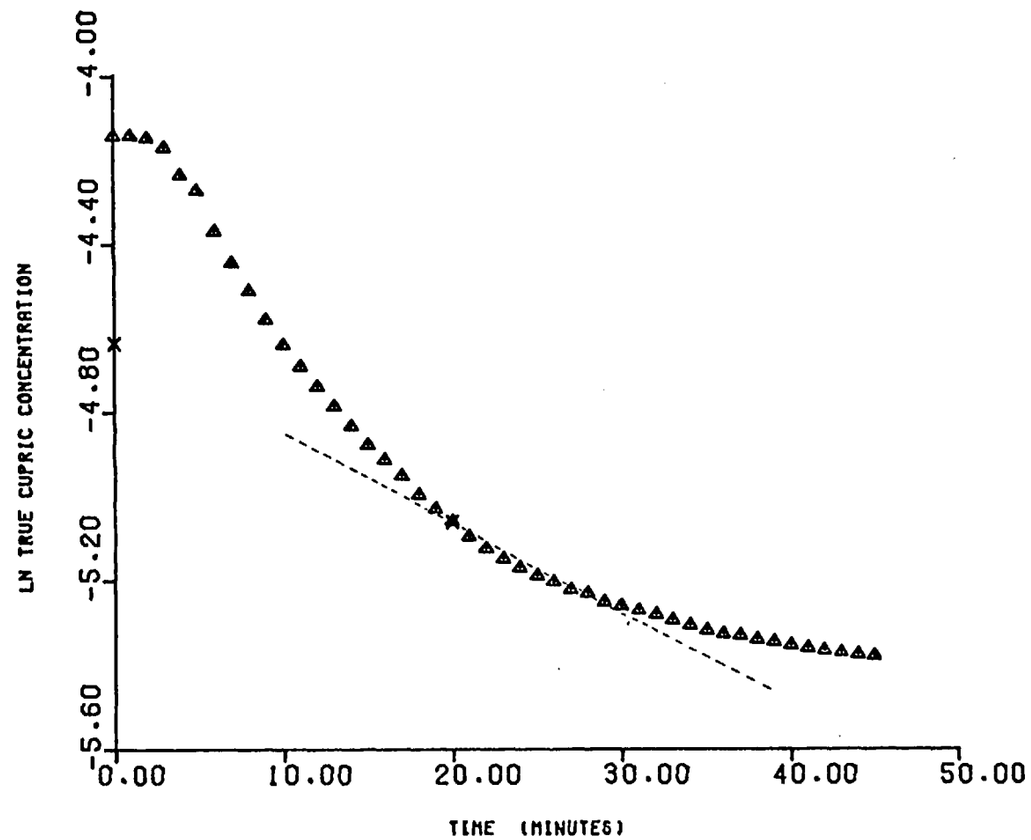
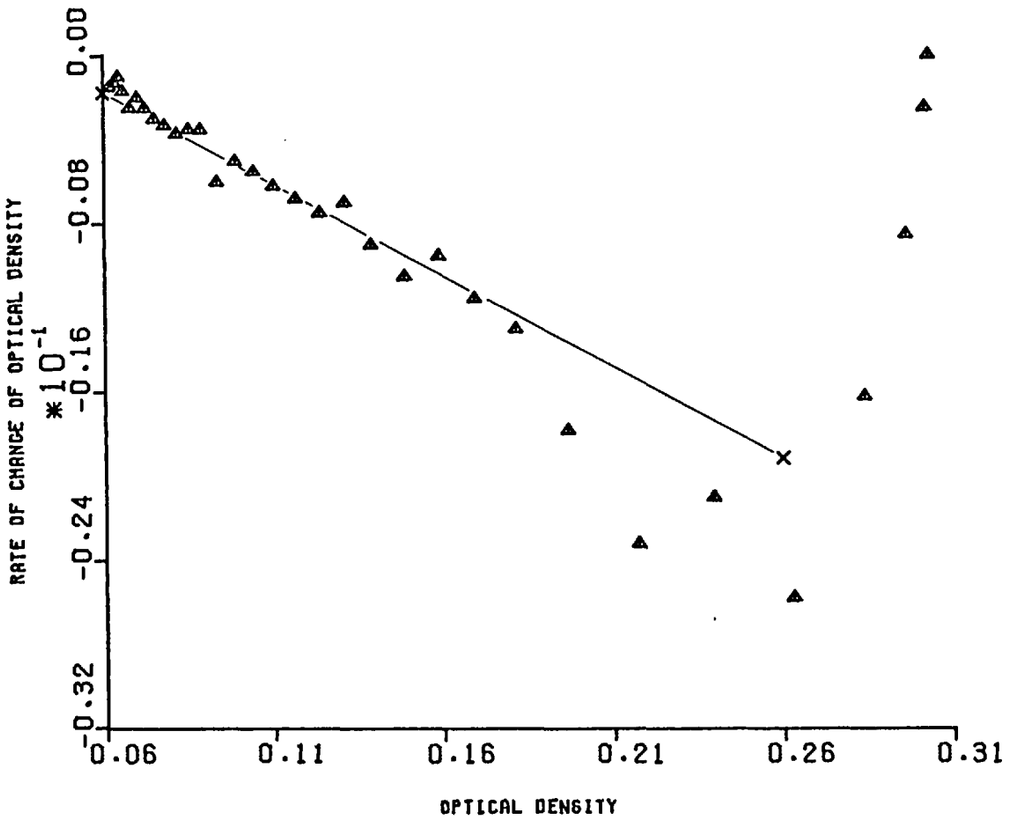
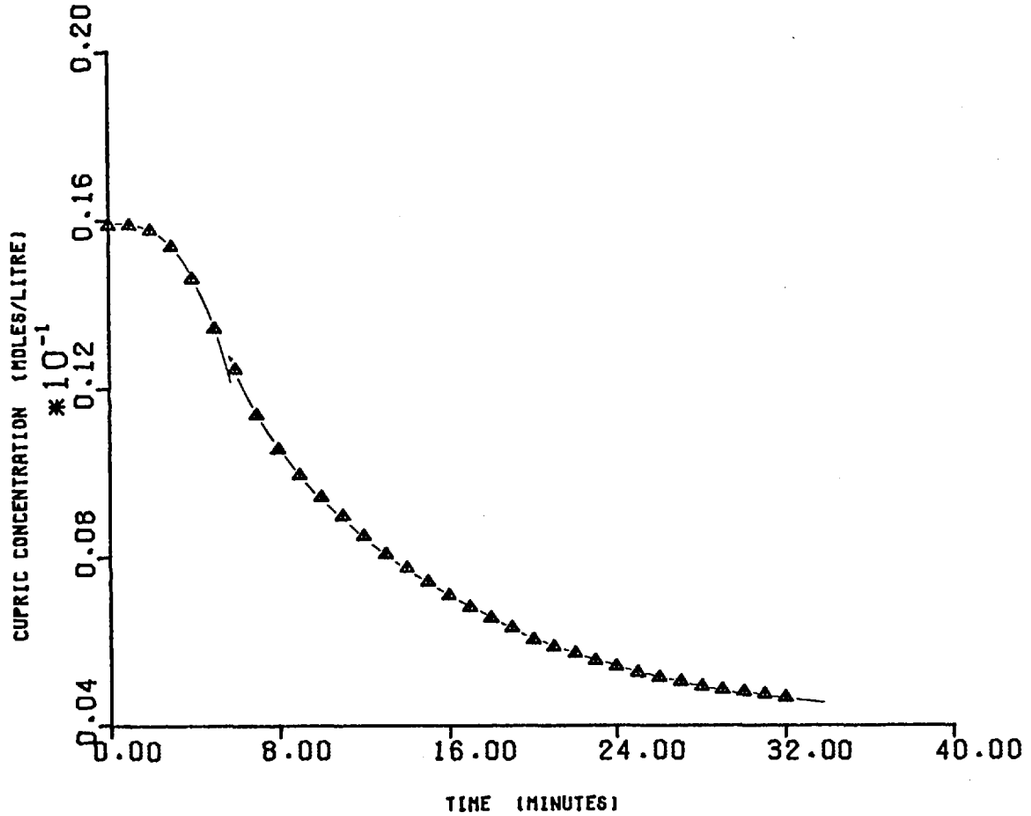


FIGURE 3.1.xii.





CONDITIONS OF REACTION :

Constant pressure controlled at : 690 p.s.i. ± 5.0 p.s.i. total
650 p.s.i. ± 5.0 p.s.i. hydrogen

Temperature : 130°C ± i.0°C

Initial cupric concentration : 0.0159 molar

Total acetate concentration : 0.2418 molar

PRODUCT OF THE REDUCTION REACTION :

No insolube reduced species were observed at the reaction conditions.
Cuprous oxide precipitated upon cooling to room temperature.

RATE CONSTANT :

The rate constant was found to be :

$$k_h = 0.042025 \pm 0.000966$$

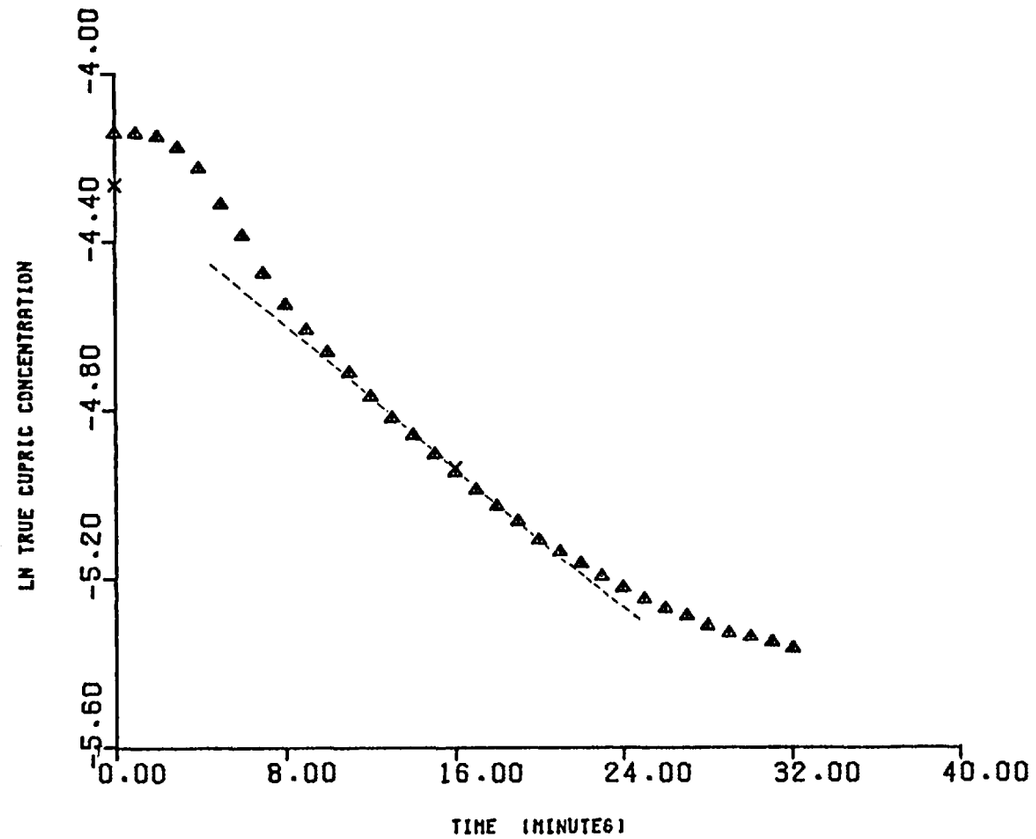
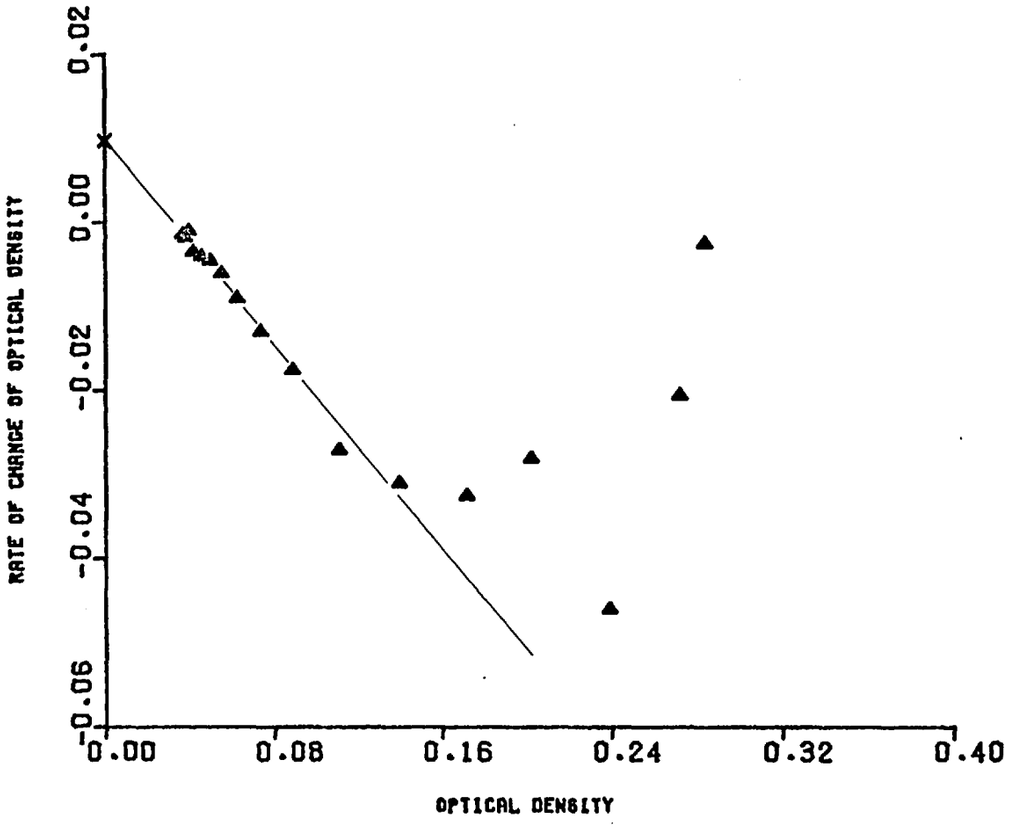
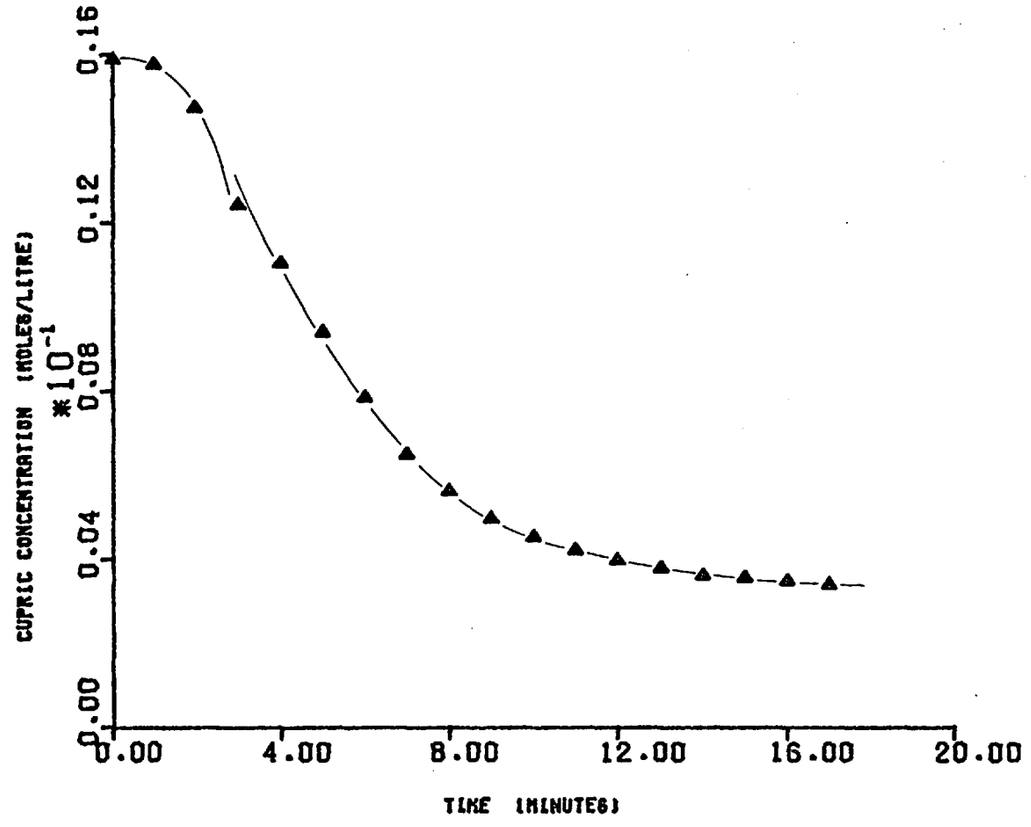


FIGURE 3.1.xiii.





CONDITIONS OF REACTION :

Constant pressure controlled at : 700 p.s.i. ± 5.0 p.s.i. total
650 p.s.i. ± 5.0 p.s.i. hydrogen
Temperature : 140°C ± 1.0°C
Initial cupric concentration : 0.0159 molar
Total acetate concentration : 0.2418 molar

PRODUCT OF THE REDUCTION REACTION :

No insoluble species were observed at the reaction conditions.
Cuprous oxide precipitated upon cooling to room temperature.

RATE CONSTANT :

The rate constant was found to be :

$$k_h = 0.14827 \pm 0.00916$$

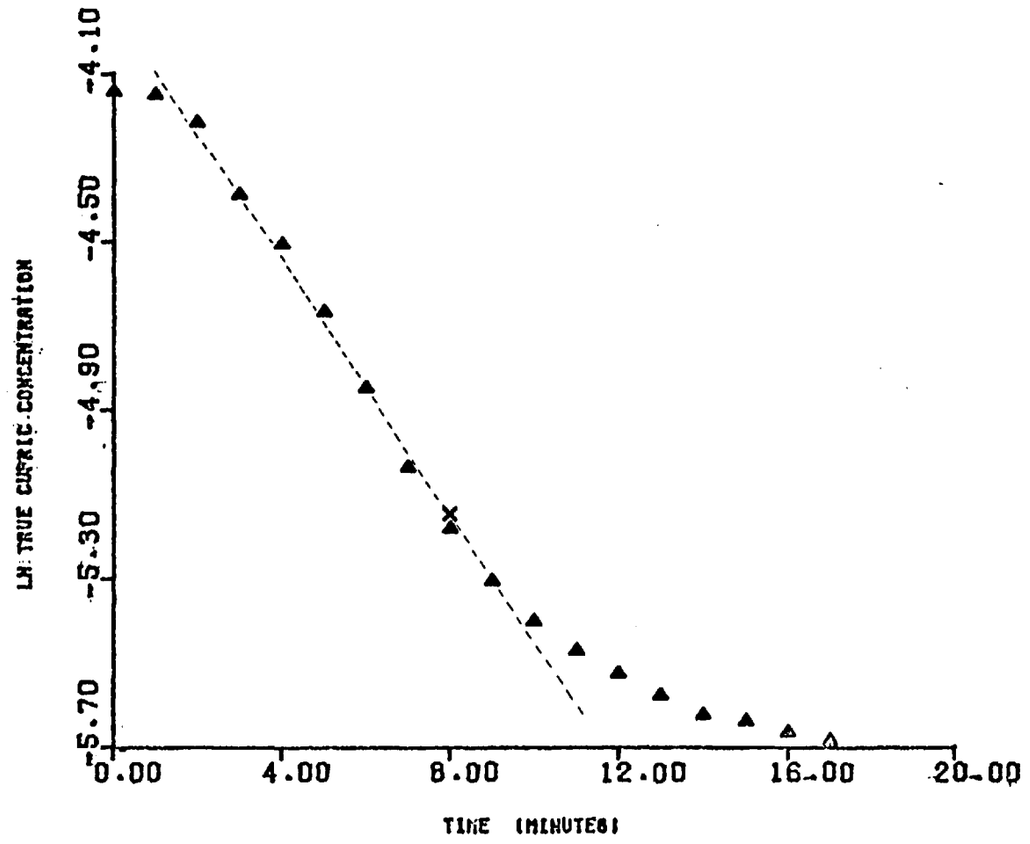
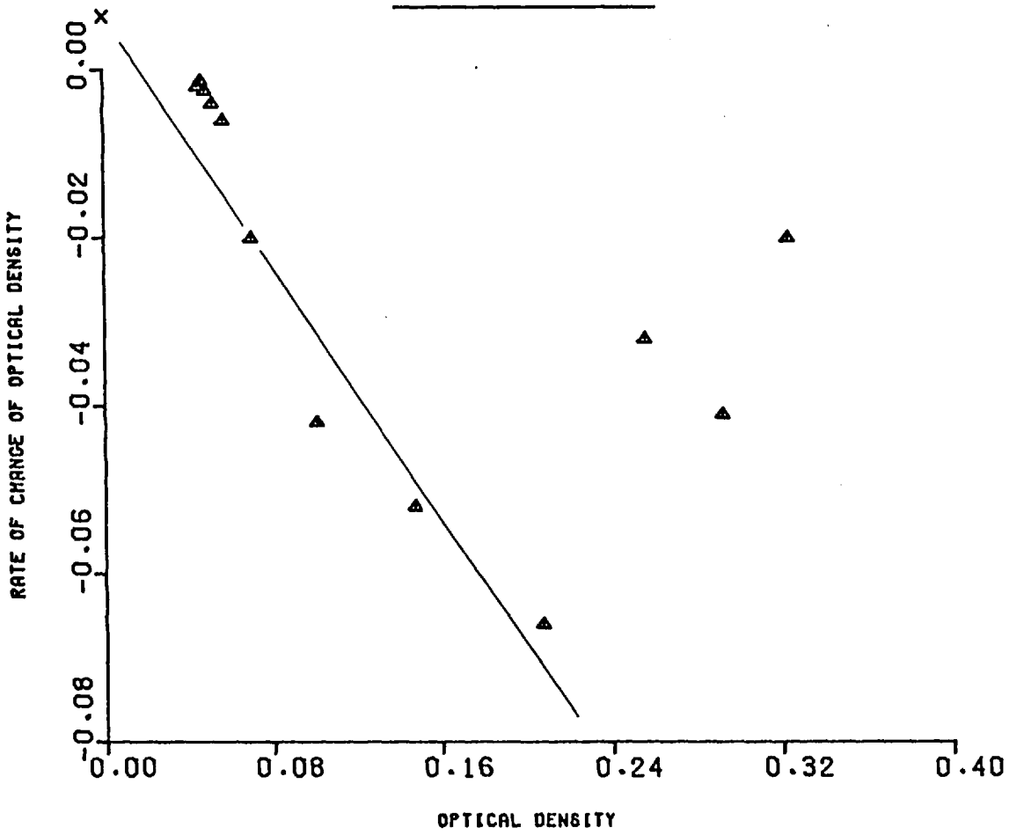
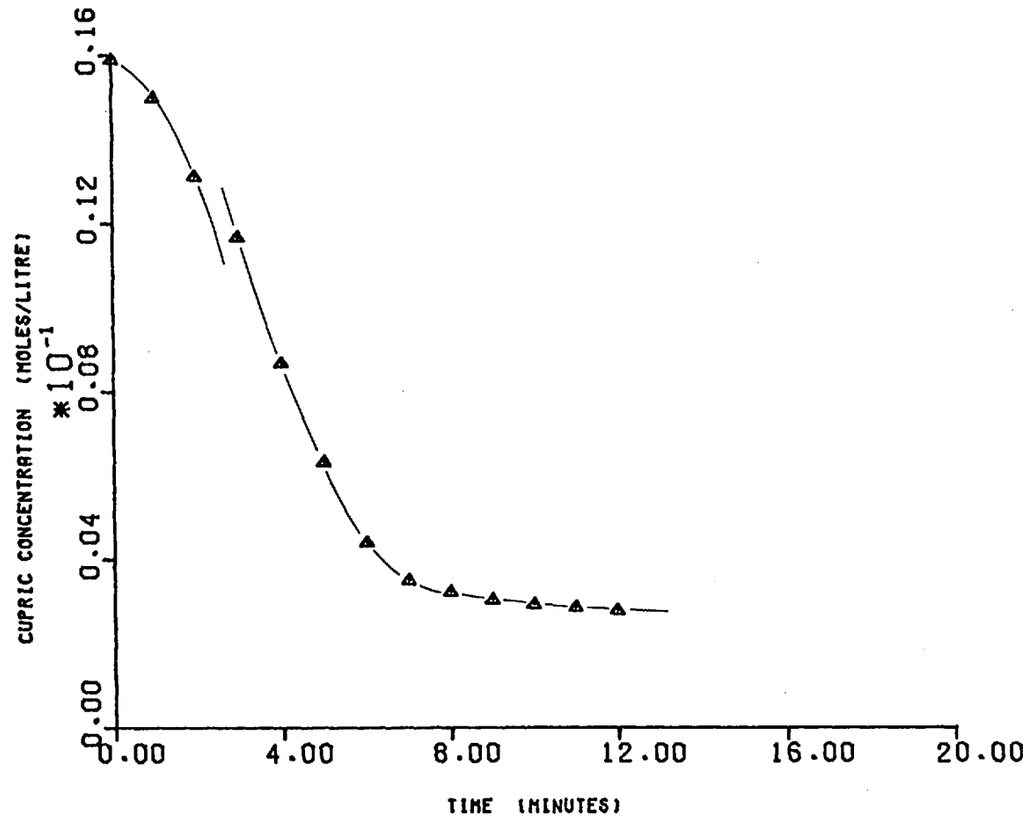


FIGURE 3.1.xiv.





CONDITIONS OF REACTION :

Constant pressure controlled at : 720 p.s.i. ± 5.0 p.s.i. total
650 p.s.i. ± 5.0 p.s.i. hydrogen
Temperature : 150°C ± 1.0°C
Initial cupric concentration : 0.0159 molar
Total acetate concentration : 0.2418 molar

PRODUCT OF THE REDUCTION REACTION :

No insoluble reduced species were observed at the reaction conditions.
Cuprous oxide precipitated upon cooling to room temperature.

RATE CONSTANT :

The rate constant was found to be :

$$k_h = 0.308596 \pm 0.010564$$

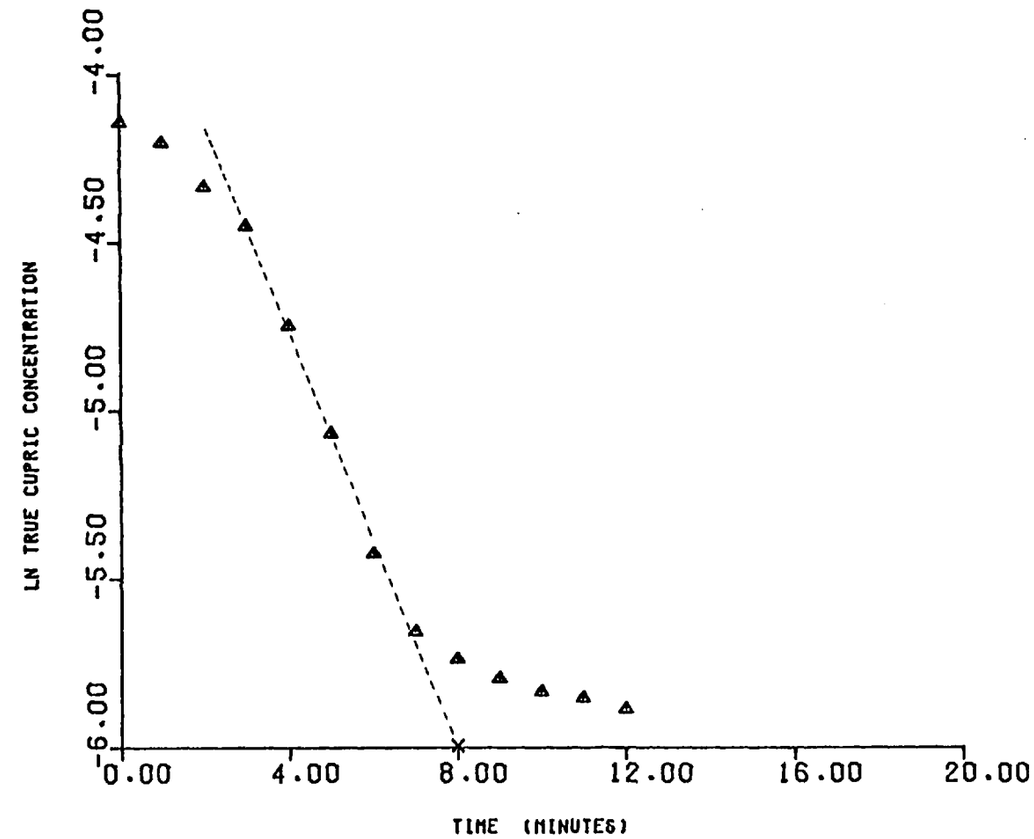
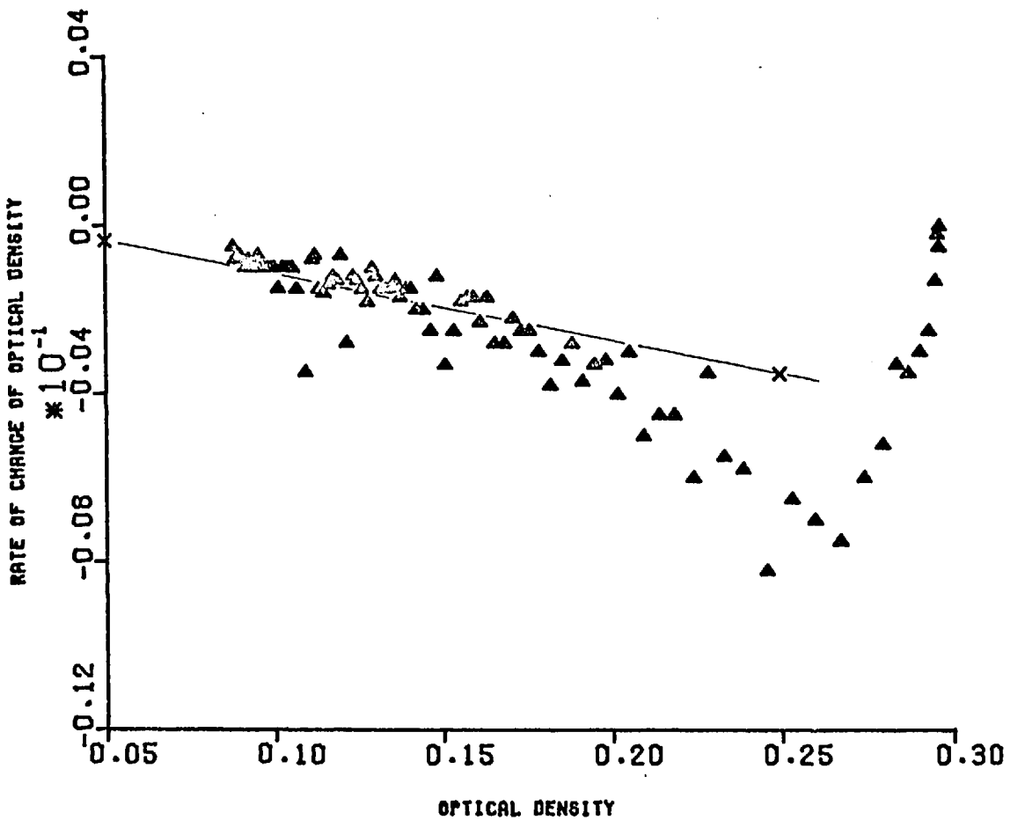
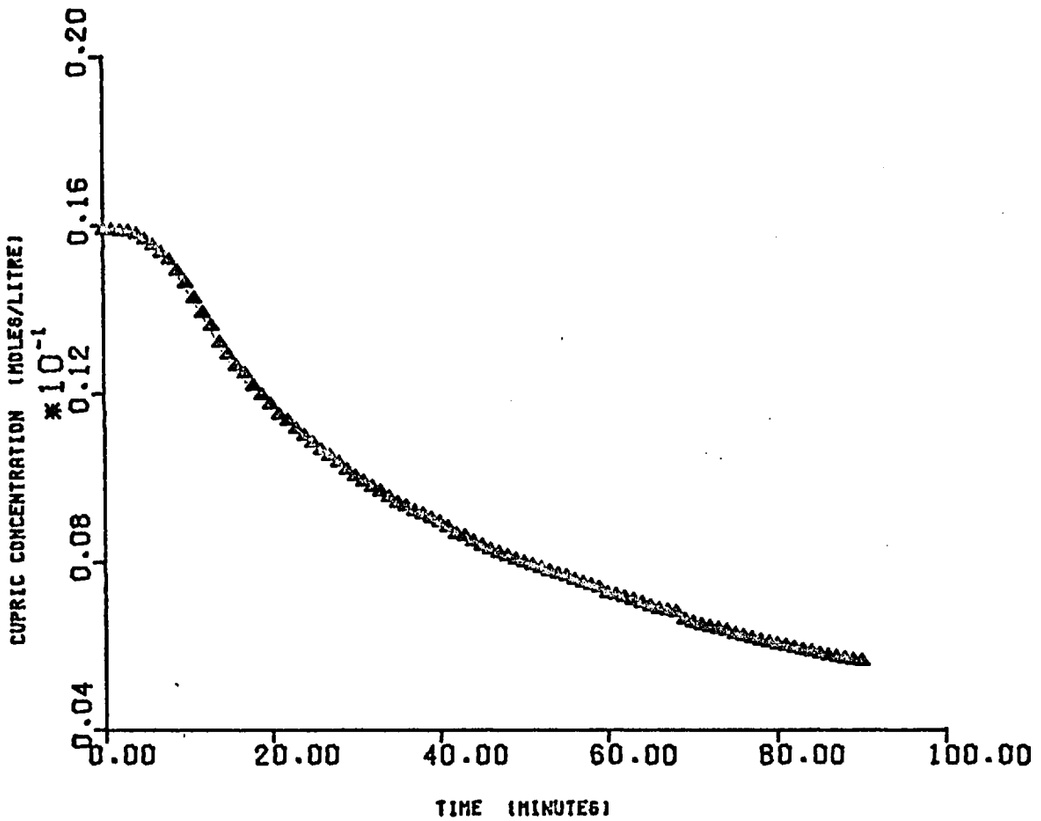


FIGURE 3.1.xv.





CONDITIONS OF REACTION :

Constant pressure controlled at : 520 p.s.i. ± 5.0 p.s.i. total
500 p.s.i. ± 5.0 p.s.i. hydrogen
Temperature : 110°C ± 1.0°C
Initial cupric concentration : 0.0159 molar
Total acetate concentration : 0.2418 molar

PRODUCT OF THE REDUCTION REACTION :

No insoluble reduced species were observed at the reaction conditions.
Cuprous oxide precipitated upon cooling to room temperature.

RATE CONSTANT :

The rate constant was found to be :

$$k_h = 0.0097483 \pm .0000748$$

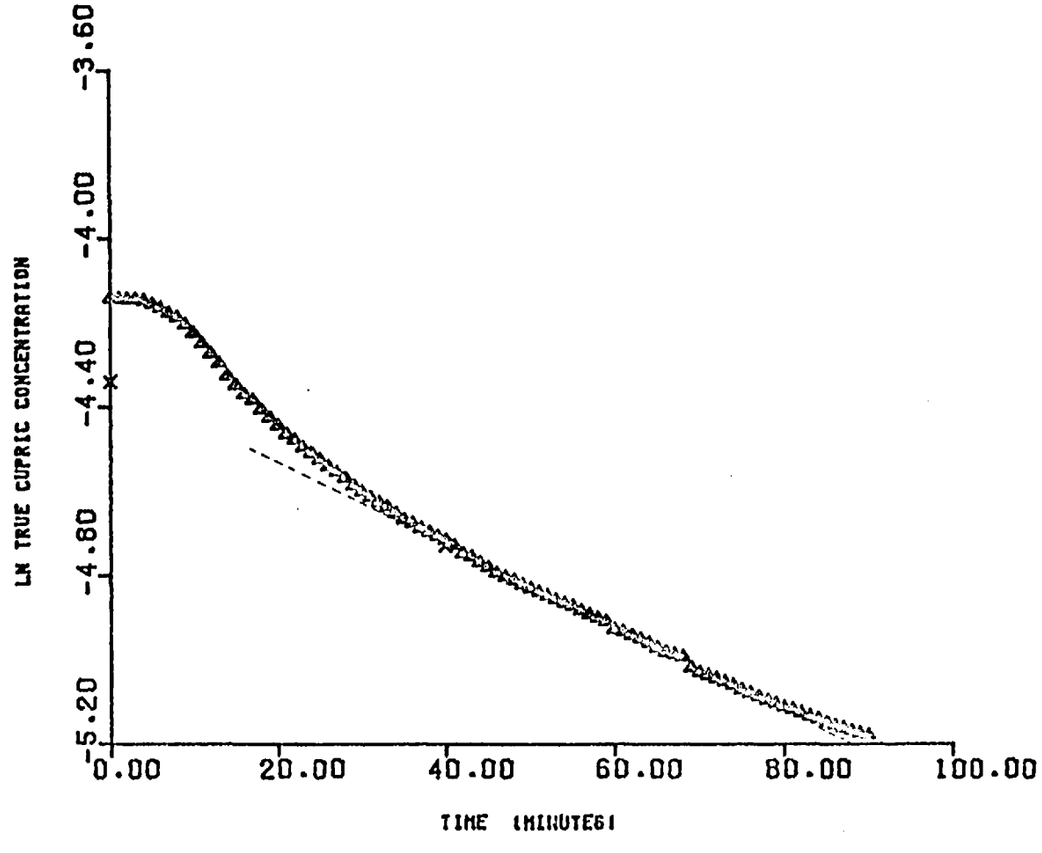
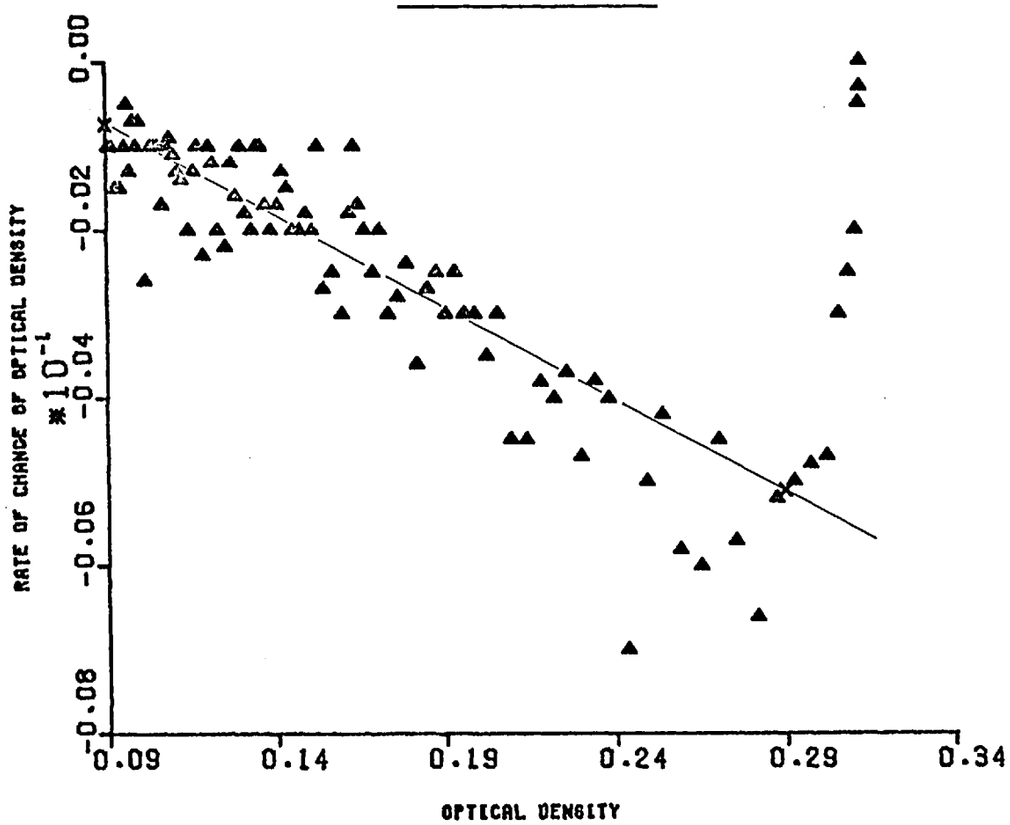
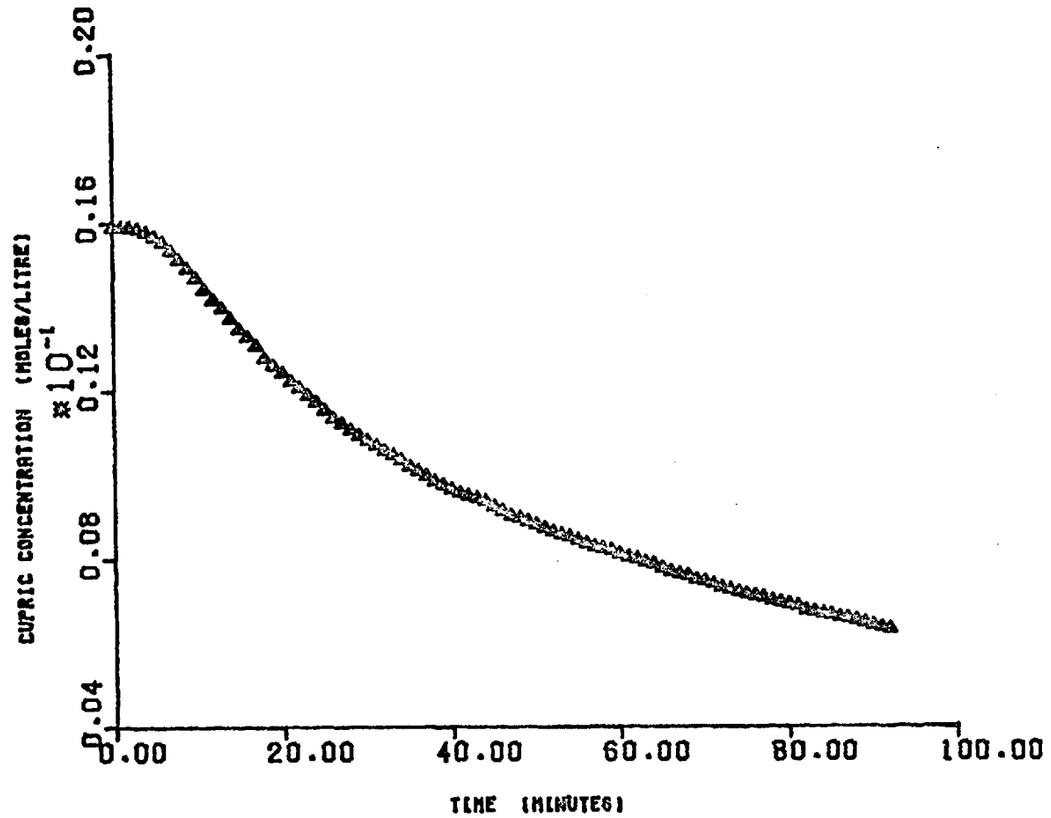


FIGURE 3.1.xvi.





CONDITIONS OF REACTION :

Constant pressure controlled at : 530 p.s.i. ± 5.0 p.s.i. total
500 p.s.i. ± 5.0 p.s.i. hydrogen

Temperature : 120°C ± 1.0°C

Initial cupric concentration : 0.0159 molar

Total acetate concentration : 0.2418 molar

PRODUCT OF THE REDUCTION REACTION :

No insoluble reduced species were observed at the reaction conditions.
Cuprous oxide precipitated upon cooling to room temperature.

RATE CONSTANT :

The rate constant was found to be :

$$k_h = 0.009077 \pm 0.000089$$

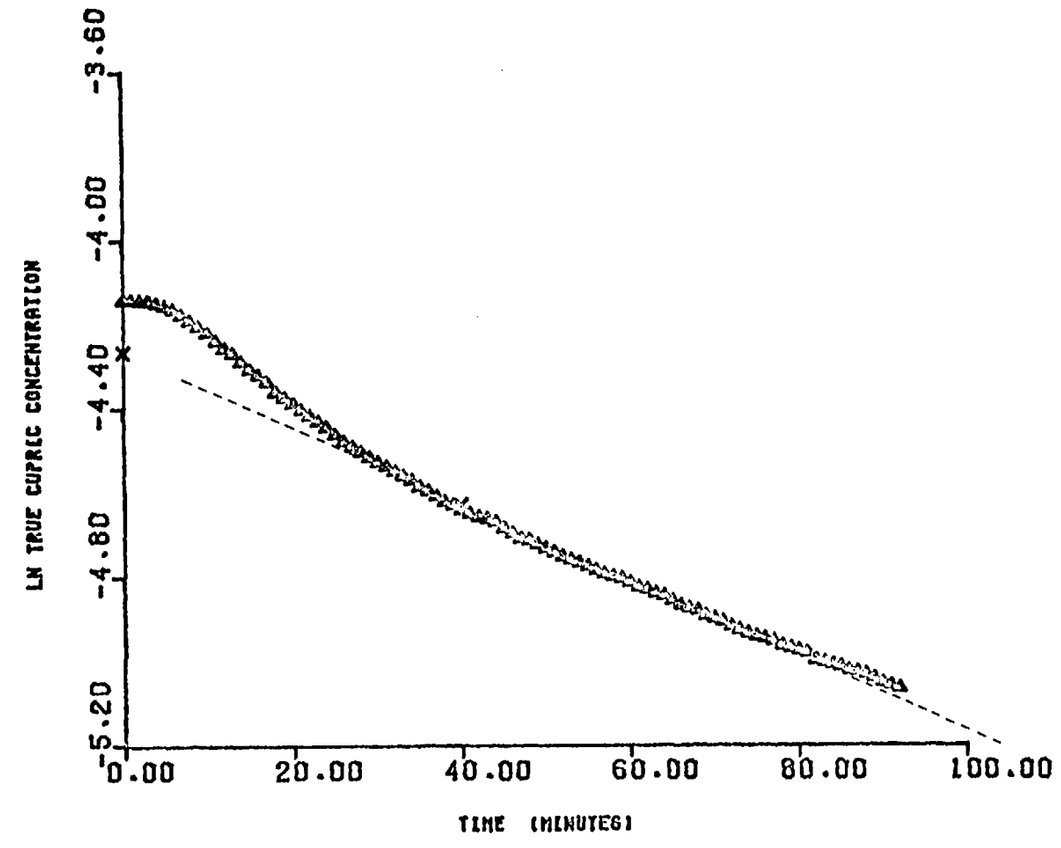
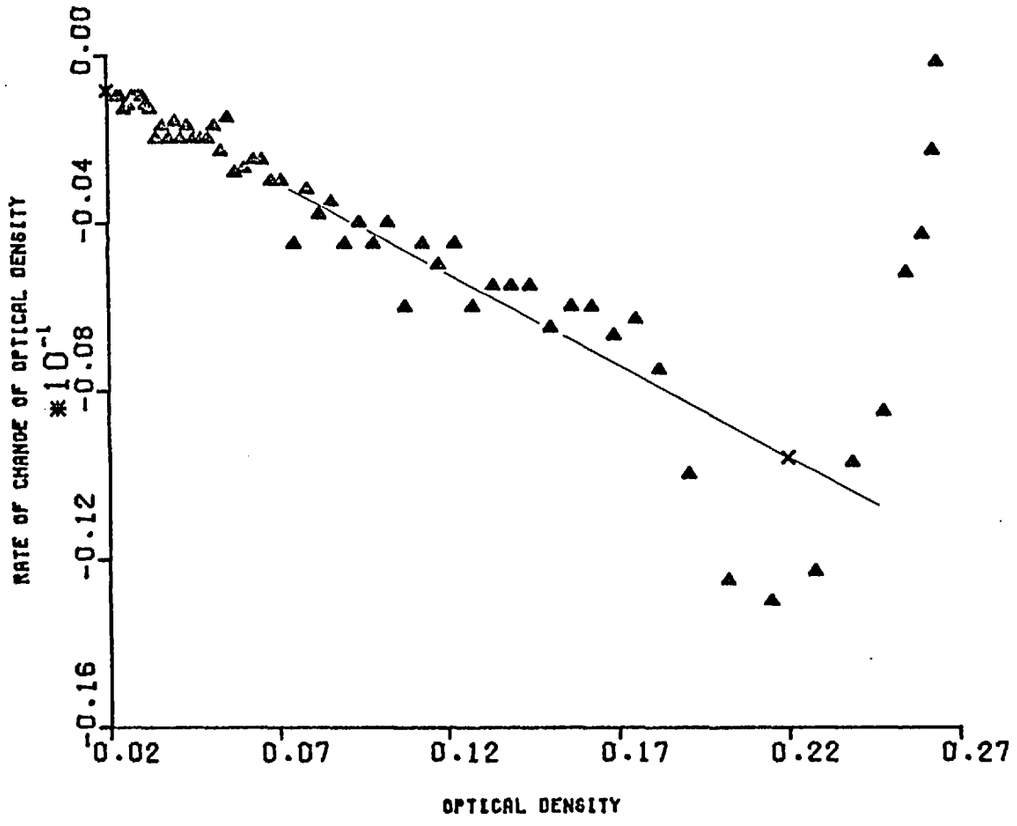
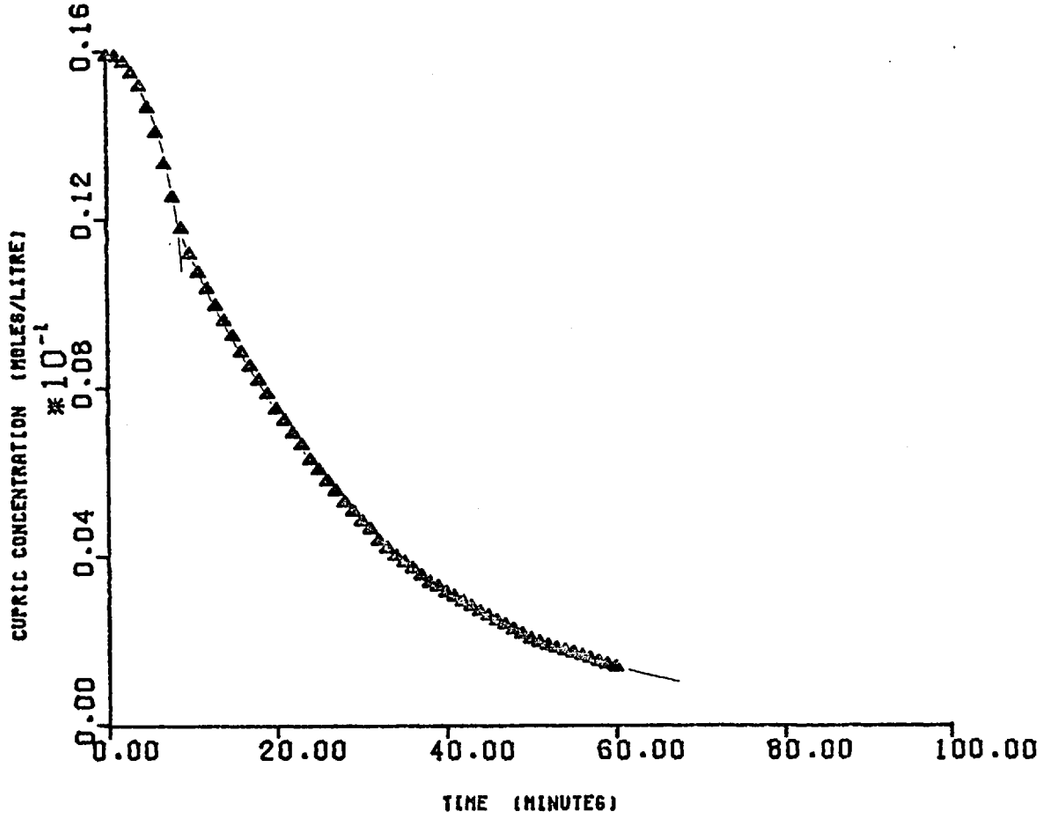


FIGURE 3.1.xvii.





CONDITIONS OF REACTION :

Constant pressure controlled at : 540 p.s.i. ± 5.0 p.s.i. total
500 p.s.i. ± 5.0 p.s.i. hydrogen

Temperature : 130°C ± 1.0°C

Initial cupric concentration : 0.0159 molar

Total acetate concentration : 0.2418 molar

PRODUCT OF THE REDUCTION REACTION :

No insoluble reduced species were observed at the reaction conditions.
Cuprous oxide precipitated upon cooling to room temperature.

RATE CONSTANT :

The rate constant was found to be :

$$k_h = 0.041875 \pm 0.000302$$

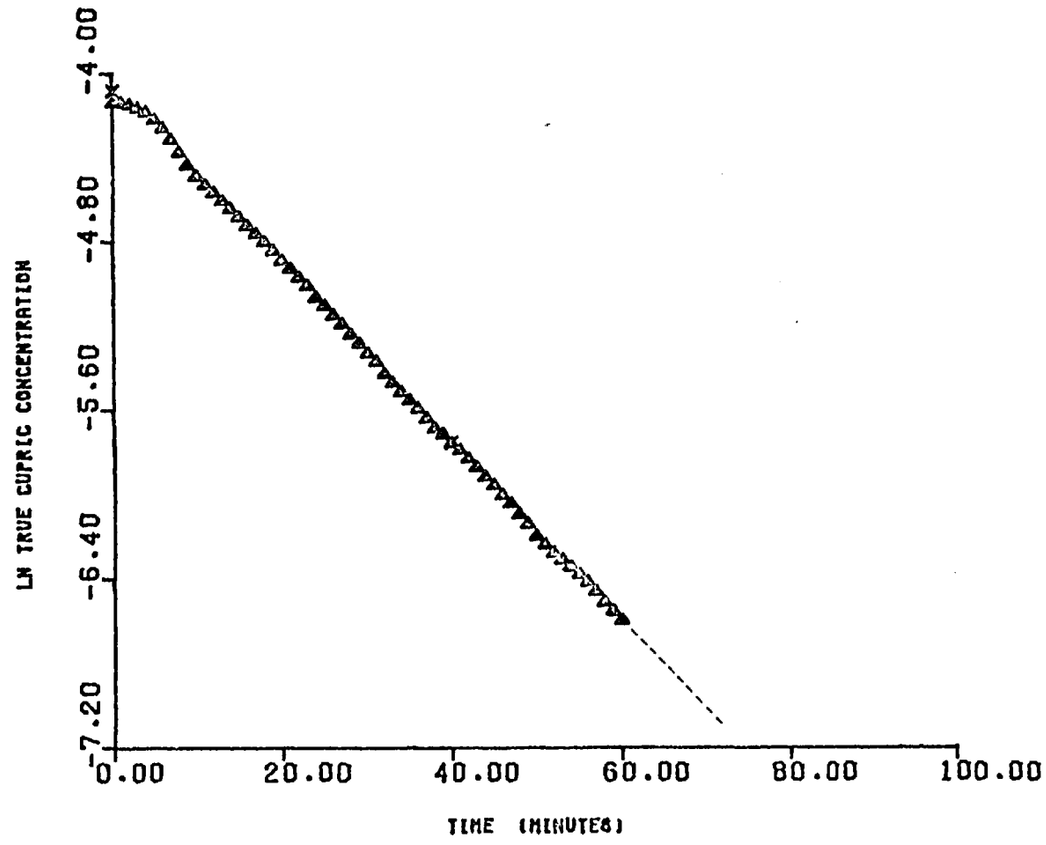
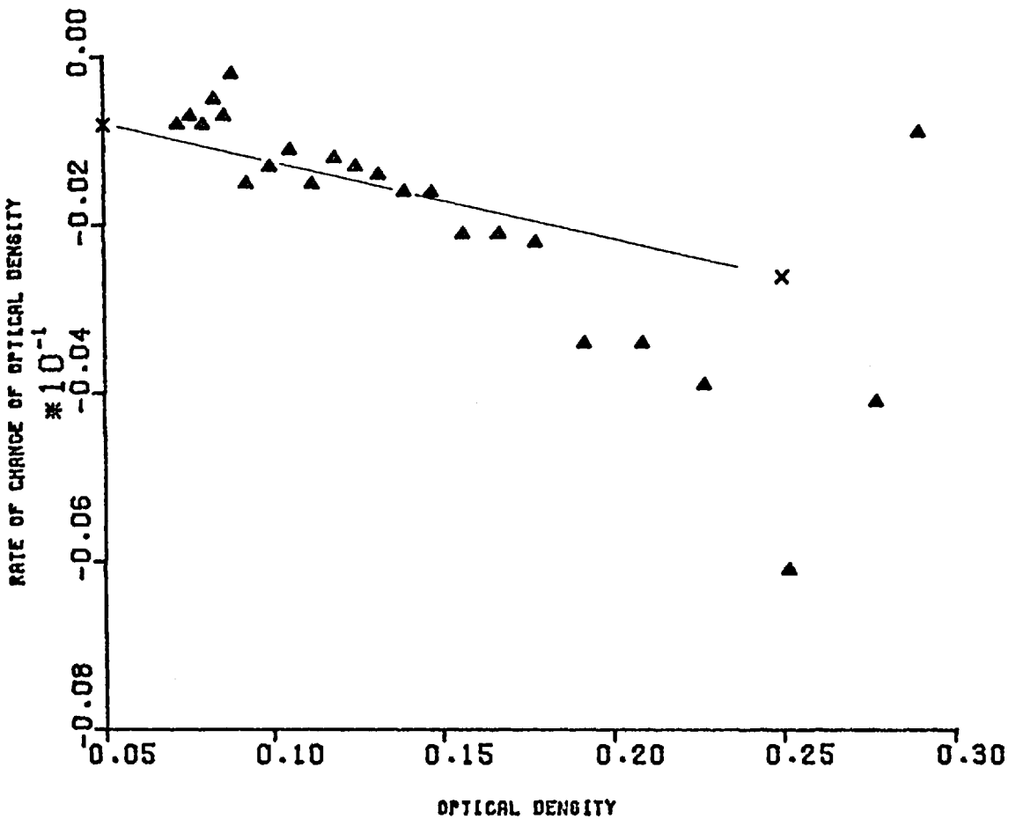
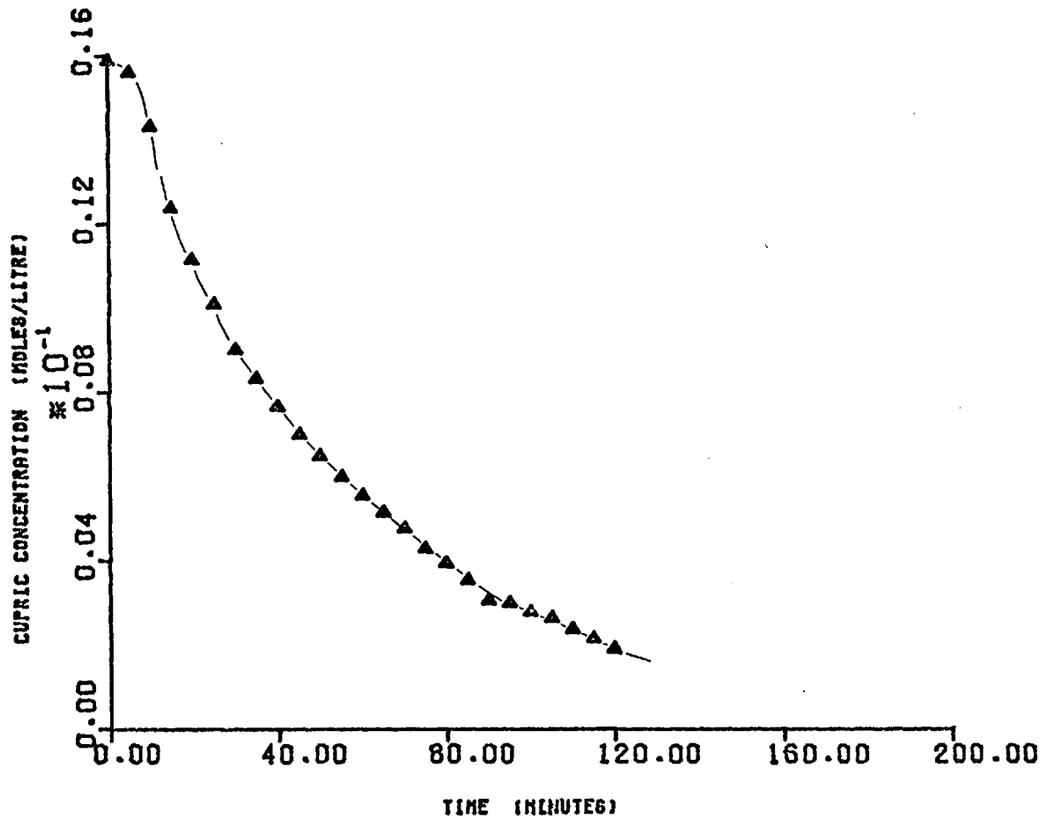


FIGURE 3.1.xviii.





CONDITIONS OF REACTION :

Constant pressure controlled at : 420 p.s.i. ± 5.0 p.s.i. total
400 p.s.i. ± 5.0 p.s.i. hydrogen
Temperature : 110°C ± 1.0°C
Initial cupric concentration : 0.0159 molar
Total acetate concentration : 0.2418 molar

PRODUCT OF THE REDUCTION REACTION :

No insoluble reduced species were observed at the reaction conditions.
Cuprous oxide precipitated upon cooling to room temperature.

RATE CONSTANT :

The rate constant was found to be :

$$k_h = 0.016767 \pm 0.000308$$

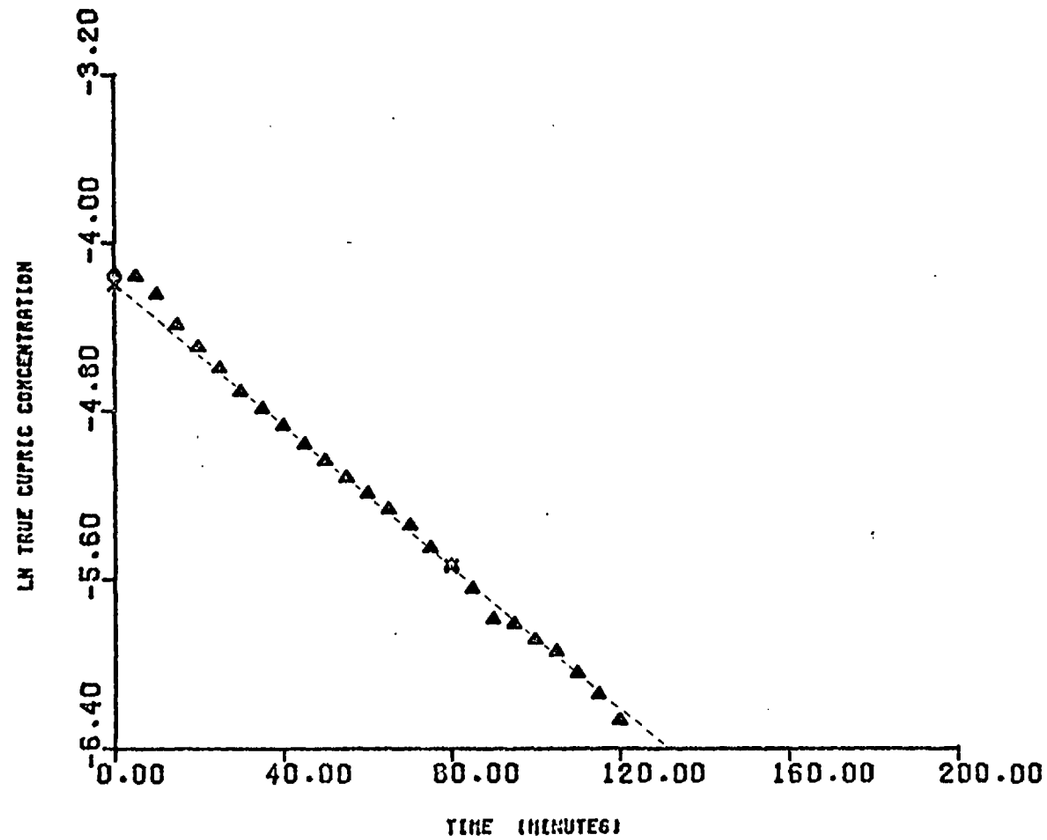
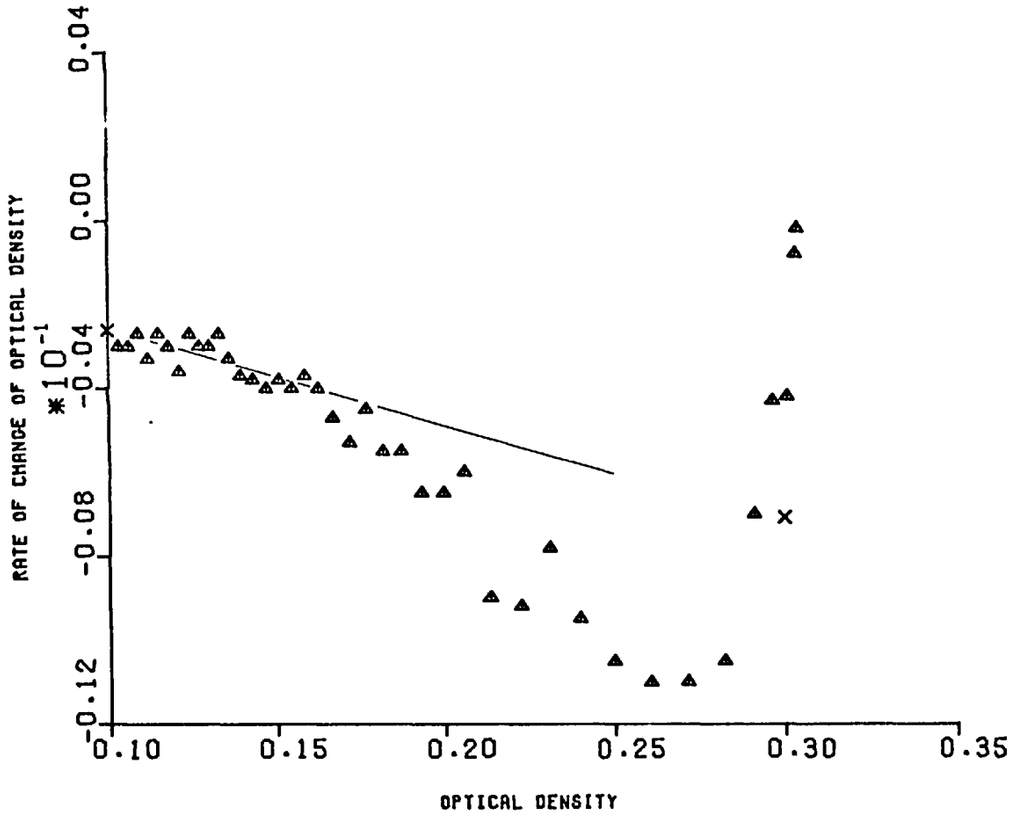
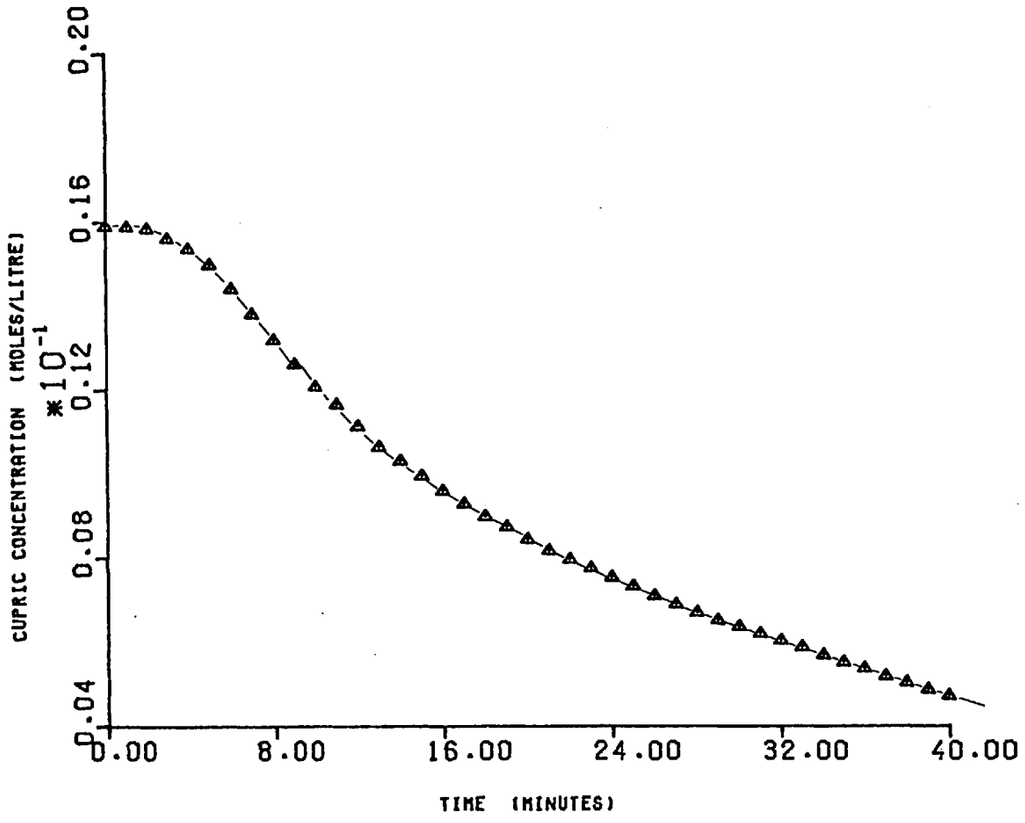


FIGURE 3.1.xiv.





CONDITIONS OF REACTION :

Constant pressure controlled at : 430 p.s.i. ± 5.0 p.s.i. total
400 p.s.i. ± 5.0 p.s.i. hydrogen
Temperature : 120°C ± 1.0°C
Initial cupric concentration : 0.0159 molar
Total acetate concentration : 0.2418 molar

PRODUCT OF THE REDUCTION REACTION :

No insoluble reduced species were observed at the reaction conditions.
Cuprous oxide precipitated upon cooling to room temperature.

RATE CONSTANT :

The rate constant was found to be :

$$k_h = 0.028474 \pm 0.000236$$

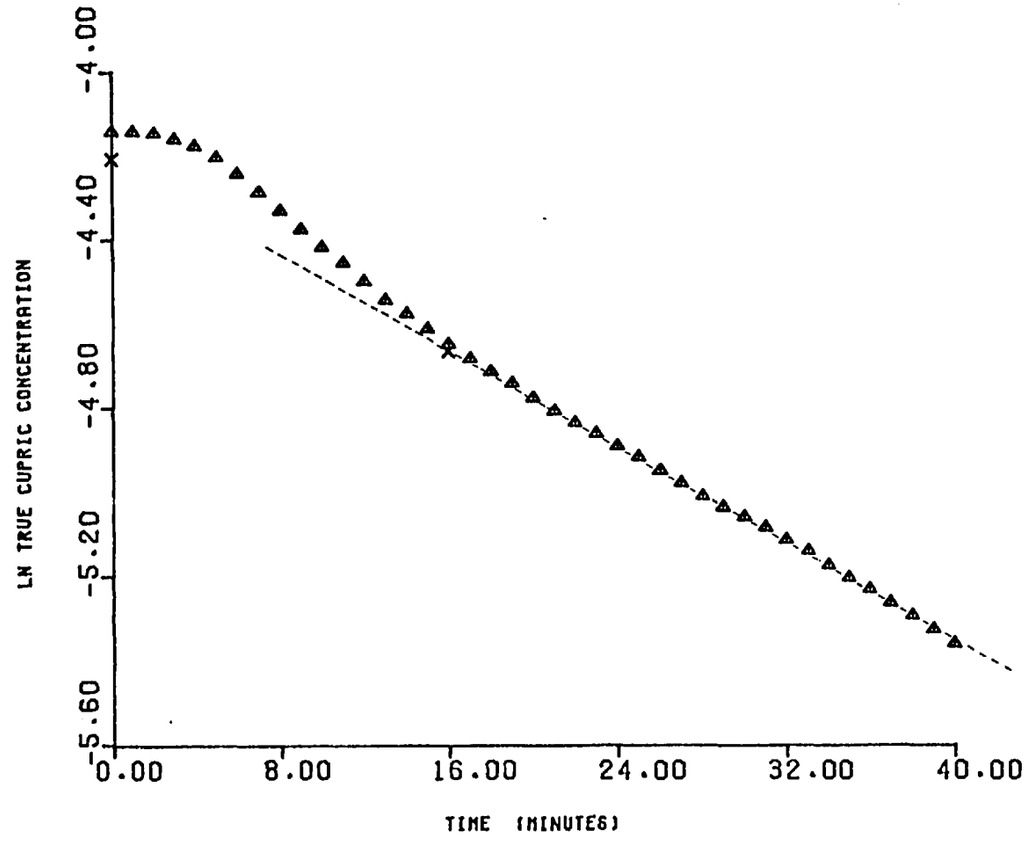
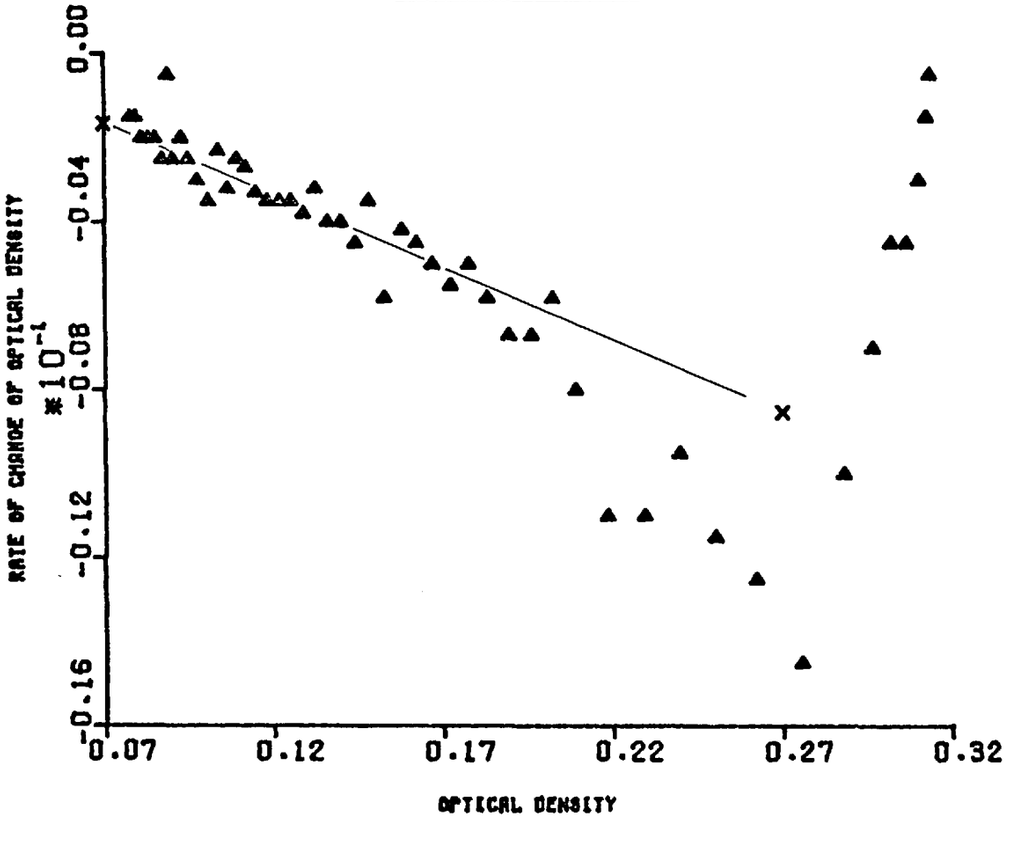
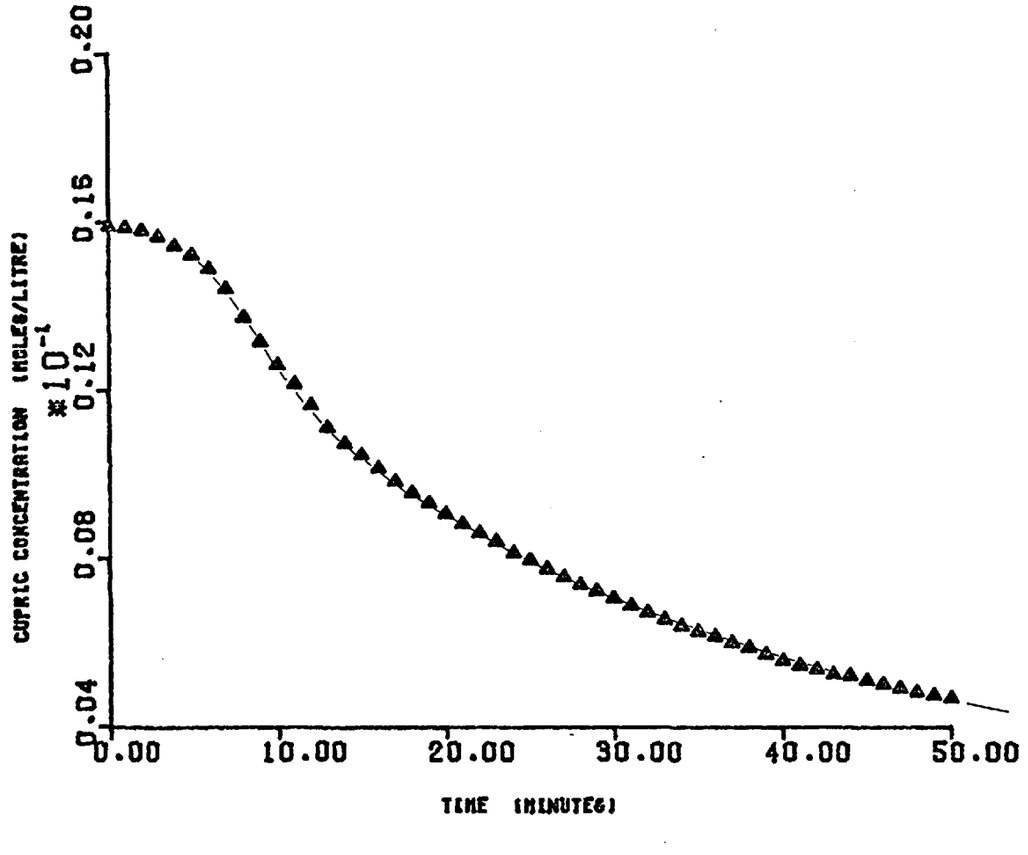


FIGURE 3.1.xx.





CONDITIONS OF REACTION :

Constant pressure controlled at : 430 p.s.i. ± 5.0 p.s.i. total
400 p.s.i. ± 5.0 p.s.i. hydrogen

Temperature : 120°C ± 1.0°C

Initial cupric concentration : 0.0159 molar

Total acetate concentration : 0.2418 molar

PRODUCT OF THE REDUCTION REACTION :

No insoluble reduced species were observed at the reaction conditions.
Cuprous oxide precipitated upon cooling to room temperature.

RATE CONSTANT :

The rate constant was found to be :

$$k_h = 0.024182 \pm 0.000169$$

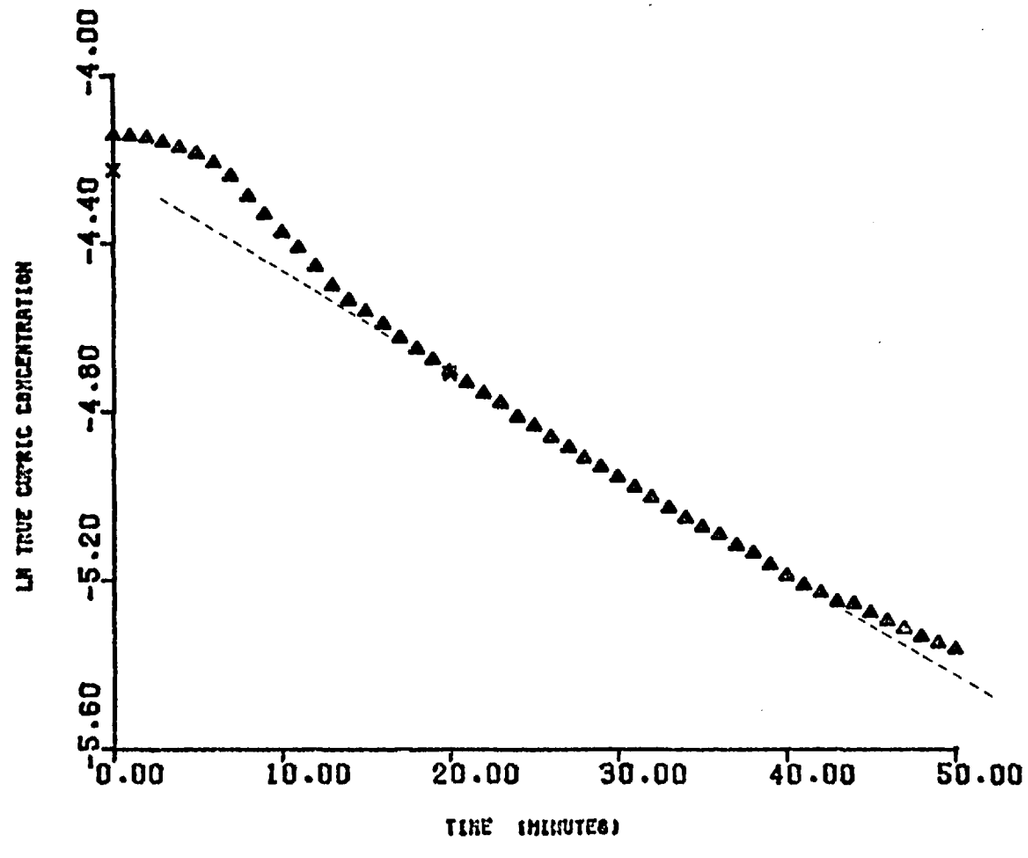
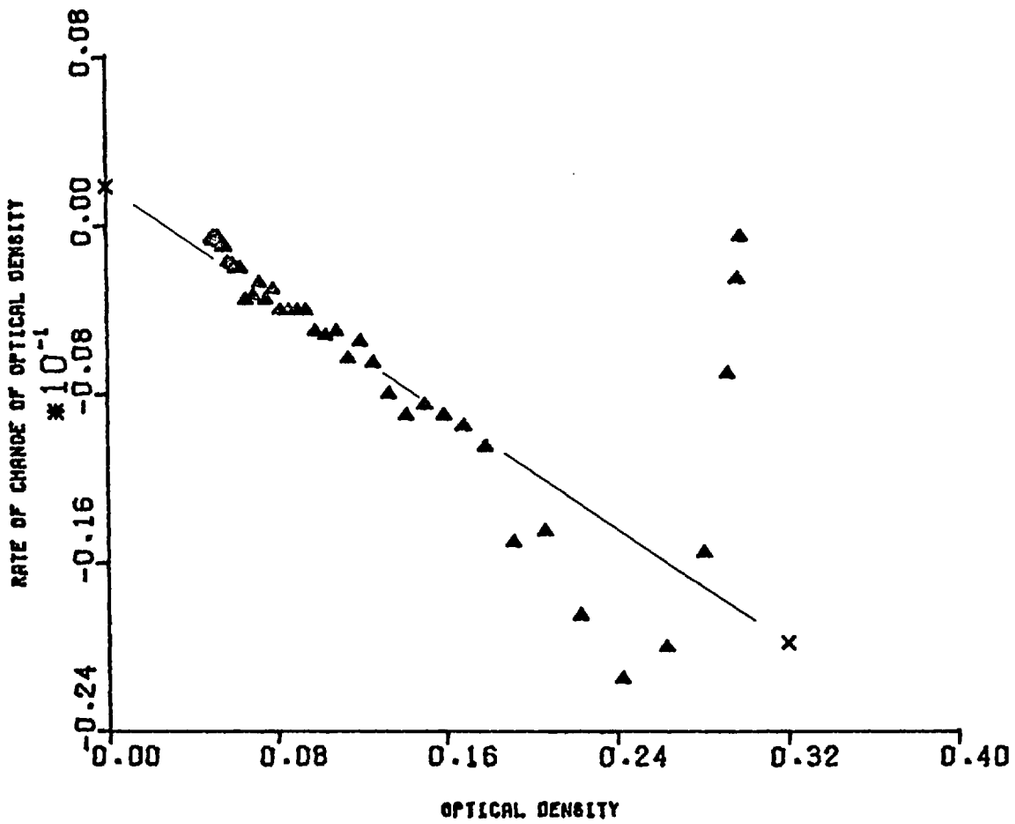
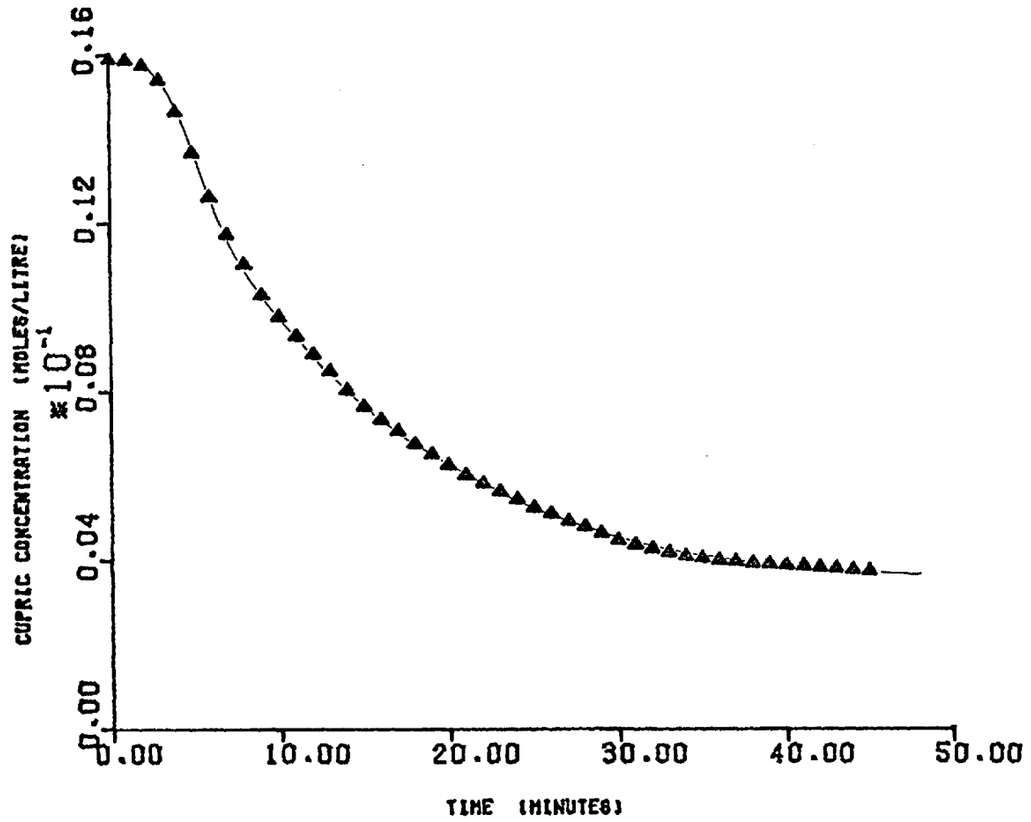


FIGURE 3.1.xxi.





CONDITIONS OF REACTION :

Constant pressure controlled at : 439 p.s.i. ± 5.0 p.s.i. total
400 p.s.i. ± 5.0 p.s.i. hydrogen
Temperature : 130°C ± 1.0°C
Initial cupric concentration : 0.0159 molar
Total acetate concentration : 0.2418 molar

PRODUCT OF THE REDUCTION REACTION :

No insoluble reduced species were observed at the reaction conditions.
Cuprous oxide precipitated upon cooling to room temperature.

RATE CONSTANT :

The rate constant was found to be :

$$k_h = 0.033629 \pm 0.000515$$

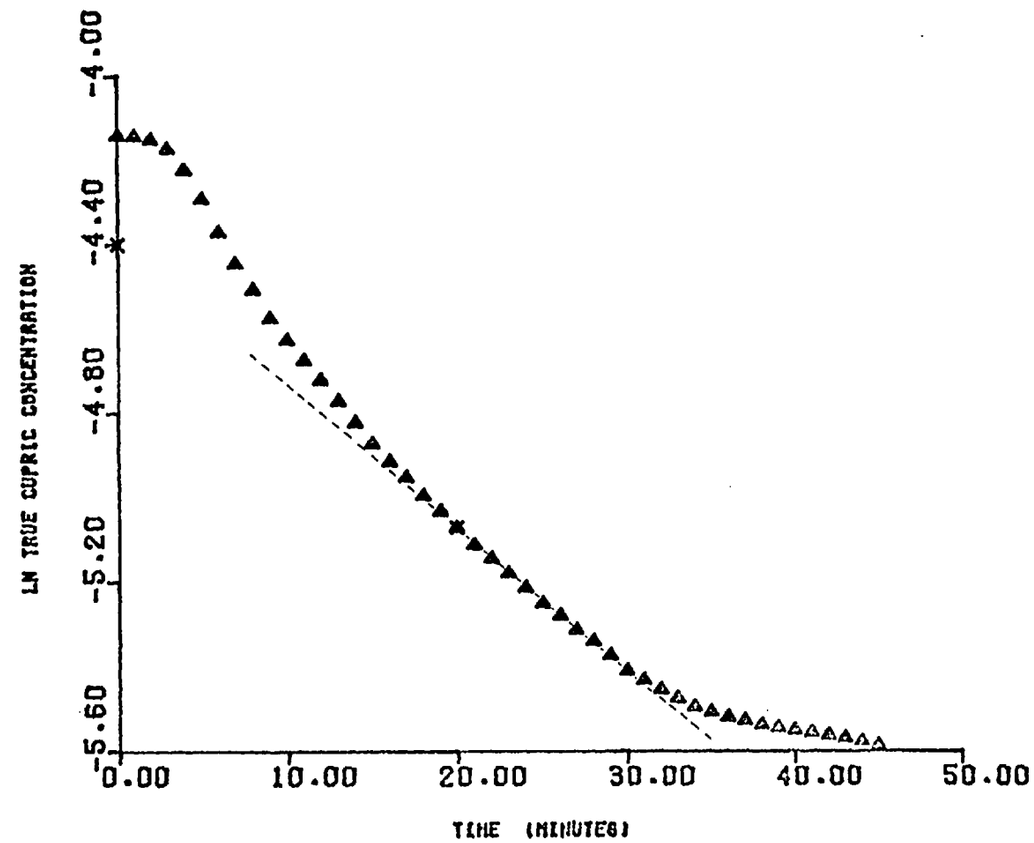
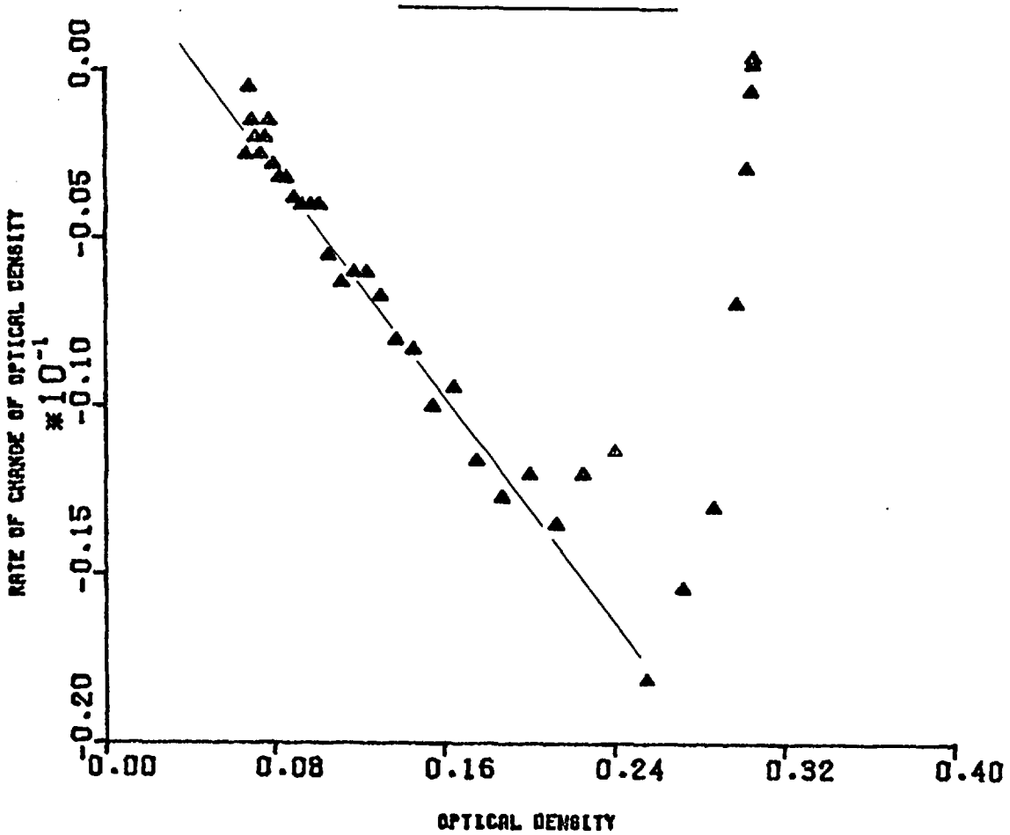
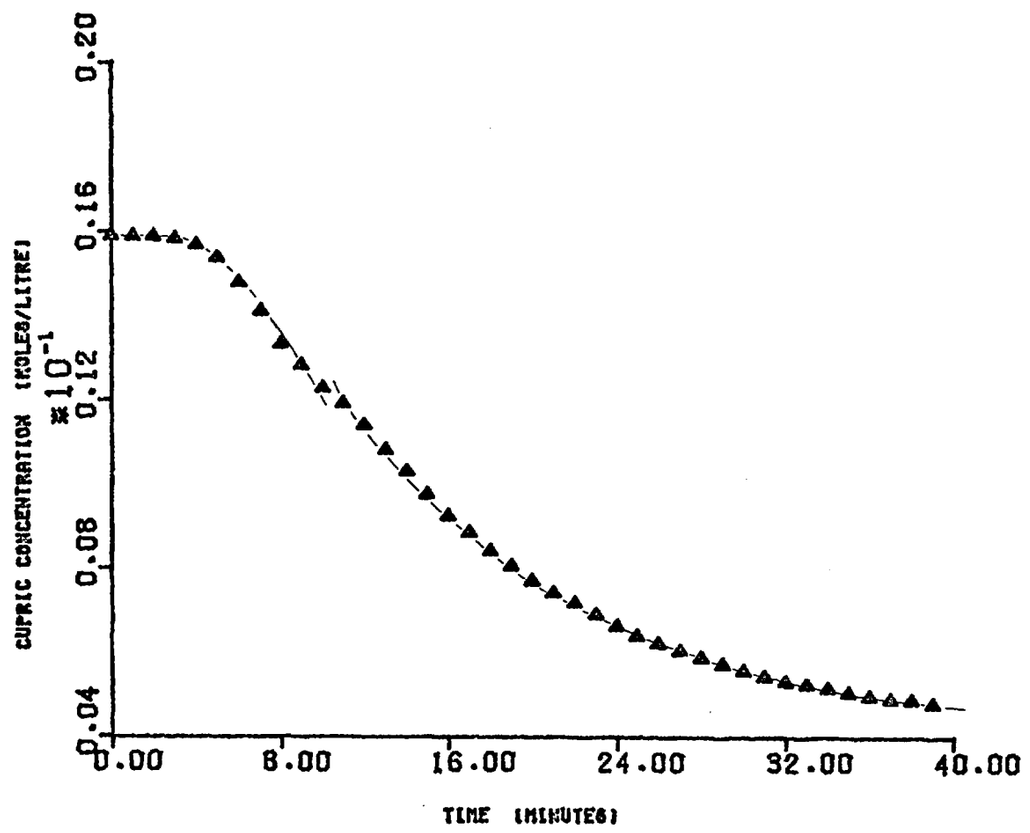


FIGURE 3.1.xxii.





CONDITIONS OF REACTION :

Initial pressure :	439 p.s.i. ± 5.0 p.s.i. total
	400 p.s.i. ± 5.0 p.s.i. hydrogen
Temperature :	130°C ± 1.0°C
Initial cupric concentration :	0.0159 molar
Total acetate concentration :	o.2418 molar

A steel stirrer rod was used.

PRODUCT OF THE REDUCTION REACTION :

No insoluble reduced species were observed at the reaction conditions.
Cuprous oxide precipitated upon cooling to room temperature.

RATE CONSTANT :

The rate constant was found to be :

$$k_h = 0.047047 \pm 0.000903$$

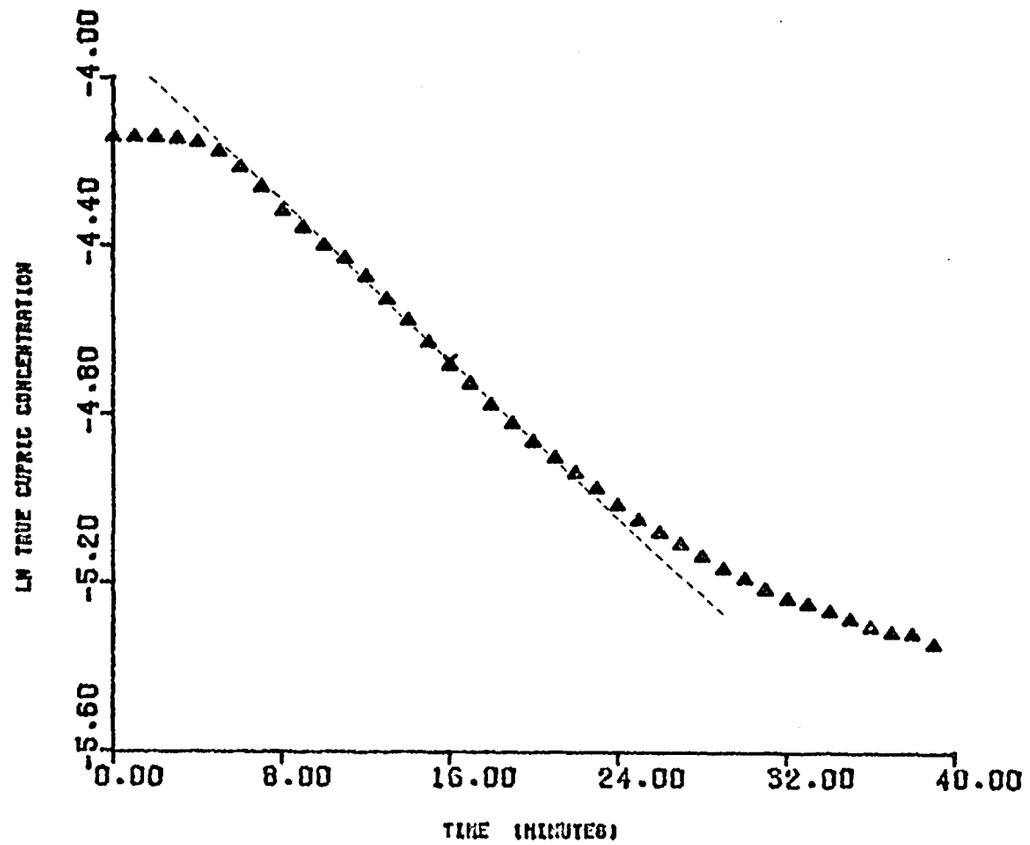
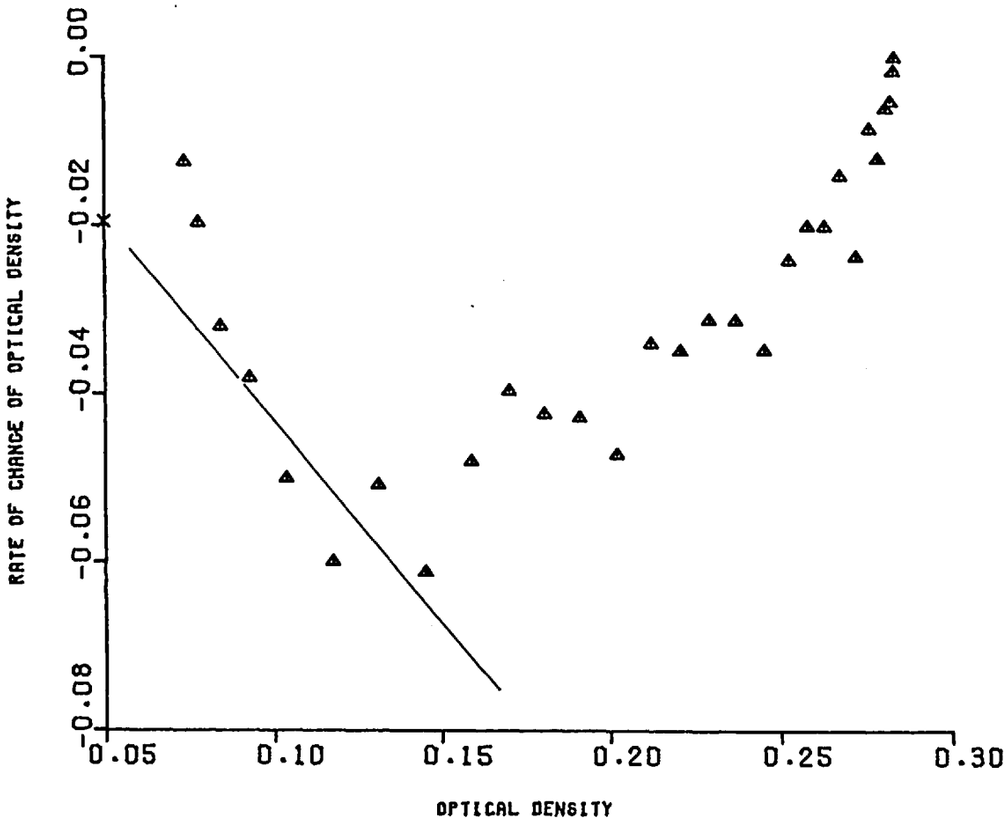
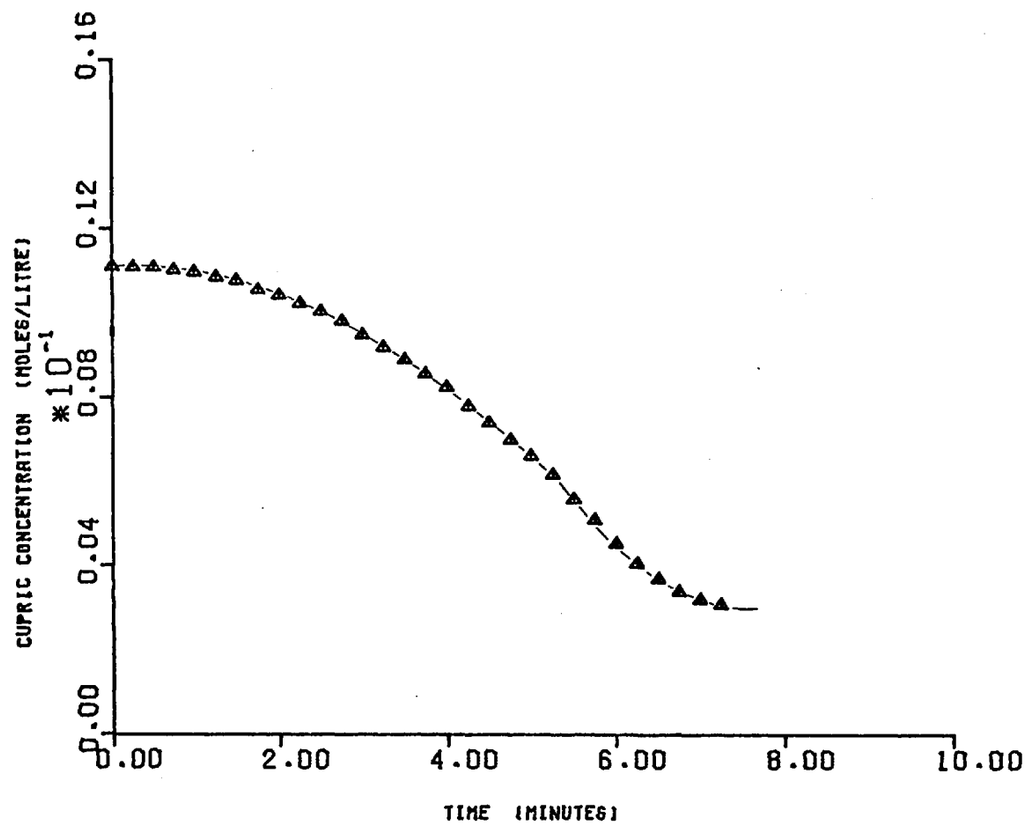


FIGURE 3.1.xxiii.





CONDITIONS OF REACTION :

Initial pressure :	496 p.s.i. ± 5.0 p.s.i. total
	400 p.s.i. ± 5.0 p.s.i. hydrogen
Temperature :	150°C ± 1.0°C
Initial cupric concentration :	0.01112 molar
Total acetate concentration :	4.92948 molar
Total ammonium concentrate :	0.2667 molar
Initial pH :	3.68

PRODUCT OF THE REDUCTION REACTION :

Precipitation of reduction product commenced at 7.50 minutes after the initiation of the reaction. The solid reduction product was metallic copper.

RATE CONSTANT :

The rate constant was found to be :

$$k_h = 0.42188 \pm 0.01078$$

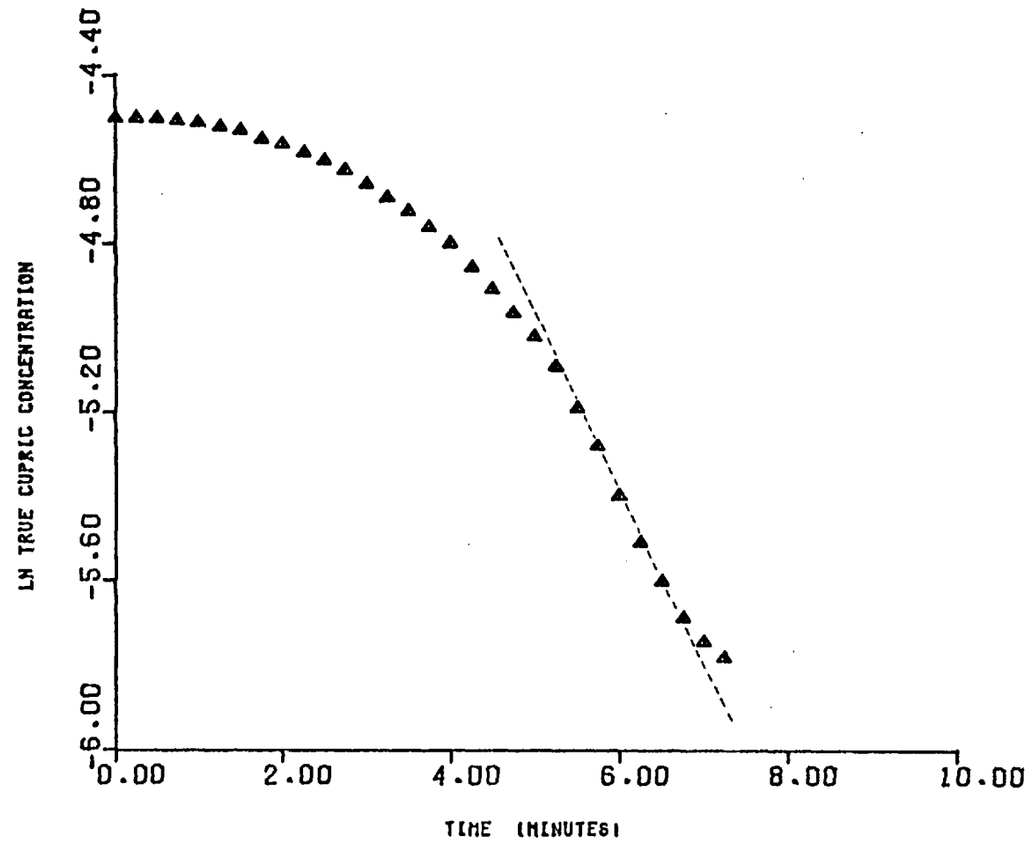
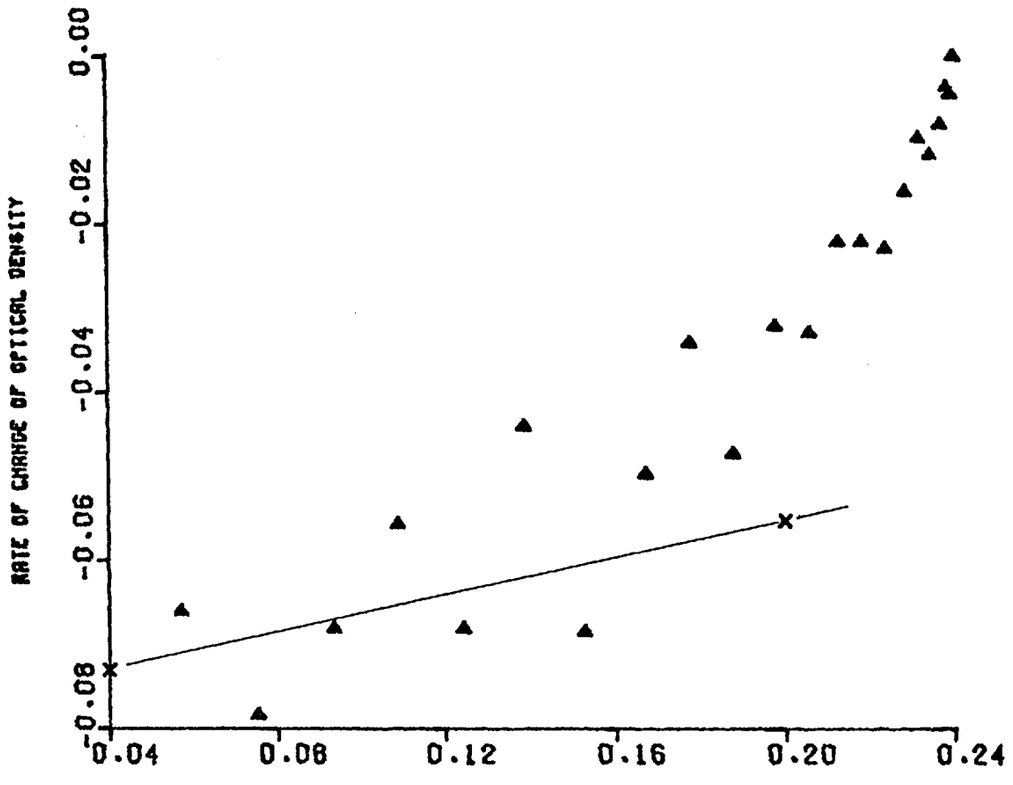
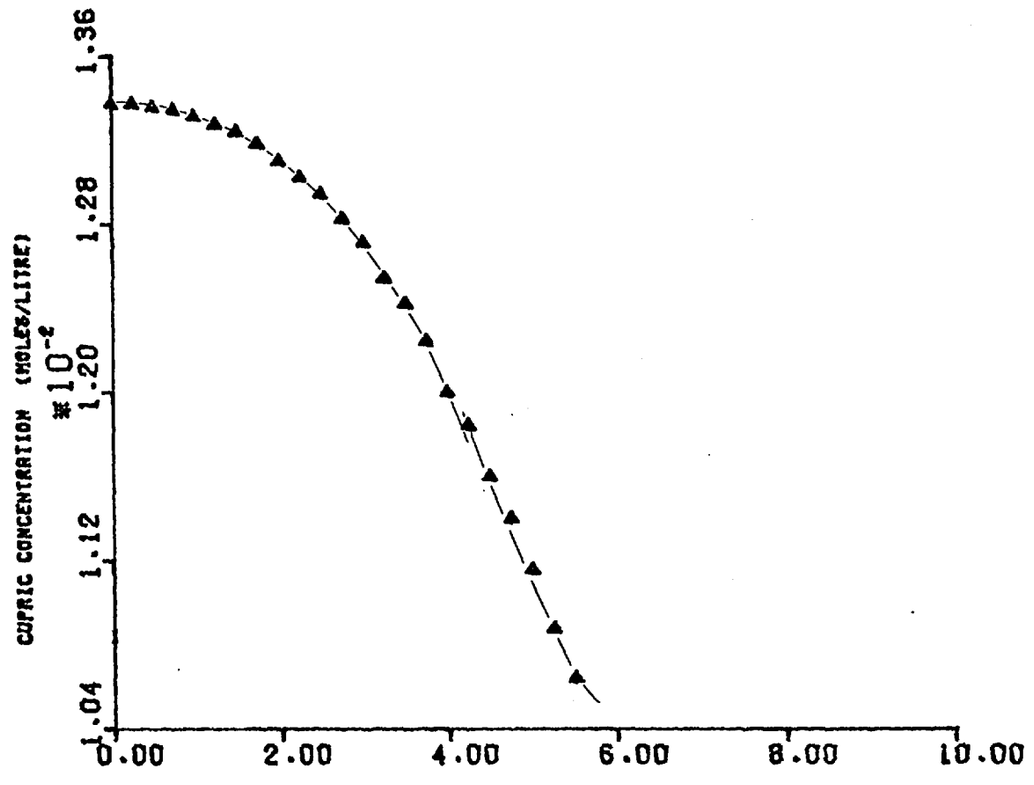


FIGURE 3.1.xxiv.





CONDITIONS OF REACTION :

Initial pressure :	480 p.s.i. ± 5.0 p.s.i. total
	410 p.s.i. ± 5.0 p.s.i. hydrogen
Temperature :	150°C ± 1.0°C
Initial cupric concentration :	0.01338 molar
Total acetate concentration :	1.83187 molar
Total ammonium concentrate :	0.08333 molar
Final pH :	3.25

PRODUCT OF THE REDUCTION REACTION :

Precipitation of reduction product commenced at 5.85 minutes after the initiation of the reaction. The solid reduction product was metallic copper.

RATE CONSTANT :

The rate constant was found to be :

$$k_h = 0.083533 \pm 0.003237$$

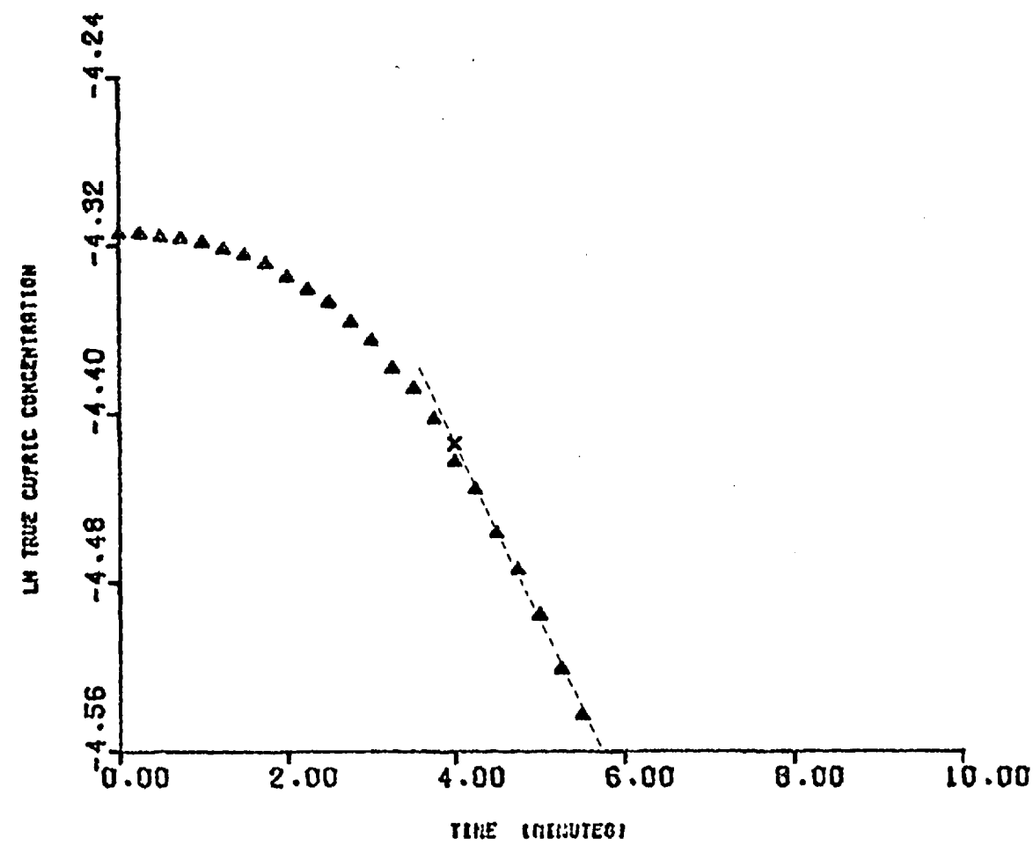
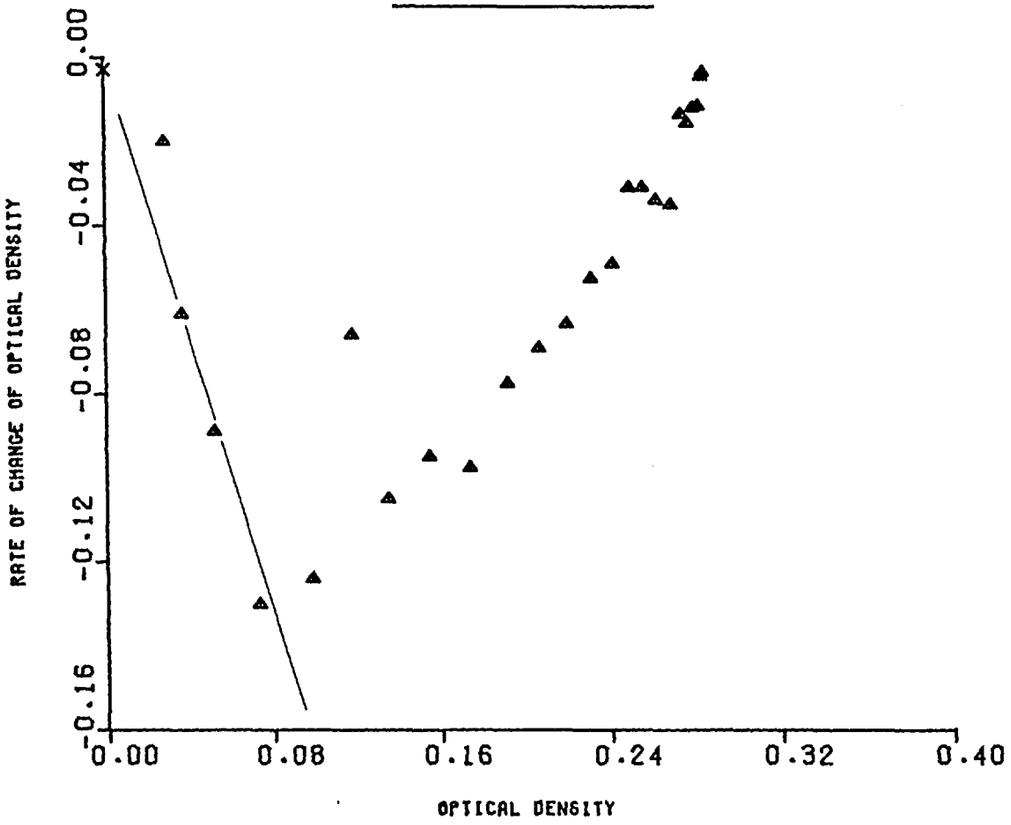
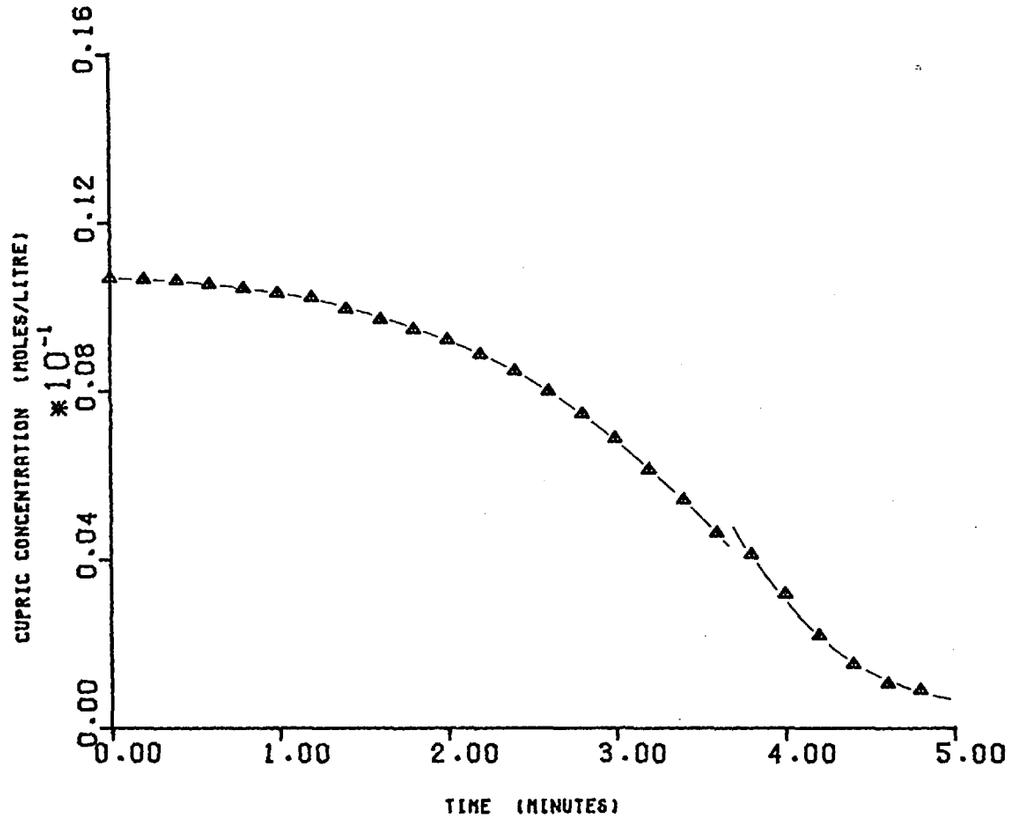


FIGURE 3.1.xxv.





CONDITIONS OF REACTION :

Initial pressure :	480 p.s.i. ± 5.0 p.s.i. total
	410 p.s.i. ± 5.0 p.s.i. hydrogen
Temperature :	150°C ± 1.0°C
Initial cupric concentration :	0.016053 molar
Total acetate concentration :	2.19825 molar
Total ammonium concentrate :	0.1 molar
Final pH :	3.23

PRODUCT OF THE REDUCTION REACTION :

Precipitation of reduction product commenced at 4.75 minutes after the initiation of the reaction. The solid reduction product was metallic copper.

RATE CONSTANT :

The rate constant was found to be :

$$k_h = 1.72325 \pm 0.06072$$

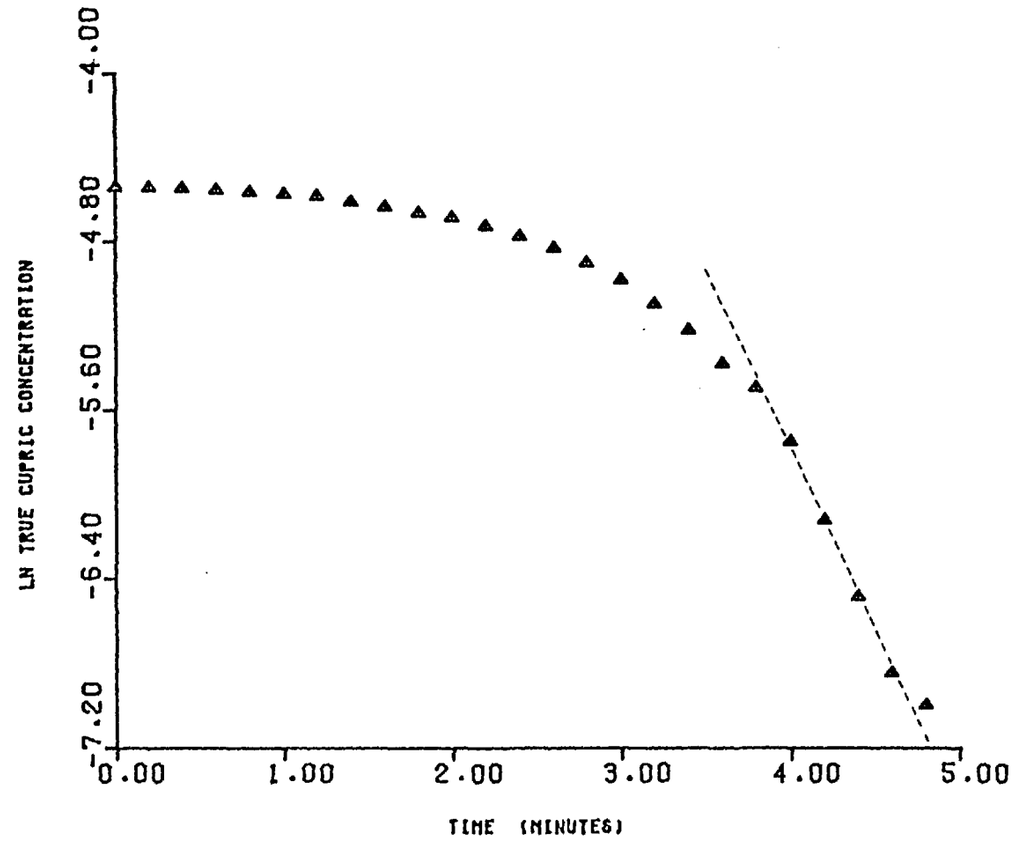
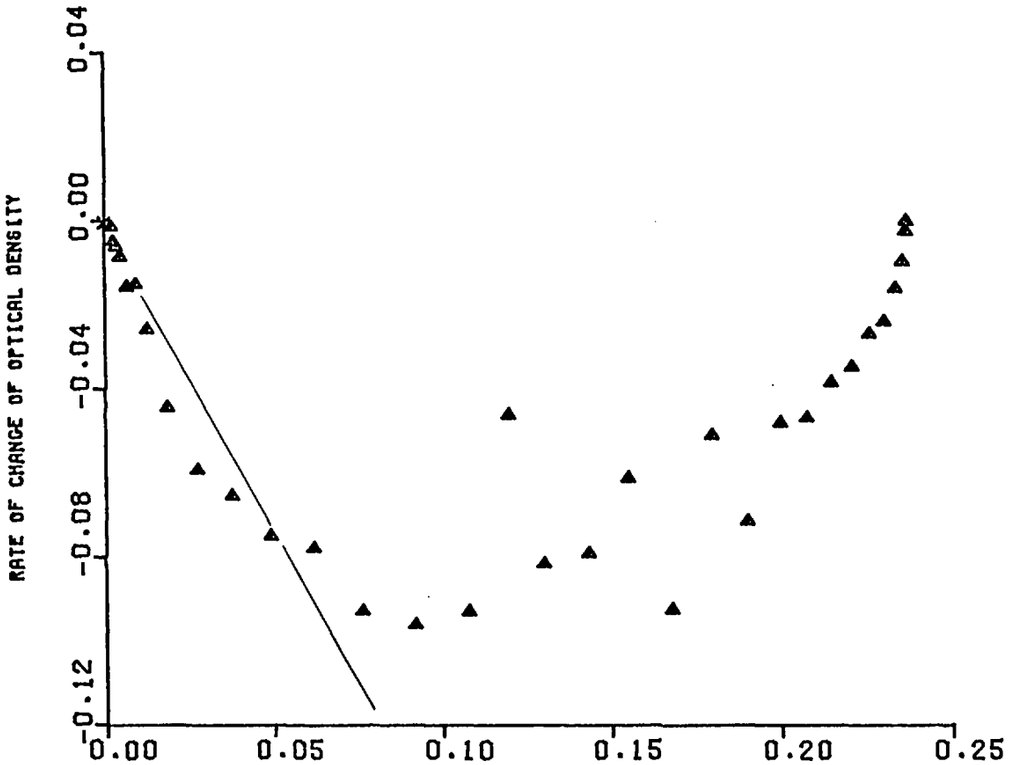
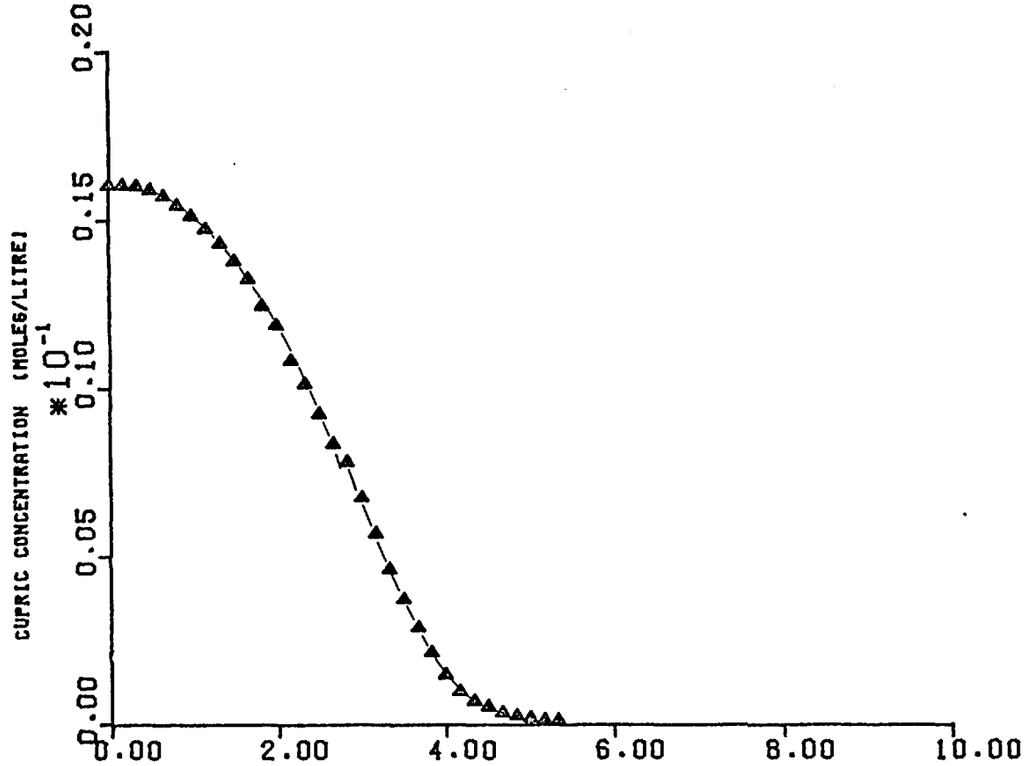


FIGURE 3.1.xxvi.





CONDITIONS OF REACTION :

Initial pressure :	480 p.s.i. ± 5.0 p.s.i. total
	410 p.s.i. ± 5.0 p.s.i. hydrogen
Temperature :	150°C ± 1.0°C
Initial cupric concentration :	0.016053 molar
Total acetate concentration :	2.19825 molar
Total ammonium concentrate :	0.1 molar
Final pH :	3.155

PRODUCT OF THE REDUCTION REACTION :

Precipitation of reduction product commenced at 5.00 minutes after the initiation of the reaction. The solid reduction product was metallic copper.

RATE CONSTANT :

The rate constant was found to be :

$$k_h = 2.06216 \pm 0.02499$$

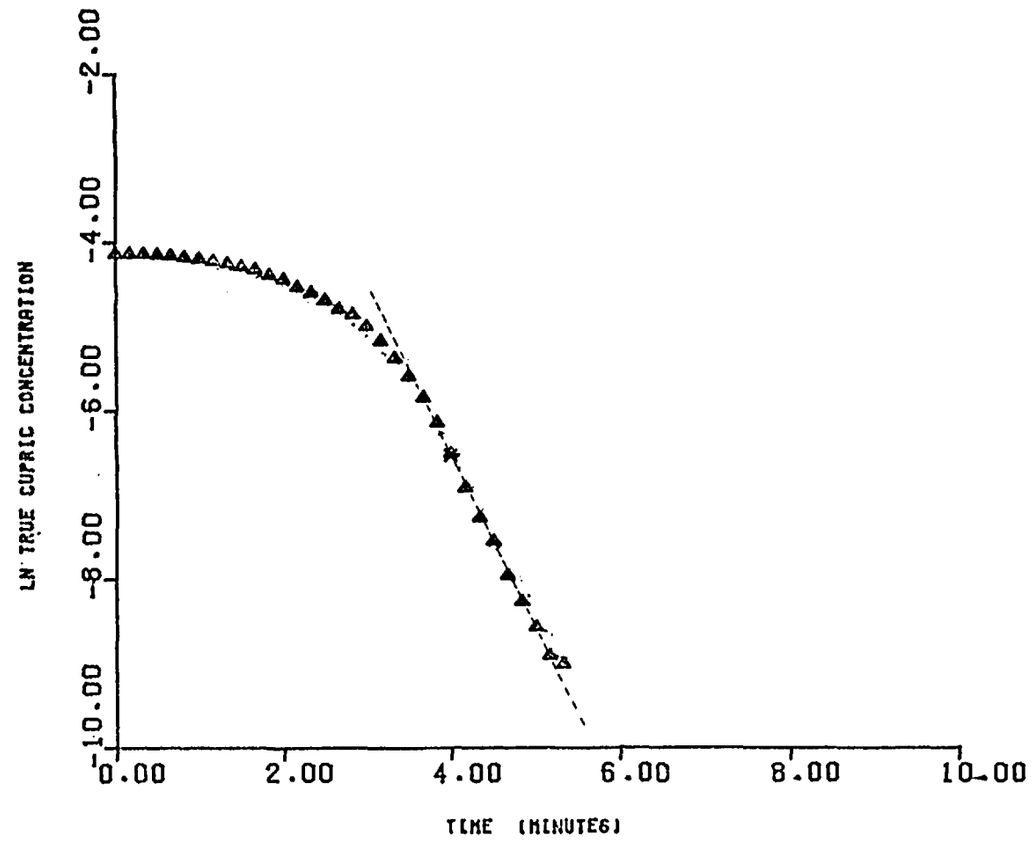
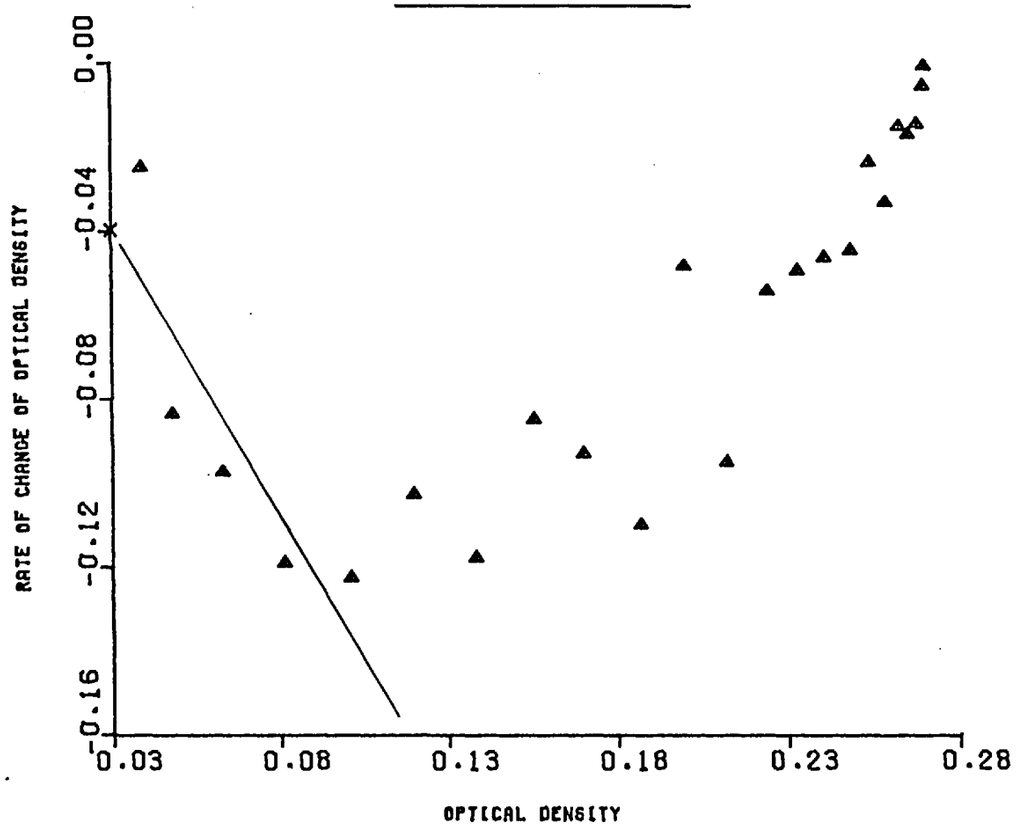
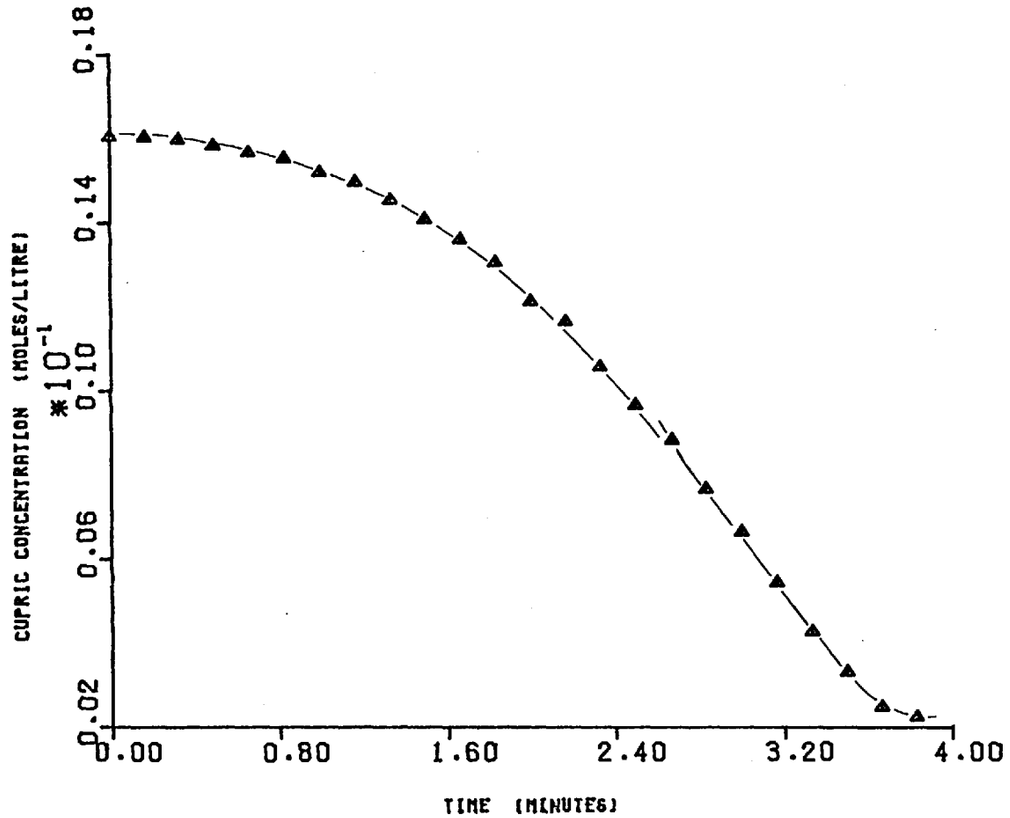


FIGURE 3.1.xxvii.





CONDITIONS OF REACTION :

Initial pressure :	470 p.s.i. ± 5.0 p.s.i. total
	410 p.s.i. ± 5.0 p.s.i. hydrogen
Temperature :	150°C ± 1.0°C
Initial cupric concentration :	0.016053 molar
Total acetate concentration :	2.19825 molar
Total ammonium concentrate :	0.1 molar
Final pH :	3.23

PRODUCT OF THE REDUCTION REACTION :

Precipitation of reduction product commenced at 3.88 minutes after the initiation of the reaction. The solid reduction product was metallic copper.

RATE CONSTANT :

The rate constant was found to be :

$$k_h = 1.47654 \pm 0.05381$$

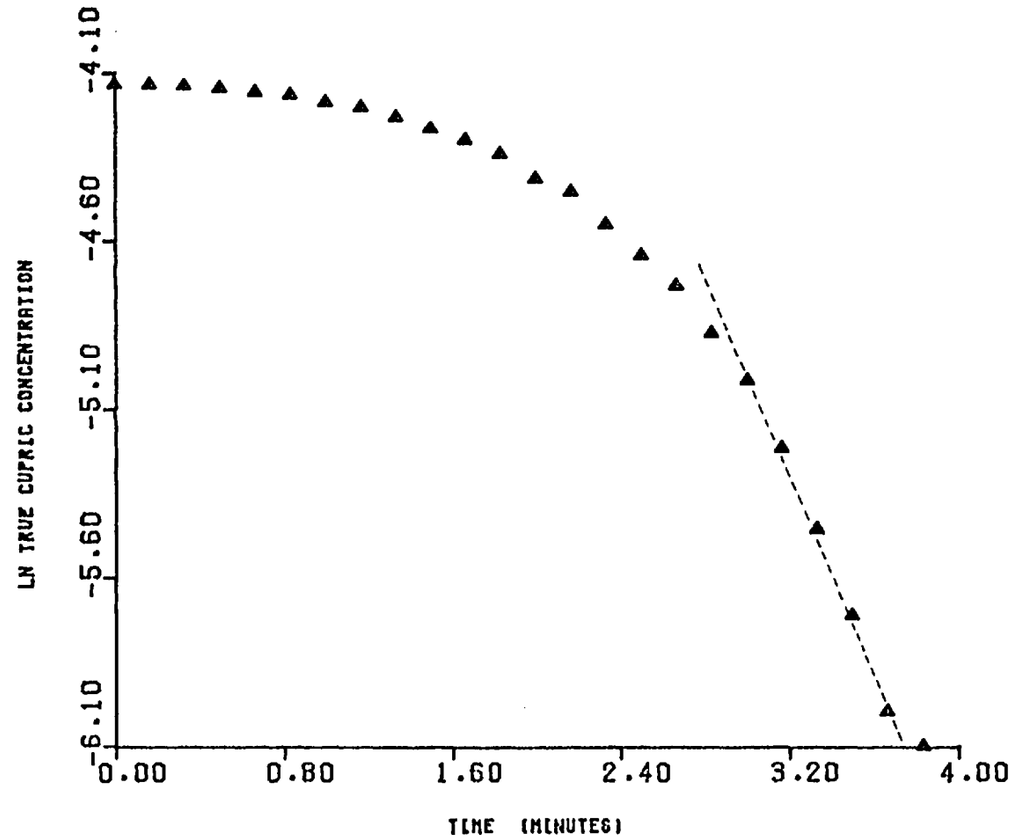
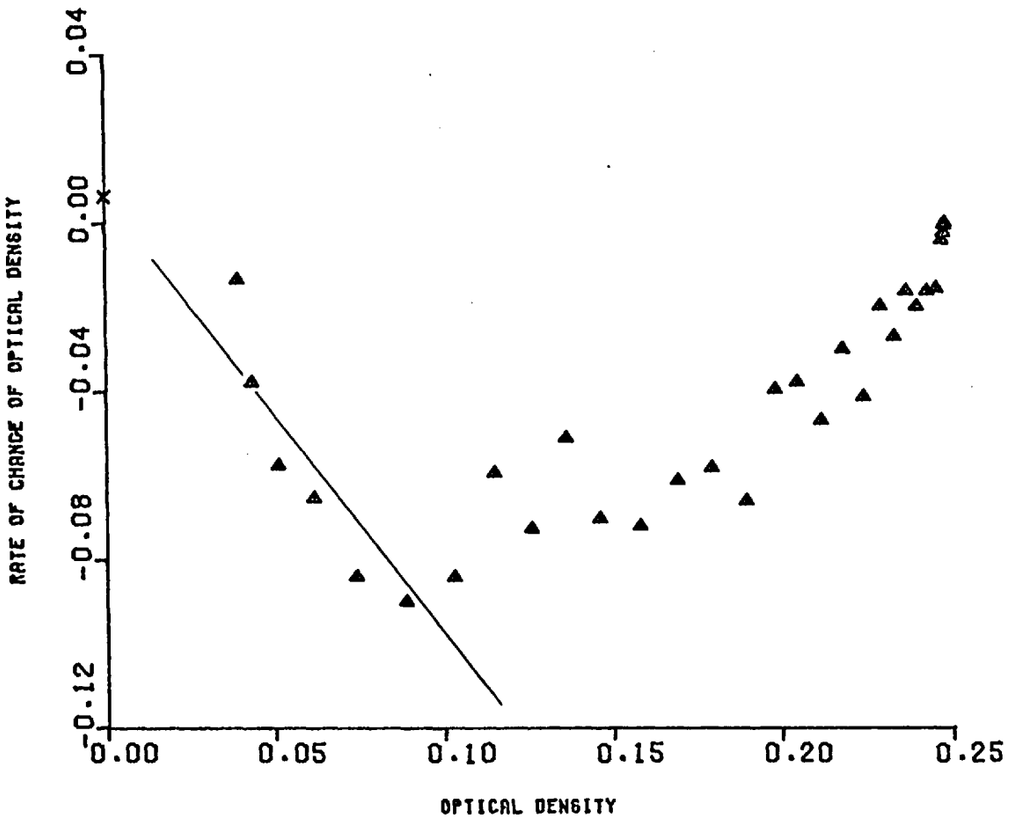
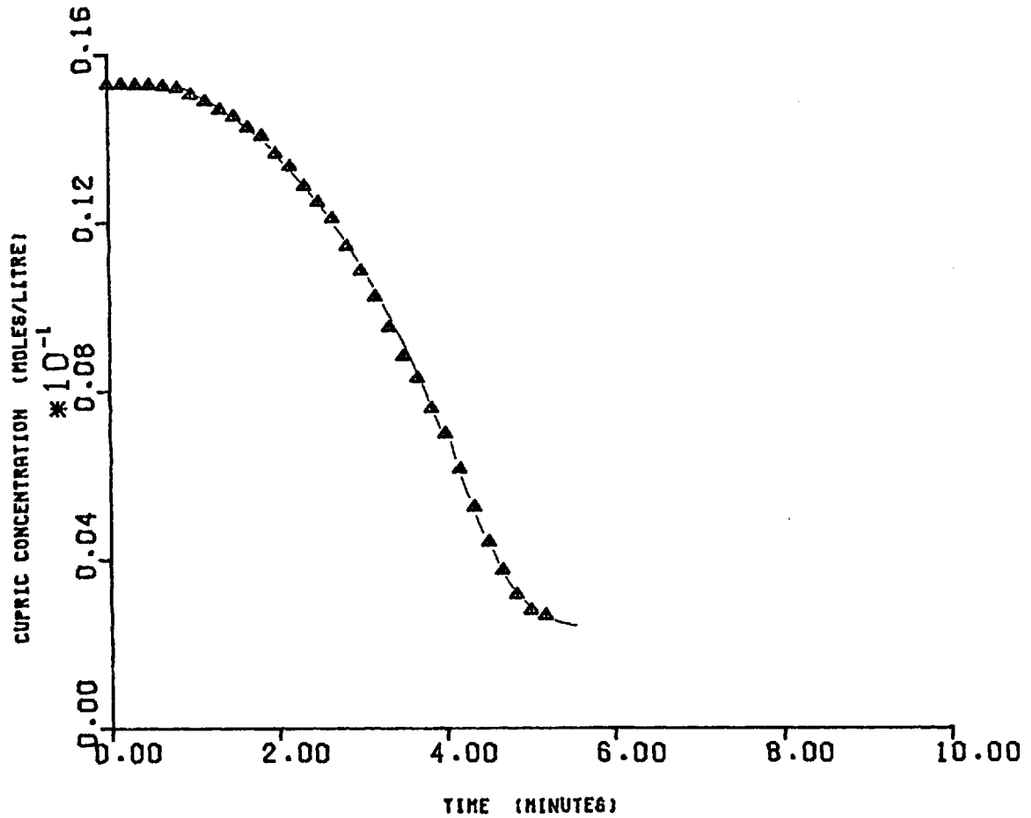


FIGURE 3.1.xxviii.





CONDITIONS OF REACTION :

Initial pressure :	470 p.s.i. ± 5.0 p.s.i. total
	400 p.s.i. ± 5.0 p.s.i. hydrogen
Temperature :	150°C ± 1.0°C
Initial cupric concentration :	0.01529 molar
Total acetate concentration :	2.10548 molar
Total ammonium concentrate :	0.10714 molar
Initial pH :	3.3
Final pH :	3.29

PRODUCT OF THE REDUCTION REACTION

Precipitation of reduction product commenced at 5.20 minutes after the initiation of the reaction. The solid reduction product was metallic copper.

RATE CONSTANT :

The rate constant was found to be :

$$k_h = 0.94605 \pm 0.01718$$

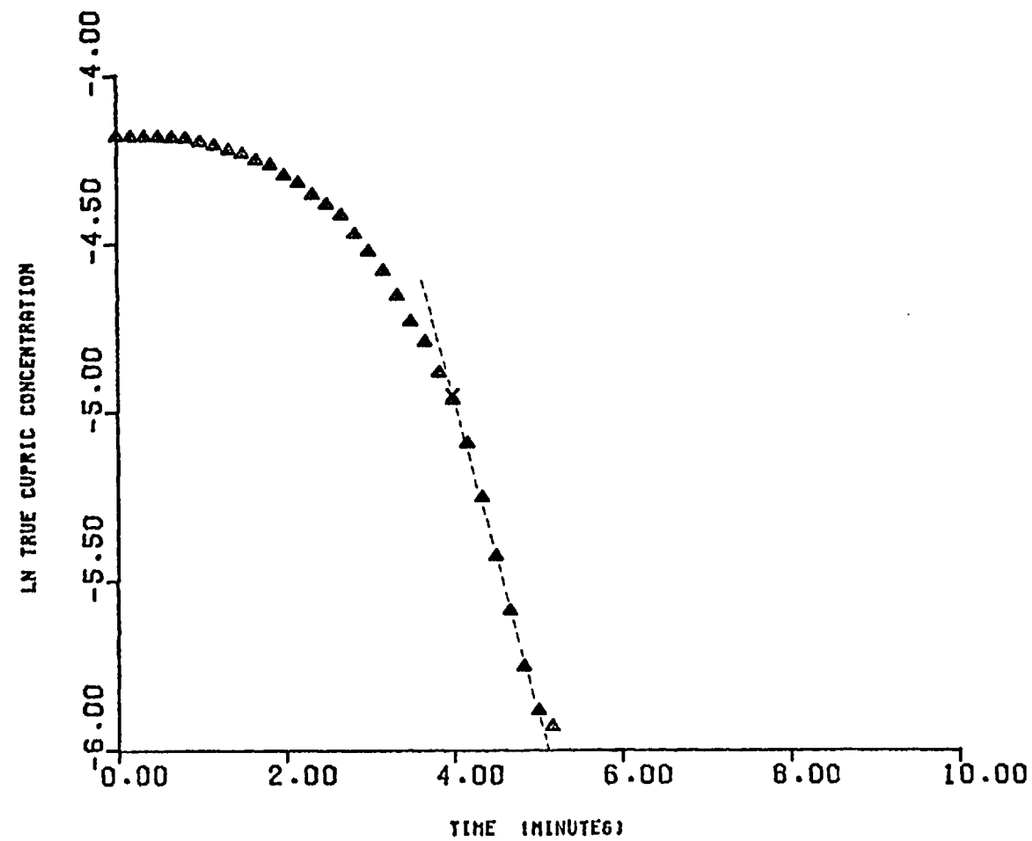
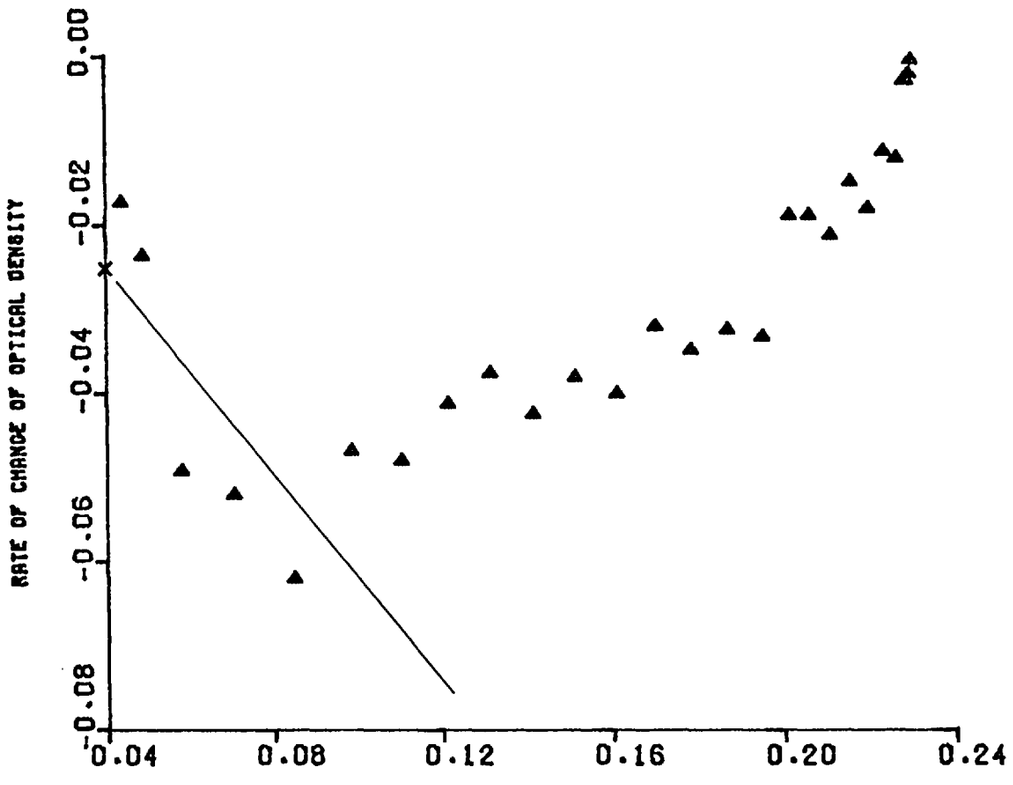
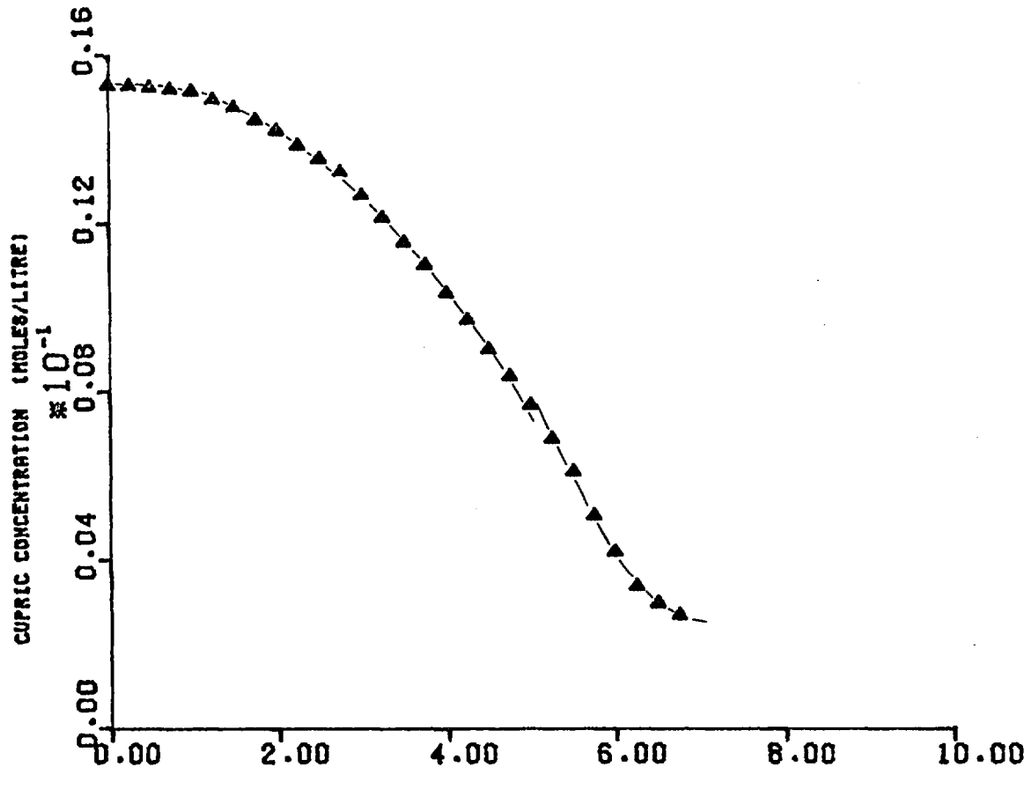


FIGURE 3.1.xxix.





CONDITIONS OF REACTION :

Initial pressure :	460 p.s.i. ± 5.0 p.s.i. total
	400 p.s.i. ± 5.0 p.s.i. hydrogen
Temperature :	140°C ± 1.0°C
Initial cupric concentration :	0.01529 molar
Total acetate concentration :	2.10548 molar
Total ammonium concentrate :	0.10714 molar
Final pH :	3.305

PRODUCT OF THE REDUCTION REACTION :

Precipitation of reduction product commenced at 6.80 minutes after the initiation of the reaction. The solid reduction product was metallic copper.

RATE CONSTANT :

The rate constant was found to be :

$$k_h = 0.700803 \pm 0.027933$$

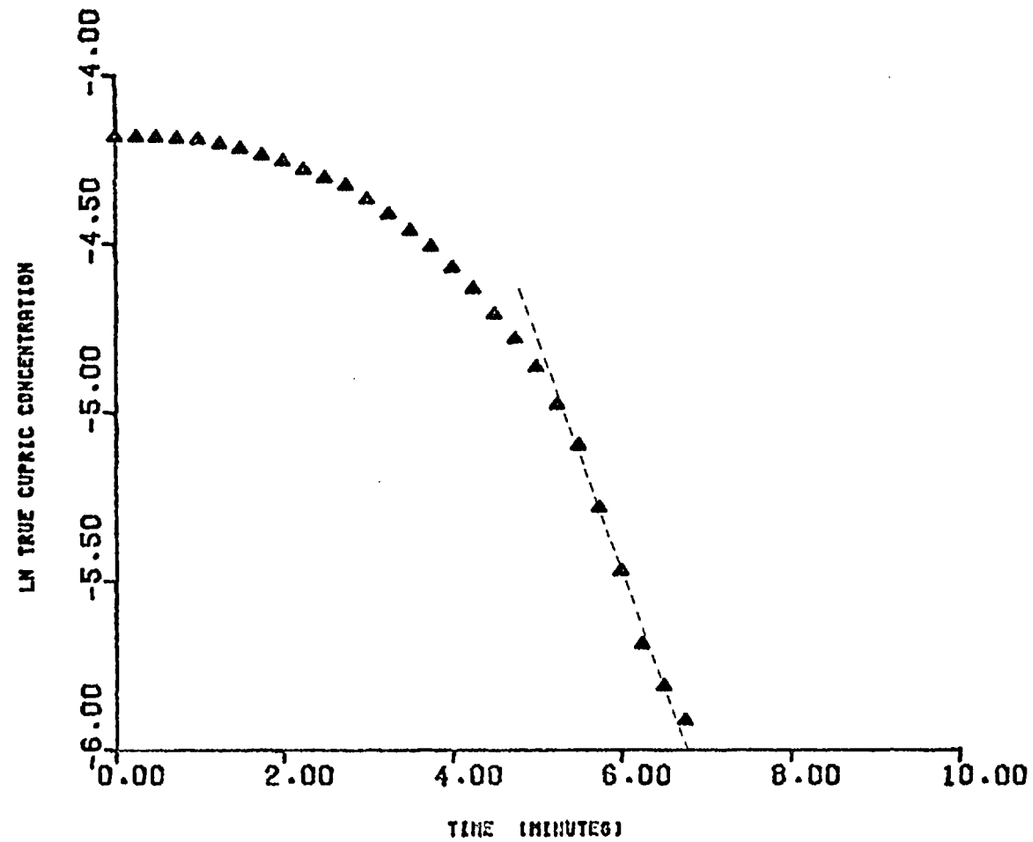
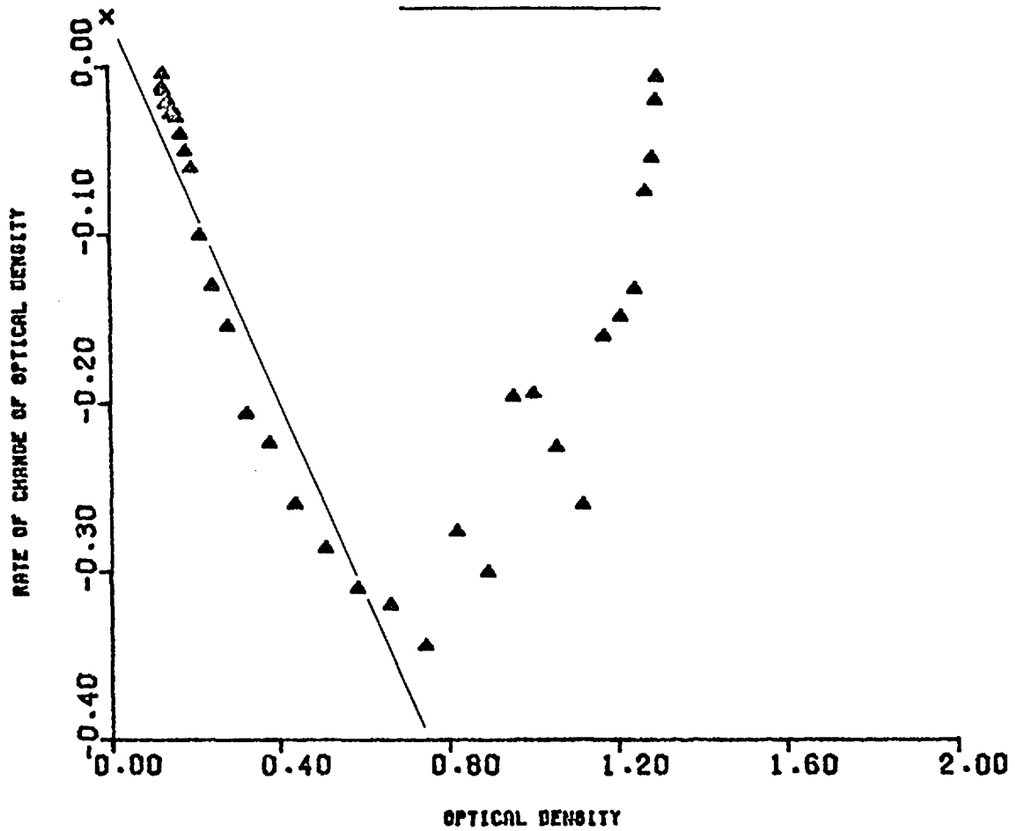
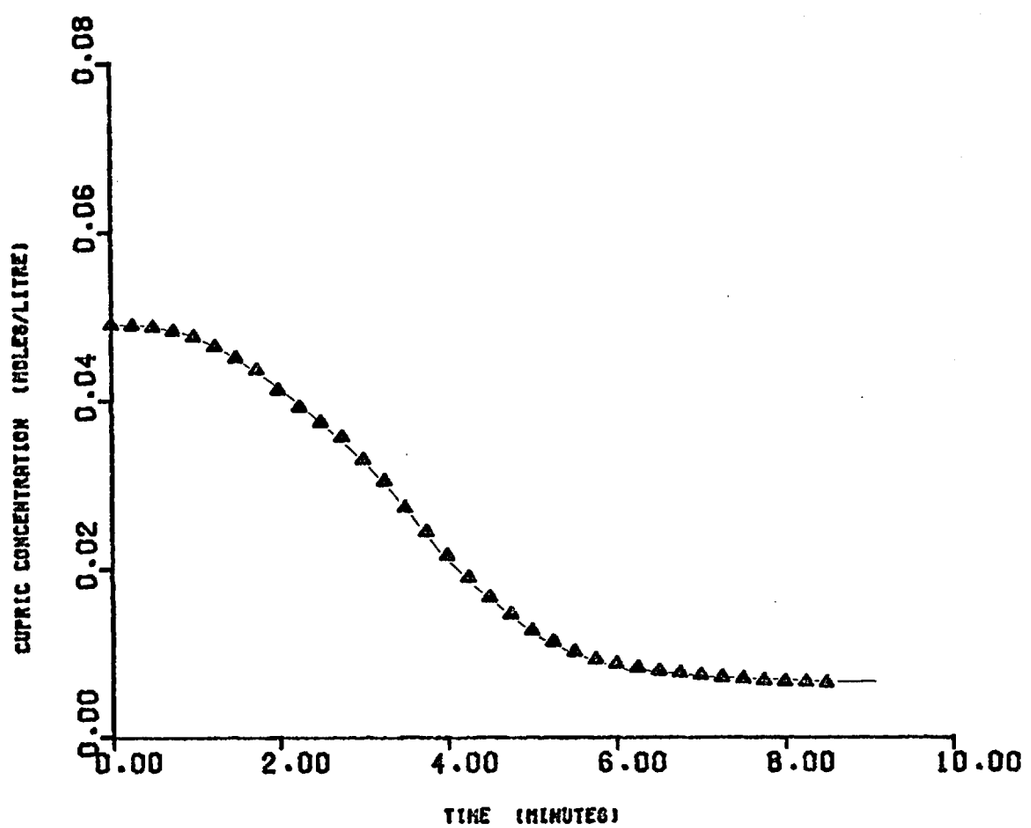


FIGURE 3.1.xxx.





CONDITIONS OF REACTION :

Initial pressure :	500 p.s.i. ± 5.0 p.s.i. total
	400 p.s.i. ± 5.0 p.s.i. hydrogen
Temperature :	150° C ± 1.0°C
Initial cupric concentration :	0.04905 molar
Total acetate concentration :	6.41132 molar
Total ammonium concentrate :	1.71263 molar
Initial pH :	4.0

PRODUCT OF THE REDUCTION REACTION :

Precipitation of reduction product commenced at 9.20 minutes after the initiation of the reaction. The solid reduction product was metallic copper.

RATE CONSTANT

The rate constant was found to be :

$$k_h = 0.42212 \pm 0.01743$$

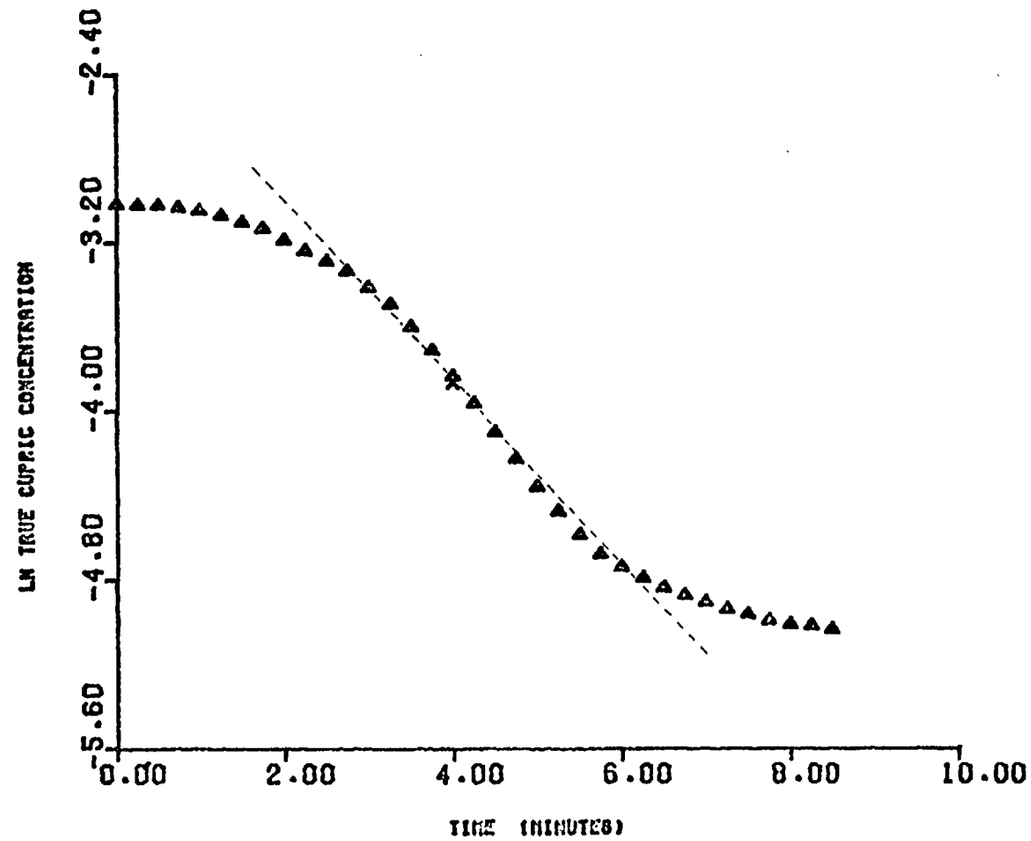
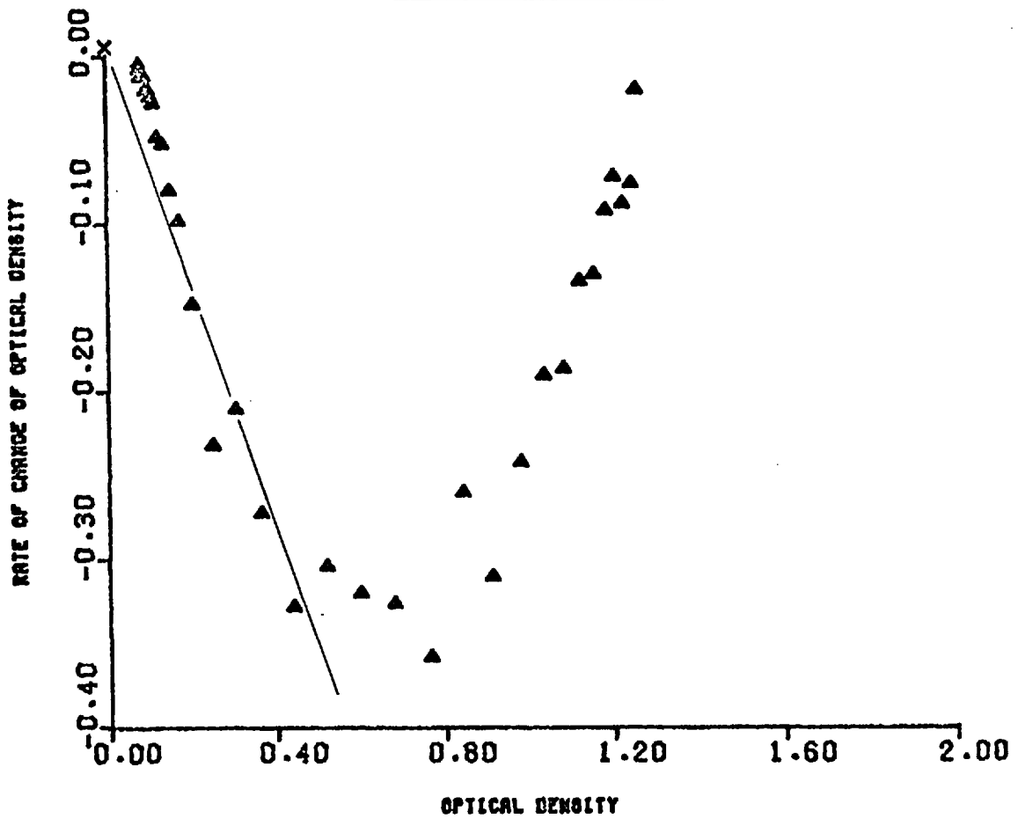
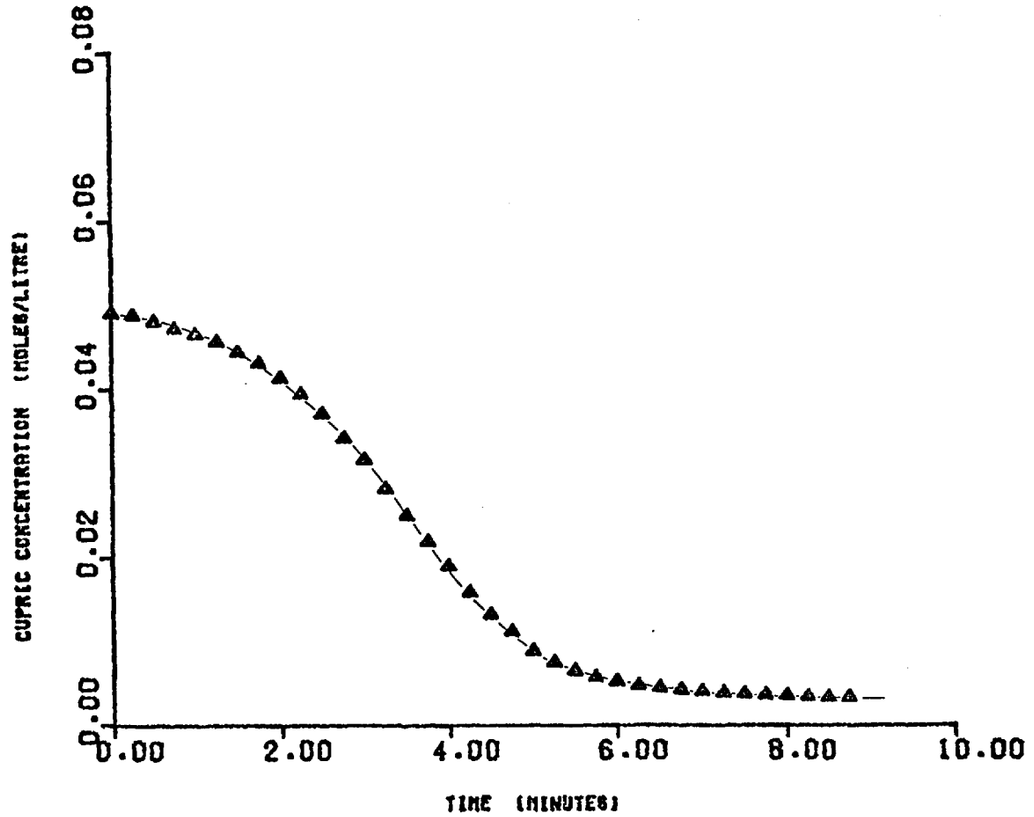


FIGURE 3.1.xxxi.





CONDITIONS OF REACTION :

Initial pressure :	500 p.s.i. $\pm$ 5.0 p.s.i. total
	400 p.s.i. $\pm$ 5.0 p.s.i. hydrogen
Temperature :	$150^{o}C \pm 1.0^{o}C$
Initial cupric concentration :	0.04905 molar
Total acetate concentration :	6.41132 molar
Total ammonium concentrate :	1.71263 molar
Initial pH :	4.0

PRODUCT OF THE REDUCTION REACTION :

Precipitation of reduction product commenced at 9.70 minutes after the initiation of the reaction. The solid reduction product was metallic copper.

RATE CONSTANT :

The rate constant was found to be :

$$k_h = 0.69796 \pm 0.01526$$

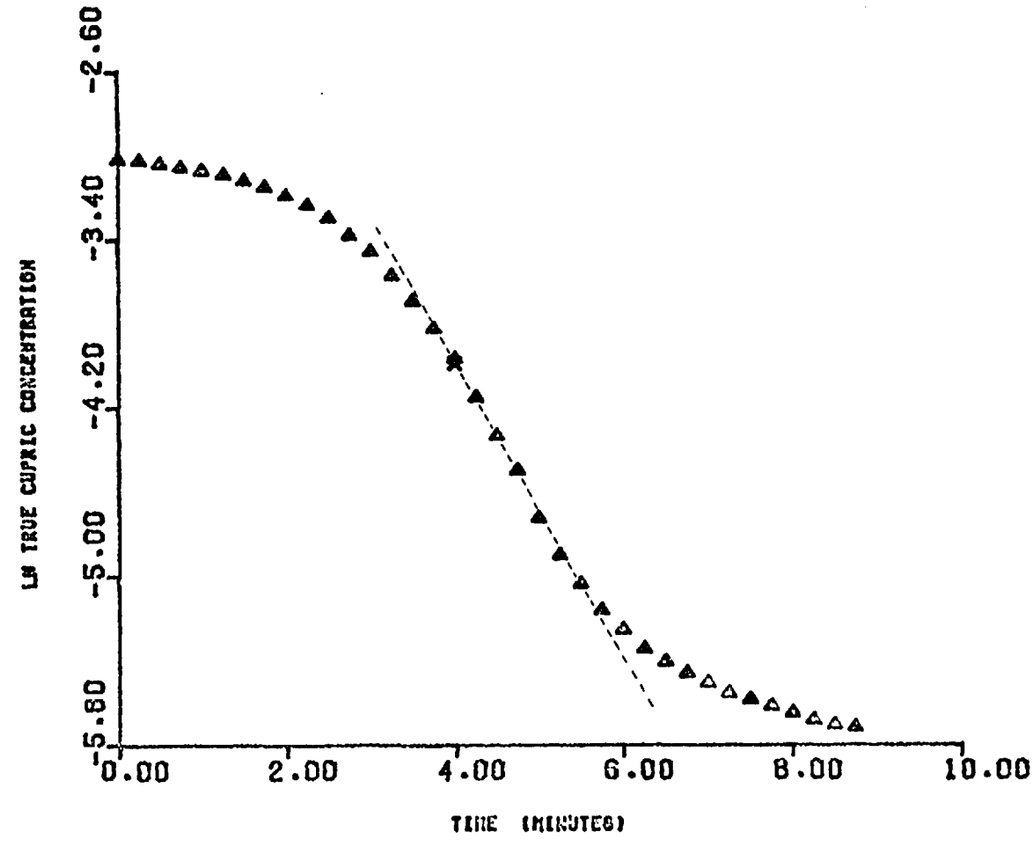
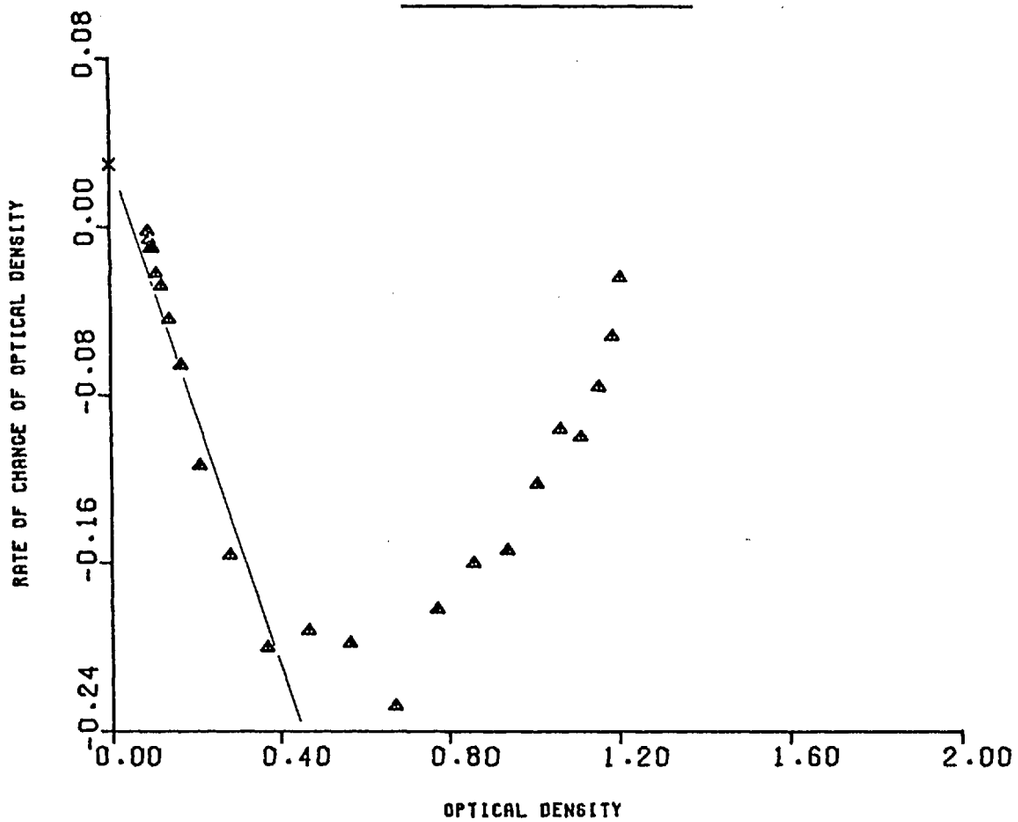
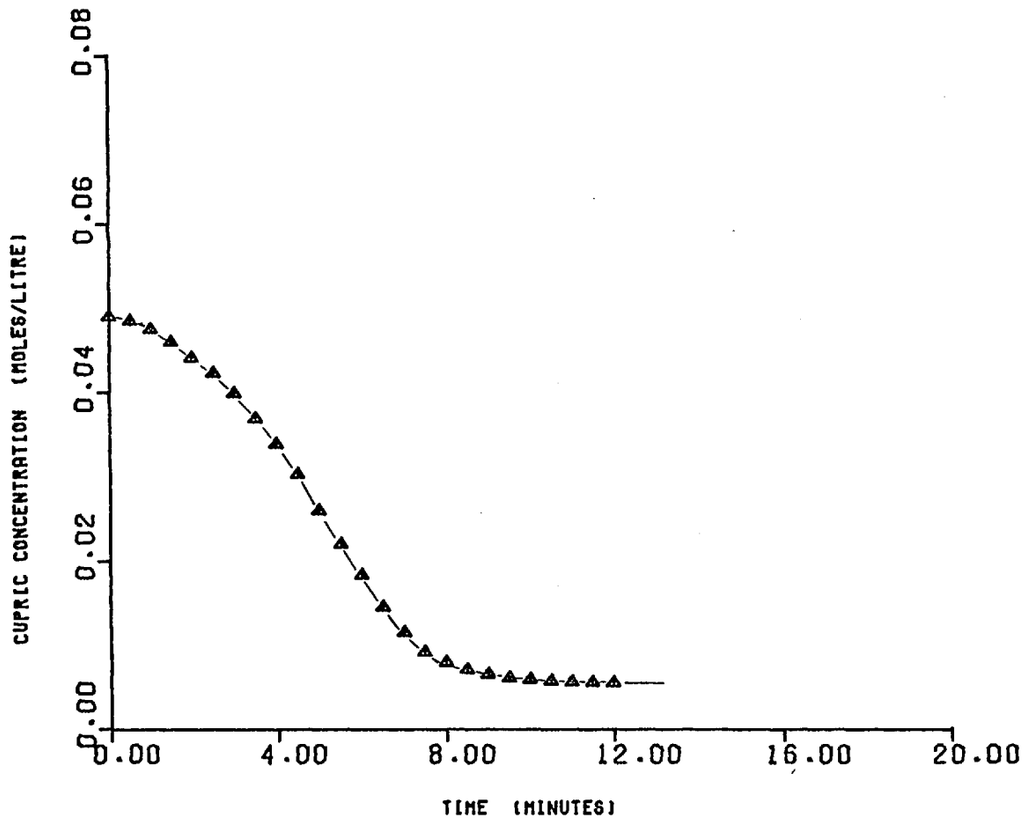


FIGURE 3.1.xxxii.





CONDITIONS OF REACTION :

Initial pressure :	500 p.s.i. $\pm$ 5.0 p.s.i. total
	400 p.s.i. $\pm$ 5.0 p.s.i. hydrogen
Temperature :	140°C $\pm$ 1.0°C
Initial cupric concentration :	0.04905 molar
Total acetate concentration :	6.41132 molar
Total ammonium concentrate :	1.71263 molar
Initial pH :	4.0

PRODUCT OF THE REDUCTION REACTION :

Precipitation of reduction product commenced at 13.00 minutes after the initiation of the reaction. The solid reduction product was metallic copper.

RATE CONSTANT :

The rate constant was found to be :

$$k_h = 0.33251 \pm 0.02474$$

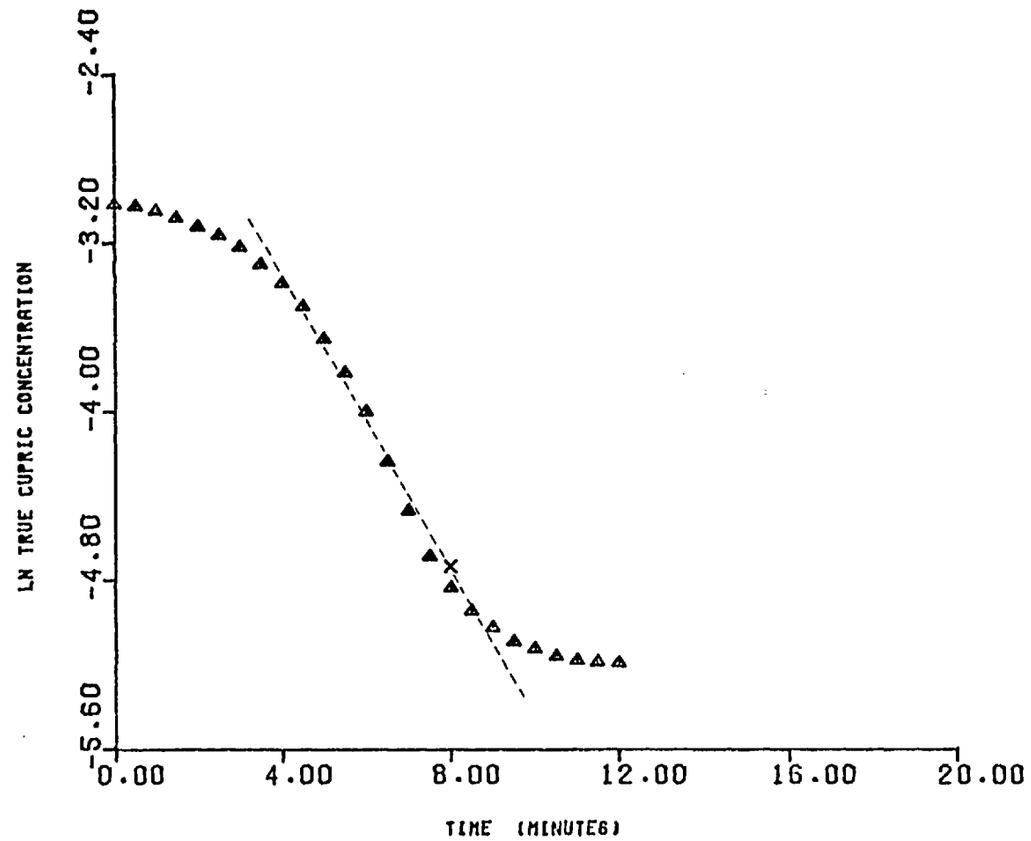
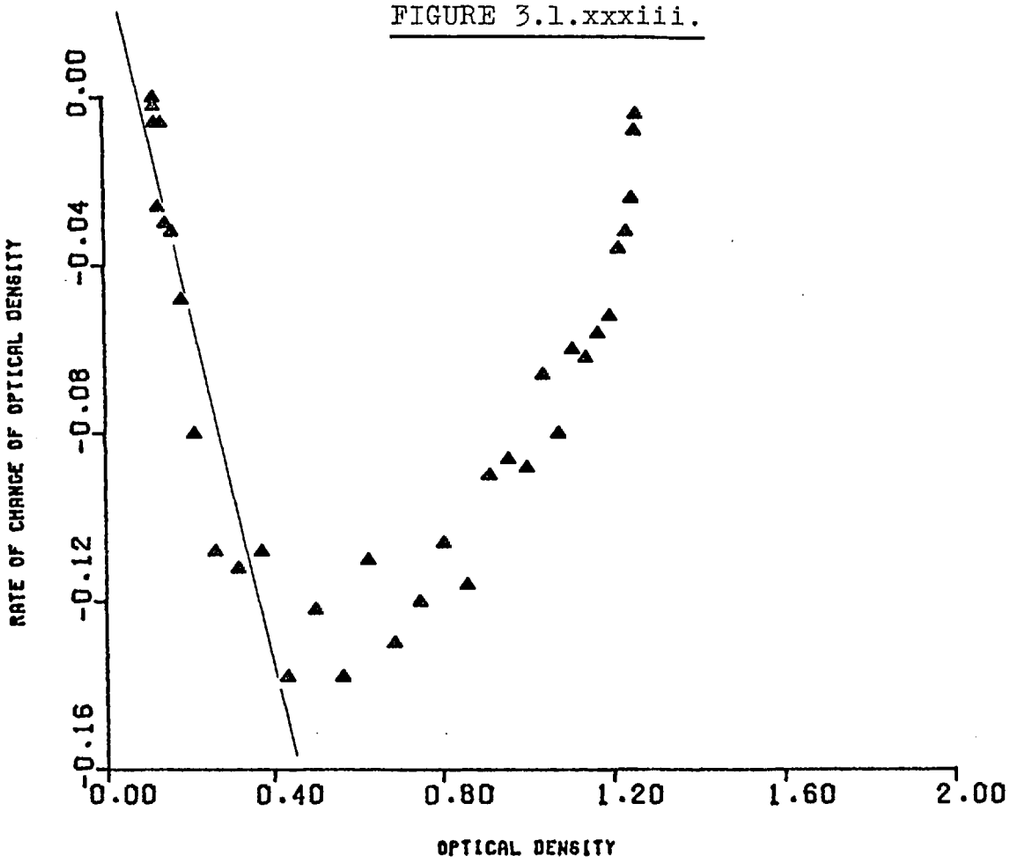
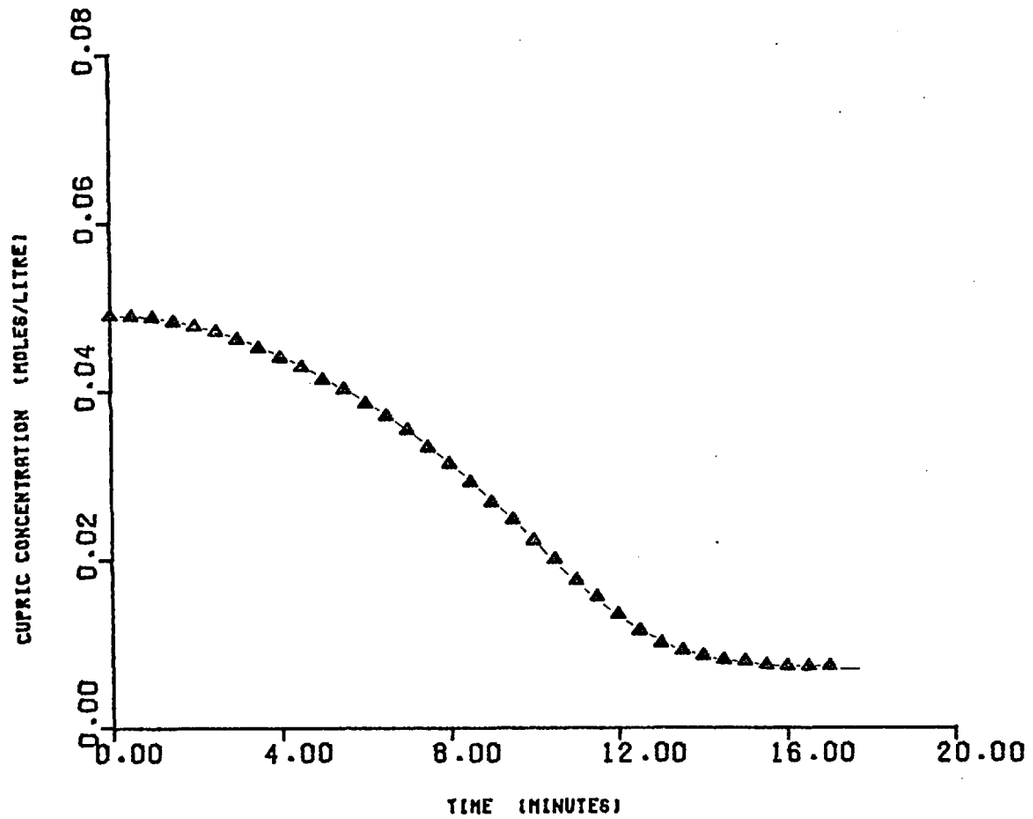


FIGURE 3.1.xxxiii.





CONDITIONS OF REACTION :

Initial pressure :	500 p.s.i. ± 5.0 p.s.i. total
	400 p.s.i. ± 5.0 p.s.i. hydrogen
Temperature :	130°C ± 1.0°C
Initial cupric concentration :	0.04905 molar
Total acetate concentration :	6.41132 molar
Total ammonium concentrate :	1.71263 molar
Initial pH :	4.0

PRODUCT OF THE REDUCTION REACTION :

Precipitation of reduction product commenced at 17.10 minutes after the initiation of the reaction. The solid reduction product was metallic copper.

RATE CONSTANT :

The rate constant was found to be :

$$k_h = 0.23068 \pm 0.01412$$

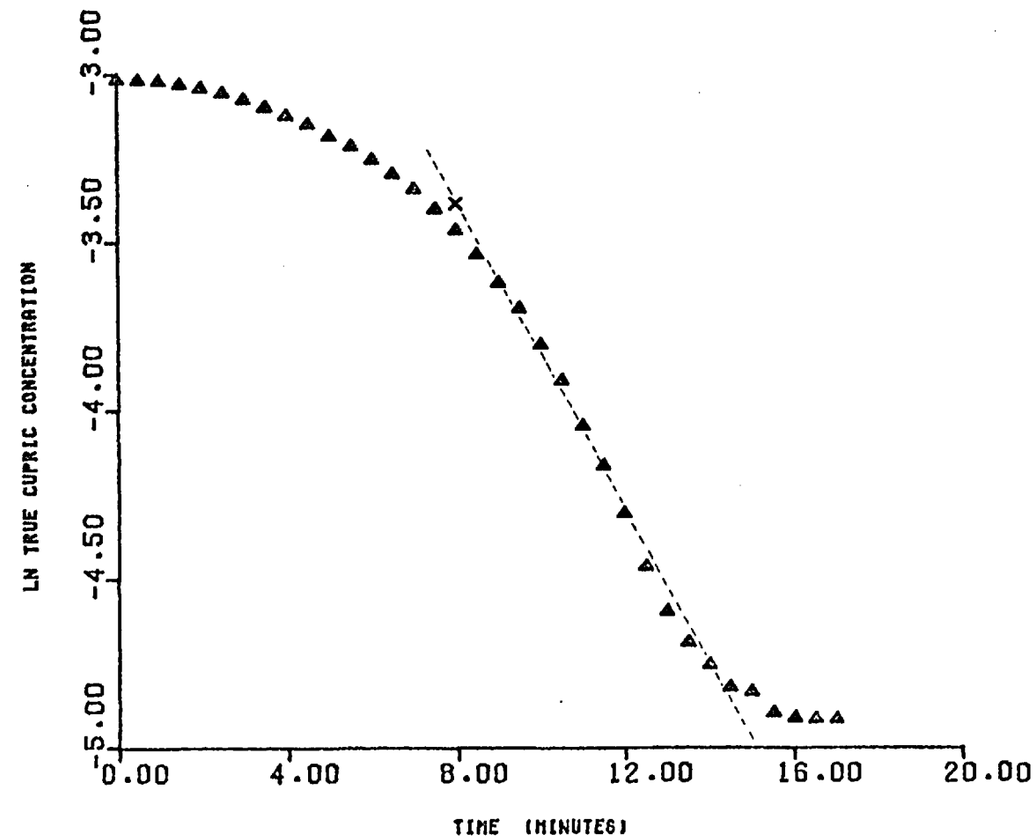


TABLE 3.T.i.

The times at which changes in the rate curves of metal producing reactions occur, and a comparison with the changes of gradient of the pressure drop curves.

Concentrations (Molar.)		Temperature. °C.	Times at which changes occured. (Minutes.)					
			Steady reaction.	End of the 1st. portion.	Formation of metal.	Discontinuities of the pressure drop curves.		
Acetate.	Cupric.					1st.	2nd.	3rd.
4.93	0.011	150		5.25	7.50			
1.83	0.013	150		2.25	5.85			
2.20	0.016	150		3.60	4.75			
2.20	0.016	150		2.70	5.00			
2.20	0.016	150		2.56	3.88			
2.10	0.015	150		3.80	5.20			
2.10	0.015	140		5.00	6.80			
6.41	0.049	150		3.00	9.20			
6.41	0.049	150	1.00	3.55	9.70	0.0	3.40	9.00
6.41	0.049	140	1.50	5.00	13.00	1.00	7.00	14.00
6.41	0.049	130	3.00	10.5	17.10	2.50	10.50	16.00

3.2. Results and discussion of the experimental investigation of cupric sulphate reduction.

3.2.i. The methods of analysing the results of the accelerating portion of the reaction.

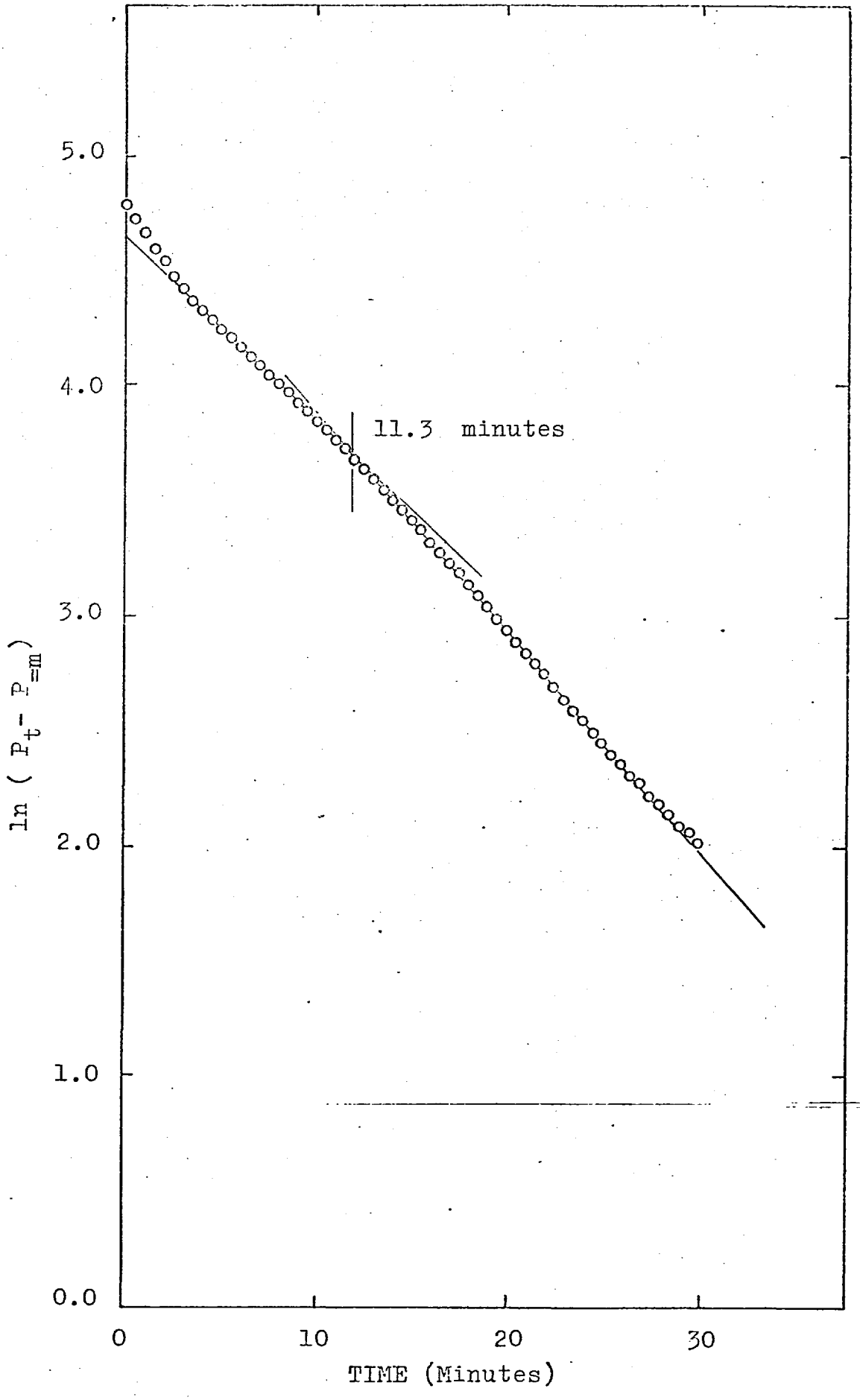
Limited investigation was performed upon the initial portion of the reaction of hydrogen gas with cupric sulphate solutions, thus no catagorical prediction as to the mechanism of the reaction could be made.

The single hydrogen use measurement which was made, in conjunction with a turbidity monitoring, was found to have an identical form to those described for the investigation of the acetate system.

The pressure drop measurements made for a cupric sulphate reaction may be seen in Figure 3.2.i. From this graph a change in gradient of the curve was observable at a point which would be very close to the time after initiation of the reaction where the cupric concentration against time curve should change from accelerating to decaying. This observation was identical to that of the acetate reduction hydrogen consumption determinations.

On this very limited information it was proposed that similar reactions would occur in the sulphate solutions as in acetate solutions if interference from corrosion products had not effected the reactions.

Figure 3.2.i.



The rate of hydrogen pressure drop during a cupric sulphate reduction reaction at 150°C

3.2.ii. The methods of analysing the results of the decaying portion of the rate curve of reduction of cupric sulphate.

Program ALFRED was also used in the analyses of data determined by measurement of the optical density change with time records produced during reduction of cupric sulphate solutions in the spectrophotometer reaction cell.

The analysis used was identical to that employed for acetate solution reduction investigation and is described in detail in section 3.1.i and in Appendix A.5.2.

The validity of the rate constants which were obtained by the method described and quoted, together with a statistical error which is one standard deviation, is dubious due to the corrosion problems encountered in the apparatus used. (As described in Appendix A.1.1. x.). However by use of the technique linearity was observed for the expression:

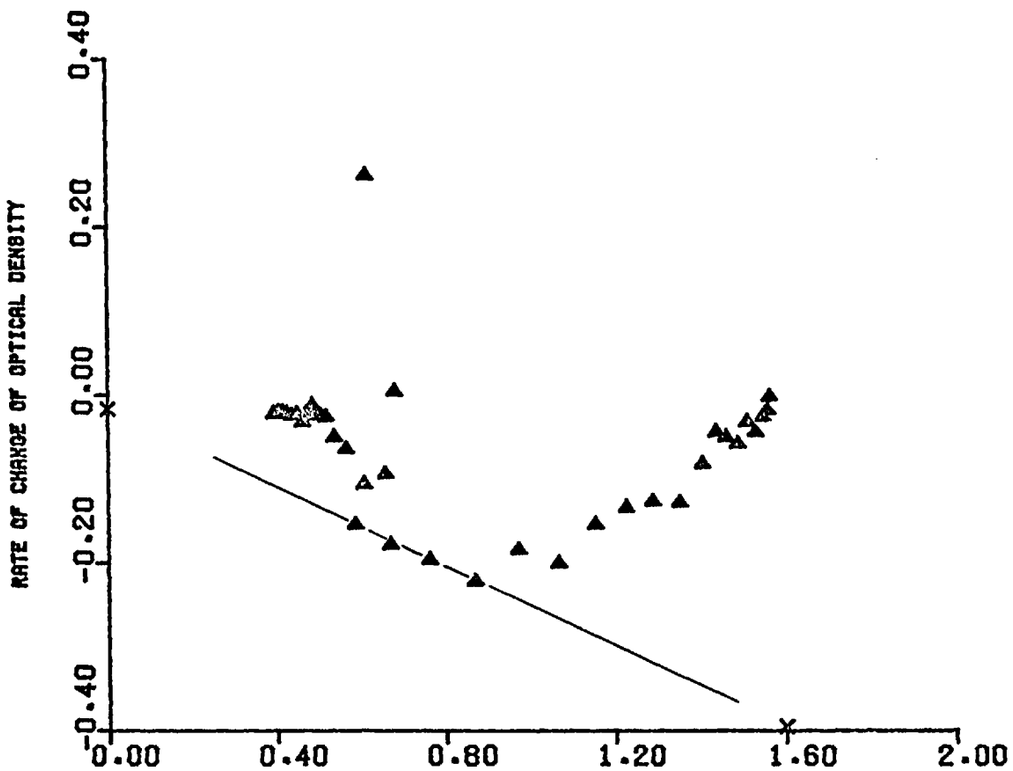
$$-\frac{d[Cu^{2+}]}{dt} = k_h [Cu^{2+}]$$

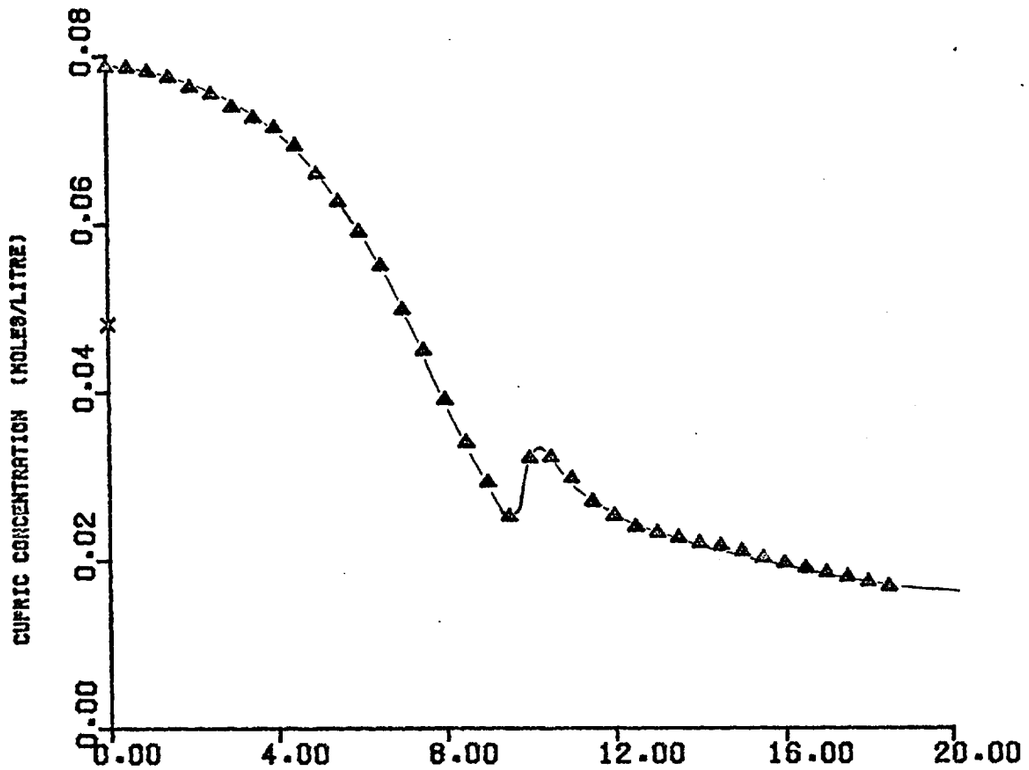
Eq. 3.1.xiii.

for the second portion of the reaction.

Plotted results of change of cupric concentration with time, change of rate of change of optical density with optical density and $\log_e$ cupric concentration with time are displayed in figures 3.2.ii. to 3.2.xi.

FIGURE 3.2.ii.





CONDITIONS OF REACTION :

Gas pressure held constant at: 670 p.s.i. ± 10 p.s.i. total.
600 p.s.i. ± 10 p.s.i. hydrogen.

Temperature : 150°C ± 2.0°C .

Initial cupric concentration : 0.0787 molar.

Initial solution volume : 90 mls.

Initial pH (25°C) : 2.17

Final pH (25°C) (After 13.4 mins.)
1.37

PRODUCT OF THE REDUCTION REACTION:

The solid reduction product was metallic copper.

RATE CONSTANT :

The calculated rate constant was :

$$k_h = 0.2856 \pm 0.0030 .$$

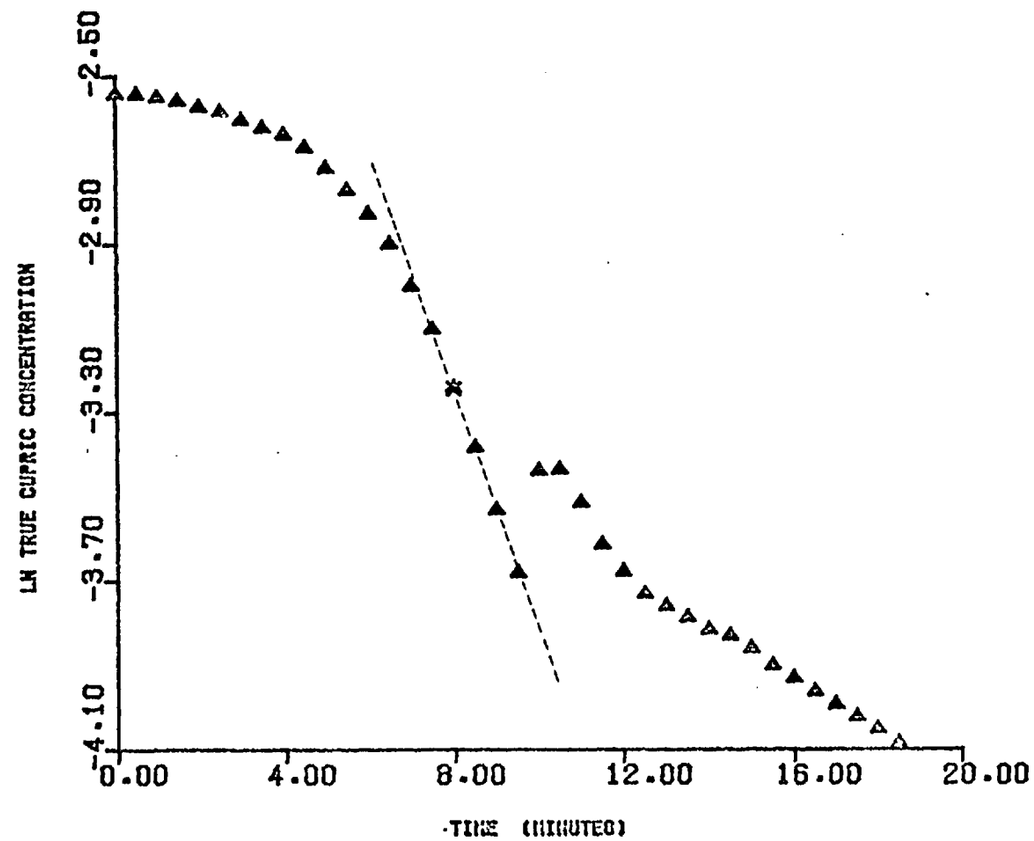
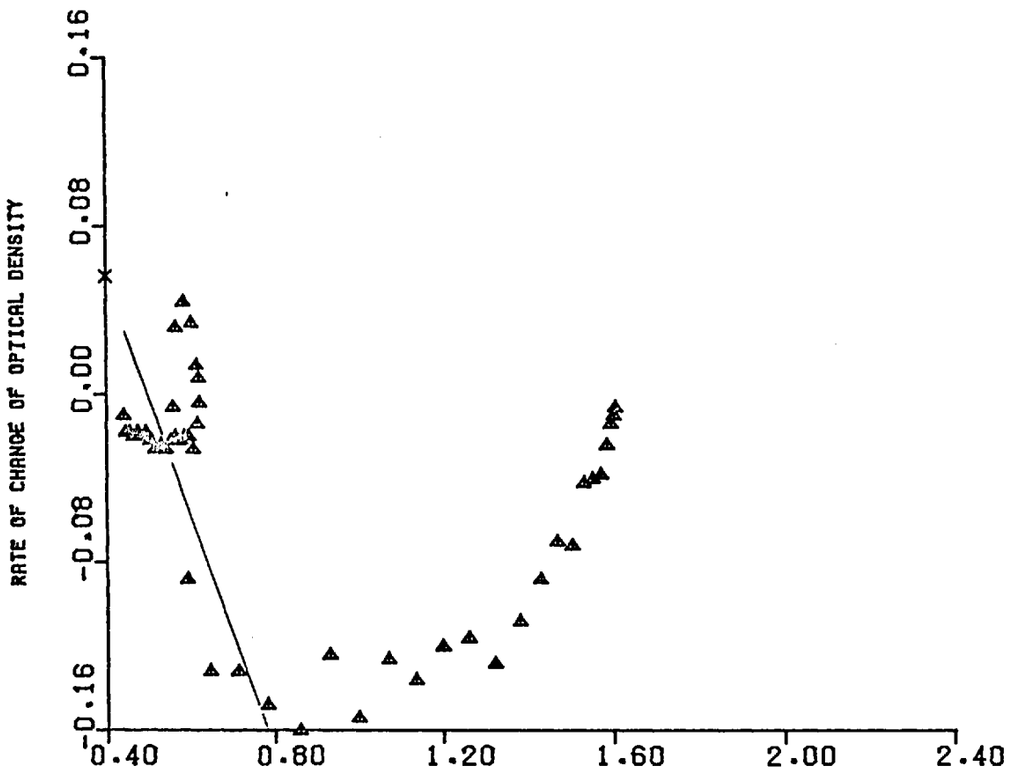
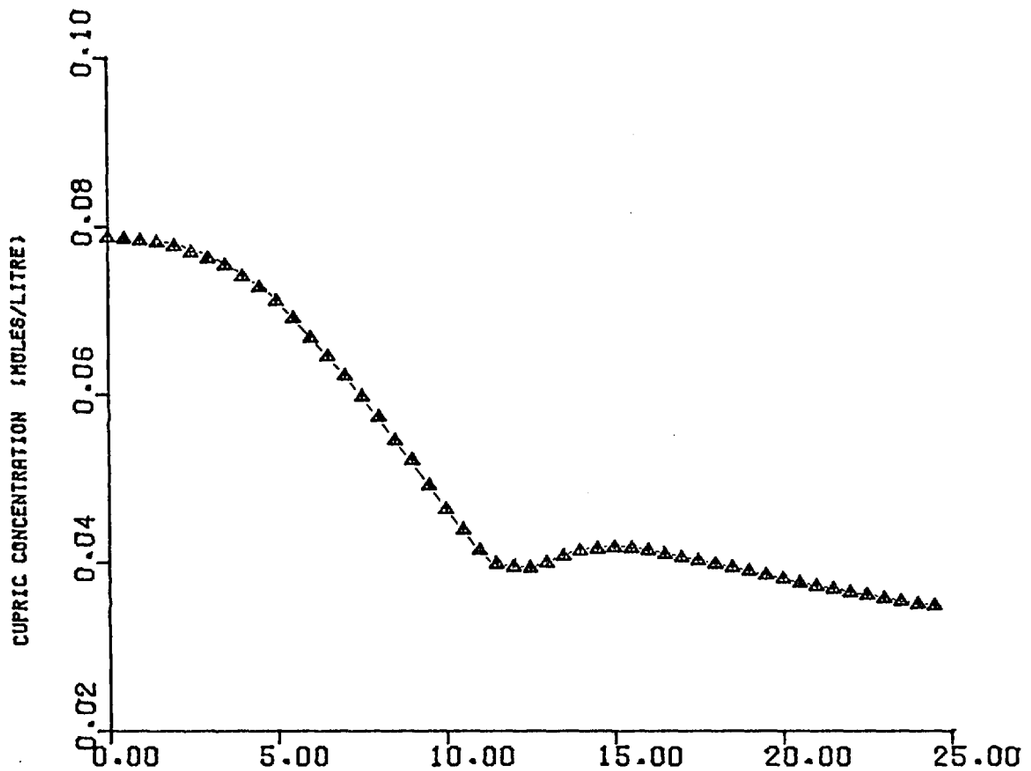


FIGURE 3.2.iii.





CONDITIONS OF REACTION :

Gas pressure held constant at: 670 p.s.i. $\pm$ 10 p.s.i. total.
600 p.s.i. $\pm$ 10 p.s.i. hydrogen.

Temperature : $150^{o}C \pm 2.0^{o}C$.

Initial cupric concentration : 0.0787 molar.

Initial solution volume : 90 mls.

Initial pH ($25^{o}C$) : 2.18 .

Final pH ($25^{o}C$) : 1.238 .

PRODUCT OF THE REDUCTION REACTION :

The solid reduction product was metallic copper.

RATE CONSTANT :

The calculated rate constant was :

$$k_h = 0.0925 \pm 0.0086 .$$

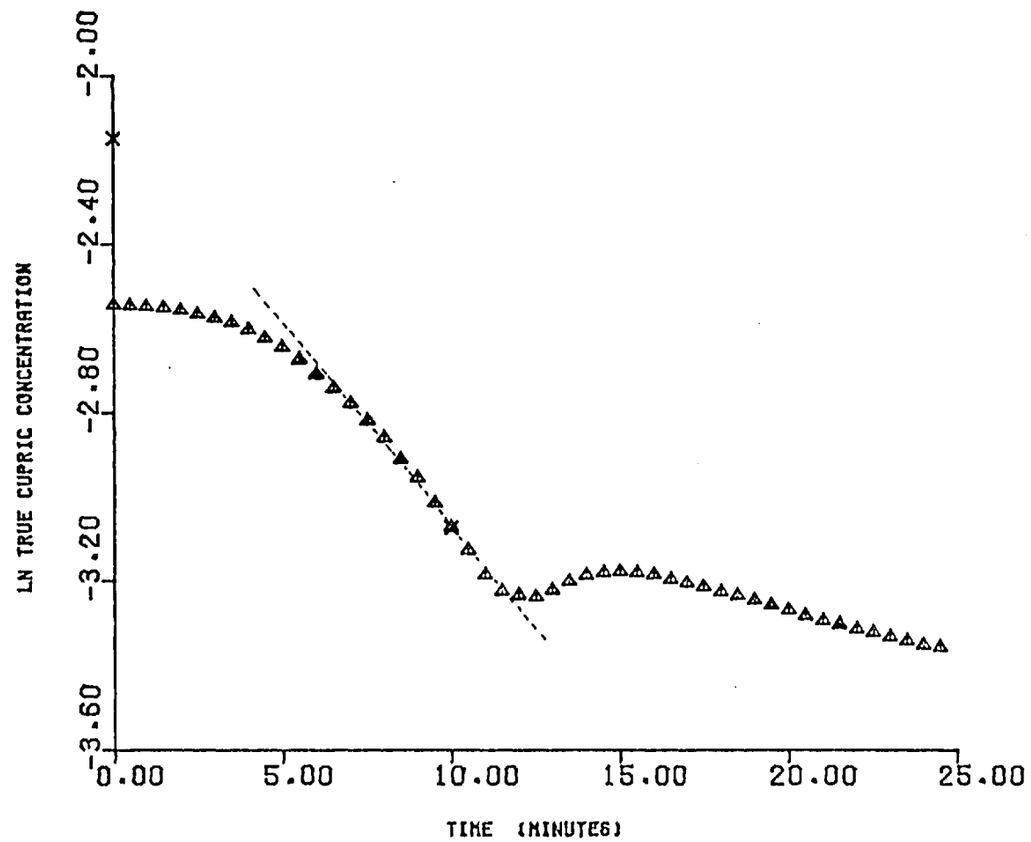
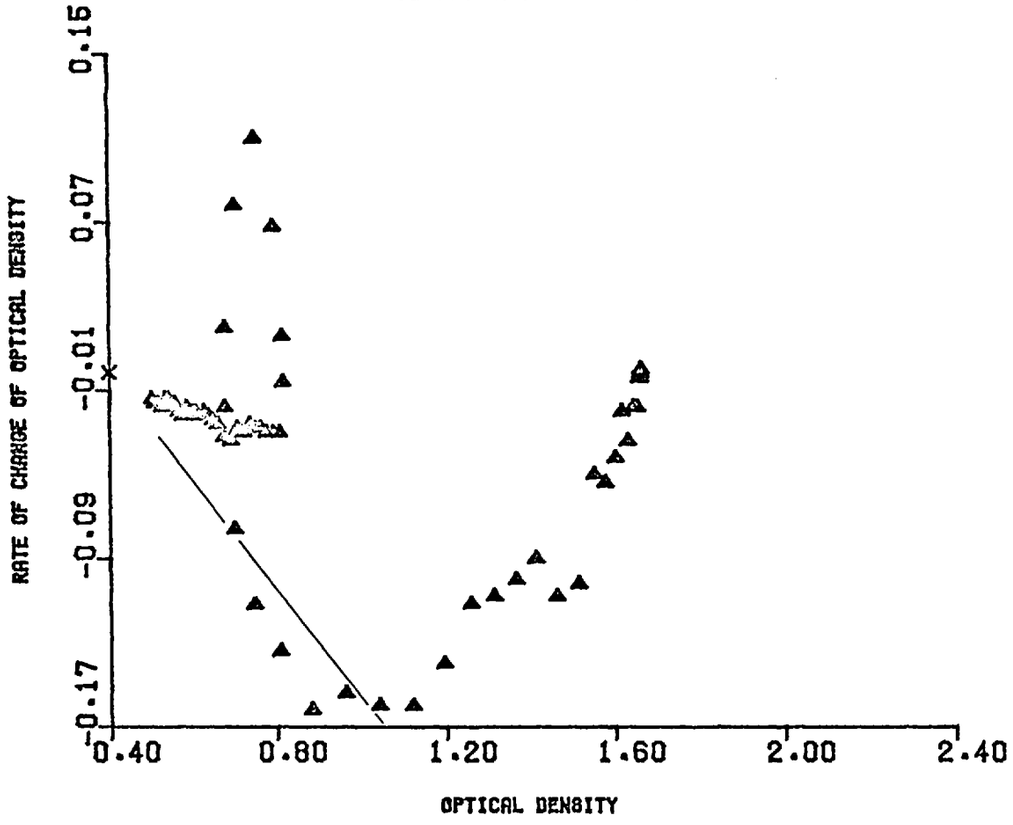
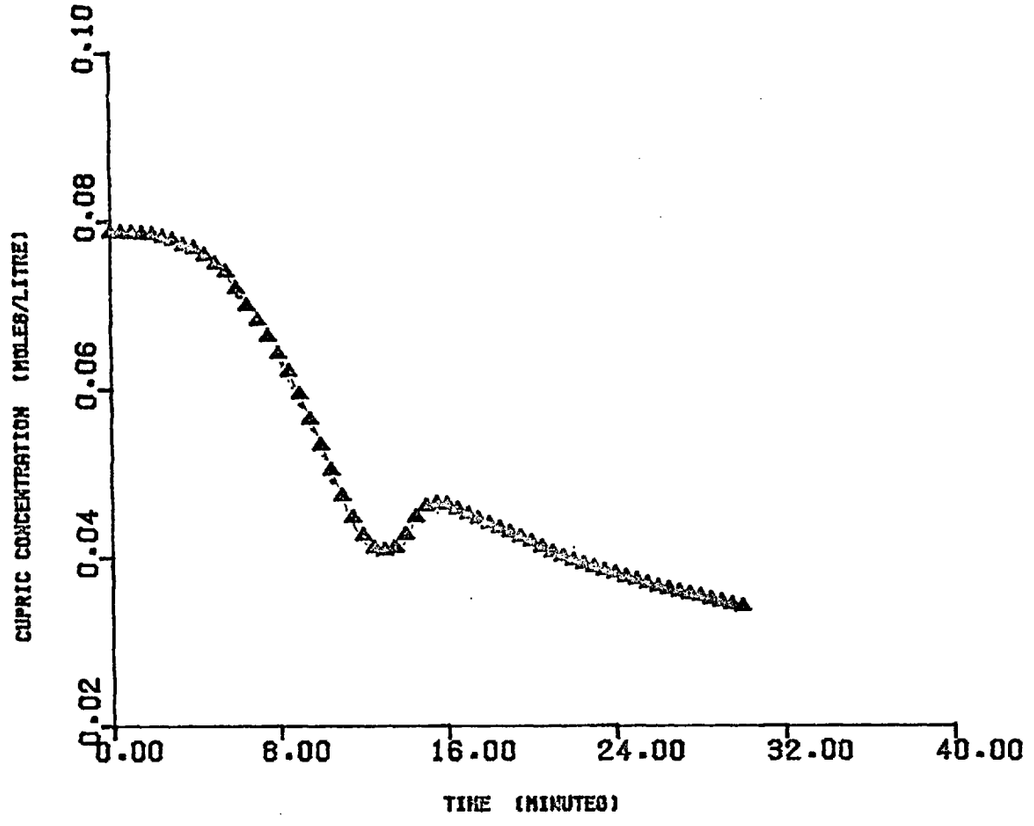


FIGURE 3.2.iv.





CONDITIONS OF REACTION :

Gas pressure held constant at; 670 p.s.i. ± 5.0 p.s.i. total.
600 p.s.i. ± 5.0 p.s.i. hydrogen.

Temperature : 150°C ± 1.0°C.

Initial cupric concentration : 0.0787 molar.

Initial volume of solution : 90 mls.

Initial pH (25°C) : 2.02

Final pH (25°C) : 1.26

PRODUCT OF THE REDUCTION REACTION.:

The solid reduction product was metallic copper.

RATE CONSTANT :

The rate constant calculated was :

$$k_h = 0.10888 \pm 0.00268.$$

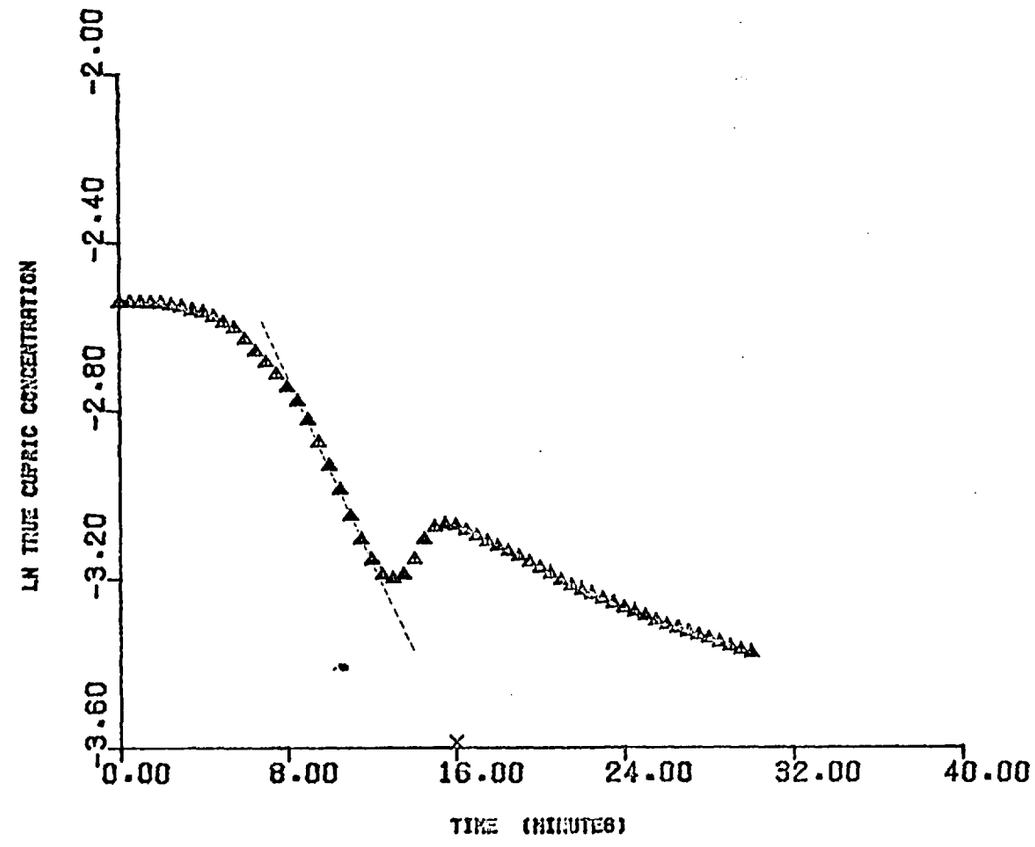
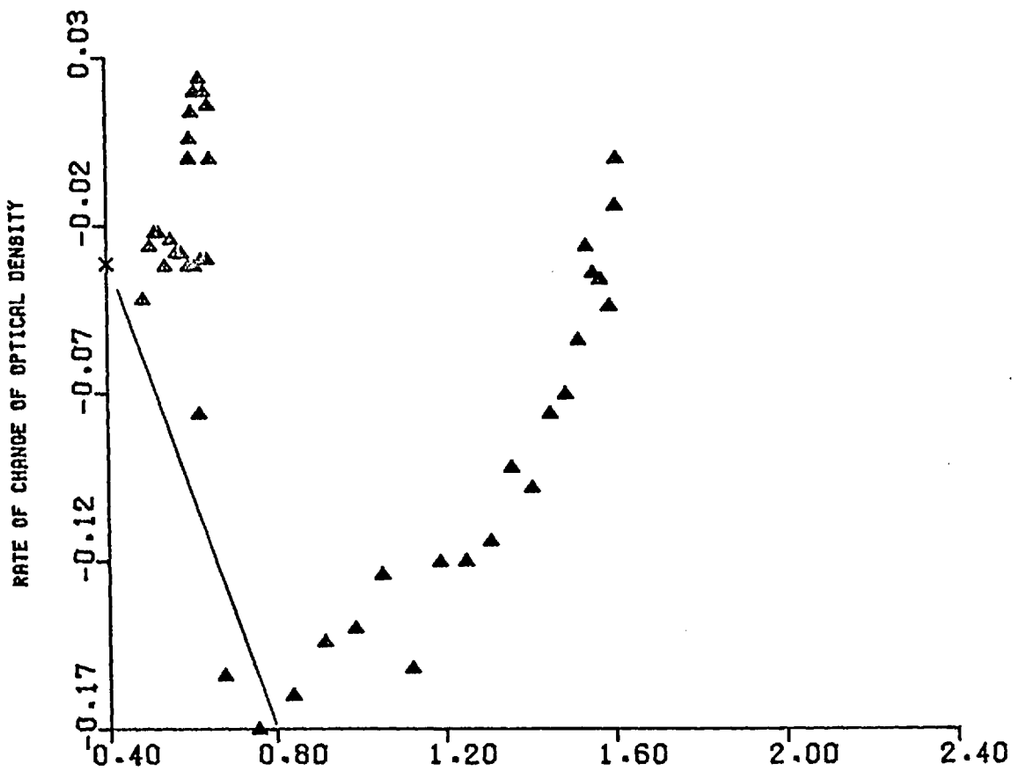
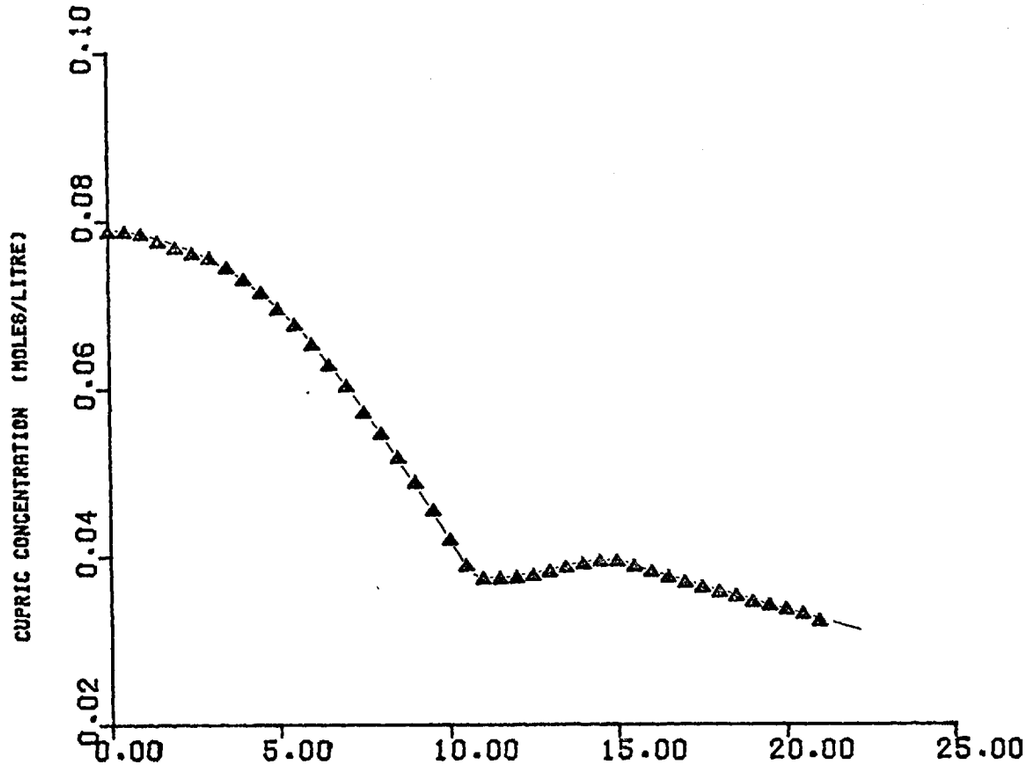


FIGURE 3.2.v.





CONDITIONS OF REACTION :

Gas pressure held constant at: 670 p.s.i. $\pm$ 10 p.s.i. total.
600 p.s.i. $\pm$ 10 p.s.i. hydrogen.

Temperature : 150°C $\pm$ 2.0°C .

Initial cupric concentration : 0.0763 molar.

Initial pH (25°C) : 2.180

Final total copper : 0.0169 molar.

Final pH (25°C) : 1.170

PRODUCT OF THE REDUCTION REACTION :

The solid reduction product was metallic copper.

RATE CONSTANT :

The calculated rate constant was :

$$k_h = 0.1527 \pm 0.0032 .$$

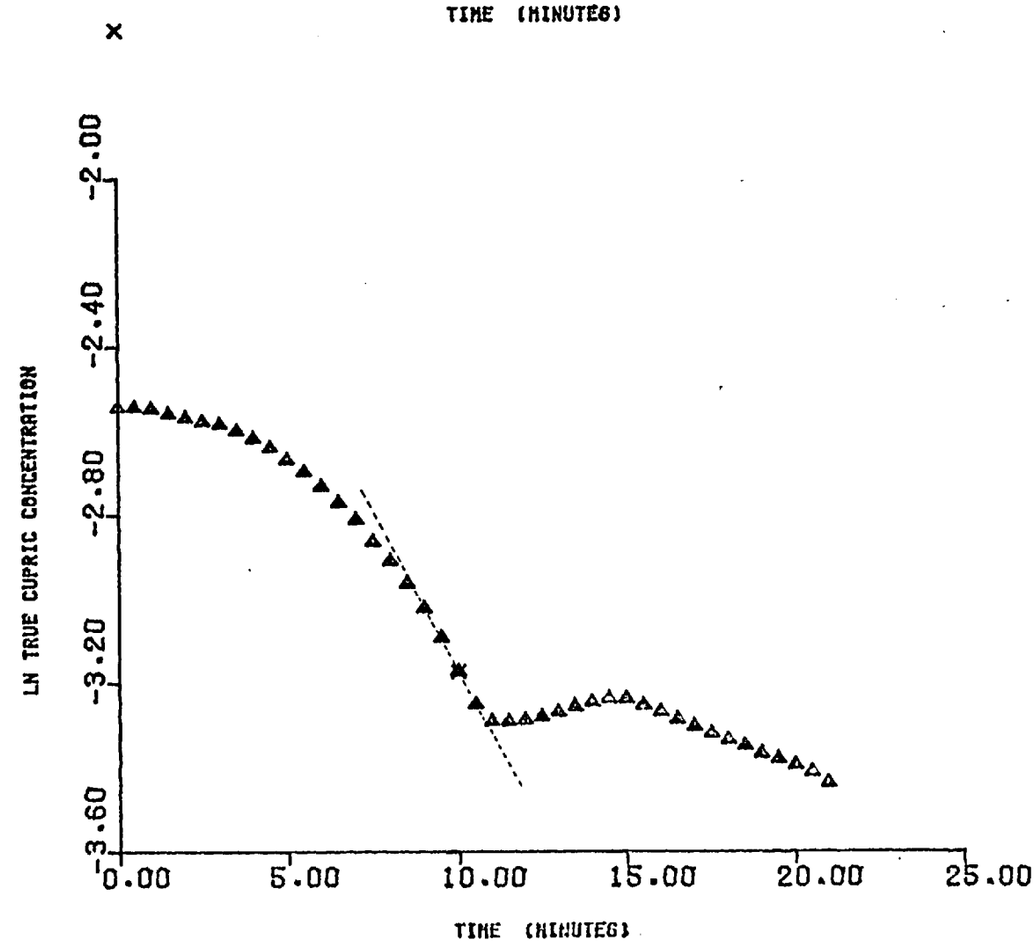
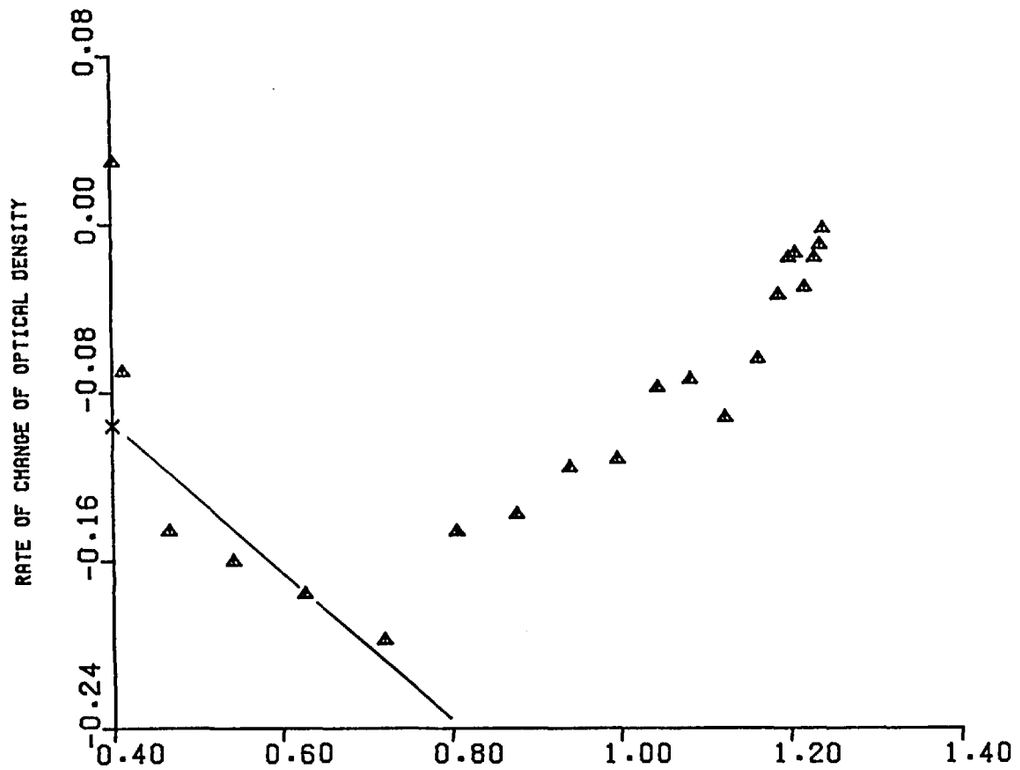
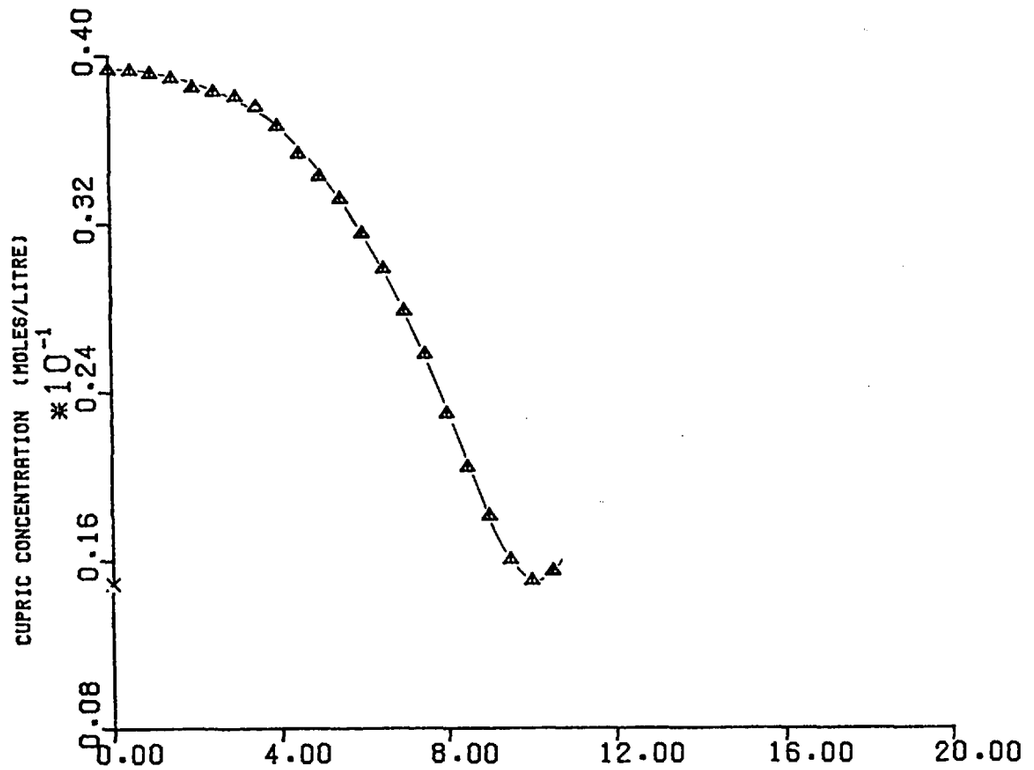


FIGURE 3.2.vi.





CONDITIONS OF REACTION :

Gas pressure held constant at: 670 p.s.i. ± 10 p.s.i. total

600 p.s.i. ± 10 p.s.i. hydrogen.

Temperature : 150°C ± 2.0°C.

Initial cupric concentration : 0.0393 molar.

Initial solution volume : 90 mls.

Initial pH (25°C) : 1.95 .

A glass stirrer was employed instead of the usual P.T.F.E. stirrer.

PRODUCT OF THE REDUCTION REACTION :

The solid reduction product was metallic copper.

RATE CONSTANT :

The calculated rate constant was :

$$k_h = 0.2374 \pm 0.0015 .$$

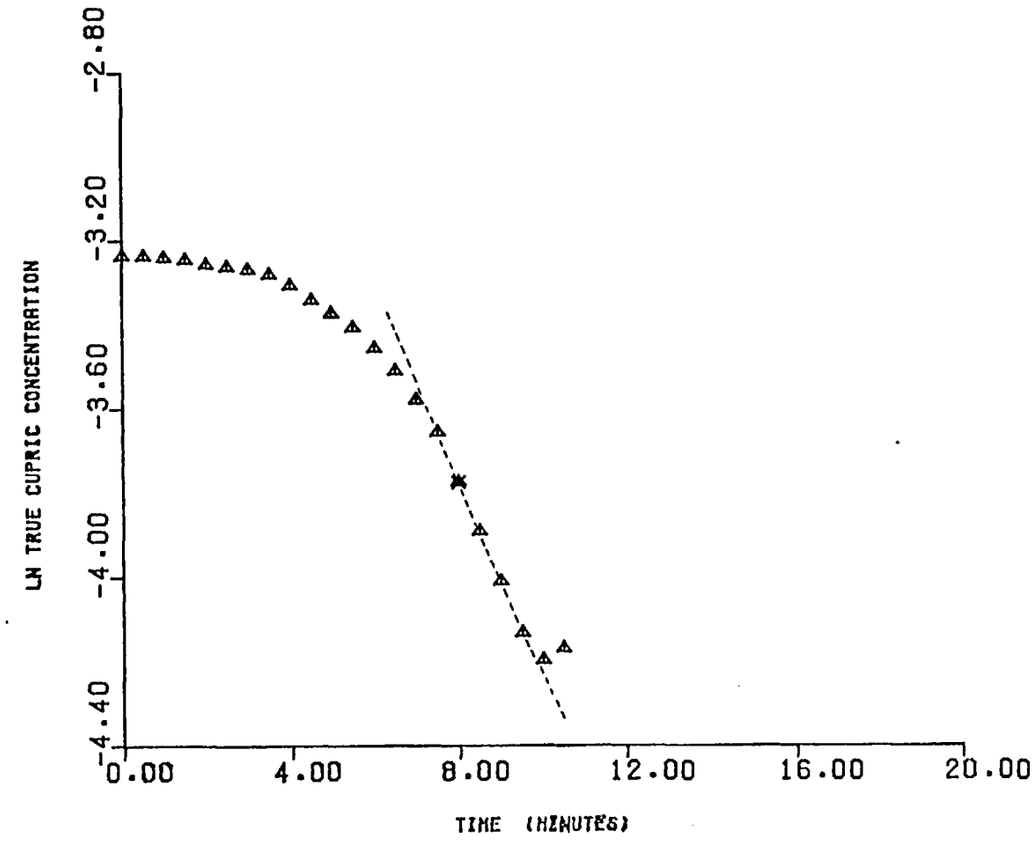
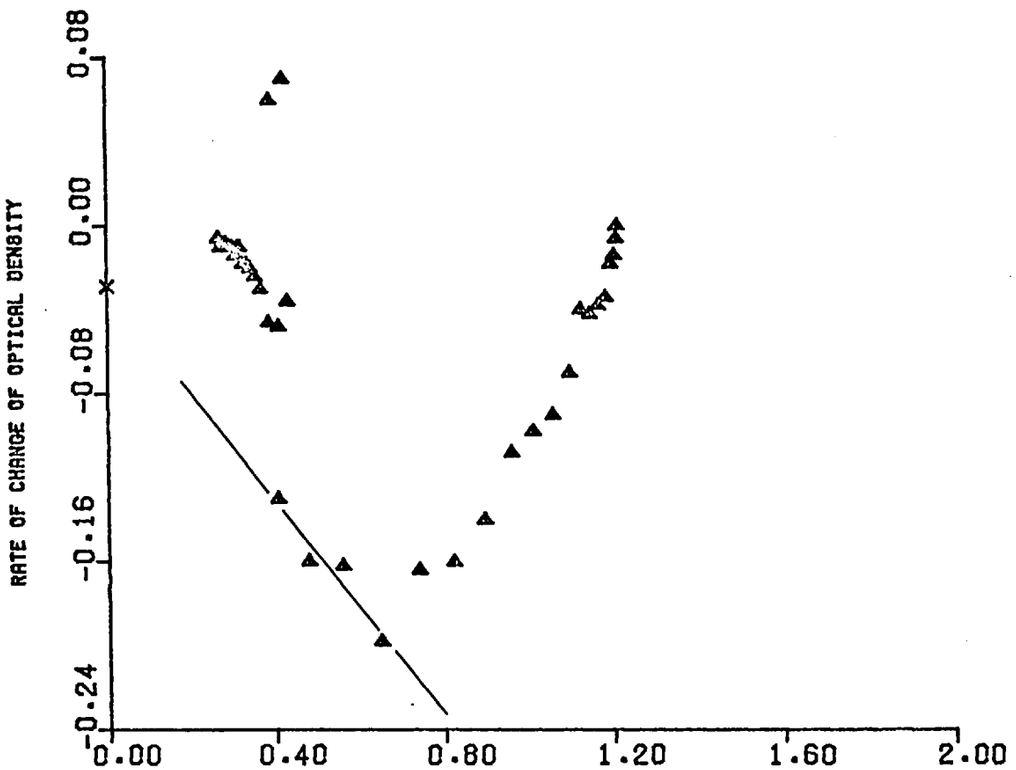
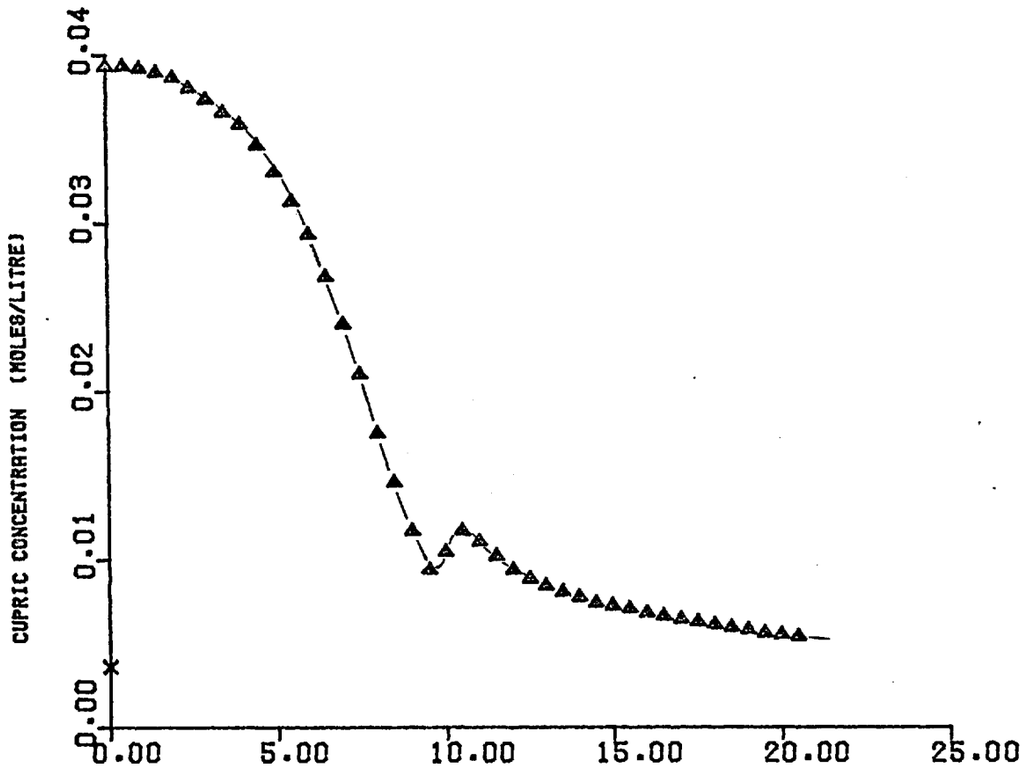


FIGURE 3.2.vii.





CONDITIONS OF REACTION :

Gas pressure held constant at: 670 p.s.i. ± 10 p.s.i. total.
600 p.s.i. ± 10 p.s.i. hydrogen.

Temperature : 150°C ± 2.0°C.

Initial cupric concentration : 0.0393 molar.

Initial solution volume : 90 mls.

Initial pH (25°C) 1.95

PRODUCT OF THE REDUCTION REACTION :

The solid reduction product was metallic copper.

RATE CONSTANT :

The calculated rate constant was :

$$k_h = 0.3874 \pm 0.0122 .$$

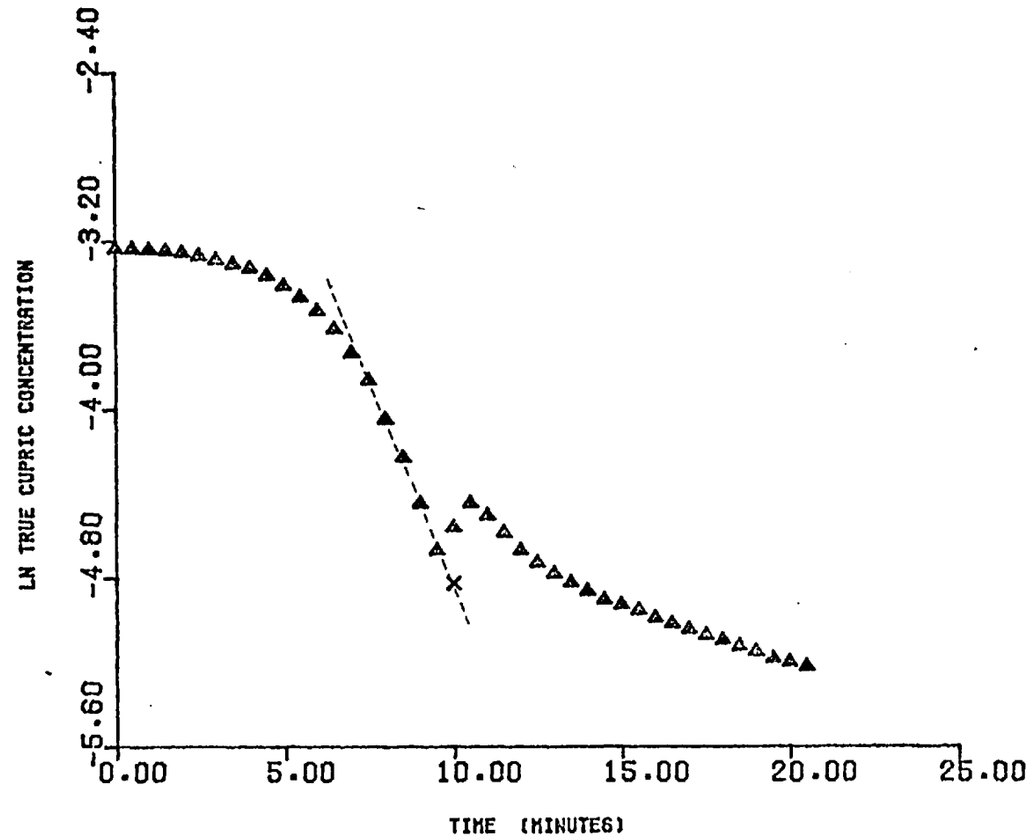
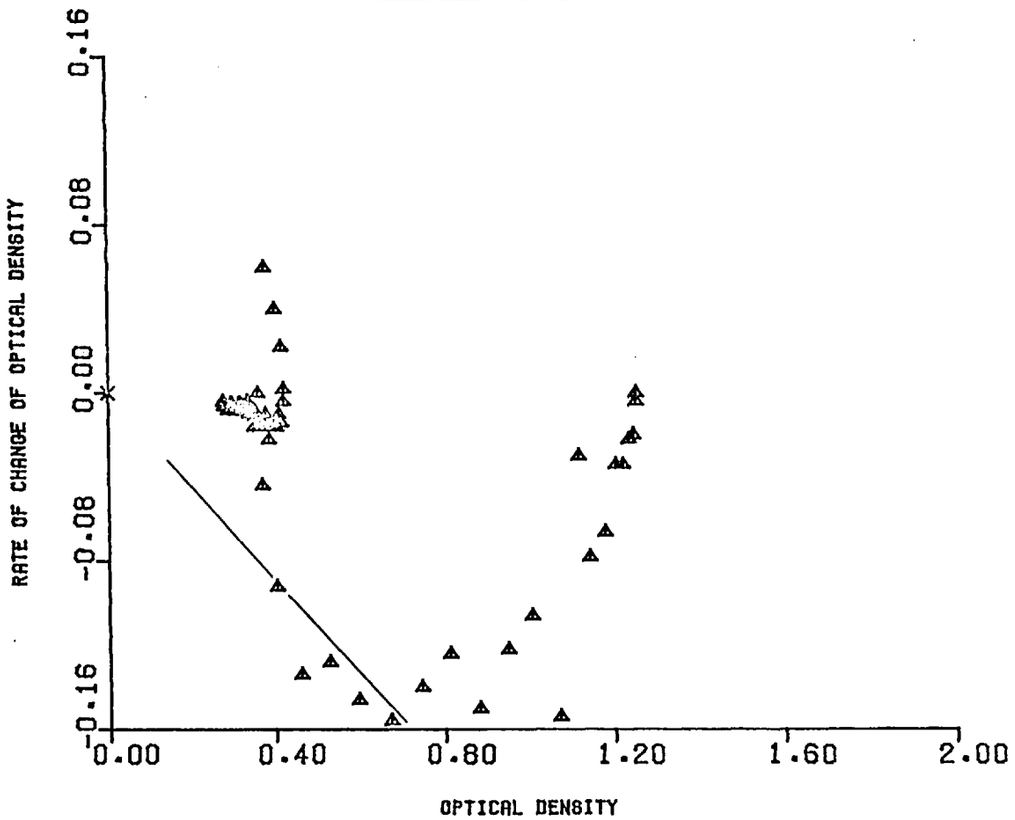
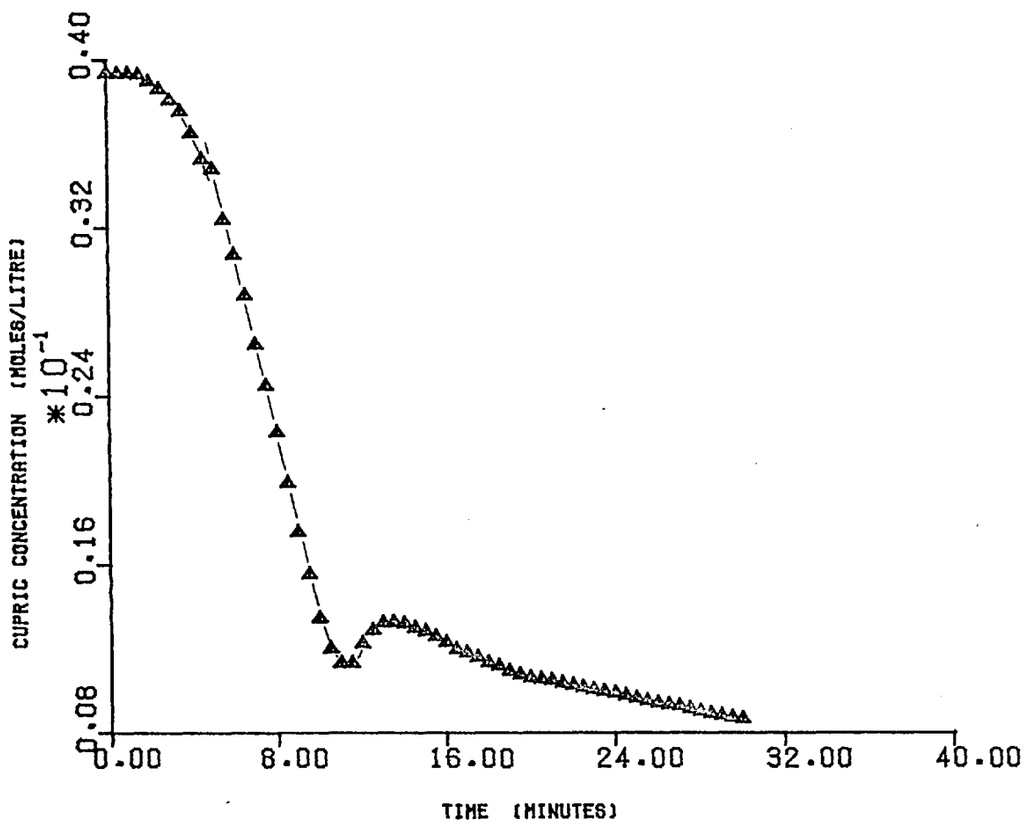


FIGURE 3.2.viii.





CONDITIONS OF REACTION :

Gas pressure held constant at: 670 p.s.i. ± 10 p.s.i. total.
600 p.s.i. ± 10 p.s.i. hydrogen.

Temperature : 150°C ± 2.0°C.

Initial cupric concentration : 0.0393 molar.

Initial pH (25°C) : 1.95

Final pH (25°C) (After standing in the presence of copper powder for 3 days) : 1.60

PRODUCT OF THE REDUCTION REACTION :

The solid reduction product was metallic copper.

RATE CONSTANT :

The calculated rate constant was :

$$k_h = 0.24261 \pm 0.00547 .$$

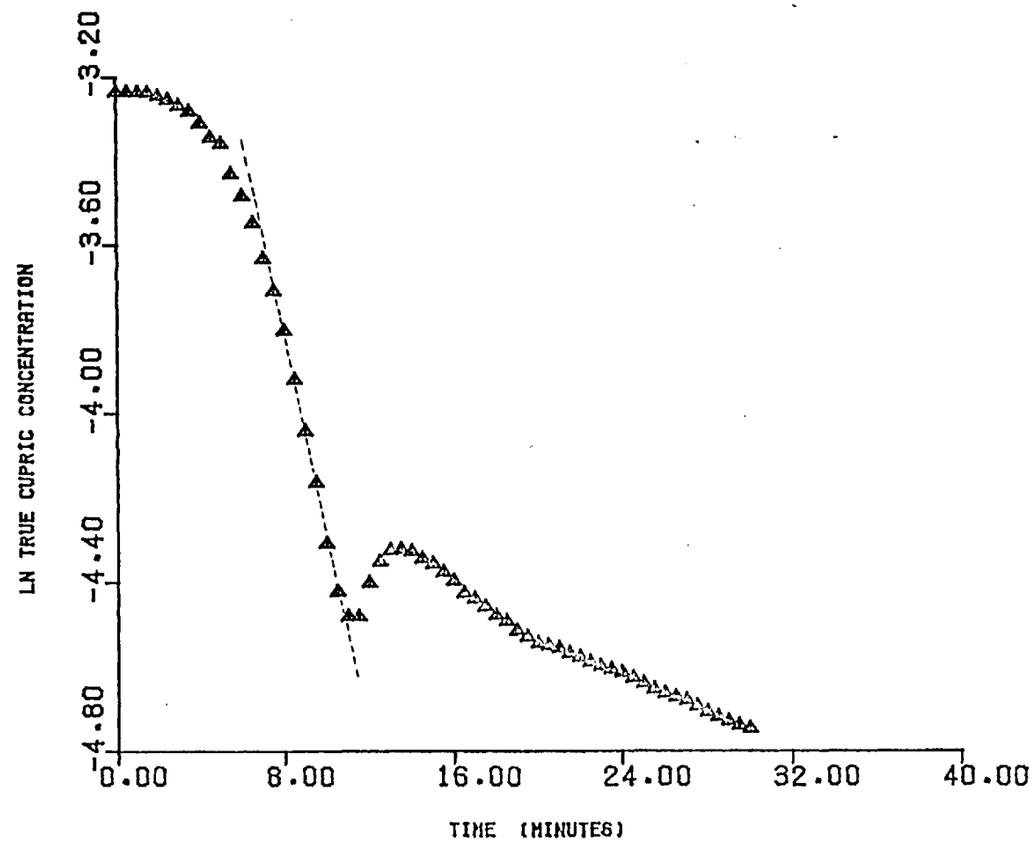
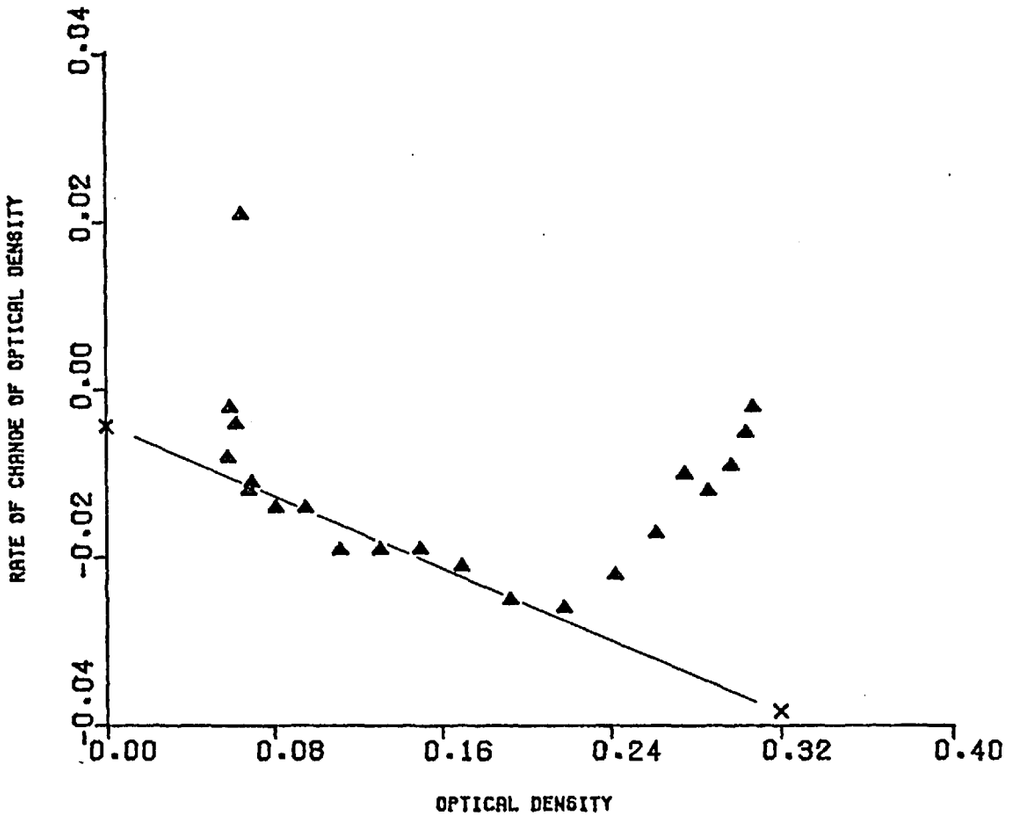
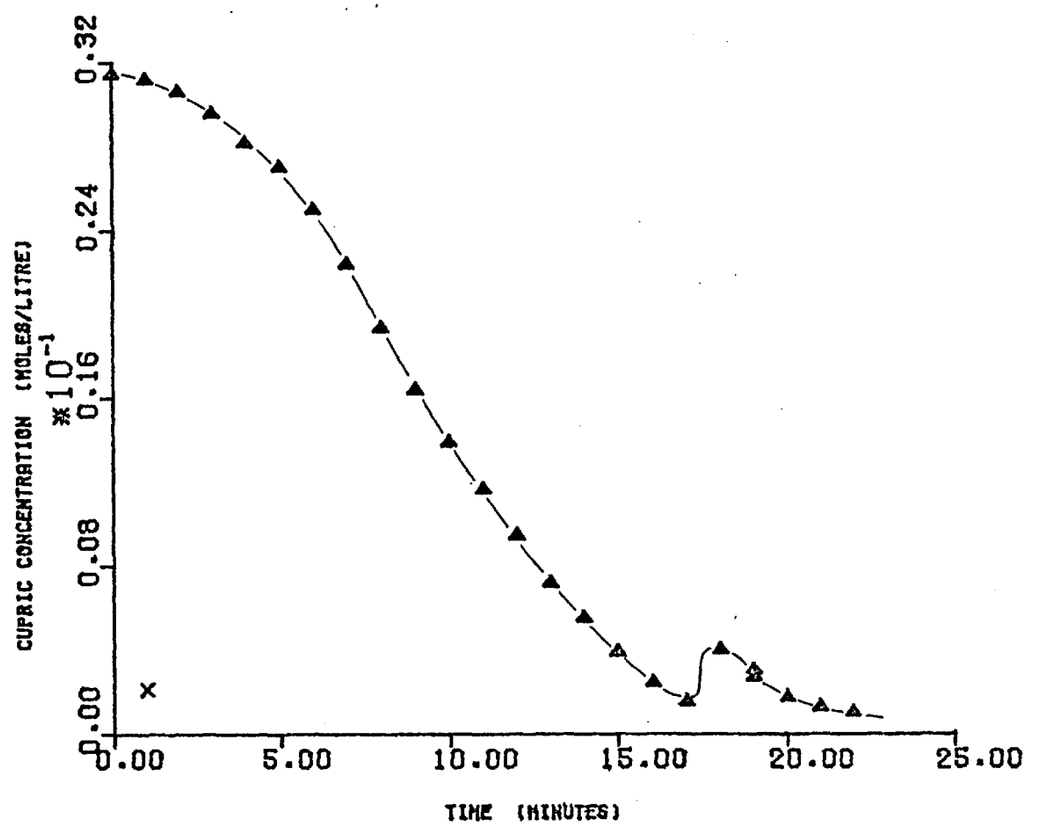


FIGURE 3.2.ix.





CONDITIONS OF REACTION :

Gas pressure held constant at: 670 p.s.i. ± 10 p.s.i. total.
600 p.s.i. ± 10 p.s.i. hydrogen.

Temperature : 150°C ± 2.0°C.

Initial cupric concentration : 0.0315 molar.

Initial pH (25°C) : 2.28

Final total copper : 0.0068 molar.

PRODUCT OF THE REDUCTION REACTION :

The solid reduction product was metallic copper.

RATE CONSTANT :

The calculated rate constant was :

$$k_h = 0.2467 \pm 0.0166 .$$

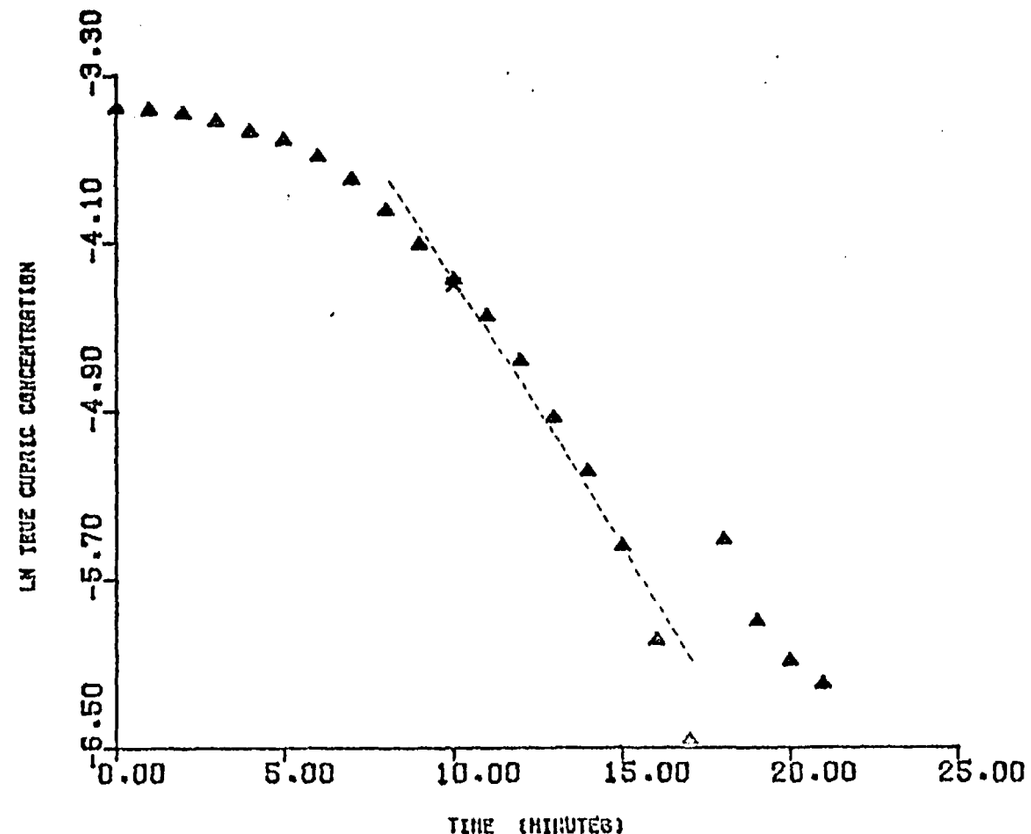
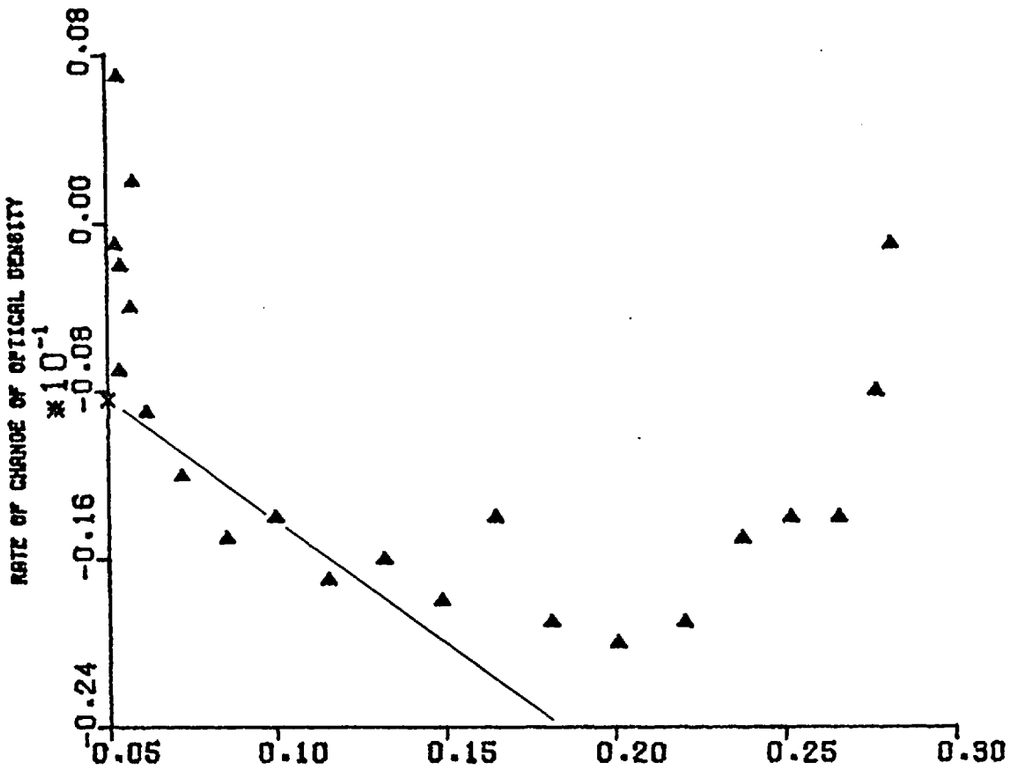
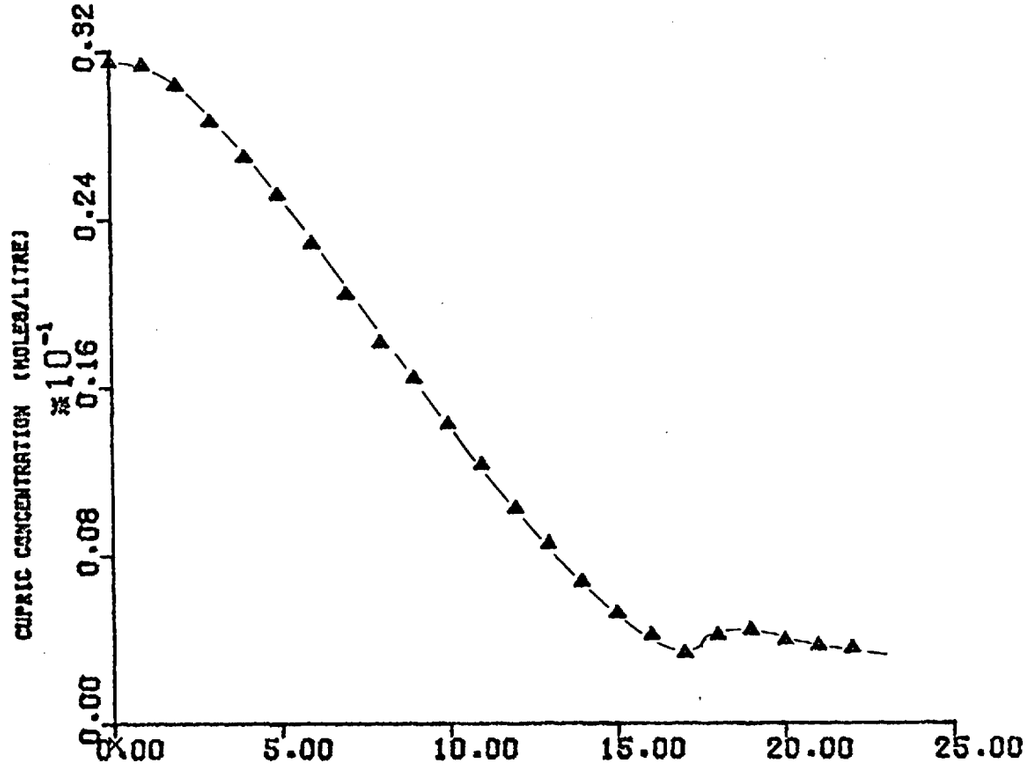


FIGURE 3.2.x.





CONDITIONS OF REACTION :

Gas pressure held constant at: 670 p.s.i. ± 10 p.s.i. total.
600 p.s.i. ± 10 p.s.i. hydrogen.

Temperature : 150°C ± 1.0°C .

Initial cupric concentration : 0.0315 molar.

Initial pH (25°C) : 2.28

Final total copper : 0.0050 molar.

PRODUCT OF THE REDUCTION REACTION :

The solid reduction product was metallic copper.

RATE CONSTANT :

The calculated rate constant was :

$$k_h = 0.2061 \pm 0.0080 .$$

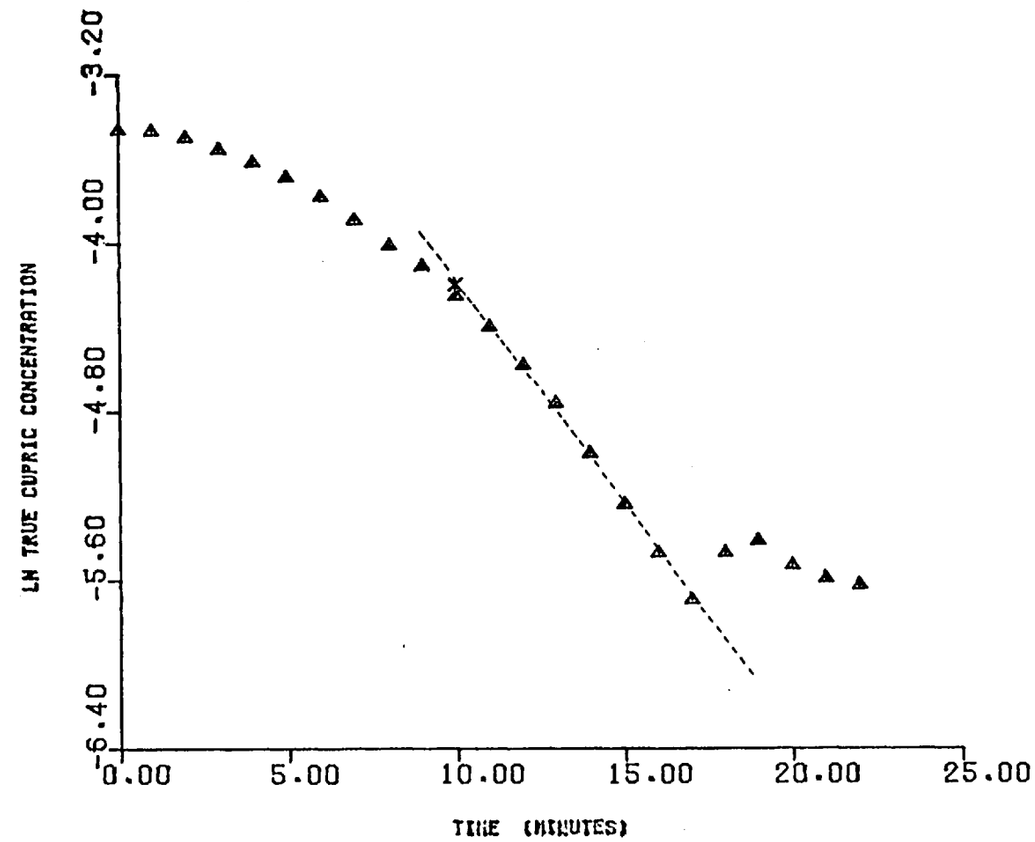
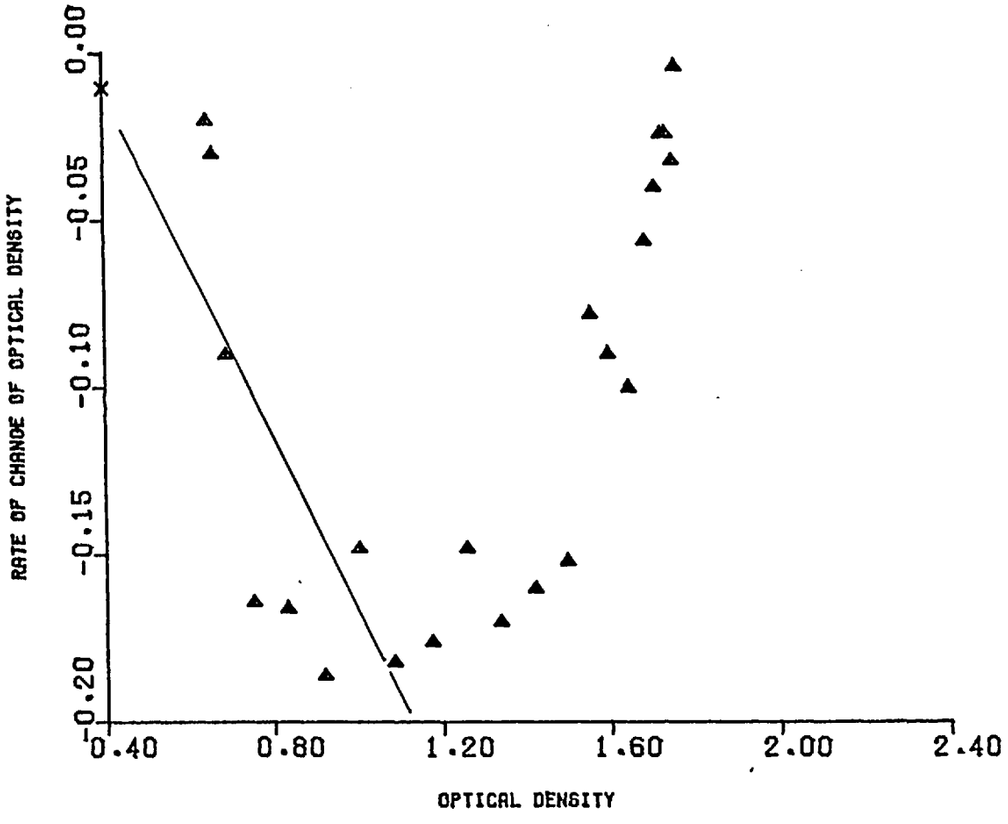
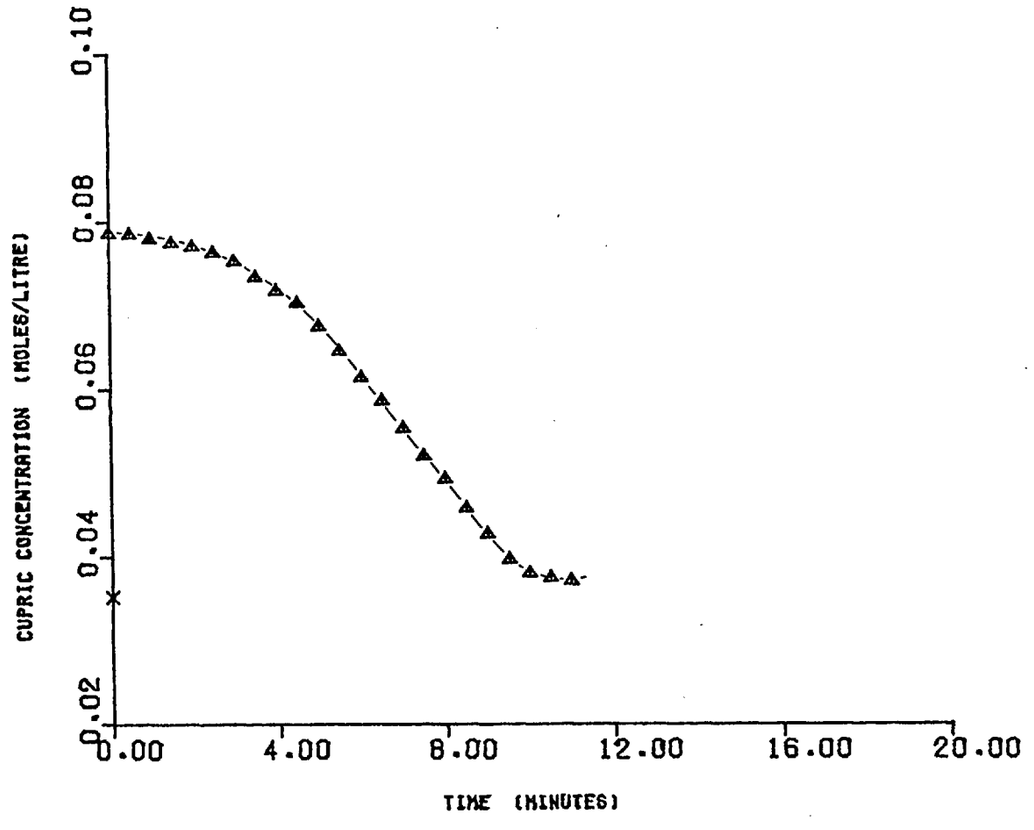


FIGURE 3.2.xi.





CONDITIONS OF REACTION :

Gas pressure held constant at: 670 p.s.i. ± 5 p.s.i. total.
600 p.s.i. ± 5 p.s.i. hydrogen.

Temperature : 150°C ± 2.0°C .

Initial cupric concentration : 0.0787 molar.

Initial solution volume : 90 mls.

Initial pH (25°C) : Approximately 1.5 .

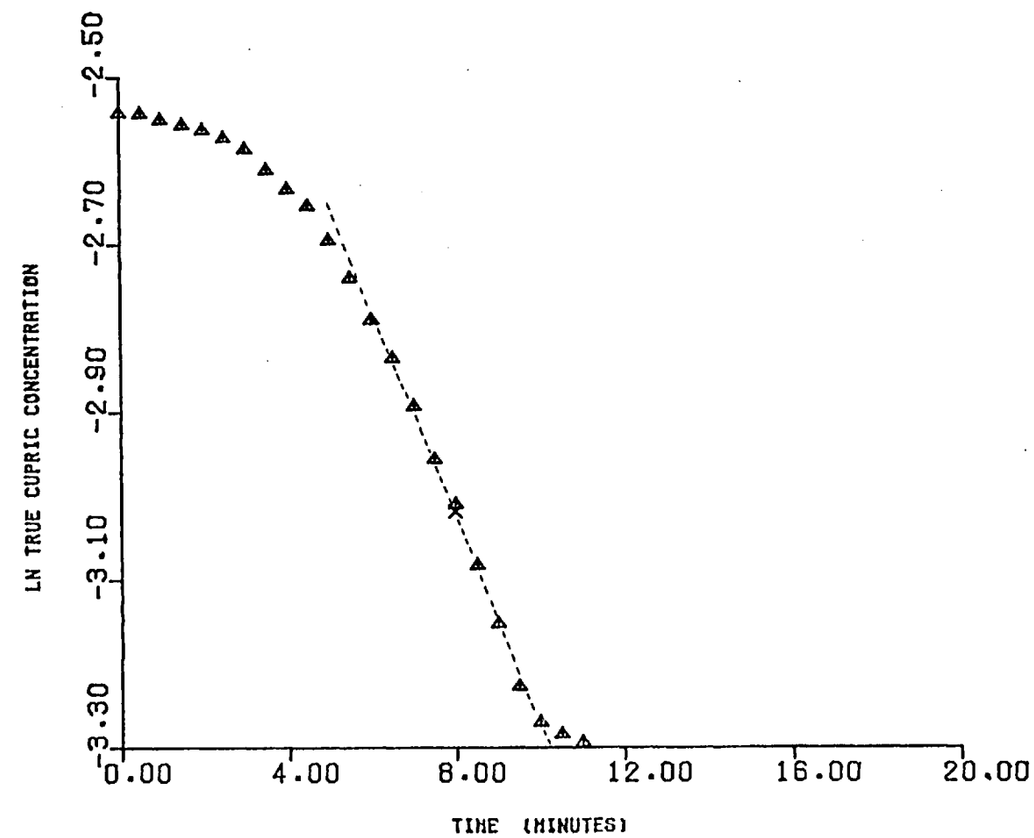
Very rapid corrosion occured at the end of the reaction as may be seen sketched in Figure 2.4.i.

Final pH (25°C) : Approximately 1.6.

RATE CONSTANT :

The calculated rate constant was :

$$k_h = 0.1202 \pm 0.0048 .$$



3.3. Discussion of information determined from the results used and analyses employed.

3.3.i. a)

The significance of the rate constants obtained, and mechanism proposal for the accelerating portion of cupric acetate reduction.

The rate constants which were determined for the accelerating portion of cupric acetate reduction reaction, by the method described in section 3.i.i. may be seen in a tabulated form in Table 3.T.ii.

From this information an Arrhenius plot was made, and thus an apparent activation energy for the first stage of the reaction could be determined.

The graph of $\log_e k_o$ against T^{-1} ('T' being the temperature in ^oK) may be seen in Figure 3.3.i. From the gradient of the line of this graph the Arrhenius activation energy was found to have a value of 1.906 K Joule. mole $^{-1}$.

The linearity of the Arrhenius plot, over the three points considered, can be seen to be very accurate. This observation gives support to the proposed mechanism of the reaction.

From the data analytical method used for the first part of the reaction the following equation, as an overall reaction may be proposed to be applicable over the considered time range:

$$Cu^{2+}_{spec.} + \tfrac{1}{2} H_2 \xrightarrow{\frac{1}{2}k_o} Cu^{1+}_{spec.} + H^+$$

Eq. 3.i.vii

The rate of reaction being directly dependent upon the presence of molecular hydrogen at the reaction sites in the solution.

$$- \frac{d [Cu^{2+}]}{d t} = k_o [H_2]_{solution}$$

Eq. 3.1.xi.

This was the premise upon which the analysis was based, and which appears to have been shown to be valid.

The reaction equation may be more acceptably re-written with the inclusion of an assumed intermediate species, hydrogenated cuprous ions or cupric hydride, the existence of which has been proposed by previous workers. (Van Hahn & Peters)(26)

$$Cu^{2+}_{spec.} + H_2 \xrightarrow{k'_o} CuH^+ + H^+$$

Eq. 1.4.ii

cupric species — hydrogenated cuprous species

$$CuH^+ + Cu^{2+}_{spec} \xrightarrow{k''_o} 2\, Cu^+_{spec.} + H^+$$

Eq. 1.4.iii

cuprous species.

Under these proposed reactions agreement with the premises used in the data analyses continues to exist. If k''_o is fast compared to k'_o then the

control of the reaction could remain to be with the presence of hydrogen molecules at the reaction sites. Also the cupric species removed from solution remains twice the hydrogen used by the reaction.

If k_o'' was large, the rate of reaction would be dependent upon the rate of formation of the hydrogenated cuprous ions, since the cupric concentration was large over the whole of the accelerating range of the reaction. Thus the formation of the hydrogenated species would be controlled in the first reaction by hydrogen concentration in the solution.

3.3.i. b)

The significance of the rate constants obtained, and the mechanism proposal for the decaying portion of cupric acetate reductions.

From the rate constants obtained by the data analyses method described in section 3.1.ii., using program Alfred, for reactions occuring under the same conditions apart from a temperature variation, Arrhenius activation energy values could be determined.

Table 3.T. iii. shows the values of the apparent activation energys obtained, together with the rate constants and the temperature of each of the

reactions studied.

Figures 3.3.ii. to 3.3.v. are the Arrhenius plots obtained from the available data.

The treatment of the data used, in program Alfred, assumed dependence of the rate of reaction upon the remaining cupric concentration in the solution. The linearity of the plotted results indicate that this assumption was legitimate, thus it may be proposed that the reaction kinetics do in fact obey the expression:

$$-\frac{d[Cu^{2+}]}{dt} = k_h[Cu^{2+}] \qquad \text{Eq. 3.1.xiii.}$$

It is also proposed that the reaction which occurs during the decaying portion of the reduction is the same as that proposed for the accelerating part. Instead of the rate being controlled by the presence of hydrogen at the reaction site it is controlled by the availability of cupric species.

The reactions proposed for the first part were:

$$Cu^{2+}_{spec.} + H_{2\,solution} \longrightarrow CuH^{+}_{spec.} + H^{+} \qquad \text{Eq. 1.4.ii.}$$

Followed by :

$$CuH^{+}_{spec.} + Cu^{2+}_{spec.} \xrightarrow{k''_o} 2Cu^{+}_{spec.} + H^{+} \qquad \text{Eq. 1.4.iii.}$$

where the concentration of dissolved hydrogen in the solution is greater than that required to give a steady reaction rate.

The evidence of the occurrence of the second reaction is unobtainable. The inclusion of this reaction during the second portion of the reduction does not agree with the rate expression, since two cupric ions are then used in one overall reaction. It must be assumed therefore that the proposed second half of the reaction occurs only when the reaction rate is controlled by the concentration of hydrogen. This proposal may be seen to be supported by the way in which the elemental copper precipitation occurs, as described in section 3.4.ii.

The reason for the decrease in the significance of second equation may be due to the lowering of the cupric concentration, or to the increase in the hydrogen concentration in the solution over the decaying part of the reaction compared to the accelerating part.

A first order dependence on cupric concentration was found to exist. It must be assumed that a bimolecular reaction is involved between cupric ion complexes and molecular hydrogen in the solution. The semi-reduced product must then be in the form of a cupric hydride, or hydrogenated cuprous species.

TABLE 3.T.ii

Rate constant and activation energy values for the accelerating portion of the reaction.

Temperature. (°C)	Pressure. (p.s.i.)	Rate constant	Apparent activation energy.
150	400	1.5170	
140	400	0.6194	1.9058 ±0.0126
130	400	0.2351	

TABLE 3.T.iii.

Rate constant and activation energy values for the decaying portion of the reactions.

Temperature. (°C)	Pressure (p.s.i.)	Rate constant	Apparent activation energy
110	650	0.0221	
110	650	0.0157	
120	650	0.0362	1.32
130	650	0.0212	± 0.165
130	650	0.0420	
140	650	0.1483	
150	650	0.3086	

TABLE 3.T.iii. (Cont)

Temperature (°C)	Pressure (p.s.i.)	Rate constant	Apparent activation energy
110	500	0.0097	1.34 ± 0.878
120	500	0.0091	
130	500	0.0419	
110	400	0.0168	0.65 ± 0.137
120	400	0.0285	
120	400	0.0242	
130	400	0.0336	
130	400	0.0470	
150	400	0.4219	
150	400	0.0835	
150	410	1.7232	
150	410	2.0622	
150	400	1.4765	
150	400	0.9491	
140	400	0.7008	
150	400	0.4221	0.89 ± 0.316
150	400	0.6980	
140	400	0.3325	
130	400	0.2307	

Apparent activation energy values in K Joules. Mole^{-1}

Figure 3.3.i.

Arrhenius plot for the accelerating portion of the cupric acetate reduction reaction

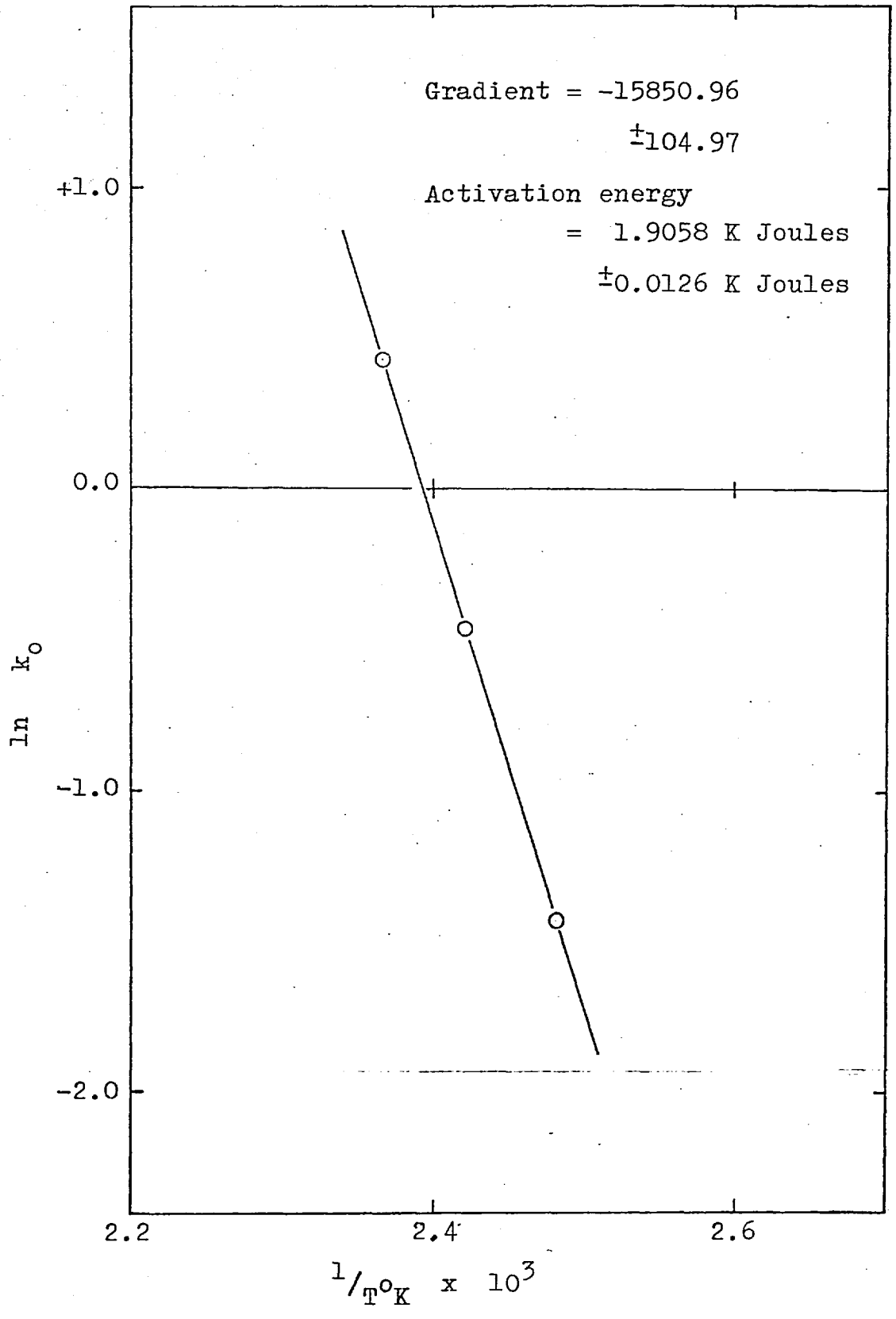
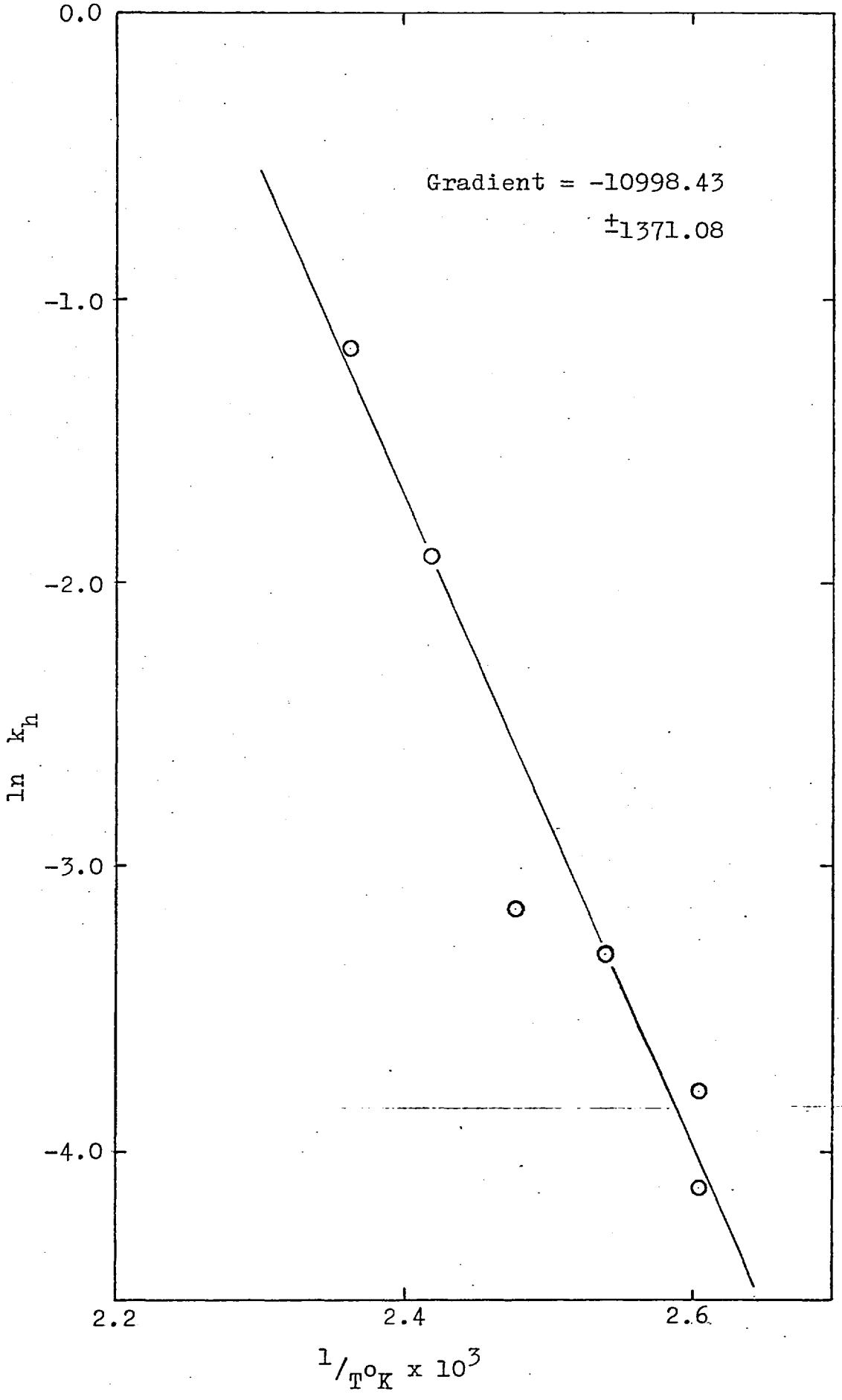
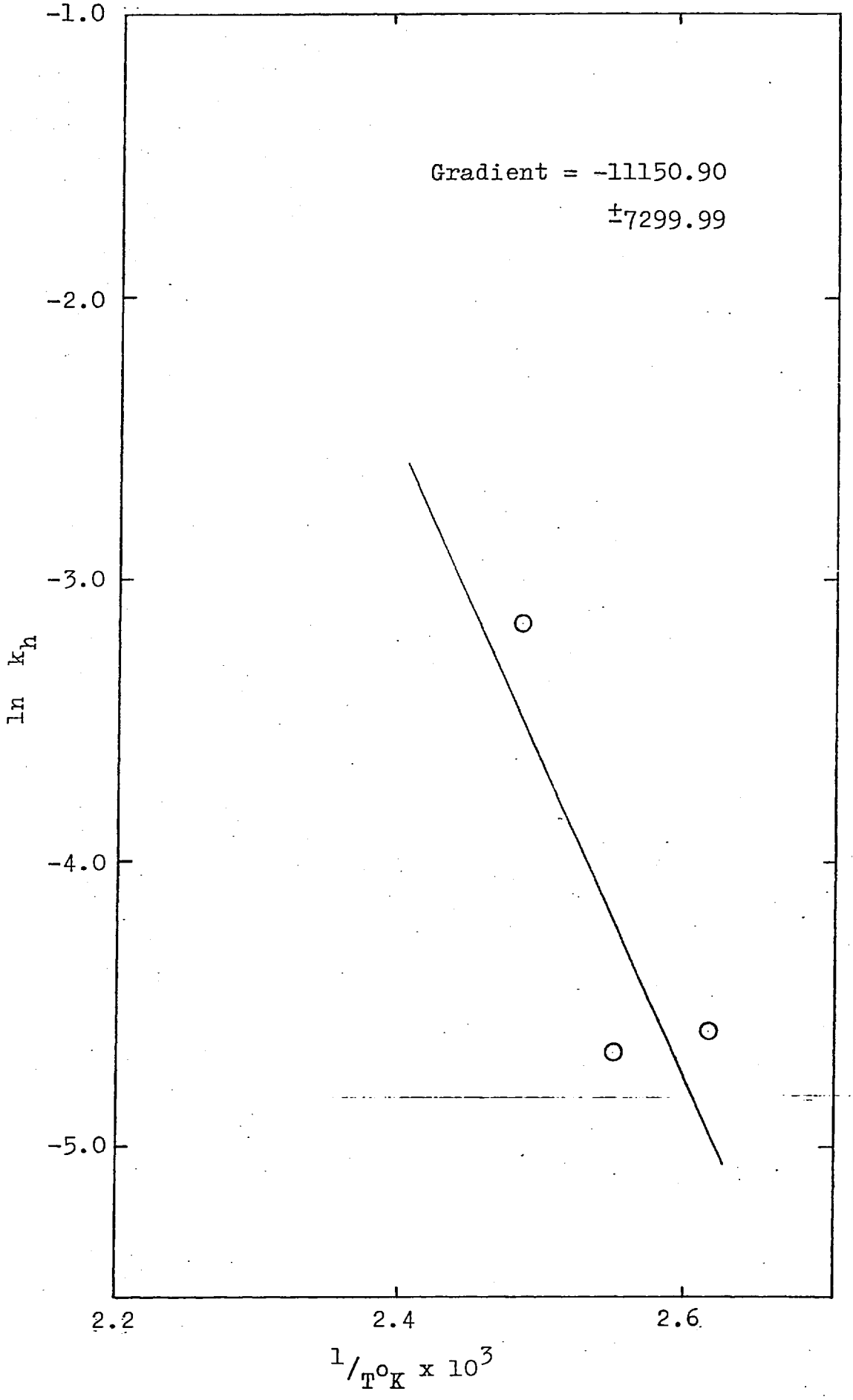


Figure 3.3.ii.



Arrhenius plot for the decaying portion of cupric acetate reduction (Figures 3.1.viii. to 3.1.xiv.)

Figure 3.3.iii.



Arrhenius plot for the decaying portion of the cupric acetate reduction reaction. (Figures 3.1.xv. to 3.1.xvii.)

Figure 3.3.iv.

Arrhenius plot for the decaying portion of cupric acetate reduction reaction. (Figures 3.1.xviii to 3.1.xxi.)

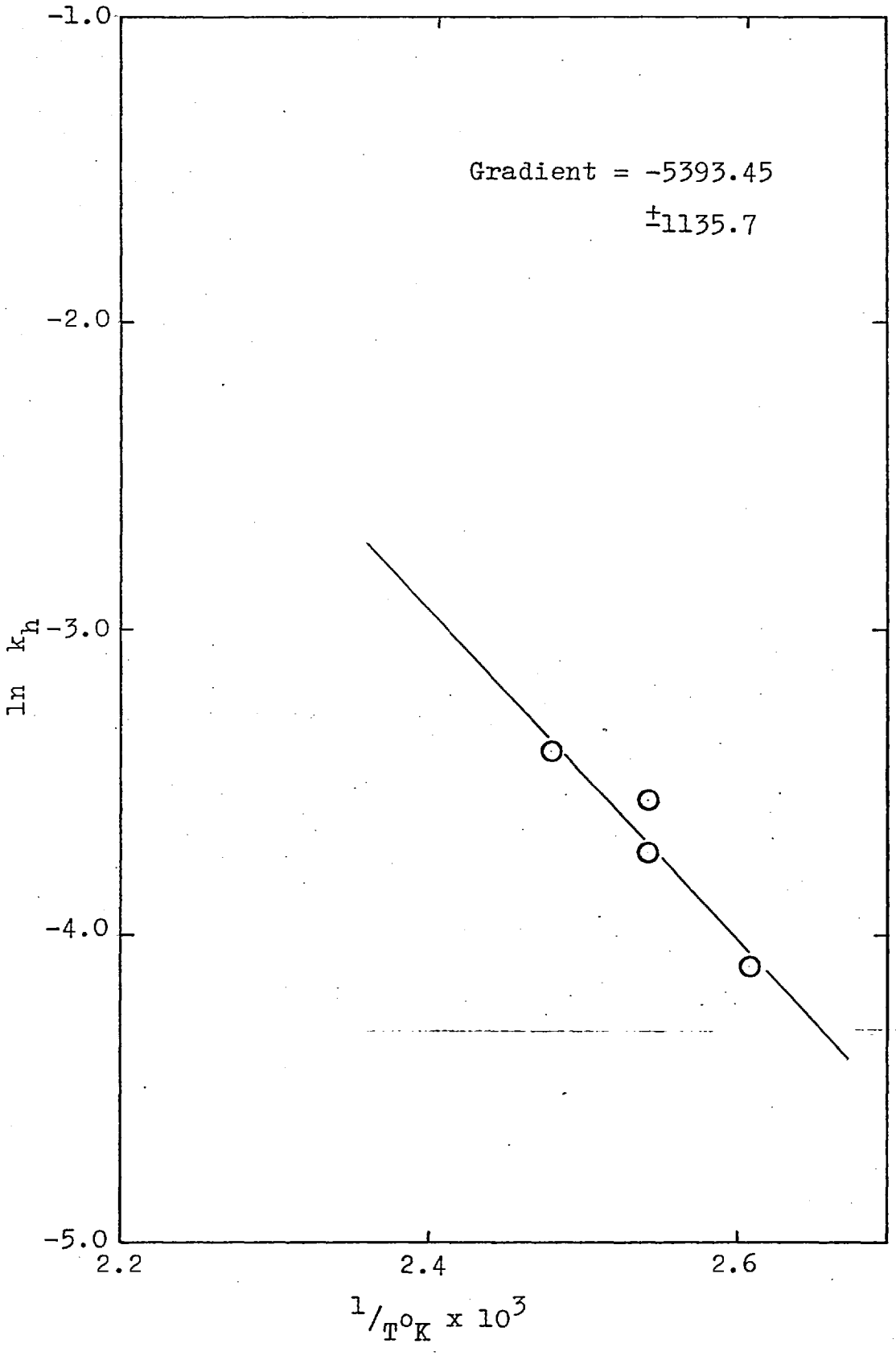
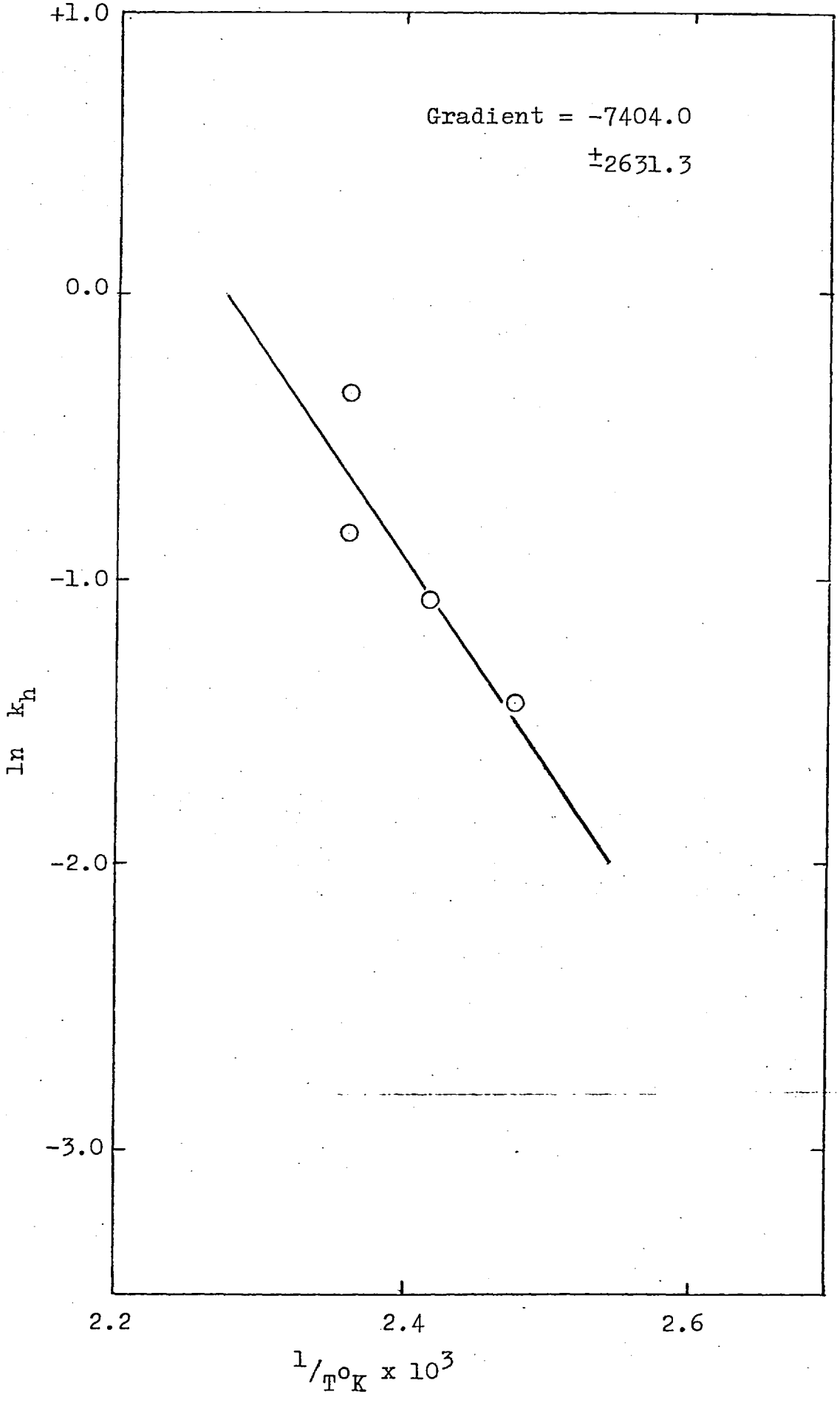


Figure 3.3.v.



Arrhenius plot of the decaying portion of the cupric acetate reduction reaction. (Figures 3.1.xxx to 3.1.xxxiii.)

3.3.ii. Significance of the information determined on the reduction of cupric sulphate solutions.

The reactions investigated for hydrogen gas reduction of cupric sulphate solutions were effected by corrosion of the reaction vessel. As a result the information attained did not have sufficient reliability for mechanism of reaction proposals to be made on their values.

However by comparison of the reaction of cupric acetate with hydrogen, with the rate curves measured for cupric sulphate, a very marked similarity is observable. Moreover, as indicated in section 3.2.i., the only information obtained for the reducing agent consumption, during the reaction, shows that a change in the rate of dissolution of hydrogen corresponds to that expected, if the reactions occuring were of the same type as those proposed for the acetate system.

On the basis of these observations it is proposed that the reactions are similar, independent of whether an acetate or sulphate cupric solution is being reduced.

The values of the measured rate constants for the cupric sulphate reduction reaction data which was analysed can be seen in ~~Table 3.T.ix.~~ Figures 3.2.ii. to 3.2.xi.

TABLE 3.T.iv.

This table shows the times at which precipitation occurs when cupric acetate solutions are reduced by hydrogen at a pressure of 400 p.s.i.

Time of precipitation (mins)	Temp. (°C)	Acetate Ion Conc'n (Molar)		Semi-reduced species conc'n. (Molar) at precipitation
		Method a	Method b	
7.50	150	0.281	2.360	0.0080
5.85	150	0.108	0.326	0.0073
4.75	150	0.123	0.373	0.0099
5.00	150	0.117	0.314	0.0159
3.88	150	0.119	0.314	0.0138
5.20	150	0.126	0.420	0.0126
6.80	140		0.420	0.0126
9.20	150	1.768	6.411	0.0256
9.70	150	1.765	6.411	0.0457
13.00	140		6.411	0.0435
17.10	130		6.411	0.0417

3.4. Precipitation of solid reduction products.

3.4.i. Semi-reduced species concentration at the time of initiation of precipitation.

The proposed reactions for the decaying part of the reduction gives a semi-reduced species, supposedly hydrogenated cuprous ions.

It is proposed that at a certain concentration of the hydrogenated semi-reduced species a further reaction occurs:

$$CuH^{+}_{spec.} \longrightarrow Cu^{o} + H^{+}$$

Eq. 3.4.i.

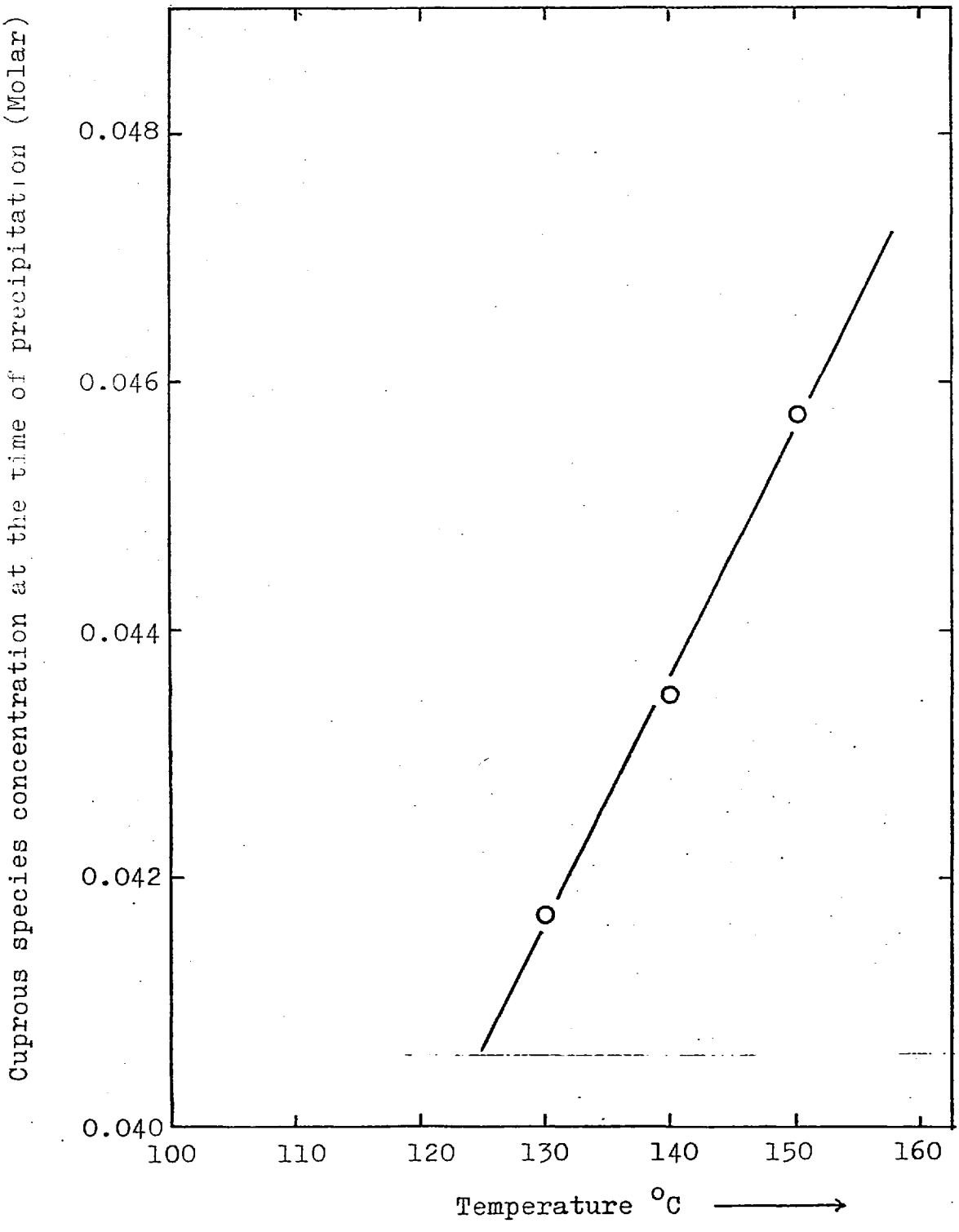
If the proposed reaction is initiated by a specific concentration of hydrogenated cuprous ions, then for identical conditions the remaining cupric concentration should be the same at the point of precipitation. This value would be expected to change with temperature.

Table 3.T.iv. shows the times at which precipitation occurs and the semi-reduced species concentration at precipitation, assuming that all "disappeared" cupric ions are in the form of one semi-reduced species.

Figure 3.4.i. shows the variation of the maximum concentration of hydrogenated cuprous ions with change of temperature for cupric acetate solution reduction, in high acetate concentration, when elemental copper precipitation does occur.

Figure 3.4.i.

Change in the maximum cuprous concentration with temperature



If the initiation of the formation of solid reduction products is dependent only upon the semi-reduced species concentration and temperature, then the original cupric concentration and the original hydrogen pressure would have no effect on this condition.

However it can be seen by examination of Table 3.T.iv. that the semi-reduced species concentration at initiation of the solid formation reaction is not independent of the other constituents of the solutions. It was decided that this variation may be due to the degree of complexing of the cuprous species in the solution. In order to test this proposal the concentration of acetate ions in the solution was estimated and these estimated values plotted against the cuprous concentration at the point at which precipitation began.

Two approximate methods were employed to estimate the acetate concentration in the solutions at the temperature:

a) Using the assumption that the system as a whole was electrically neutral, and that ammonium acetate was totally dissociated, then:

$$[NH_4^+] + [H^+] + [Cu^+_{spec.}] + [2\ Cu^{2+}_{spec.}] = [Ac^-] + [OH^-]$$

Hydroxyl ions are at a concentration of approximately 10^{-10} to 10^{-11}M and were consequently ignored, as was the existence of any species other than those

in the equation. No attempt was made to use the concentration value estimated to derive activity data at the temperature of the reaction (150°C.) since further assumptions were unwarranted, especially when in addition to those already made.

b) Using an approximate value of the dissociation constant for acetic acid, making the assumption that acetic acid, acetate ions and hydrogen ions only were in the solution.

The value of the dissociation constant K_a used was :

$$K_a = 10^{-4}$$

This compares well with the room temperature value of K_a, where:

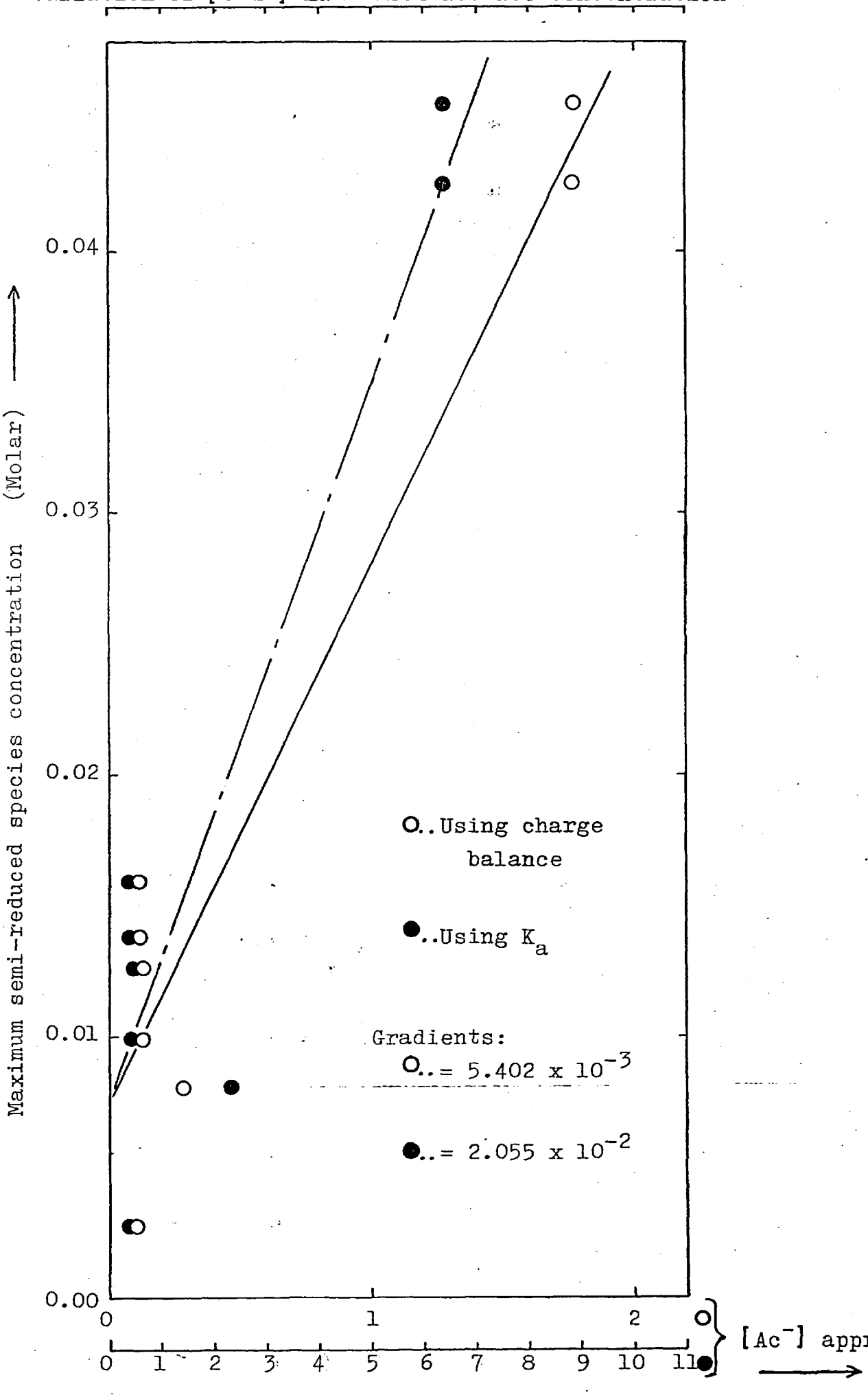
$$\log_{10} K_a = -4.69 \pm 0.90$$

The lack of precision in this value was considered acceptable since the method makes use of the hydrogen ion activity at 150°C, in a complicated solution. This value is at present undeterminable and it must therefore be estimated. An error in this value would also have a large effect upon the value of the acetate ion activity obtained.

Both approximate methods used treat all solution conditions identically. Thus the object of

Figure 3.4.ii.

Variation of $[CuH^+]$ max with acetate concentration



showing some dependence of reduced species concentration, at the point of precipitation on the acetate ion concentration, was still maintained, despite inaccuracies in the values used.

Figure 3.4.ii. shows that at high acetate activity, or concentration, the precipitation reaction is not initiated until a high cuprous species concentration is attained. Also, at lower acetate concentration the reaction begins at a lower hydrogenated cuprous ion concentration.

These observations would indicate the existence of a complex formation at higher acetate concentrations which stabilises the semi-reduced species with respect to de-hydrid ation to the elemental copper. The existence of this stabilisation does not agree with the knowledge that at low acetate concentrations (less than 1.0 molar) complete stability of the cuprous ions exists at the temperatures at which investigations were performed. Solid products did not form until the temperature fell.

3.4.ii. Proposals for reactions occuring during the formation of elemental copper.

It was observed from examination of the turbidity change measurements made, an example of which may be seen in figure 2.5.iii., that the solid forms very rapidly after initiation of the precipitation reaction. It was also observed that the increase in

turbidity was usually not quite as large as the increase in the optical density plus turbidity measurements. No quantitative discussion can be made on this observation since the change in absorbance of a solution due to the formation of a fine powder in suspension is very sensitive to small changes in the conditions at which the reaction occurs. However from the observation of the inequivalence of the changes of turbidity over the precipitation reaction it was proposed that at some stage during the copper powder formation disproportionation of a cuprous species must occur in order to cause a rise in the cupric concentration.

A rise in cupric species concentration and hence a rise in optical density at 775nm. to 800nm. may be caused by the reaction:

$$2Cu^{+}_{spec.} \longrightarrow Cu^{o} + Cu^{2+}_{spec.}$$

Eq. 1.3.i.

If this were the only reaction producing elemental copper then the rise in optical density due to the cupric species formation would be equivalent to a cupric concentration change of one half of the cuprous concentration at the initiation of the precipitation. This situation was never observed to exist.

The proposal for the reactions causing the precipitation of copper metal are:

$$CuH^{+} \longrightarrow Cu^{o} + H^{+}$$

Eq. 3.4.i.

with the concentration at which the reaction is initiated being controlled by the degree of stabilisation of the cuprous species by acetate groups.

And:

$$2Cu^{+}_{spec.} \longrightarrow Cu^{o} + Cu^{2+}_{spec.}$$

Eq. 1.3.i.

occuring to a small extent at some stage during metal formation.

3.4.iii. The effect of temperature on the hydrogenated cuprous ion concentration at precipitation.

Figure 3.4.i. shows the way in which the cuprous species concentration at the point of beginning of the metal formation reactions varies with temperature.

This graph indicates that at higher temperatures the cuprous species is more stable than at lower temperatures. Higher cuprous concentrations are maintained without the metal formation reaction proceeding, at the higher temperature.

The observation of the increase in stability of cuprous ions with increase in temperature was expected, and has been predicted, notably by Ugarte [35], from theoretical thermodynamic considerations.

3.4.iv. Cuprous oxide formation reactions upon cooling of low acetate cupric acetate reduction solutions.

If the proposed reactions in solution are correct then it follows that at low acetate ion concentration, when precipitation of elemental copper did not occur, the semi-reduced species must stabilise with respect to de-hydridation. Furthermore under these conditions no solid reduction product was formed at the temperature of the investigations. On cooling of the solution another reaction must take place, to give rise to the formation of cuprous oxide.

As suggested in section 3.4.ii. the stabilisation of the semi-reduced hydride species could be due to the complex formation with acetate groups.

The cuprous oxide formation reaction proposed by Dakers and Halpern [28], was that between a doubly hydrogenated cupric acetate complex and an unhydrogenated cupric acetate complex:

$$Cu(OAc)_2.H_2 + Cu(OAc)_2 + H_2O \longrightarrow \underset{\text{cuprous oxide}}{Cu_2O} + \underset{\text{acetic acid}}{HOAc}\ .$$

Eq. 3.4.ii

This proposed reaction assumes that upon cooling some cupric acetate remains in the solution.

From the present investigation it is known that

the optical density at the absorption peak for cupric ions falls to close to zero; thus the cupric concentration also falls to zero during the reaction. It follows therefore that this proposal must be incorrect.

Knowing that the entire copper content of the solution after reduction with hydrogen at raised temperature is in the form of a semi-reduced species, such as the hydrogenated cuprous ion, the following reaction is proposed. This occurs at a temperature where cuprous oxide is more stable than the cuprous species:

$$2CuH^{+}_{Aq.Complex.} + H_2O \longrightarrow Cu_2O_{solid.} + H_2 + 2H^{+}$$

Eq. 3.4.iii.

This gives an overall reaction, occuring in two different temperature conditions of:

$$2Cu^{2+} + H_2O + H_2 \longrightarrow Cu_2O + 4H^{+}$$

Eq. 3.4.iv.

No reason can be proposed as to why a different reaction should occur at the temperature of the investigations depending upon the acetic acid concentration in the solution; thus the same reaction is proposed.

Section 4

AUTO-REDUCTION OF CUPRIC ACETATE SOLUTIONS

4.1. The investigations

Several cupric acetate solutions were examined in order to observe the phenomenon of auto-reduction.

All solutions used were of high acetate concentration, approximately 6.5 molar, and of cupric concentration approximately 0.052 molar.

Examinations were all performed at 150°C, and resulted in the production of very pure metallic copper powder. The product in each case was examined by X-ray powder photography.

The product was found to be independent of the source of the cupric acetate solution, whether it was from G.P.R. hydrated copper acetate, or produced by dissolving copper in acetic acid.

4.1.i. Auto-reduction monitoring using spectrophotometry

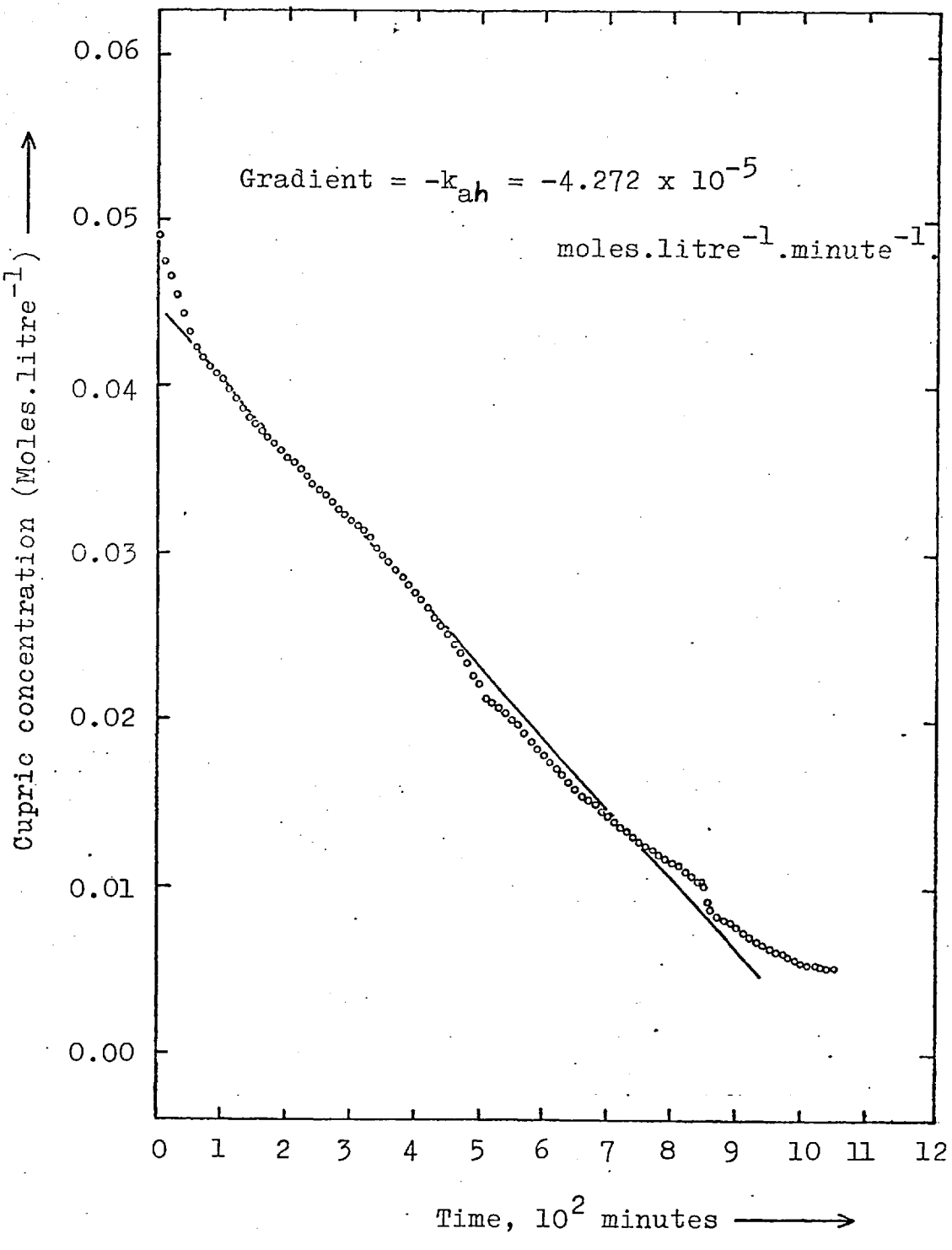
One investigation was made of auto-reduction by following the procedure of the reaction in a high temperature spectrophotometer cell, as described in section 2.2.ii. and Appendix A.1.1.ii.

The optical density of a cupric acetate solution was monitored over a period of just over 20 hours.

Decrease in cupric concentration appeared to

Figure 4.1.i.

The auto-reduction reaction rate curve for a cupric acetate solution at 150°C.



proceed approximately linearly with time over the period of the measurements, although a tendency to 'tail off' was observed towards the end of the reaction, when very little cupric species remained in the solution.

A plot of cupric concentration against time can be seen in Figure 4.1.i.

No evidence of powder formation was observed over most of the duration of the experiment, however an increase in the optical density/turbidity was noticed during the final 30 minutes of observation.

Although a change in the optical density equivalent to the removal of nearly 100% of the cupric species in the solution was observed, only a small quantity of copper metal was recovered from the spectrophotometer cell. This indicates the existence of a two or more stage reaction, similar to that which is proposed to occur when reduction by hydrogen gas is performed.

4.1.ii. Autoclave auto-reduction of cupric acetate solutions

When solutions were heated, without stirring, in a pair of small pressure vessels, for 200 hours, at $150^{o}C \pm 2.0^{o}C$, a very fine powder product of copper was found on removal of the vessel lids. This fine suspension was photographed in a laser beam, as described in section 2.5.ii. The result

of the photograph can be seen in figure 2.5.2.

Analyses of the solution and residual gases over the solutions in the autoclaves, indicates the presence of carbon dioxide, approximately 70% and hydrogen, about 25% to 30%.

Some evidence of the existence of a further constituent of the solution was observed, as described in section 2.4.iv., but catagorical identification could not be made. The decomposition of a component of the solution to carbon monoxide, carbon dioxide and water at about 190°C does indicate a probability of the existence of oxalic acid in the solution.

It was proposed from this information that a reaction of the form: (from Eq. 2.4.i.)

$$(CH_3COO)_2Cu + 4H_2O \xrightarrow[Cu^+, Cu^{2+}; \text{ catalysts.}]{\text{slow}} \begin{pmatrix} COO \\ | \\ COO \end{pmatrix}.Cu^{2+} + 2CO_2 + 7H_2.$$

Eq. 4.1.i.

The decomposition of acetic acid, in the presence of cupric and cuprous ions, controls the reduction reaction by the slow production of molecular hydrogen in the solution. The hydrogen may then be assumed to perform the reduction in a similar manner to that proposed when external hydrogen is introduced.

In order to reduce 0.052 moles of cupric ions to metallic copper, 0.052 moles of molecular hydrogen

are required, the production of this quantity of hydrogen uses 0.0074 moles of acetate ions, approximately. Therefore it may be assumed that the acetate concentration remains constant, since the change is less than 0.12%, in a total acetate concentration of approximately 6.1 molar.

If the rate of decomposition of acetate were dependent upon the acetate concentration:

$$- \frac{d[Ac]}{dt} = k_{ah}[Ac]$$

Eq. 4.1.ii

this rate would remain constant over the change of acetate concentration of only 0.12%.

As no reasonable concentration of oxalic acid could be traced in the remaining solution after auto-reduction, the possibility of the following reactions occuring must be considered:

$$\underset{\text{oxalic acid}}{(COOH)_2} \longrightarrow \underset{\text{carbon monoxide}}{CO} + CO_2 + H_2O \ .$$

Eq. 2.4.ii

However the presence of carbon monoxide was not found in the gas over the remaining solution.

Carbon monoxide could have been consumed by the overall reaction:

$$CO + Cu^{2+} + H_2O \longrightarrow Cu^{o} + CO_2 + 2H^{+} \ .$$

Eq. 4.1.iii.

(The steps proposed for this reaction by Byerley and Peters [29] may be seen in section 1.4.iii., Eq. 1.4.xiv. to 1.4.xix., they do however observe cuprous oxide as the reduction product, and it must be assumed that this product is only formed during cooling of a dilute solution)

Due to the slow rate of hydrogen production the cupric ion reduction is slow and controlled by the rate at which hydrogen could be obtained from the decomposition.

When autoclave reductions were performed, over a period of 200 hours, the decomposition appears to have proceded after equilibrium of elemental copper and cupric or cuprous species had been attained, hence a excess of hydrogen and carbon dioxide were found in the vessel.

The vessel used for the auto-reduction investigations is described in detail in Appendix A.1.4.

Section 5

CONCLUSIONS

5.1 Cupric acetate reduction by hydrogen

By the experimental techniques which have been described to determine the reactions which proceed when cupric acetate solutions are reduced by hydrogen, and by making use of the data analyses which have been described, the following reaction has been proposed:

$$Cu^{2+} + H_2 \longrightarrow CuH^+ + H^+ .$$

It is supposed that this simple reaction proceeds in solution during the whole of the reduction.

During the first part, the accelerating part, of the reaction the rate was found to be controlled, as far as the available information could show, by the concentration of hydrogen in the solution. Because of the control of the rate of the reaction being by molecular hydrogen concentration in the solution, the rate of reaction was observed to increase as the amount of gas 'dissolved' in the solution increased.

The proposal that has been maintained by previous workers that the accelerating portion of the reaction was due to auto-catalytic effect of the presence of an increasing concentration of a semi-reduced species, does not appear to agree with the

information obtained in this investigation.

At a certain hydrogen concentration, or hydrogen to cupric concentration ratio it is proposed that the rate does not continue to be controlled by the hydrogen concentration. At this point the hydrogen in solution was proposed to be available for reactions at a greater frequency than were the remaining cupric ions. Due to the change in the controlling species the shape of the rate curve may be seen to go through a point where the gradient has an inflection.

It appears that even after the concentration of hydrogen has ceased to control the rate of the reaction, the increasing concentration of the reaction products does not influence the rate of the reduction.

Thus over the first period:

$$-\frac{d\,[Cu^{2+}]}{d\,t} = k_o\,[H_2]_{solution}$$

And over the second period:

$$-\frac{d\,[Cu^{2+}]}{d\,t} = k_h\,[Cu^{2+}]_{solution}$$

After a certain activity of hydrogenated cuprous ions, the semi-reduced species, has been attained further reduction occurs, forming elemental copper.

This part of the reaction only proceeds when the cuprous species is not sufficiently stabilised by the acetate ions in the solution for them to remain in solution complexed with acetate groups.

The reactions under which elemental copper powder was formed were not easily predictable, but due to a small increase in cupric concentration which was observed during the formation of the metal powder, it may be concluded that at some stage some disproportionation occurs:

$$2CuH^{+} \longrightarrow Cu^{2+} + Cu^{o} + H_2$$

Possibly a small amount of none-hydrogenated cuprous ions were formed in the earlier parts of the reduction, by the reaction:

$$CuH^{+} + Cu^{2+} \longrightarrow 2Cu^{+} + H^{+}$$

Followed by disproportionation of the cuprous ions:

$$2Cu^{+} \longrightarrow Cu^{2+} + Cu^{o}$$

The increase in cupric concentration was noticed to be insufficient for either of these reactions to be the major one in the formation of copper powder. The main reaction equation proposed was:

$$CuH^{+} \longrightarrow Cu^{o} + H^{+}$$

the simple de-hydrogenation of the cuprous species.

It can be seen from the turbidity change example curve that this reaction occurs very rapidly, although no measure of the rate of reaction could be made.

The stability of cuprous ions in solution was

found to be effected by the activity of acetate ions in the solution and by the temperature of the solution. At acetate total concentration of less than about 0.3 molar ($25^{o}C$) the cuprous species were stable at all temperatures between $110^{o}C$ and $150^{o}C$. At acetate concentrations above 2.0 molar ($25^{o}C$) the cuprous species was found to be sufficiently unstable for formation of metallic copper to occur. However the trend reverses as the acetate rises further and the cuprous ions become more stable at higher acetate concentration.

The cuprous species were found to be increasingly stable as the temperature of the solution increased.

Under the conditions where metallic copper was not formed at the temperature of the investigation, the reaction proposed when the temperature falls and the cuprous species becomes unstable is:

$$2CuH^{+} + H_2O \longrightarrow Cu_2O + H_2 + 2H^{+}$$

giving a fine cuprous oxide powder product.

Both the copper product and the cuprous oxide formed from low acetate cupric acetate reduction were found to be in the form of quite evenly sized nearly spherical particals.

An example of the cuprous oxide powder may be seen in the photograph in Figure 5.1.ii. This photograph was made from a scanning electron microscope image.

FIGURE 5.2.i.

A photo-micrograph of the copper product from the reduction of cupric sulphate solution. This photo-graph shows the 'needle' structure of the powder.



x 610

FIGURE 5.1.ii.

A photograph of a scanning electron microscope image of the cuprous oxide powder product from the reduction of cupric acetate solution.



x 2000.

5.2. Cupric sulphate reduction by hydrogen

On the evidence of the experimental work, and the analyses which could be performed, for cupric sulphate reduction by gaseous hydrogen, a similar mechanism is proposed as that which has been described for the reduction of cupric actate in high acetate concentration.

Thus:

$$-\frac{d\,[Cu^{2+}]}{d\,t} = k_1\,[H_2]_{solution}$$

$$-\frac{d\,[Cu^{2+}]}{d\,t} = k_h\,[Cu^{2+}]_{solution}$$

And reaction equations the same as those written for the acetate reduction.

Due to the presence of dissolved impurities no interpretation of the results regarding cuprous species concentration at the point of precipitation of copper powder could be made.

The copper powder product was found to be in the form of a mixture of spheroid particals, 'wires' and plates.

An example of the needles, spheres and plates may be seen in the photo-micrograph in Figure 5.2.i.

5.3. Auto-reduction of cupric acetate solutions

When cupric acetate, in an acetate solution of high concentration, greater than about 2.0 molar, is heated for a long period at 150°C, the cupric ions are reduced, finally producing copper powder. The reactions proposed for this phenomenon were:

$$\underset{\text{acetate ion}}{(CH_3COO)_2^{2-}} + 4H_2O \longrightarrow \underset{\text{oxalate ion}}{\begin{pmatrix} COO \\ | \\ COO \end{pmatrix}^{2-}} + 2CO_2 + 7H_2$$

$$Cu^{2+} + H_2 \longrightarrow CuH^+ + H^+$$

$$CuH^+ \longrightarrow Cu^o + H^+$$

The following reactions might also occur to some extent:

$$\begin{pmatrix} COO \\ | \\ COO \end{pmatrix}^{2-} + H_2O \longrightarrow CO_2 + CO + 2OH^-$$

Carbon monoxide produced by this reaction may have been consumed in the reduction of some cupric ions, and:

$$2CuH^+ \longrightarrow Cu^o + Cu^{2+} H_2$$

No positive evidence existed to support the possibility of the decomposition of oxalic acid, but neither

could a reasonable concentration of oxalic acid be found in the remaining solution.

The overall reaction was controlled by the rate of production of molecular hydrogen in the solution by the decomposition of acetate ions. This rate being dependent upon the acetate ion concentration which remained effectively constant over the period of observation.

The rate constant for the reduction of cupric species was:

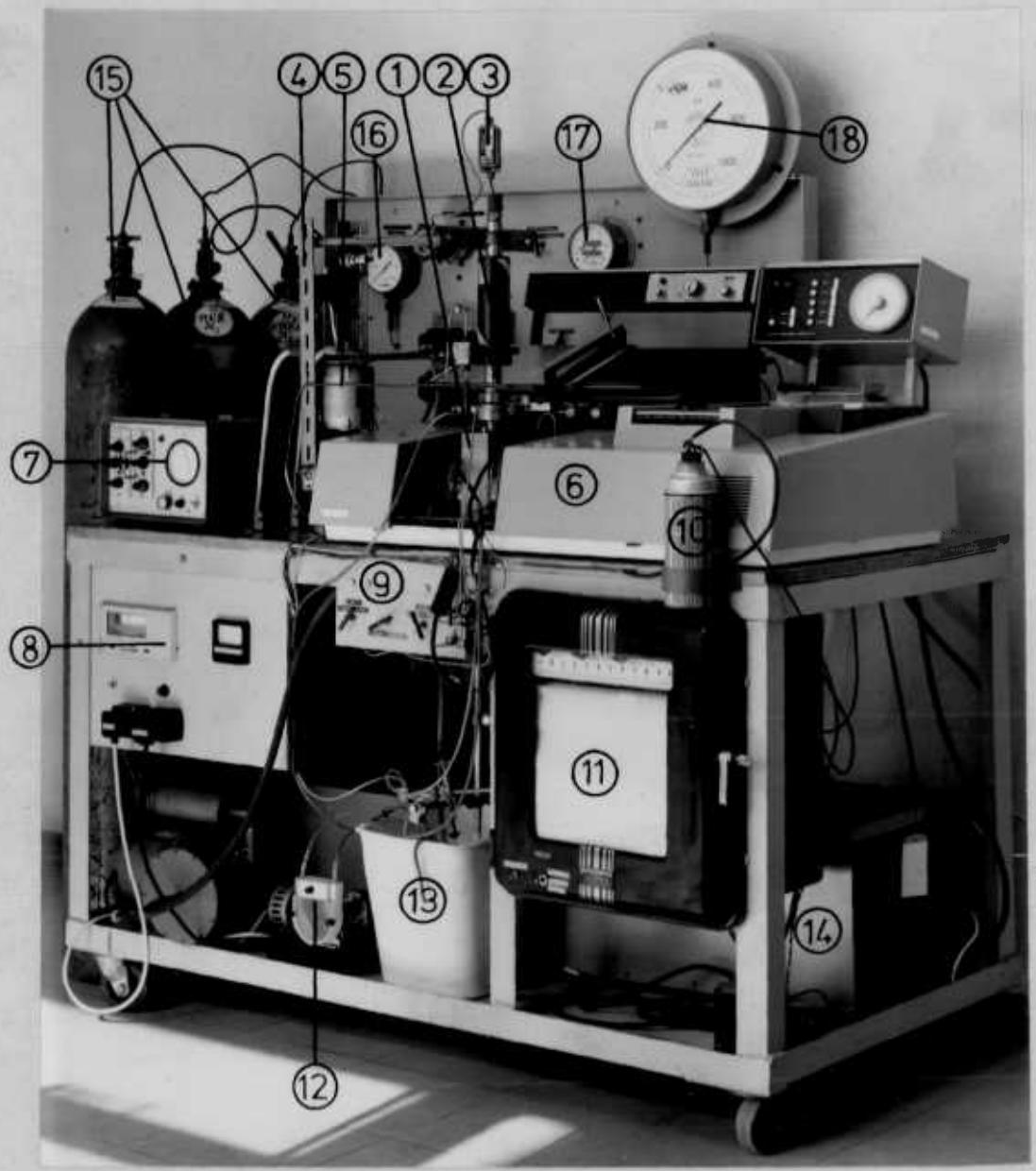
$$k_{ah} = 4.272 \times 10^{-5} \text{ moles. litre}^{-1}. \text{ minute}^{-1}.$$

The copper powder product from the auto-reduction reaction was of extremely fine partical size. Particals could not be observed separately, but a suspension of fine powder was shown to exist by observing a laser beam in the solution.

Appendix 1.

DESIGN OF THE APPARATUS.

The photograph below, together with the key to the numbers on the photograph and the description in Appendix A.1.1., shows the experimental equipment for the investigation of the reduction of cupric solutions by gaseous hydrogen.



The key may be seen in the following list.

Appendix 1.

Key to the components which are numbered on the photograph of the apparatus.

1. Reaction vessel block.
2. Stirrer coupling.
3. Transducer.
4. Support frame for the stirrer coupling and the stirrer motor.
5. Stirrer motor.
6. Spectrophotometer.
7. Transducer convertor.
8. Heater controller equipment.
9. 'Front panel' valves for exhausting, flushing and interconnection of the reaction vessel.
10. Cold junction thermostat for the measurement thermocouple.
11. External 'Slave' recorder.
12. Cooling water circulation pump.
13. Refrigerated cooling water reservoir.
14. Refrigeration units.
15. Nitrogen and hydrogen supply.
16. Pneumatic hydrogen controller dome pressure gauge.
17. Reaction vessel nitrogen pressure gauge.
18. Reaction vessel hydrogen pressure gauge.
19. Connections to the reaction vessels for gas supply, cooling water, thermocouples and power for the heating elements.

Appendix 1

A.1.1. DESIGN OF THE EQUIPMENT

A.1.1.i. Design of the spectrophotometer vessel with circular chambers

A spectrophotometer reaction vessel with circular chambers was employed for the investigation of the reaction of cupric sulphate solutions with hydrogen gas. The design of this vessel can be understood from the drawing; Figure A.I.i.

This equipment was designed by Mr. Roger Hughes prior to the beginning of the present investigation.

The apparatus consisted of two cylindrical, identical, reaction vessels, as described in section 2.2.ii., which were machined out of a single block of stainless steel B.S. E.N.58 J. The chambers were positioned in the body in such a way that window holes cut diametrically into each could be aligned with the double optical paths of the spectrophotometer. In this way, one vessel could be used as a reference cell so that comparative observation of the absorbance change during a reaction proceding in the other cell could be observed.

Each vessel, or cell, was equipped with a lid also made of B.S. E.N. 58 J. A pressure seal was maintained between the lid and the main body block by means of a silicon rubber 'O' ring.

The 'O' rings used were of 'Viton' supplied

by James Walker. These seals fitted in the chamber in the upper end of each vessel, and were forced into the correct position by the flanged portion of the lids.

The windows of the cells were of a double cylindrical design, and were manufactured by Thermal Syndicate Ltd. out of silica 'Spectrosil B'. The pressure seal of the windows was attained by the use of another set of 'O' rings, also supplied by James Walker. These 'O' rings fitted circumferencially about the smaller diameter 'nose' of the windows and in a machined groove for the purpose in the chamber window ports. The large diameter flange of each window was supported by an external retaining plate which took the force transmitted along the windows when the vessels were pressurised.

The polished inside faces of the nose of each window just formed a chord to the cylindrical cell. Therefore, an optical path length of 3.97 cms. was achieved.

Pressure induction, flushing, etc. of the reaction vessel was done by the use of gas ports situated in the side of the block, just under the lid of the chamber. Pressurisation of the reference chamber was made by a single gas port situated in the lid of the vessel.

A small thermocouple well was situated cent-

AN EXPLODED PICTORIAL SECTIONED VIEW OF BOTH THE REACTION VESSELS

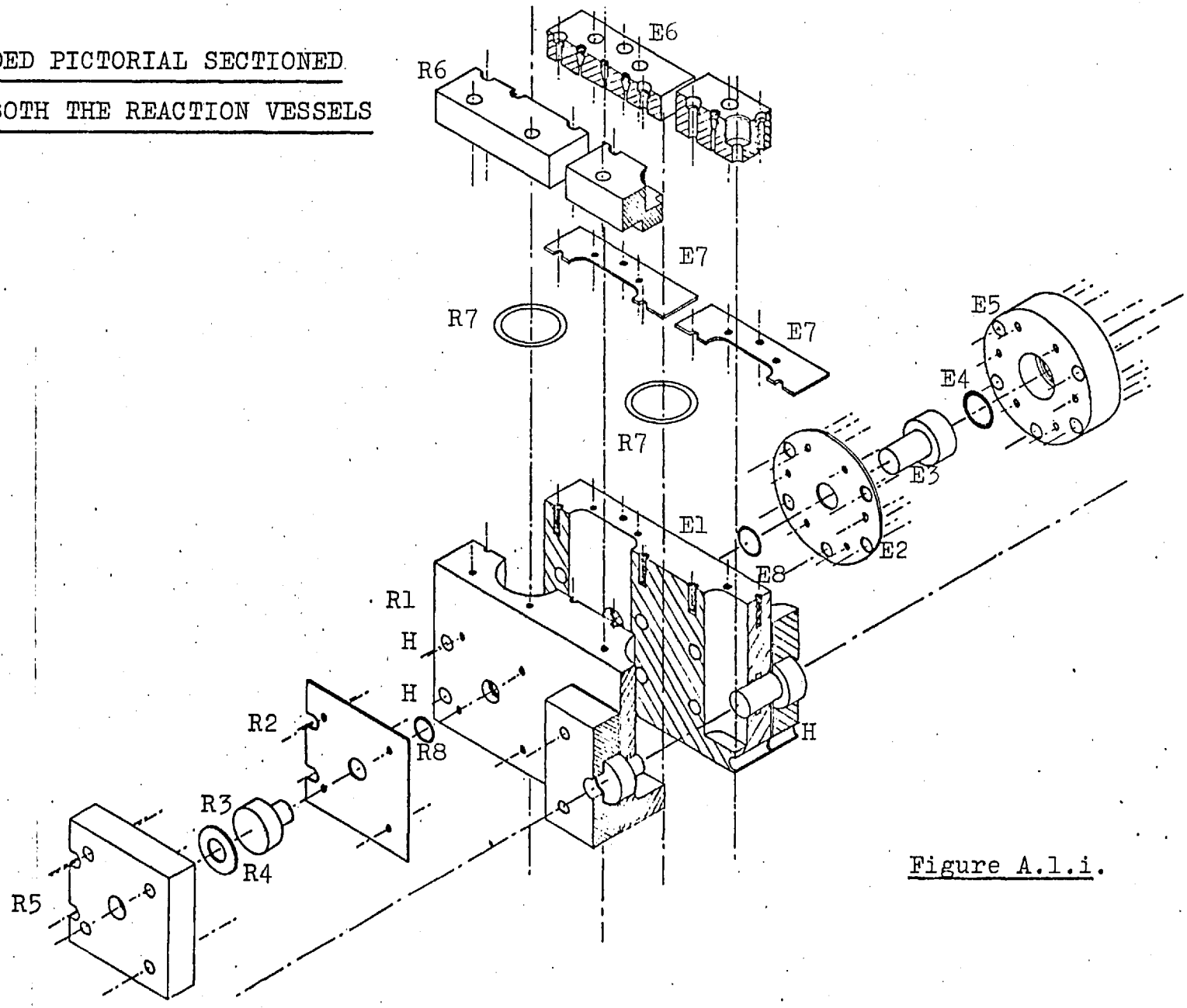


Figure A.1.i.

Appendix 1

Key to the labelling on figure A.1.i.

The precedent letter "R" indicates the label refers to the round celled vessel.

The precedent letter "E" indicates the label refers to the oblated ellipsoidal vessel

1 Main cell body.

2 Inside window cushion and gasket.

3 Quartz windows.

R4 Outside 'Walkerite' cushion.

E4 Outside 'O' ring cushion.

5 Window support blocks.

6 Vessel lids, one in each type of cell having a connector for the stirrer unit or stirrer unit adaptor.

R7 'O' ring lid seal for the round cells

E7 Flat gasket seals for the oblated ellipsoidal vessel.

8 Window seal 'O' ring.

The blank holes in each vessel body, marked 'H' are to accommodate the heating rods.

rally in the main body block. This well was of sufficient diameter to accommodate two thermocouples. One was for control of the heating of the equipment, and the other for accurate measurement of the temperature.

Heating, temperature control and measurement, and gas feed and control to the apparatus is described in conjunction with the description of these parts of the oblate ellipsoidal chambered equipment used.

A.1.1.ii. Design of the spectrophotometer vessel containing oblated ellipsoidal chambers.

A double chambered spectrophotometer reaction cell, having ellipsoidal 'pots' was used during the investigation of cupric acetate reduction by gaseous hydrogen.

This apparatus was also designed and built previously to the beginning of the present work. The equipment was designed primarily by Dr. I.J. Grayson-Smith; however, some modifications were made to the design to allow stirring of the solution undergoing reduction reactions.

The method of manufacture of this apparatus was very similar to the previously described equipment. The material used was again stainless steel B.S. E.N. 58 J. The two sets of vessels differed

most significantly from one another in that the arrangement used for the cupric acetate work had chambers with an oblated elliptical section, instead of circular.

The reaction chambers were again fitted with lids. Because of the non—symetrical section of the chamber, an 'O' ring seal could not be employed; instead a plain flat gasket, of James Walker "Wallisic" was used to attain lid seals.

The window design was very similar to that already described in Appendix A.1.1.i., with the exception that longer 'noses' were used so that an optical path length through the solution being investigated of 0.5 cms. was obtained.

The lid of the reference chamber was fitted with a union, to allow pressurisation. A thermocouple well was also fitted to allow a heater controller thermocouple to be inserted.

The reaction cell lid was equipped with an adaptor to allow a stirrer to be inserted. This adaptor was integral with the gas inlet for flushing and pressurisation. A thermocouple well was also arranged in this lid in order that temperature in the reacting solution could be accurately measured.

A third union in the reaction vessel lid could be used as an exhaust for flow through flushing of the chamber, or to allow for the entrance of a sampling tube.

A.1.1.iii. Heating and temperature control of the reaction vessels

Heating of the stainless steel main bodies of the vessels was done by the use of 'Fire-rods'. These are 40 watt insulated rod heating elements which were inserted in holes to accommodate them in the steel body.

The power supplied to these heaters was controlled by a Eurotherm PID/SCR temperature controller, with an iron/constantan thermocouple. The thermocouple was fitted into the stainless steel block or in the solution in the reference chamber as described in the chamber design.

The temperature was measured by a second thermocouple, with a chromel/alumel junction, using a standard cold junction held in an ice bath, in a Dewar vessel. The thermocouple wires from the hot to the cold junctions and the leads from the cold junction were both sheathed with a woven copper harness in order that protection from interference should be given. The shielding of the thermocouple leads avoided 'pick-up' from the effect of the moving magnets in the magnetically coupled stirrer drive, and of the proximity of the heater elements and electric circuits in the spectrophotometer.

The potential from the thermocouple cold junction was either read from a digital volt meter 'solartron L.M.1420.2', or recorded on a Honeywell potentiometric recorder.

A.1.1.iv. Stirring of the reaction vessels.

The stirring of both reaction cells described was by means of an Autoclave Engineers 'Magne-Drive' magnetically coupled stirrer unit.

The stirrer coupling was driven at 1450 r.p.m. by a synchronous motor mounted at one side of the apparatus, as shown on the photograph in Figure A.1.1.ii. The motor was connected to the stirrer coupling by a fabric 'V' belt.

The 'Magne-Drive' was either directly joined to the lid of the reaction cell, when the circular chambered equipment was used, or was joined by a diameter reducing adaptor when the ellipsoidal cell was used. Under both circumstances the seal at the 'Magne-Drive' was by means of a flat gasket made of 'Walker 'Wallisic'' and a knife edge to give a larger pressure on the gasket material. The seal between the adaptor and the vessl lid was two layers of 'Walker 'Wallisic'' gasket material, supported on a cylindrical spigot with a flange on it. The object of this arrangement was to avoid the 'spreading' of the gasket and loose pieces falling into the reacting solutions.

The adaptor also served as a gas inlet union for the flushing of the vessel, and for the induction of reaction gas.

The stirrer head was a straight parallel rod for all inveatigations. The material of the stirrer was P.T.F.E. in all investigations but one.

A.1.1.v. Securing of the position of the cells within the spectrophotometer.

In order to obtain a nearly reproducible light path through the reaction cell and the solution, and thus reproducible optical density readings from the sprectrophotometer, it is necessary to accurately locate the vessel block within the instrument. During the present work the positioning of the cells was maintained vertically by clamping the top of the 'Magne-Drive' stirrer coupling to a rigid, partially triangulated, frame over the instrument. This frame also served as a mounting for the stirrer motor.

The alignment of the main block laterally was obtained by the use of packing pieces of asbestos and gasket material between the faces of the vessel block and the walls of the spectrophotometer cell chamber.

A.1.1.vi. The cooling of the surroundings of the reaction vessel.

Certain parts of the spectrophotometer, for example the monochromater optics and the detector photo-multiplier, are quite sensitive to changes in temperature. The monochromater and collimator sections of the instrument are contained in a thermostated box, held at 37°C. If the heated reaction vessel were allowed to transfer heat to

the sensitive parts, serious reading drifts and possible permanent damage to the intrument would result.

For these reasons it was necessary to arrange cooled plates around the heated block of the reaction vessel, together with asbestos sheet to insulate the block from the cooling jacket.

The coolers consisted of three plates through which water from a refrigerated water bath was pumped. The pump used was a two channel peristaltic pump, equipped with a rheostat to allow it to operate at various speeds. The cooling water was in a closed system, being returned to the refrigerated bath after circulation through the plates. Water was pumped through the plates at a total rate of approximately one to two litres per minute.

A.1.1.vii. The arrangement for gas supply to the reaction vessel.

The pipe-work and equipment arrangement for the gas supply is described in the sketch, Figure A.1.iii.

Nitrogen (oxygen free quality from the British Oxygen Company) was supplied from a cylinder by way of a plain needle valve to the front connecting panel of the apparatus. A pressure gauge was incorporated between the inlet

valve and the front panel. By use of the interconnecting valve 'I', nitrogen could be introduced into the rear, reference cell only, or to both the front, reaction cell and the rear cell. In this way nitrogen could be flushed through the reaction cell when valve 'I' and the flow-through flushing valve were open. Exhausting of the whole assembly was made from the front connection panel valves which are marked on the diagram, Figure A.I.iii., as 'reaction cell - flush valve' and 'reference cell - flush valve'.

Hydrogen was supplied from a cylinder via a pneumatic pressure controller, in order that constant and preset induction pressures could be ensured. The controlling pressure of the pneumatic regulator was set by the nitrogen pressure in the dome of the controller. This pressure was set by a mechanical regulator. A gauge on the dome allowed measurement of the preset hydrogen pressure.

A test gauge was fitted to the induction, downstream, side of the controller so that the reaction cell hydrogen pressure could be accurately observed. An evacuation valve was fitted between the front panel and the cells. This valve was to allow the space above the solutions to be evacuated if necessary. This operation would 'de-gas' the solutions before reactions, thus ensuring that no appreciable concentration of dissolved carbon dioxide or oxygen remained in the solution.

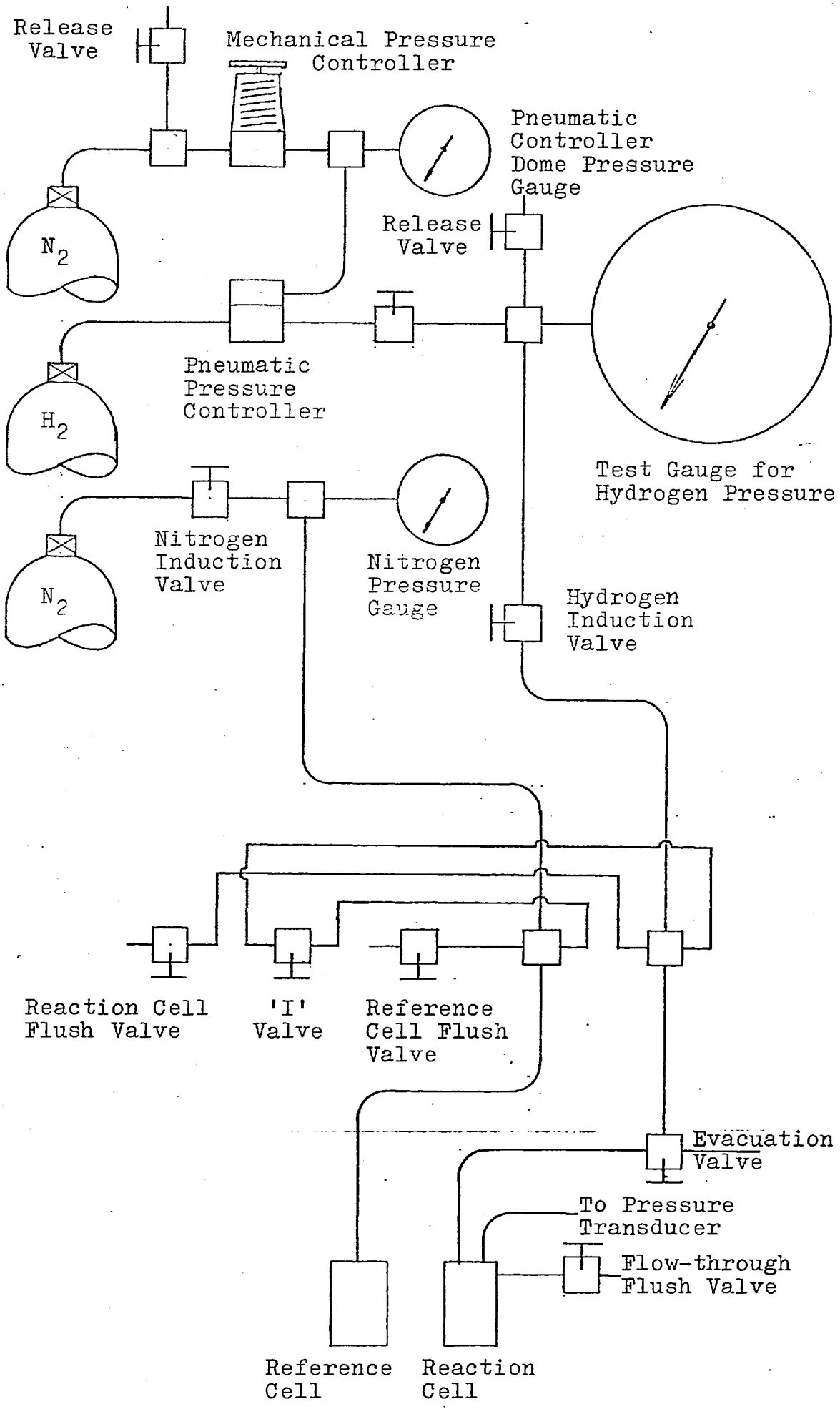


Figure A.1.iii.

Appendix 1

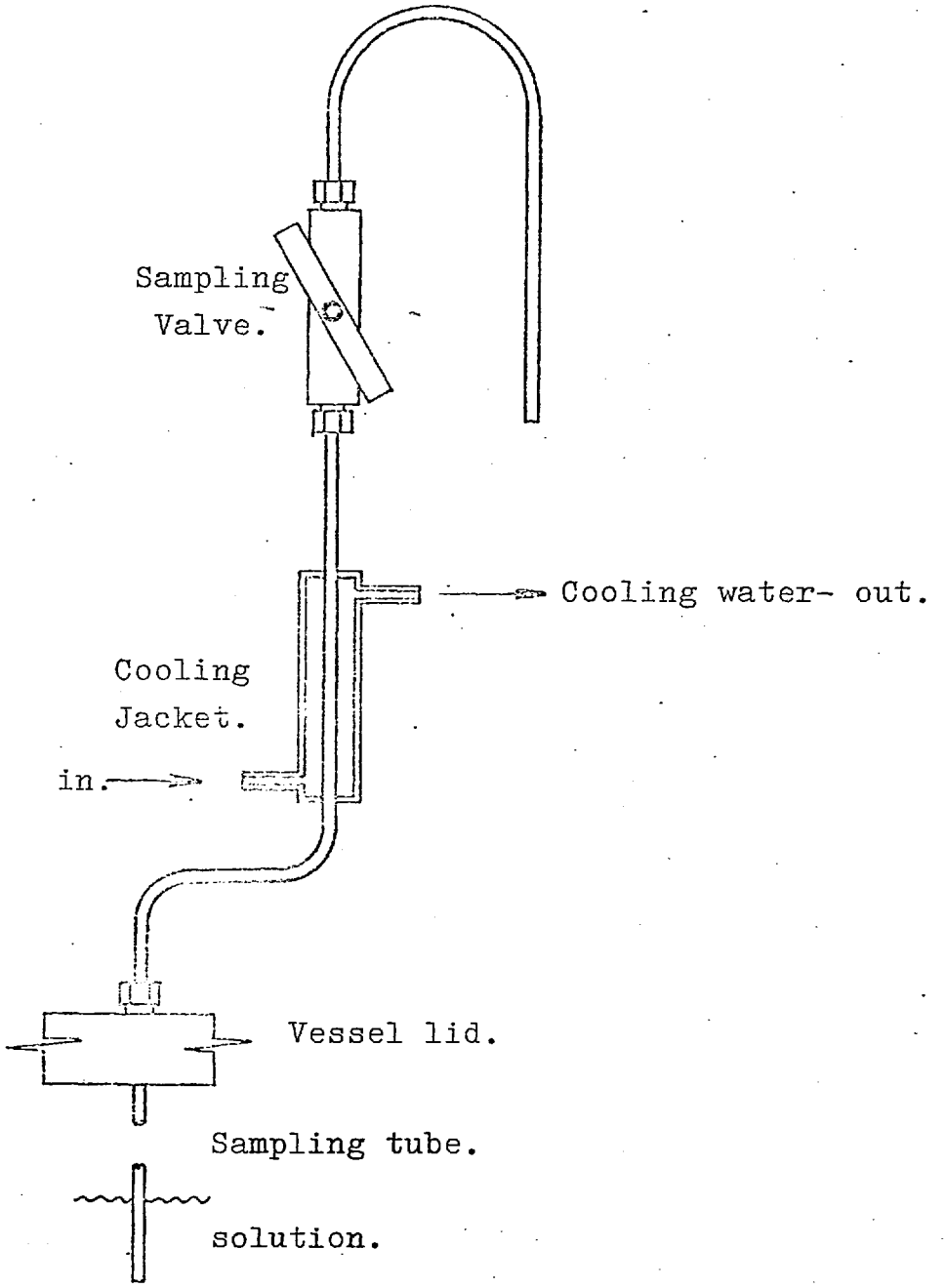
A.1.1.viii. Pressure measurement in the reaction vessels.

a) When reactions were followed at constant total pressure, supplied by the control system described above, the total pressure was then quite accurately measured on the hydrogen pressure test gauge. Since the cell was flushed with hydrogen during induction, by use of the flow-through flush valve, the hydrogen pressure could be determined since the total pressure was assumed to be due to hydrogen and to water vapour pressures.

b) When hydrogen use measurement were made during reactions the pressure was recorded throughout the duration. These measurements were made by a pressure transducer connected to the upper end of the 'Magne-Drive' unit. The gas pressure controller was then used only as a presetable regulator, in order that very swift induction of hydrogen could be made.

To avoid a time-lag occuring, due to the pressure equilibriation rate across the bearings of the magnetic coupling unit, deep slots were cut in the graphite bearing material to allow a free passage for gas. This operation facilitated almost instantaneous readings of the vessel pressure and also avoided seizing of the stirrer unit when excessive pressure differences developed across the bearings.

Output from the transducer was formed into a



THE SAMPLING TUBE AND VALVE.

Figure A.1.iv.

millivolt signal by a transducer converter. This signal was recorded on a pen recorder.

A.1.1.ix. The sampling valve used.

As described in section 2.3.i. d)., a sampling technique was used on occasions. A sketch of the sampling valve is shown in Figure A.I.iv. The cooling jacket of the sampling tube was circulated with cooled water in the same closed system as were the cooling plates surrounding the vessel block.

A.1.1.x. The gold plating of the oblate ellipsoidal chambered reaction cell

After it had been found that quite rapid corrosion was occuring on the walls of the reaction vessel during the reduction reactions, it was decided to attempt to avoid this problem by the gold plating of the inside of a cell.

Since the cylindrical chambered vessel had been quite seriously attacked, the gold plating was done on the ellipsoidal cell.

The plating of the vessel walls was done by 'Sel-Rex' Ltd.

Despite thorough precautions taken by the manufacturer during the plating procedure, a secure gold plate was not obtained on the cell walls. The surface preparation of the stainless steel included ultrasonic cleaning, degreasing,

water washing, 'striking' the surface with nickel plate, then washing and re-striking with a gold alloy. After the completion of the preparations the final layer of gold was plated. About 10 grams of gold were plated onto the whole surface.

After two attempted reaction runs at raised temperatures it was found that the gold was no longer adherent to the steel and that solution had penetrated the gap between gold and steel.

A.1.2. Calibration of the apparatus

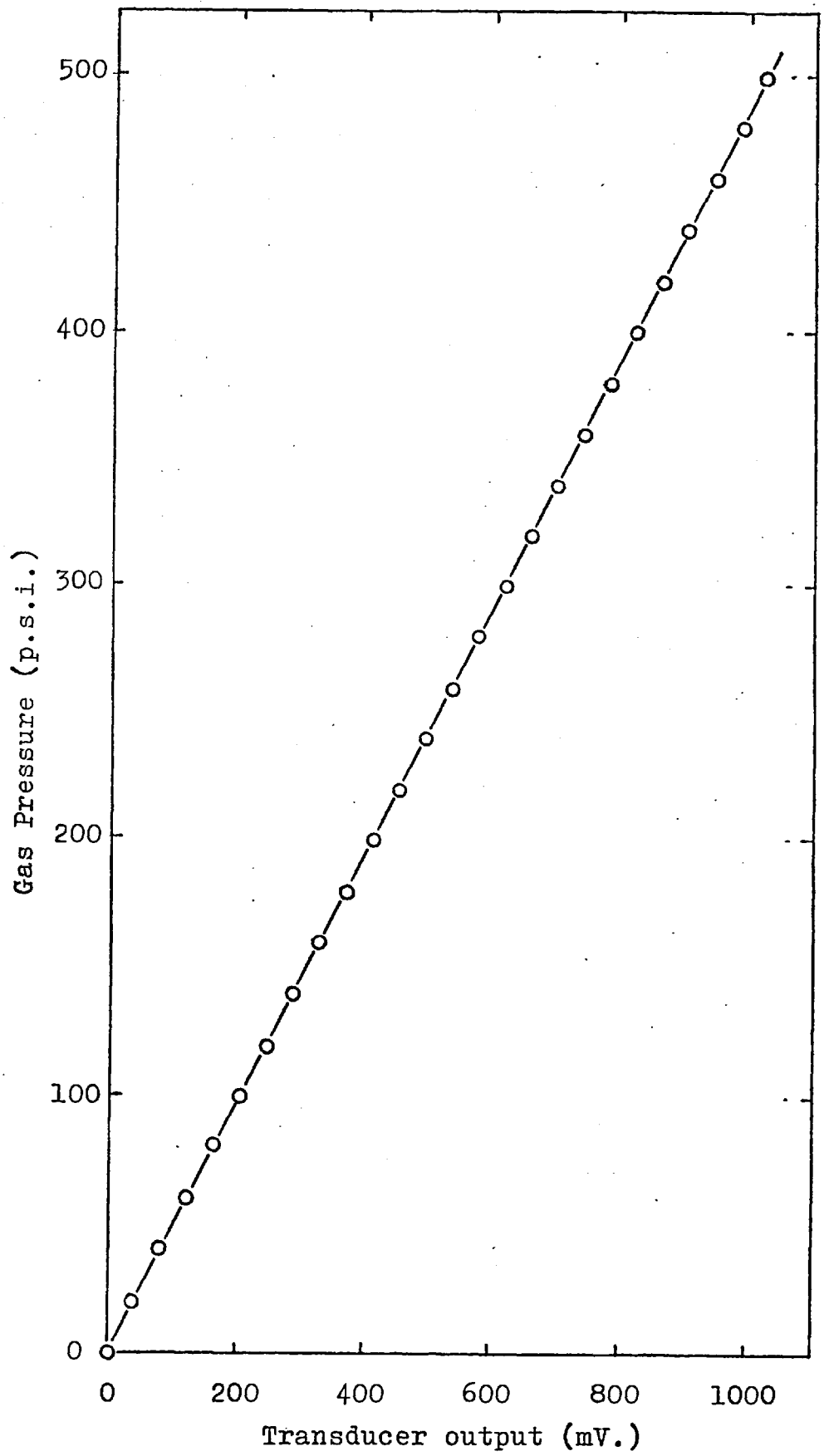
During the setting up of the experimental procedure several calibrations were necessarily made. These included the calibration of the transducers, determination of the apparent volume of the reaction vessel at various temperatures and the verification of Beers law for the solutions being used.

A.1.2.i. Calibration of the transducers.

Calibration of the S.E.L. transducers was performed by comparison with a Barnet instruments air operated low pressure 'dead-weight' tester.

The tester would operate up to 500 p.s.i., air being used as the pressure transfer fluid. Air for the tester was supplied from a cylinder

Figure A.1.v.


500
400
300
200
100
0
Gas Pressure (p.s.i.)
0
200
400
600
800
1000
Transducer output (mV.)

via an activated carbon filter and a silica gel drying column.

The tester was balanced with a particular loading on the plunger carriage, to give a convenient pressure at the testing station. The output from the transducer converter was read for each pressure, and at a particular attenuation setting on the unit.

The pressure could then be plotted against the transducer output. A calibration curve for the transducer may be seen in Figure A.1.v. From the calibration curve a very nearly linear dependence of pressure transducer reading with pressure was shown to exist. Because of the nearness of the curve to a direct dependence, a linear convertion factor was used during all the result analyses when pressure changes were required from transducer readings.

A.1.2.ii. Determination of the apparent volume of the reaction vessel.

During all investigations the reaction vessel was maintained at a constant, known, temperature. Connected to the vessel there was always ancillary equipment, gas pipes and valves. Some of the extra equipment was at the temperature of the body block, while some was at lower temperatures, down almost to room temperature. As a result of the temperature

variation over parts of the gas space within the vessel, the 'apparent volume' of the space was required to be known. The 'apparent volume' would be the volume of the vessel if all the gas in the space were at the controlled temperature of the block. Without a knowledge of the 'apparent volume' no meaningful calculations or conclusions regarding the rate of use of hydrogen gas could be made from the pressure drop measurements in the gas space.

The determination of the apparent volume of the vessel was made by the following method. The cell chamber block, fitted with all the ancillaries, was heated to the temperature at which the apparent volume was to be measured. The reaction vessel was then pressurised with nitrogen from a cylinder. The pressure in the reaction cell was then accurately adjusted to a convenient value, usually about 400 p.s.i.

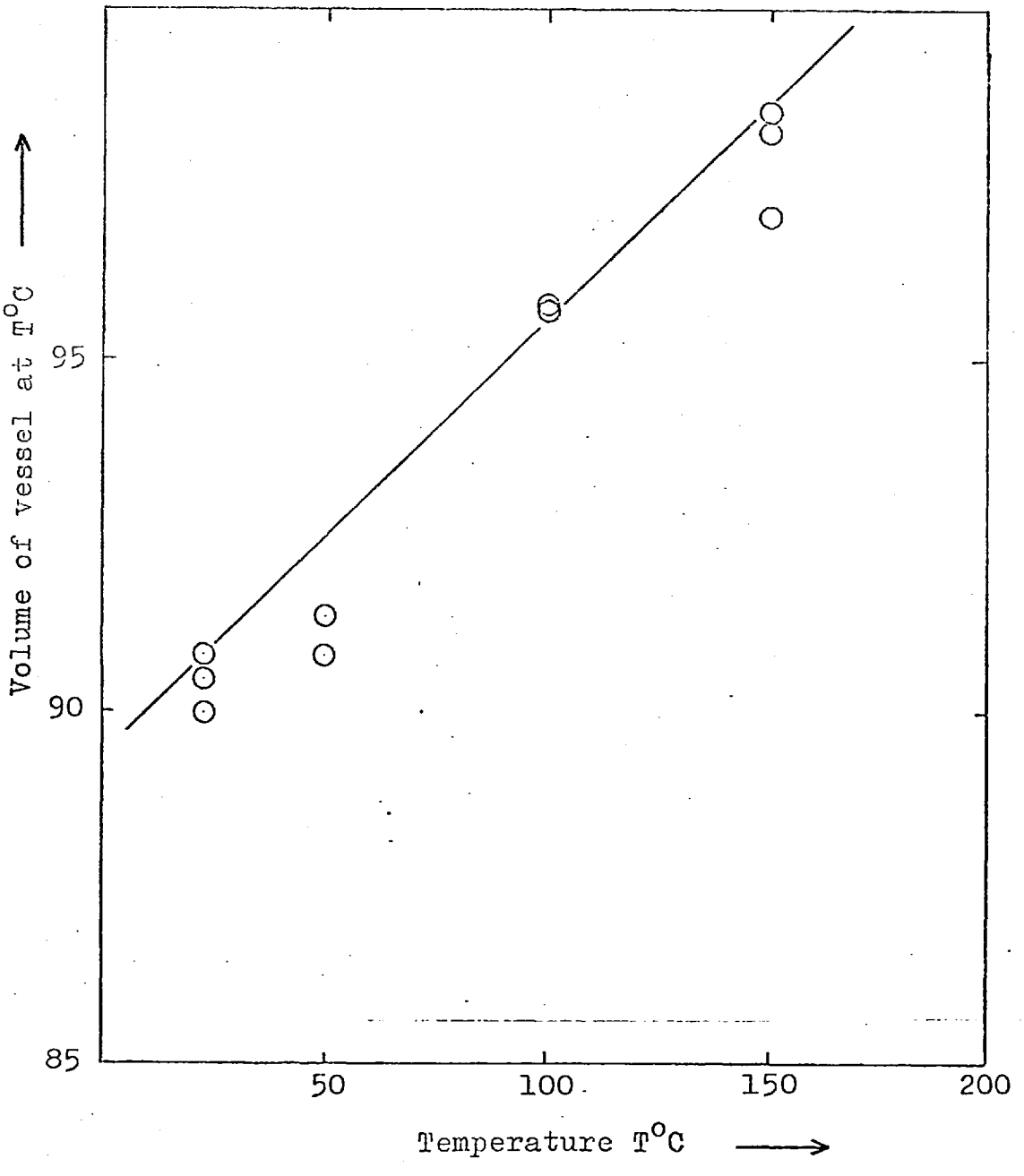
The nitrogen was allowed to remain in contact with the steel of the cell block for about 10 minutes, until a steady temperature was again attained.

When steady conditions existed in the cell chamber the nitrogen was allowed to escape very slowly, by way of a long length of steel tube, to a water filled gas volume meter. The volume of the gas which passed through the meter was measured.

It was assumed that the nitrogen behaved as an ideal gas, and that the gas flowing through the flow

Figure A.1.vi.

Variation of the apparent total volume of the ellipsoidal vessel with temperature.



meter was at room temperature and at atmospheric pressure. The temperature and pressure were measured within a short time of each volume determination being made. It was also assumed that the gas pressure in the vessel finally dropped to that of the surrounding air.

From the information obtained the apparent volume was calculated:

V_o The volume of gas which passed through the gas meter.

V_m The apparent volume of the reaction vessel.

P_A The atmospheric pressure.

P_m The initial pressure in the vessel.

T_A The room temperature (^oC).

T_m The temperature at which the apparent volume was to be determined (^oC).

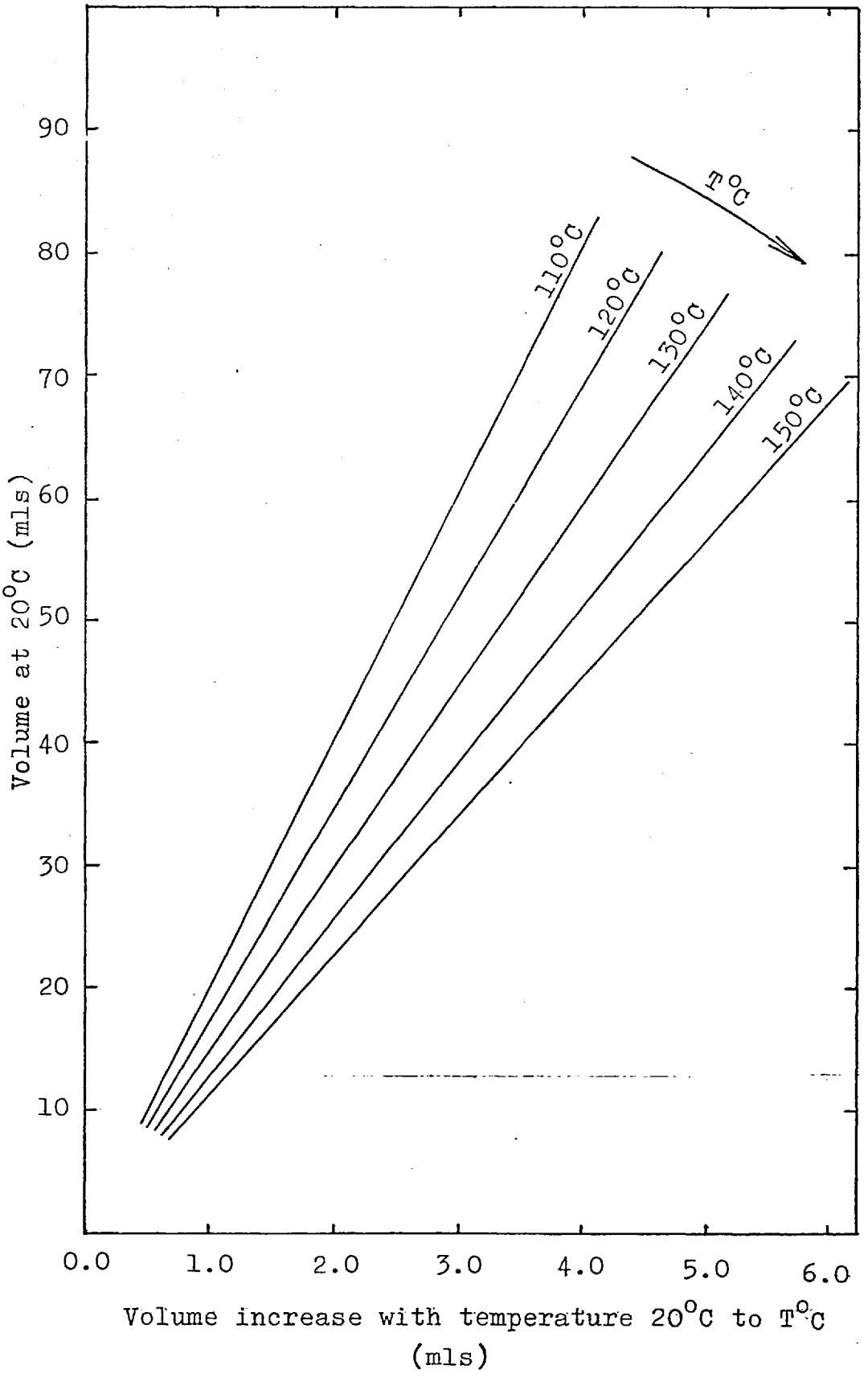
$$V_m = \frac{P_A . V_o . (T_m + 273.2)}{P_m . (T_A + 273.2)}$$

The value of V_m was determined in millilitres.

The graph shown in Figure A.I.vi. indicates the variation of the apparent volume of the vessel with temperature. The line drawn through the groups of points was placed through the largest volume values, since inaccuracy in the measurements made would give

Figure A.1.vii.

The increase in volume of various volumes of solution when heated from 20°C to 110°C, 120°C, 130°C, 140°C and 150°C.



values lower, rather than higher, than the true volume. By this reasoning it was concluded that the maximum volumes obtained at each temperature were the nearest to the true 'apparent volume'.

From the graph the apparent volume at any temperature between 20°C and 150°C can be determined.

A.1.2.iii. Determination of the apparent volume of the gas space over the solution in the reaction cell.

The volume of the solution introduced into the reaction vessel, at approximately 20°C to 25°C, was known accurately since pipettes were used during the filling operation. The volume of a solution at the temperature of an investigation is not accurately known and could not be easily measured. The volume at raised temperature could not be determined by difference from the total 'apparent volume' of an apparent gas volume measured when an amount of solution was in the cell. This method could not be used because of vapour losses as the gas was allowed to escape were replaced by evaporation from the solution, thus changing the solution volume.

The solution volume was estimated by using the assumption that the bulk, or volume, coefficient of expansion had the same value for the solution as for pure water.

Appendix 1

The graphs shown in Figure A.1.vii. show the approximate increase in the volume of a volume of solution at 20°C when it is heated to temperatures between 110°C and 150°C.

From the volume of the solution at raised temperature, and the measured apparent total volume of the chamber at the same temperature, the apparent volume of the gas space over the solution, at that temperature, could be easily determined by subtraction.

A.1.2.iv. Determination of the value of the β factor.

The β factor was used to describe the effect that one pound per square inch change in hydrogen pressure in the gas space above a solution had upon the molar concentration of hydrogen in the solution if the pressure change was due to dissolution only.

The following expression was used for the evaluation of β :

$$\frac{1}{V_{so}} \times \frac{(V_m - V_{st})}{V_{sm}} \times \frac{1}{P_o} \times \frac{(T_o + 273.2)}{(T_m + 273.2)} \times 10^3.$$

where:

V_{so} was the volume of the solution in the vessel at 25°C

V_m was the apparent total volume of the vessel

V_{st} was the volume of the solution in the vessel, at the temperature of the measurement.

V_{sm} was the ideal gas molar volume at standard conditions.

P_o was the standard pressure, 1 atmosphere or 14.59 p.s.i.

T_o the standard temperature, 25°C.

T_m was the temperature at which the measurements were made.

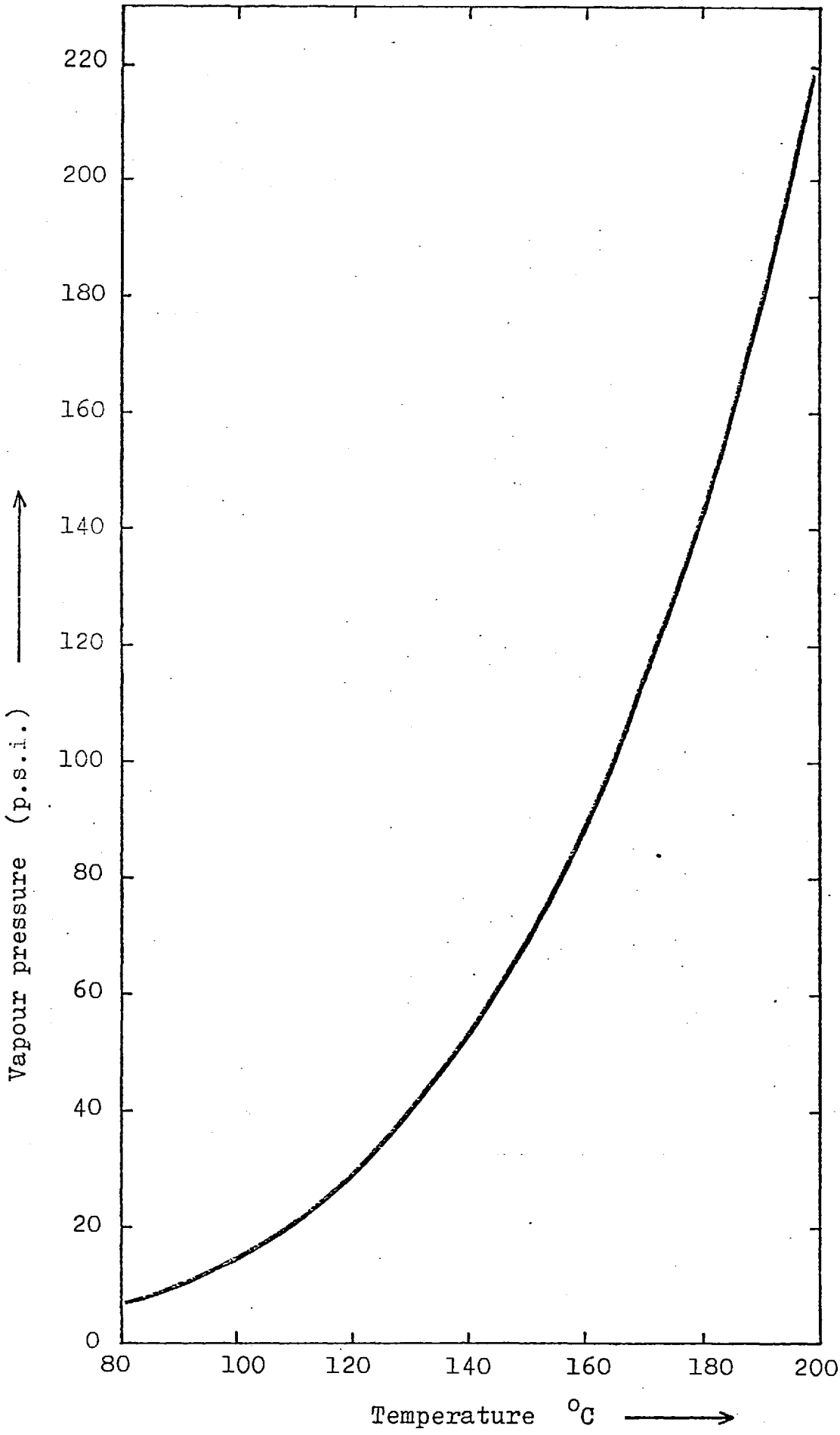
All volumes used were in milli-litres, and pressures in pounds.inches^{-2}. (p.s.i.), thus the units of β were:

moles.litres^{-1}.p.s.i.$^{-1}$.

A.1.2.v. The vapour pressure over solutions in the reaction vessel.

It was assumed, for reactions performed after flow through flushing with hydrogen, that the vapour pressure over the solutions was due to water only and that the water vapour pressure was equal to that over pure water. If this assumption were employed when high acetate concentrations were being used, it may not have been valid. Under solution conditions of ionic strength less than 0.1, as was employed during the sulphate investigations, the assumption was considered to be of sufficient accuracy.

Figure A.1.viii.



Vapour pressure variation with temperature for water.

Appendix 1

Water vapour pressure variation with temperature is much published information; the values used were obtained from the Chemical Rubber C°. manual of physical data.(36)

The plotted values of the water vapour pressure change with temperature may be seen in Figure A.1.viii. A graph of this information was used to calculate pressure settings of the gas controller during the experimentation, since set pressure values were the required hydrogen pressure plus the solution vapour pressure.

A.1.2.vi The calibration of the spectrophotometer and the validation of Beer's law.

The data analyses technique employed to obtain information from the optical density information, as described in section 3.1.i., assumed Beer's law was applicable to the solutions under examination.

To show the validity of the assumption that optical density was proportional to the concentration of the absorbing species in solution, various copper solutions were made, and the spectra of them determined. Figures A.1.ix. and A.1.x. show the variation of the cupric sulphate spectra with concentration at room temperature and with temperature. They also show the calibration plot, or Beer's law plots, at different temperatures.

Figure A.1.xi. shows the variation of the absorption spectra of copper acetate solutions

Appendix I

TABLE A.1.T.i.

Solutions used in spectra determination of cupric acetate complexes

A. 10 mls bulk solution (20.2 g Cu/l)
20 mls 5:1, acetic acid : ammonia
30 mls water

B. 10 mls bulk solution (20.2 g Cu/l)
30 mls 5:1, acetic acid : ammonia
20 mls water

C. 10 mls bulk solution (20.2 g Cu/l)
40 mls 5:1, acetic acid : ammonia
10 mls water

D. 10 mls bulk solution (20.2 g Cu/l)
50 mls 5:1, acetic acid : ammonia

Solutions A,B,C,D all measured against 5:1 acetic acid : ammonia

E. 10 mls bulk solution (20.2 g Cu/l)
50 mls water
Measured against water

F. 10 mls bulk solution (20.2 g Cu/l)
40 mls water

Appendix 1

F.(cont)

10 mls acetic acid

Measured against 5:1, water : acetic acid

G. 10 mls bulk solution (20.2 g Cu/l)

30 mls water

20 mls acetic acid

Measured against 2:1, water : acetic acid

H. 10 mls bulk solution (20.2 g Cu/l)

20 mls water

30 mls acetic acid

Measured against 1:1, water : acetic acid

I. 10 mls bulk solution (20.2 g Cu/l)

10 mls water

40 mls acetic acid

Measured against 1:2, water : acetic acid

J. 10 mls bulk solution (20.2 g Cu/l)

50 mls acetic acid

Measured against 1:5, water : acetic acid

K. 0.0530 molar Cu^{2+}

Approx. 7.0 molar acetate ions

plus 5 mls of "0.88" ammonia solution in 60 mls

L. 0.0397 molar cupric ions

Approx. 7.0 molar acetate ions

plus 5 mls of "0.88" ammonia solution in 60 mls

Appendix 1

M. 0.0265 molar cupric ions
Approx. 7.0 molar acetate ions
plus 5 mls of "o.88" ammonia solution in 60 mls

N. 0.0132 molar Cu^{2+}
Approx. 7.0 molar acetic acid
plus 5 mls of "0.88" ammonia solution in 60 mls

Solutions K,L,M,N were measured against 7.0 molar acetic acid + 5 mls of ammonia solution in 60 mls

1. 0.079 molar Cu^{2+} in sulphate solution
($5g\ Cu^{2+}.\ litre^{-1}$)

2. 0.039 molar Cu^{2+} in sulphate solution
($2.5g\ Cu^{2+}.\ litre^{-1}$)

3. 0.0197 molar Cu^{2+} in sulphate solution
($1.25g\ Cu^{2+}.\ litre^{-1}$)

Solutions 1,2,3 were contained in the circular sectioned reaction vessel. Measurements were made against a reference of water.

4. 0.0063 molar Cu^{2+} in sulphate solution
($0.4g\ Cu^{2+}.\ litre^{-1}$)

5. 0.0126 molar Cu^{2+}. in sulphate solution
($0.8g\ Cu^{2+}.\ litre^{-1}$)

6. 0.0188 molar Cu^{2+} in sulphate solution
($1.2g\ Cu^{2+}.\ litre^{-1}$)

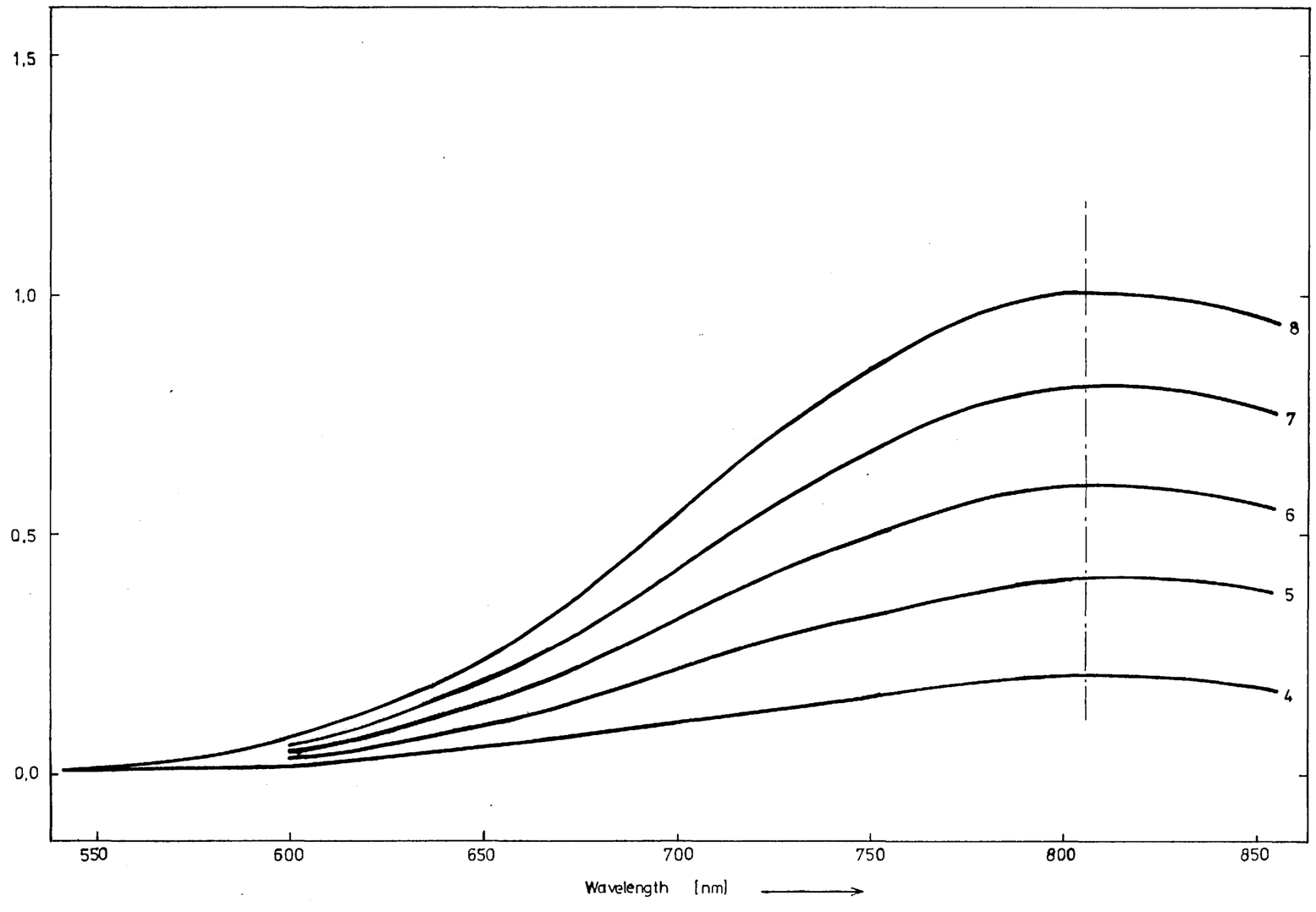
7. 0.0252 molar Cu^{2+} in sulphate solution
($1.6g\ Cu^{2+}.\ litre^{-1}$)

8. 0.0315 molar Cu^{2+} in sulphate solution
($2.0g\ Cu^{2+}.\ litre^{-1}$)

Solutions 4,5,6,7,8 were contained in 40 mm standard silica spectrophotometer cells. Measurements were made against water as a reference.

FIGURE A.1.ix.

Cupric Sulphate Spectra At Various Copper Concentrations.



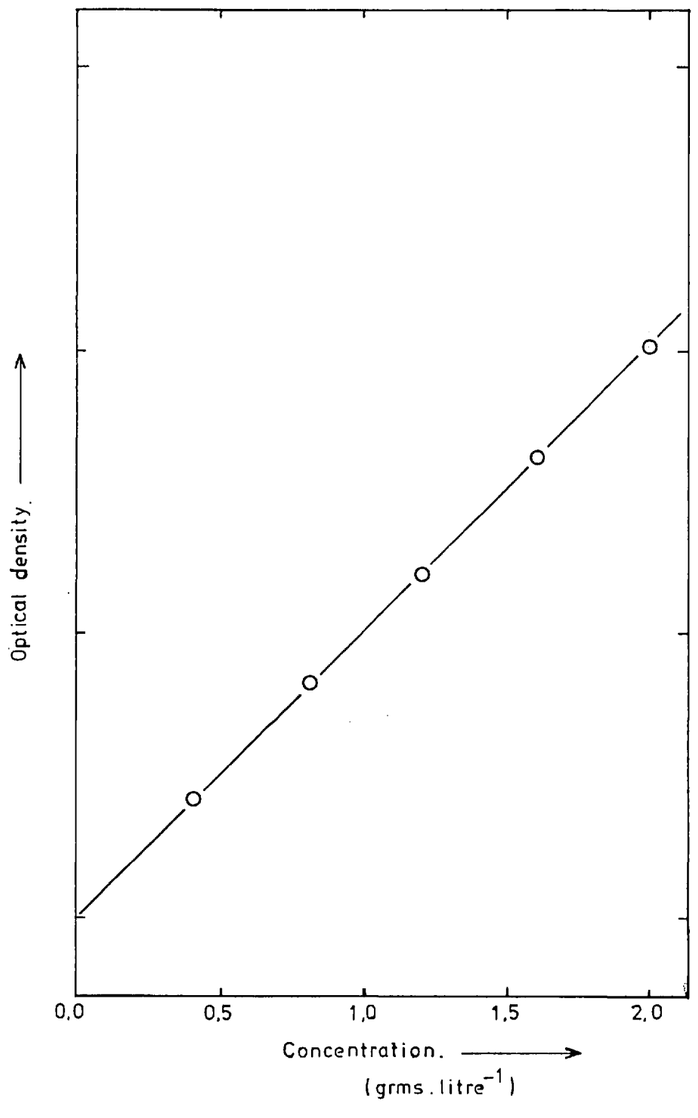
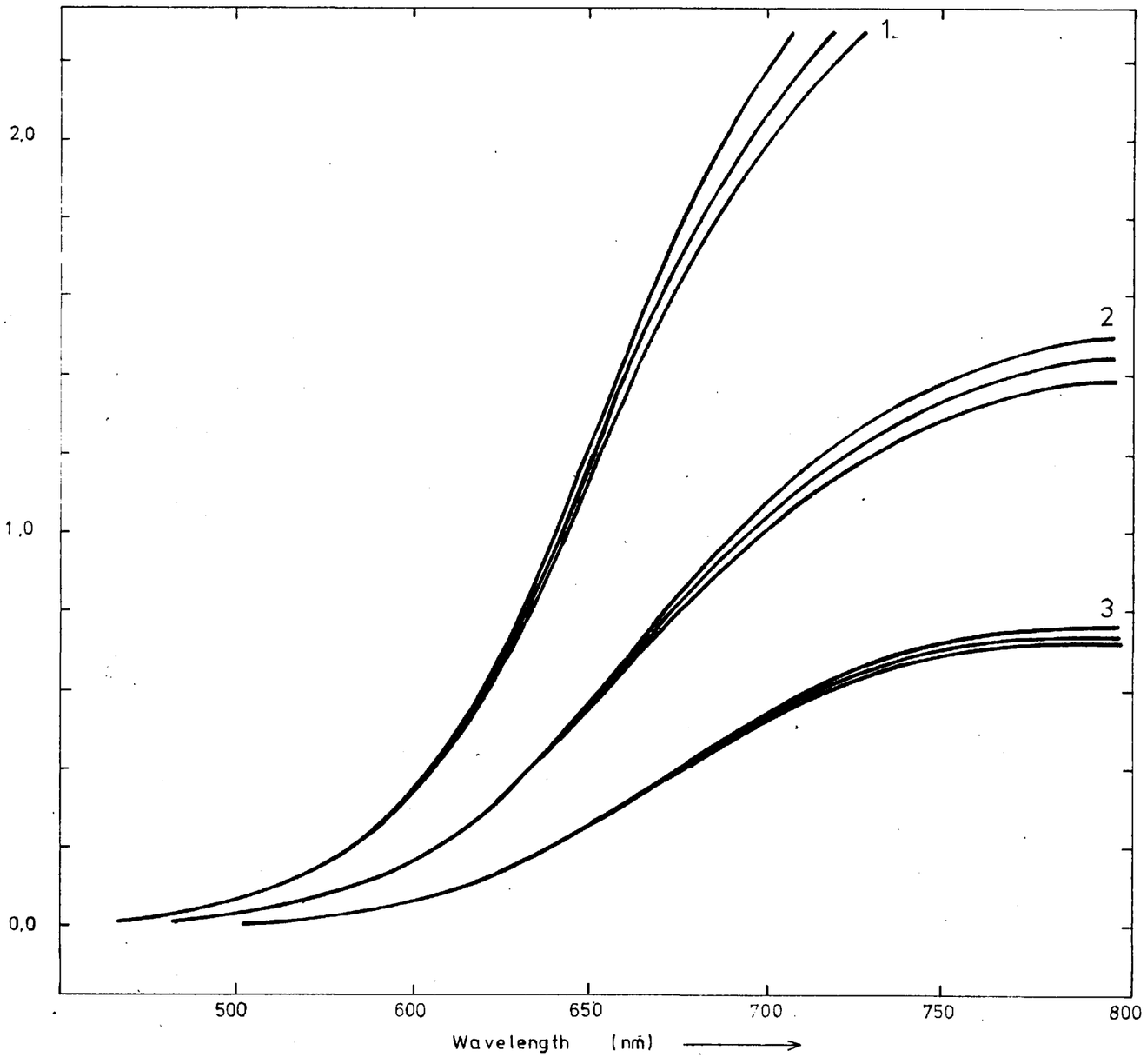


FIGURE A.1.x.

Cupric Sulphate Spectra At Various Temperatures.



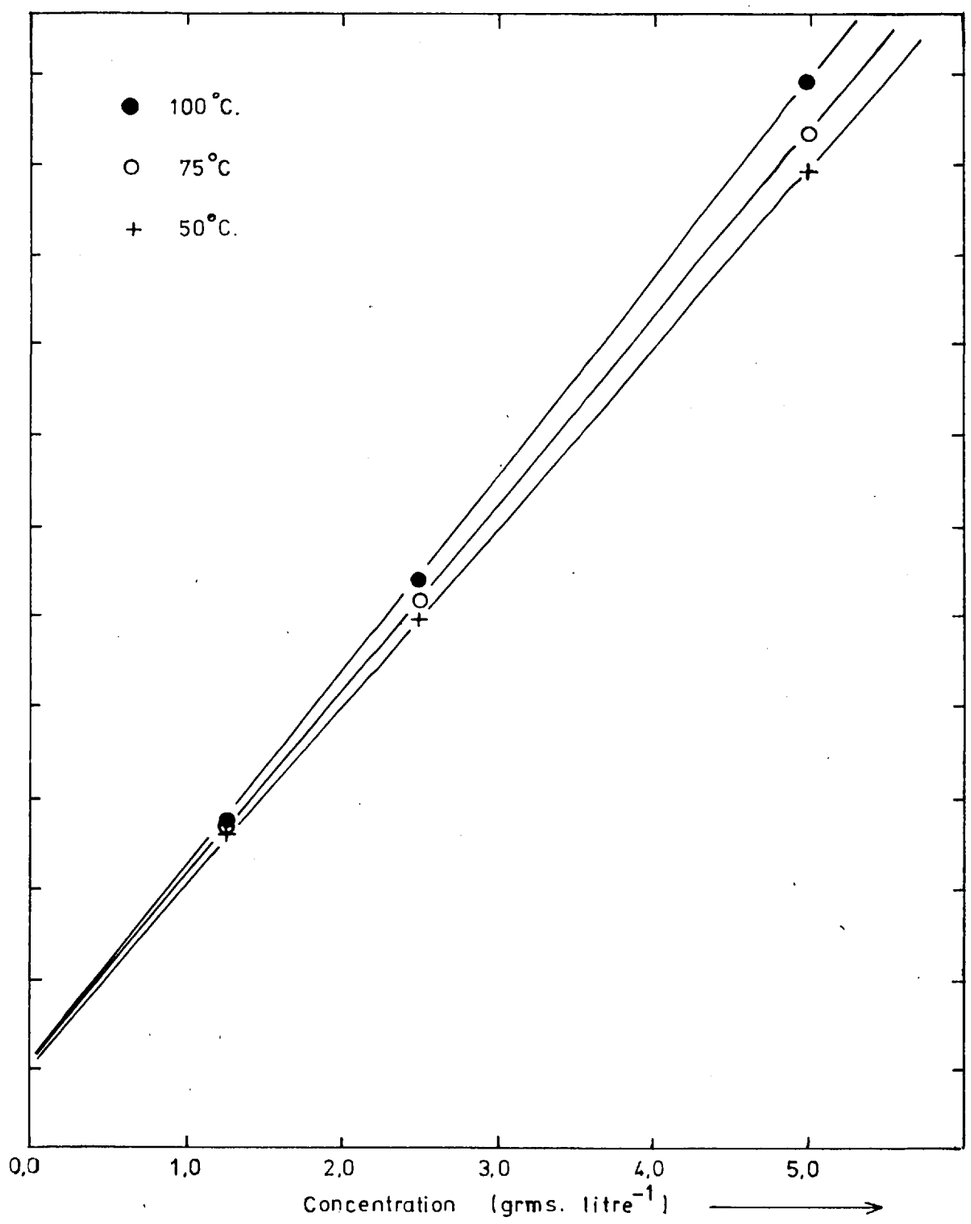
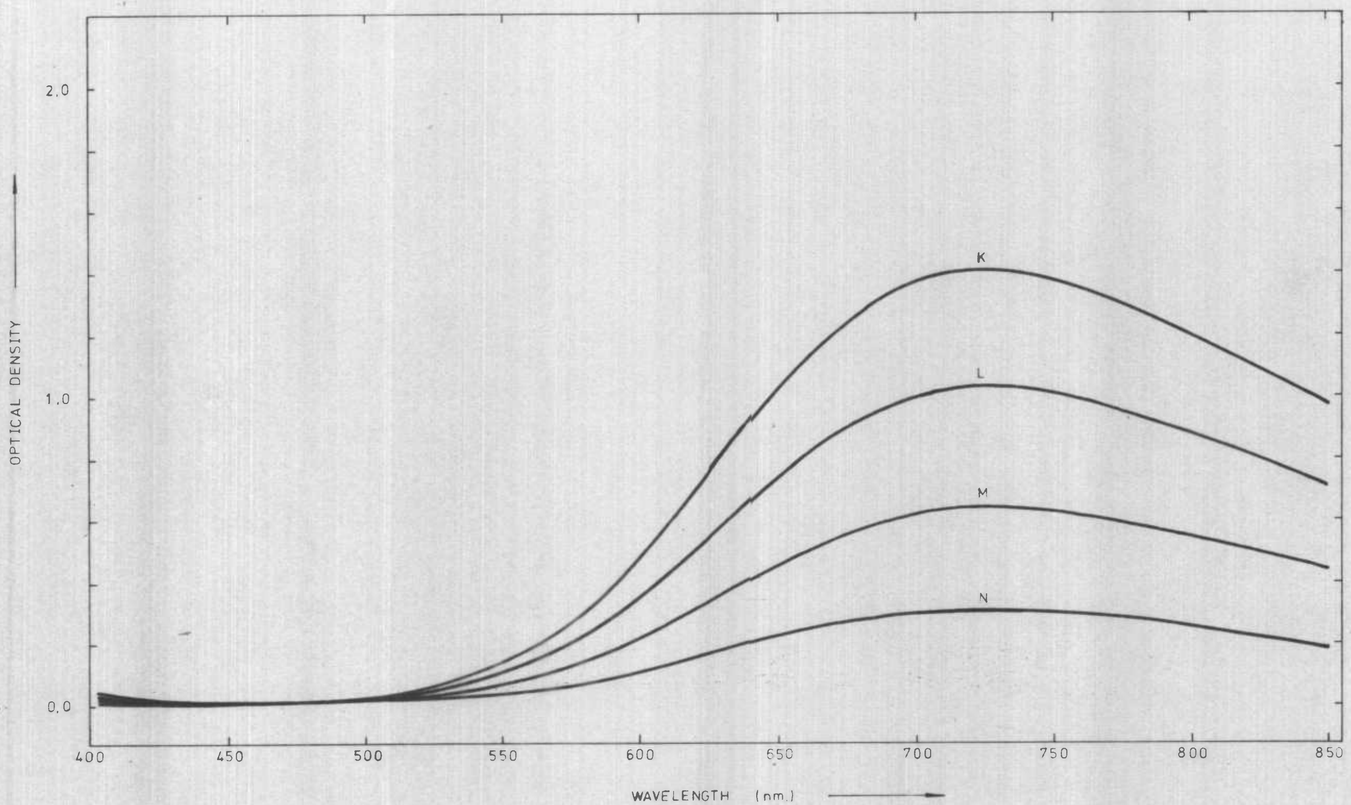


FIGURE A.1.xi.

Cupric Acetate Spectra At Various Copper Concentrations.



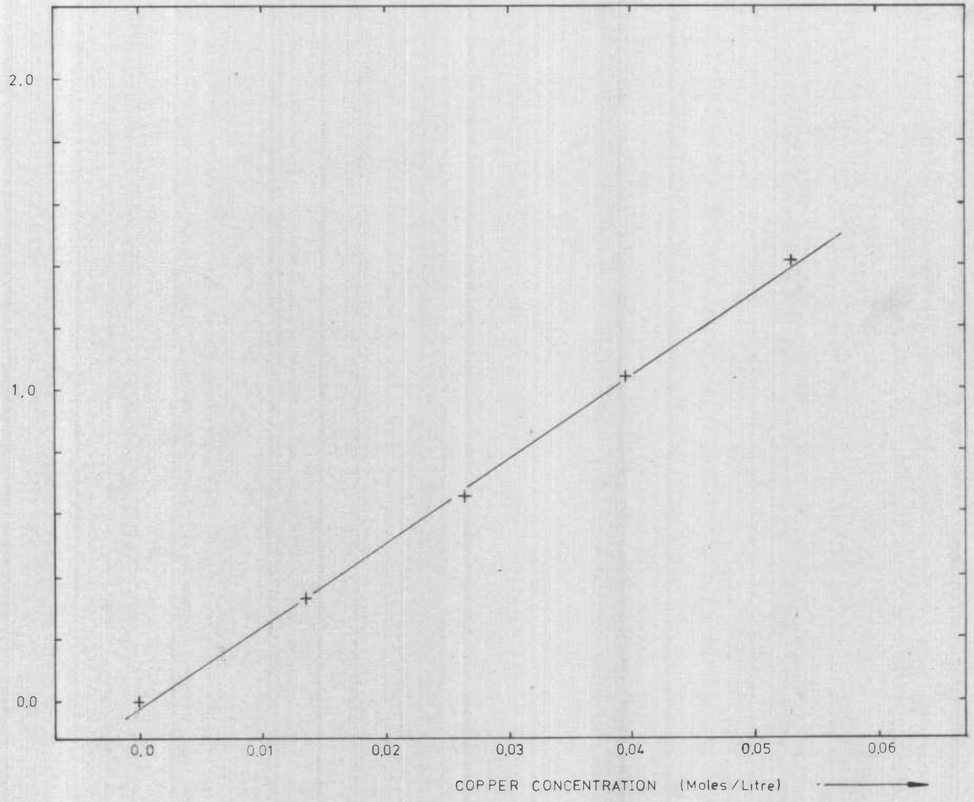
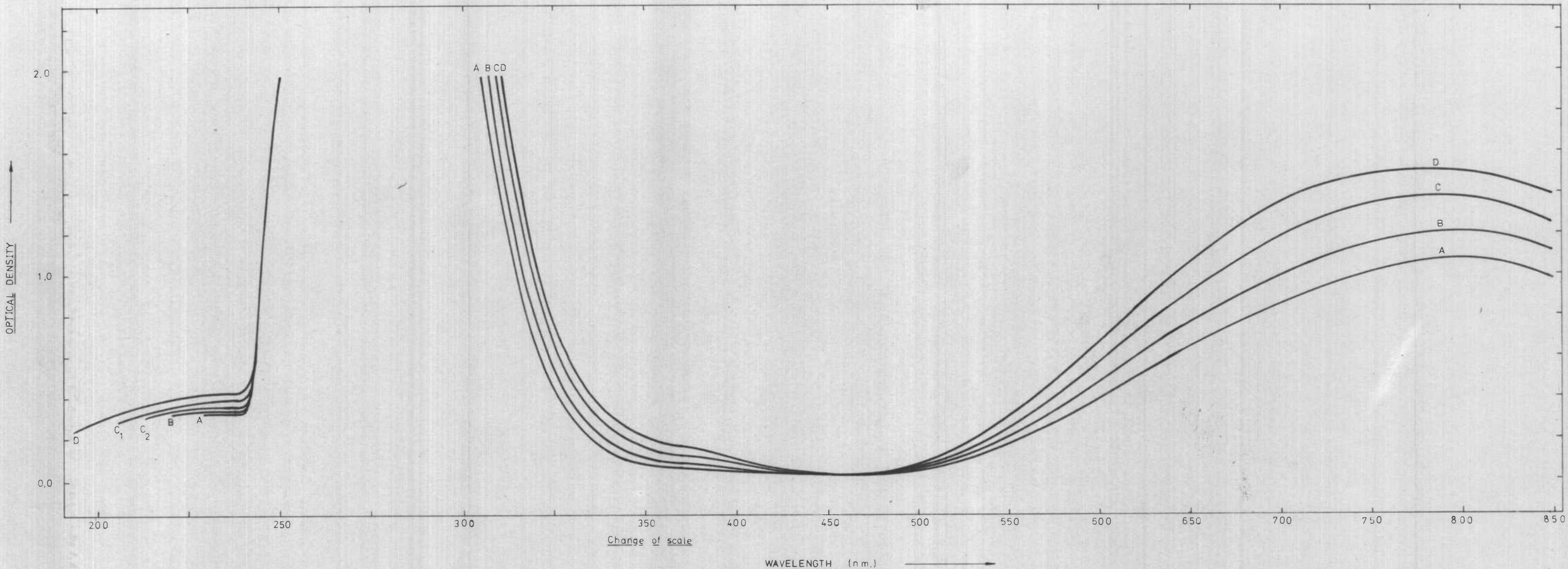


FIGURE A.1.xii.



Cupric Acetate Spectra At Various Acetate Concentrations.

Cupric Acetate Spectra At Various Acetate Concentrations.

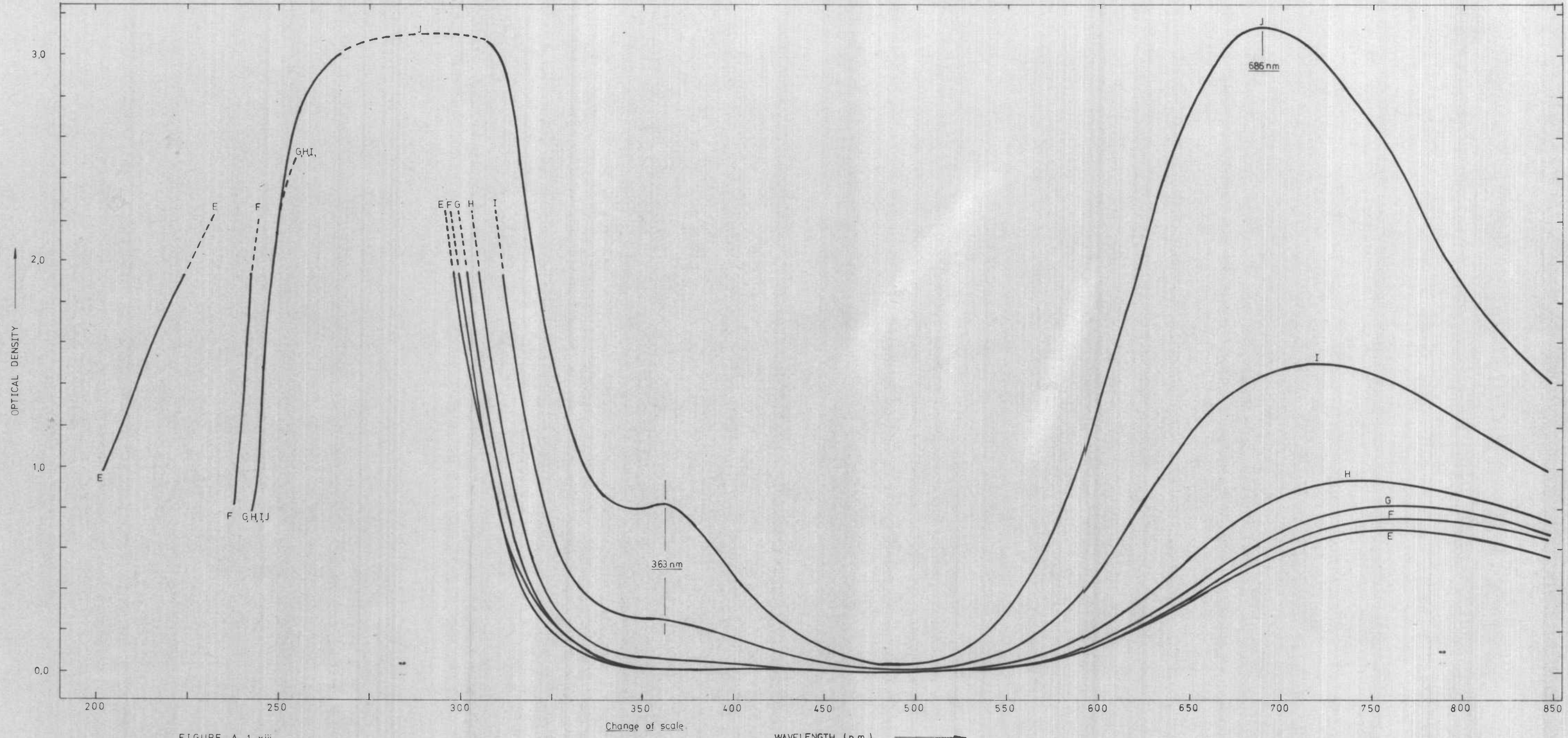


FIGURE A. 1. xiii.

with change in cupric concentration at constant acetate concentration and the Beer's law plot for this solution at room temperature.

Figure A.1.xii. and Figure A.1.xiii. show the variation of the spectra of copper acetate solutions at constant cupric concentration with change in acetate concentration.

By projecting the peak heights of the spectra curves across the diagram a dependence of optical density on concentration can be seen to exist.

Table A.1.T.i. shows the solutions used for the calibrations.

The calibration constant values here determined, were not used during the experiments. The value for each set of conditions could be determined since the optical density and cupric concentration were known at the beginning of the reduction.

A.1.3. The dissolution of hydrogen in aqueous solutions

During the course of the preparation of the experimental procedure for the examination of the reduction of cupric acetate solutions, examinations were made of the rate at which hydrogen dissolves in solutions with which it does not react.

The object of these investigations was to attempt to determine the rate of hydrogen consumption by the reduction reaction by the difference

between the rate of dissolution plus reaction and the rate of dissolution alone.

Solutions were employed which contained the same anion concentration as the copper solutions but no metal with which hydrogen could react.

Graphs of the rates of dissolution in sulphate solutions can be seen in Figure A.1.xvi. to Figure A.1.xviii. It can be seen that the rate of dissolution appears to be independent of temperature, hence the Arrhenius activation energy would be zero for this dissolution.

A.1.3.i. The purpose of the determinations

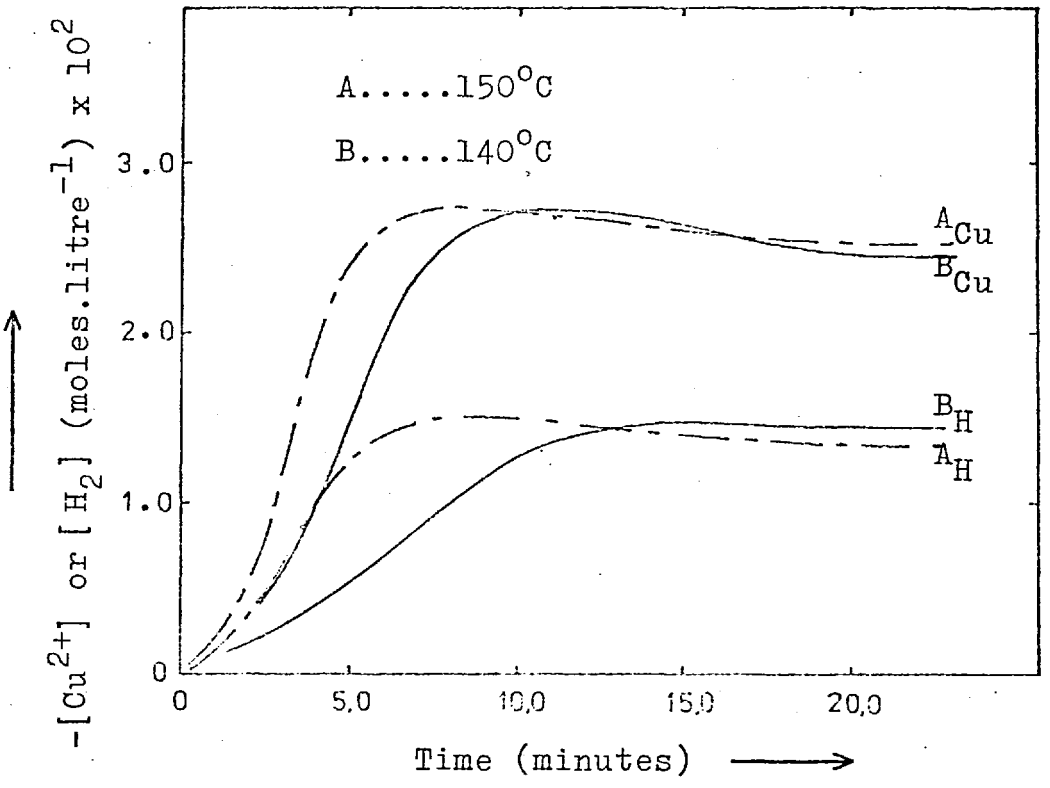
At a stage during the development of the data analysis method for the hydrogen reduction of cupric species in solution, it was thought that a knowledge of the rate of dissolution of the gas in an un-reacting solution would be of use.

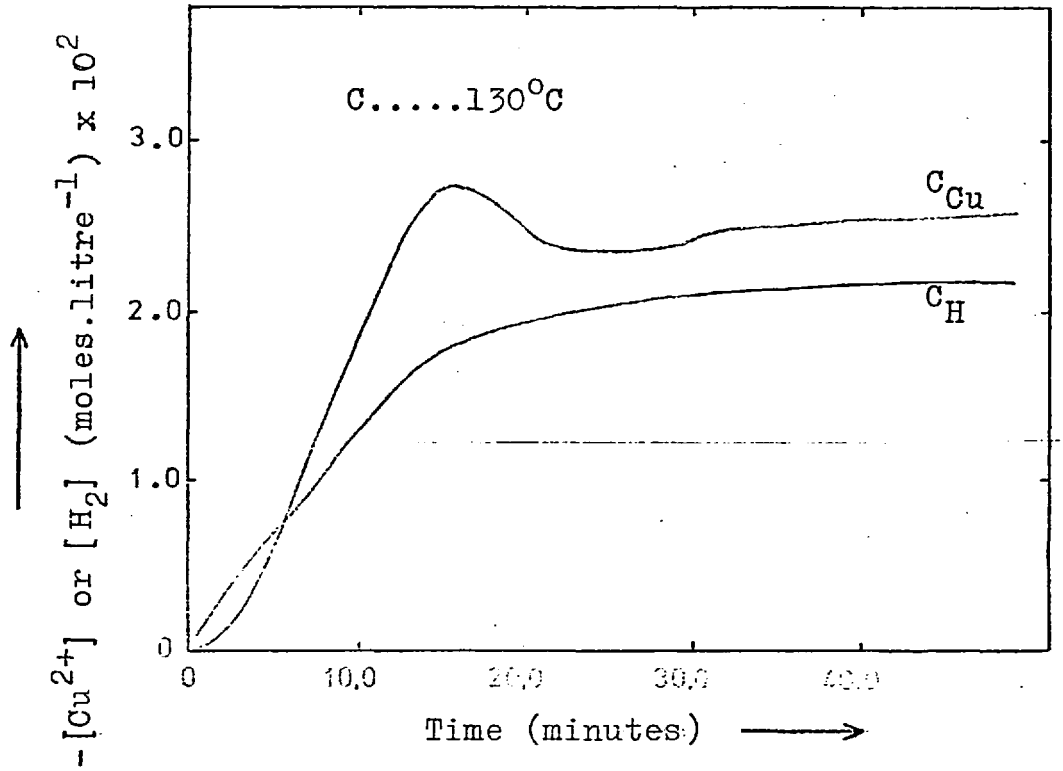
The proposed procedure was to measure the rate of dissolution of hydrogen in a solution in which a reduction reaction was occuring, and to subtract from this result the rate of dissolution in an un-reacting solution. The object of this procedure was to attempt to have a measure of the rate of use of hydrogen by the reduction reaction alone.

A surprising similarity was found to exist when the rate of hydrogen use found by this method was compared to the rate of 'disappearance' of

Figures A.1.xiv. and A.1.xv.

Rates of consumption of hydrogen curves compared with those of the rate of reaction of cupric species.





cupric species. Figure A.1.xiv. and Figure A.1.xv. show the curves, obtained as described above, for three identical cupric acetate solutions in which reduction reactions occured at 150°C, 140°C and 130°C. The similarities noted above will be seen to be evident in these graphs.

It was found that no further direct use could be made of the hydrogen rate of dissolution curves. However, they were thought to be of interest for their own merit.

The connection between the hydrogen consumption rate and reaction rate became evident from this work and the final data analytical method was developed from this point.

A.1.3.ii. The dissolution of hydrogen in unreacting sulphate solutions

These investigations were performed on two sets of sulphate solution, one equivalent to a cupric sulphate solution of about 5.0 grms.Cu^{2+}.litre^{-1}, and one equivalent to about 1.0 grms Cu^{2+}.litre^{-1}.

A variation of the rate of dissolution with temperature was considered to be within the experimental accuracy of the techniques employed, and thus a rate of dissolution which was independent of temperature was found.

The rates of dissolution were measured by the

Figure A.1.xvi.

Dissolution curves for hydrogen in sulphate solution of approximately 0.089 M, under a hydrogen pressure of 400 psi.

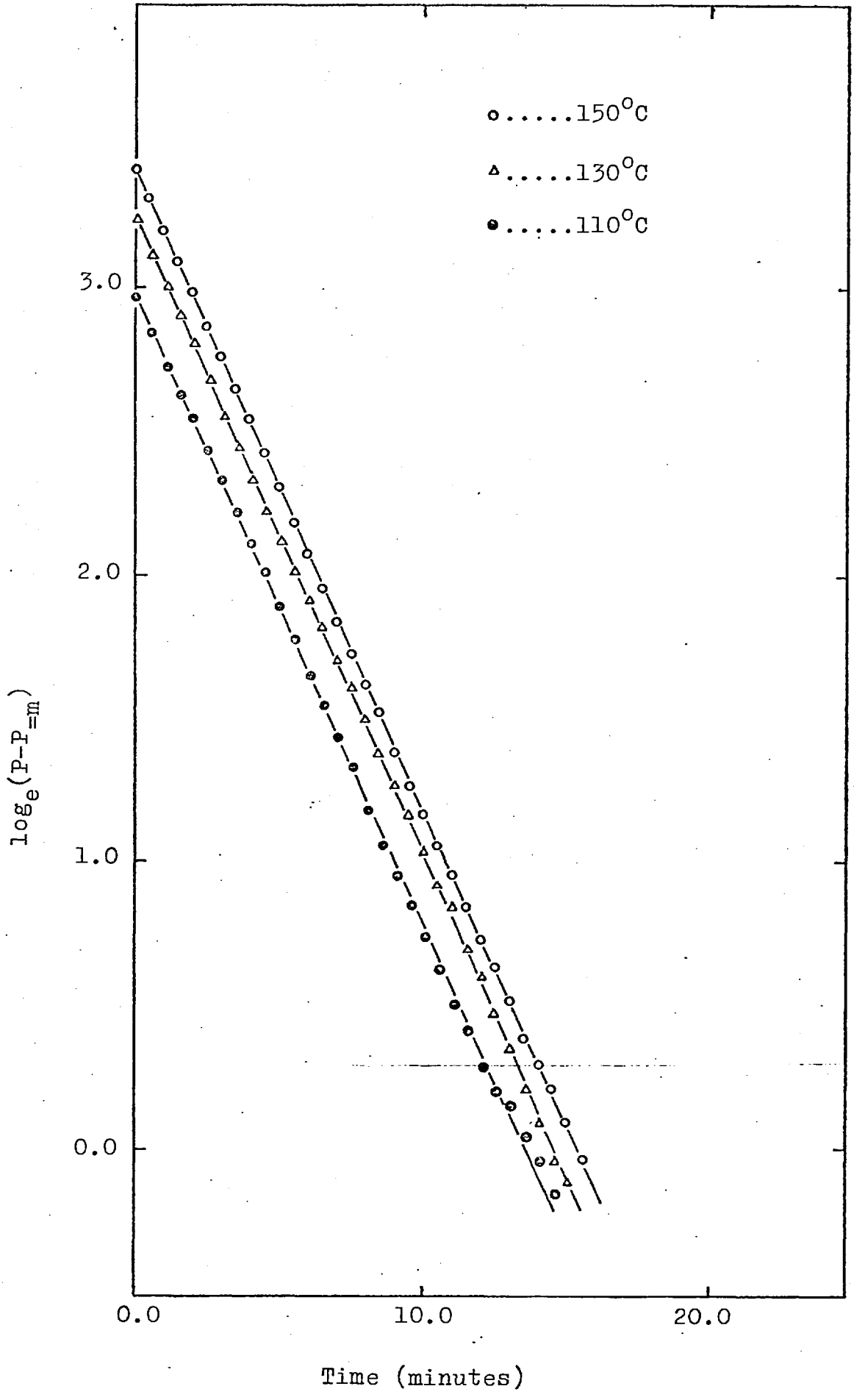


Figure A.1.xvii.

Dissolution curve for hydrogen in sulphate solution of approximately 0.089M, under hydrogen pressure of 600 psi.

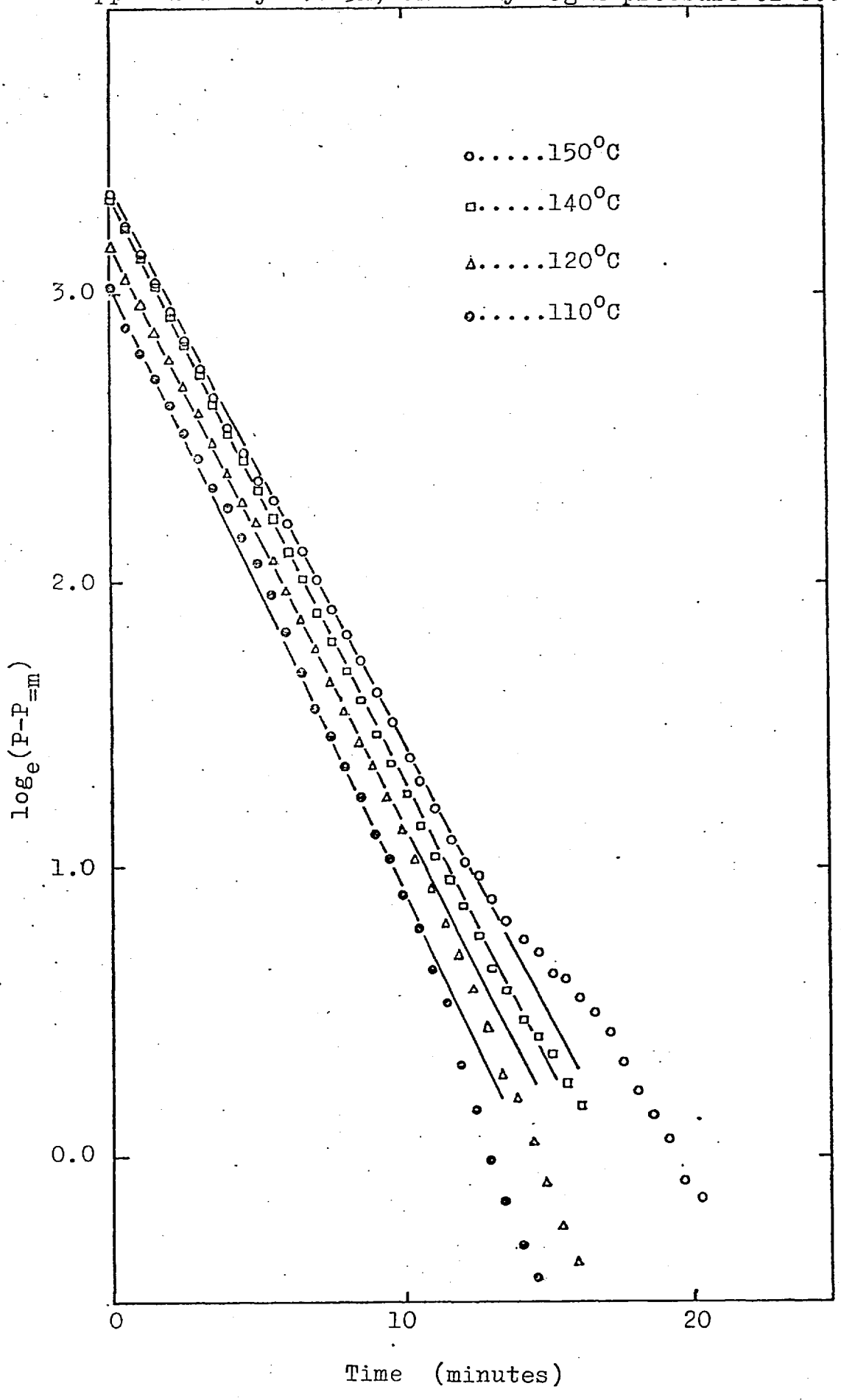
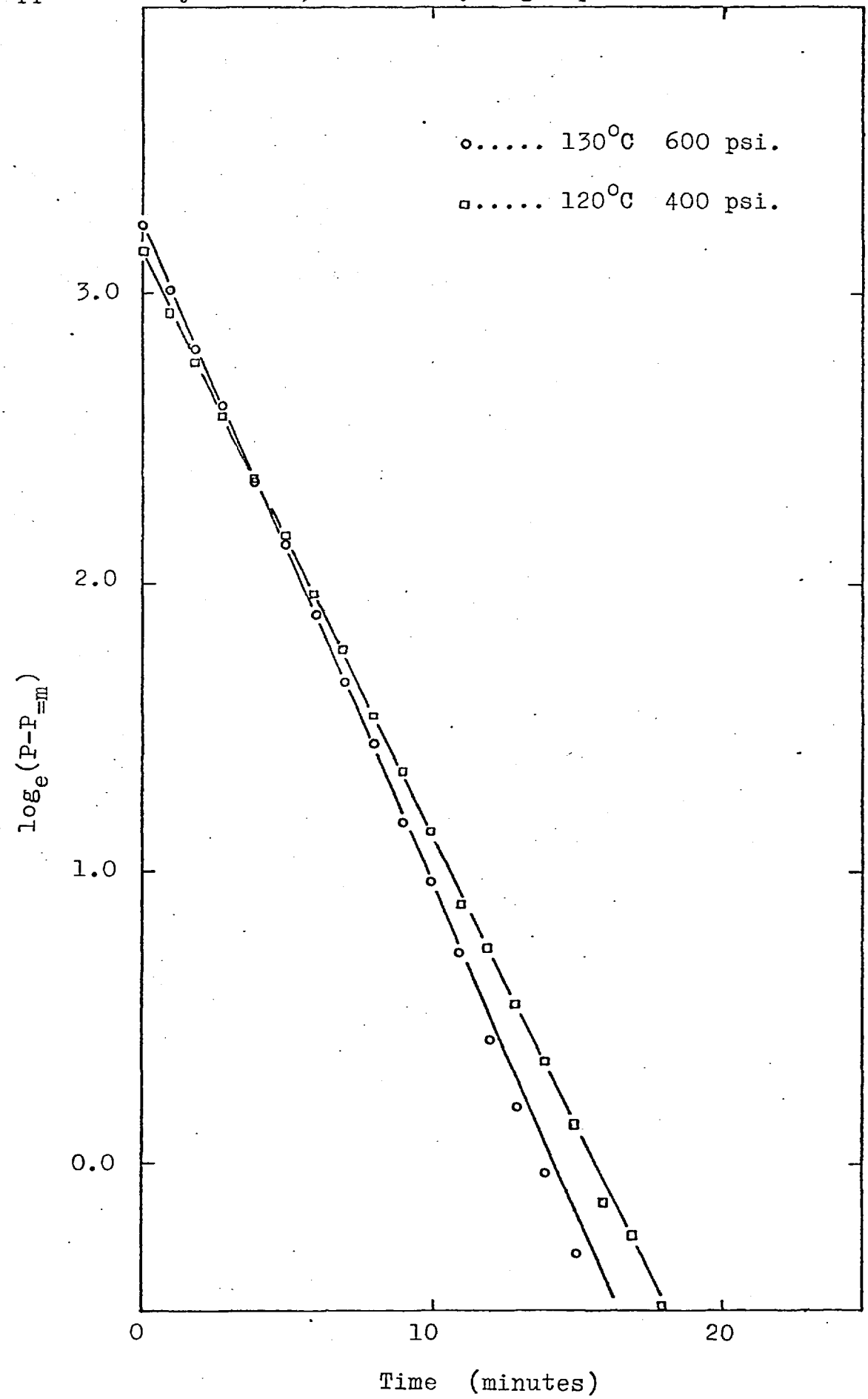


Figure A.1.xvii.

Dissolution curve for hydrogen in sulphate solution of approximately 0.025M, under a hydrogen pressure of 400 and 600psi.



gradient of the $\log_e(P_t - P_{=m})$ against time curves. These gradient values were:

Equivalent to 5.0 grms. $litre^{-1}$ = -0.204 $minutes^{-1}$

Equivalent to 1.0 grms. $litre^{-1}$ = -0.234 $minutes^{-1}$

at an initial hydrogen pressure of 600 p.s.i.; and

Equivalent to 5.0 grms. $litre^{-1}$ = -0.226 $minutes^{-1}$

Equivalent to 1.0 grms. $litre^{-1}$ = -0.208 $minutes^{-1}$

at an initial hydrogen pressure of 400 p.s.i.

Figures A.1.xvi. to A.1.xviii. show the variation of the rates of dissolution under different conditions.

A.1.3.iii. The dissolution of hydrogen in unreacting acetate solutions

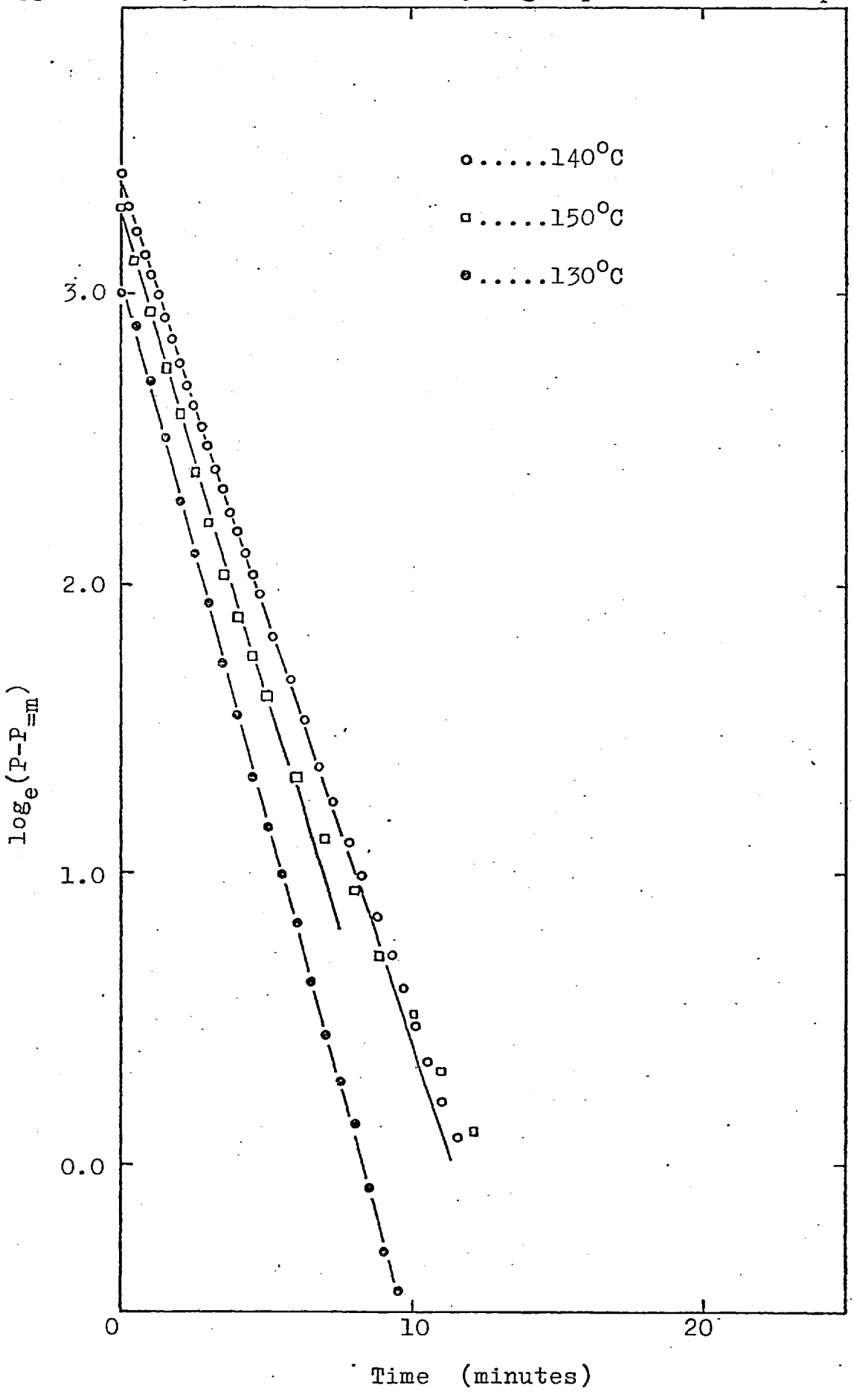
Not so many dissolution rates were determined for the acetate system as were found for the cupric sulphate equivalent solutions. However the same rules were found to apply. One concentration of acetate species only was investigated.

The rate constant for the dissolution of hydrogen in a solution of 6.41 molar acetic acid and 1.71 molar ammonia was found to be -0.36 $minutes^{-1}$.

The graph of these dissolutions may be seen in Figure A.1.xix.

Figure A.1.xix.

Dissolution curves for hydrogen in acetate solution of approximately 6.411M, under a hydrogen pressure of 400 psi.



Appendix 1

A.1.3.iv. A comparison of the results of the dissolution of hydrogen with previously published information.

Previous workers have determined the solubility and the rates of dissolution of hydrogen in aqueous solutions and in water.

Needes [37] found that in ammonia/ammonium sulphate solutions the dissolution was in two steps; both having the approximate rate equation of the form:

$$\frac{d\,[H_2]}{d\,t} = k\,[H_2]$$

where k had two different values during the course of the same dissolution reaction.

The total solubilities, that at equilibrium, found in the present work are as shown in Table A.1.T.iii. The values obtained by other workers [38], [39], [40], are presented in Table A.1.T.ii.

In the present work, good evidence was obtained to suppose that the rate constant for dissolution has a constant value throughout the transfer reaction, and that for the same solution dissolution rate constants are independent of temperature. Total solubility was found to increase slightly with temperature.

As the rate constants are independent of temperature, it follows that the apparent activation energy of the reaction must be zero.

Appendix 1

The values determined by Bruhn, Gerlach and Pawlech [38] expected a marked decrease in solubility. The decrease obtained was of approximately the expected value, however the solubilities measured were higher than those given by these authors.

Table A.1.T.ii. shows the variation of K_a, the Henry's law constant, with temperature for hydrogen dissolved in water. These values of K_a are from determination by Pray et Al [39]. This constant is in terms of pounds per square inch of gas pressure and mole fraction in solution. The values may be converted to molar concentration by assuming the number of moles of water in a litre of solution remain constant at approximately 55.56.

TABLE A.1.T.ii

$T^{o}C$	$K_a \times 10^{-5}$	Solubility 400 p.s.i. moles/litre	Solubility 600 p.s.i. moles/litre
23	11.00	0.020	0.030
52	8.72	0.025	0.038
149	9.30	0.024	0.036
179	8.34	0.027	0.040

Appendix I

The value obtained in the present work for sulphates and acetates are shown in Table A.1.T.iii.

TABLE A.1.T.ii

Solution	Pressure Hydrogen p.s.i.	Temperature °C	Solubility moles/litre	Rate const of dissolution
Sulphate approx. 0.089M	400	150	0.043	0.23
	400	130	0.037	0.23
	400	110	0.029	0.22
	600	150	0.039	0.19
	600	140	0.039	0.20
	600	120	0.034	0.20
	600	110	0.030	0.21
Sulphate approx. 0.025M	400	120	0.033	0.21
	600	130	0.036	0.23
Acetate	400	150	0.033	0.36
	400	140	0.039	0.31
	400	130	0.030	0.40

It may be noticed that the values for equilibrium hydrogen concentration in solution are considerably higher than those determined by Pray et Al. The change of solubility was not as marked as was predicted by Bruhn et Al [38]. The differences from these results was not so evident as those determined by Needes [37].

Appendix 1

A.1.4. The apparatus used for auto-reduction reactions

One investigation of the kinetics of the auto-reduction of cupric acetate solutions was made using a spectrophotometer cell reaction vessel. The remaining investigations made were in a double 'pot' autoclave.

The spectrophotometer cell used to make the single investigation showed signs of prospective failure after having been heated, at about 400 p.s.i., continually for about 22 hours. Because of the problems in use of spectrophotometric reaction vessel, a double chambered autoclave was used when further auto-reduction reactions were performed.

The autoclave arrangement used was designed by Dr. I.J. Grayson-Smith, originally for the investigation of the thermodynamics of solutions at high temperatures. The apparatus was, however, very suitable for determinations of the solution and gaseous products from an auto-reduction reaction.

The apparatus used consisted of tantalum lined chambers machined in a block of stainless steel, with lids sealed with silicon 'O' rings. The entire steel block was closely surrounded by a large aluminium block which enabled the whole assembly to be maintained at a steady temperature.

Appendix I

The aluminium 'block bath', which was designed and built to allow accurate temperature control for this investigation, was heated by means of a wire wound heating mat upon which the block rested. The entire bath and autoclave assembly was surrounded by an insulated box filled with vermiculite, with a kaoline wool blanket over the surface. Control of the heaters was performed using a Eurotherm PID/SCR controller.

The solution which was to undergo auto-reduction was introduced into one, or both, of the chambers. The apparatus was then raised to 150°C, under a small pressure of nitrogen, and held at that temperature for 200 hours. The results of the analyses of the solution after auto-reduction are described in section 4.

A.1.5. The design of new apparatus to investigate the reactions of solutions at high pressure and temperature

A.1.5.i. The design of the reaction vessel

The reaction vessels previously designed for investigating solution reactions, in a large volume of solution, by spectrophotometric techniques, have been made of stainless steel. The solution to be examined has been in contact with the steel, usually

Appendix 1

B.S. E.N.[58] J.

As has been described earlier in the thesis, corrosion problems are met with when acid solutions are in contact with the steel vessel.

To avoid the problem of corrosion a reaction vessel was designed in which no steel surfaces were allowed to come into contact with the solution.

On consideration of the available materials with which to make a reaction vessel, it was decided that the most feasible was an anodisable refractory metal.

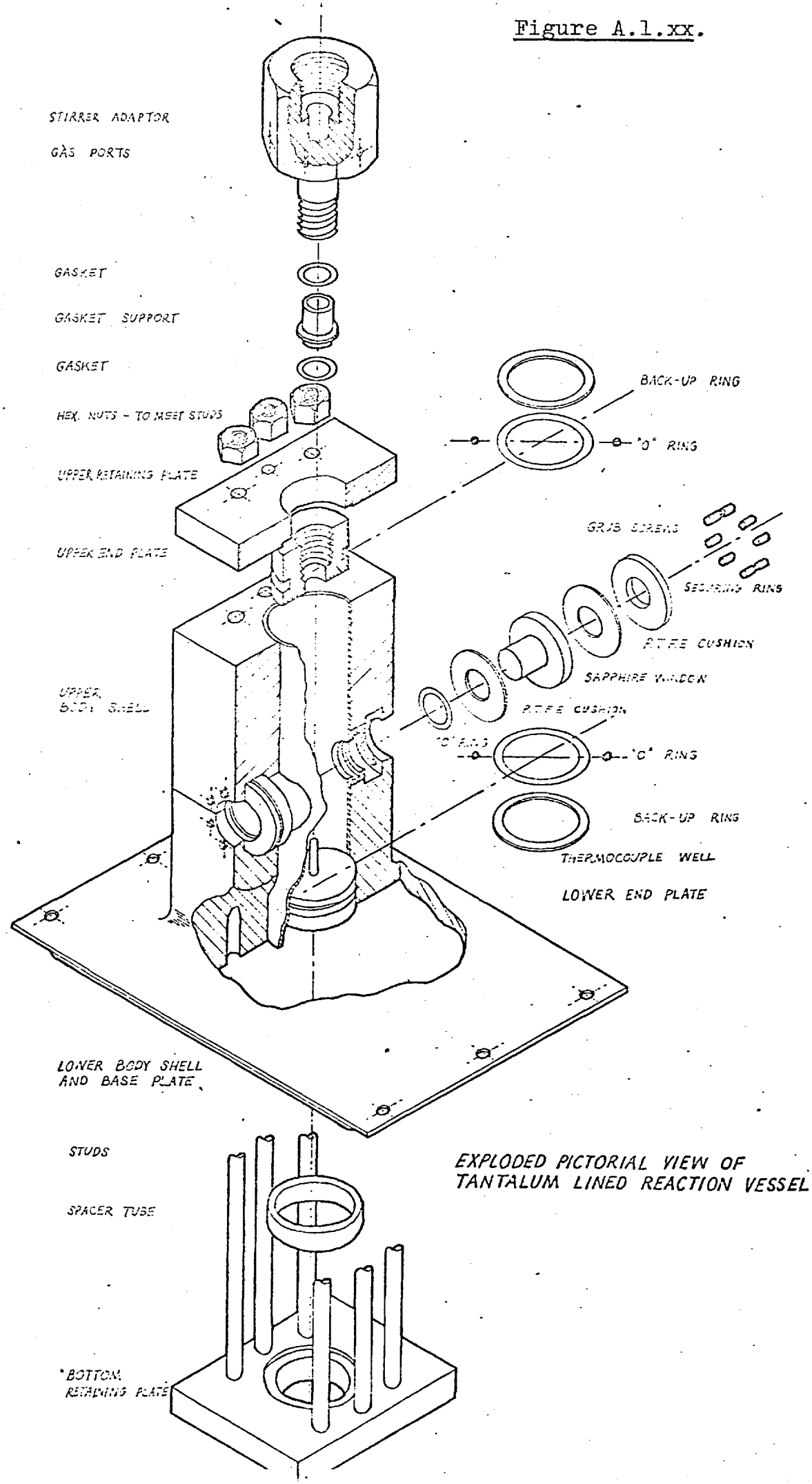
The metal chosen was tantalum, due to the ease of anodising and the relative ease of manufacture.

The cost of refractory metals, and the confined space available for the vessel caused the design to be in the form of a refractory metal lined stainless steel body. The refractory metal, tantalum, gave the required corrosion resistance, and the steel body resisted the pressure forces involved.

Design problems were encountered on consideration of the coefficients of expansion of the tantalum (approximately 6.5×10^{-6}) with that of the stainless steel (approximately 13×10^{-6}).[41] It was found that if the liner, of tantalum, was rigidly fixed to the steel body in more than one place, then rupture of the liner would occur when a temperature rise of more than approximately $100^{\circ}C$ was to be encountered.

To overcome this problem, the vessel was

Figure A.1.xx.



EXPLODED PICTORIAL VIEW OF TANTALUM LINED REACTION VESSEL

designed as a cylinder, which was supported rigidly only about the window 'ports', as may be seen in the exploded pictorial view, Figure A.1.xx. The ends of the cylinder were designed to be sealed by sliding end-plate plungers within the cylinder.

The end-plates were to be held in position by the retaining plates of the 'back-up' body, appropriately located by a spacer placed between the end plate and the retainer plates. Using spacers in this position allowed the volume of the vessel to be adjusted as required.

The mechanical design of the vessel body was done using conventional methods to allow the vessel to withstand an operating pressure of up to 2,000 p.s.i., if necessary.(42)

The mechanical properties of the materials for the manufacture of the windows of the cell were difficult to determine since very small imperfections would considerably influence the properties of materials such as sapphire.

Sapphire was decided upon as a suitable material since the price difference between quartz, the other possible material, and sapphire was very small and the mechanical properties, optical properties and resistance to chemical attack of sapphire (alumina) are considerably better than for quartz (silica).

A value of the maximum allowable shear stress was decided upon as 2,000 p.s.i. for the purposes of the design, although shear strength values of

sapphire have been found to be as high as 10^6 p.s.i.(43)

A drawing of the sapphire window design is included in the design envelope at the back of this work.

The stainless steel body, of B.S. E.N. 58 B., was designed assuming a maximum acceptable tensile stress of 20,000 p.s.i. Drawing of the final design of the vessel may also be found in the envelope at the back of this work.

The tantalum liner was produced by Murex Refractory Metals Ltd., to tolerances as close as was possible to those stated in the drawing. The liner was found, however, to have a noticeable degree of non-circularity in the section; (up to about 0.008 inches diameter difference). Therefore fitting of the steel back-up body to the liner was required.

The finished combined pressure vessel was sufficiently well fitted that any strain upon the tantalum on pressurising caused stresses which were within the acceptable limit.

The windows of the cell were designed to seal in the tantalum window 'ports' by means of 'O' rings, made of 'Viton' by James Walker Ltd. Cushions were situated on both sides of the window flange so that stress concentrations on the loaded faces of the windows were avoided. The cushions were made of P.T.F.E. and were 0.030 inches thick.

Appendix 1

The seals for the vessel end plates were also supplied by James Walker Ltd. They consisted of a 'Viton' 'O' ring in conjunction with a P.T.F.E. 'back-up' ring. The 'back-up' ring was to avoid extrusion of the viton under high pressure at raised temperature.

The stirrer adaptor / gas port assembly was to be of stainless steel, B.S. E.N. 58 J. This assembly allows a magnetically driven stirrer, similar to that described in section A.I.1.iii., to be attached to the reaction vessel. Seals between the 'Magne-Drive' and the adaptor, and the adaptor and the upper end plate are the same as those described in section A.I.1.iii. Use of a gasket support guide was again made so that contamination of the reacting solution could be avoided, and a reliable gas seal was attained.

In order to avoid prospective seizing of the tantalum liner within the stainless steel body when the liner was pressurised inside the shell, it was proposed that two small unions should be fitted in the steel body so that oil may be pumped into the interface between steel and tantalum.

The unions were to be of the form of a $\frac{1}{8}$" diameter threaded surface hole, of approximately $\frac{3}{8}$" depth, with a one sixteenth inch hole taken through to the interface. One eighth inch diameter steel

tube could be screwed into surface hole and sealed sufficiently with P.T.F.E. threading tape. By this means oil could be pumped to the interface, under a small pressure, and lift the liner from the steel surface, thus relieving the surface friction and allowing ease of removal of the tantalum from the body whilst keeping a very good fit of the liner within the steel.

In practice this precaution was found to be unnecessary since no 'binding' of the steel to the tantalum occured. The completed tantalum lined reaction vessel was hydraulically tested to 2,250 p.s.i. before use in the spectrophotometer, to ensure stability of the design.

A.1.5.ii. Design of the constant pressure gas consumption measuring apparatus

In order that the rate of use of gaseous reducing agent may be monitored continuously, whilst maintainence of a constant pressure within the reaction vessel is assured, equipment was designed to allow a measurable apparent volume change of the gas space above the solution contained in the tantalum lined reaction cell.

This equipment was not completed at the time of writing, but the major design was done. The outline of the design is described below and in the drawing, Figure A.1.xxi.

Appendix 1

The design consists of a P.T.F.E. diaphram 10.2 cms. in diameter sealed in a chamber formed by two joined spherical segments. A diaphram of this diameter may be displaced at its centre by a small amount to cause a relatively large volume displacement, whilst the increase in the diameter of the diaphram disc would be changed by a very small amount. The small change in the pressure which would be required to cause a displacement of 10 mls. would be negligable, since the subsequent increase in the diameter of the disc would be about 1.6% from 10.2 cms. to 10.36 cms. To strain a P.T.F.E. sheet of approximately 0.025 mms. thick by 1.6% requires minimal stress. Thus the pressure difference across the strained and across the unstrained diaphram may be assumed to be the same.

The lower segment portion of the chamber was to be connected to the reaction vessel gas space, shilst the upper part was to be filled with hydraulic fluid and fitted with the plunger and sleeve of a Barnet Instruments Ltd. low pressure oil operated 'dead weight' tester.

By the described arrangement, the pressure within the reaction vessel may be balanced against the load on the carriage of the hydraulic plunger, and the volume change at that pressure may be monitored by the movement of the carriage.

Movement of the plunger and weights was to be followed using a very lightly loaded position trans-

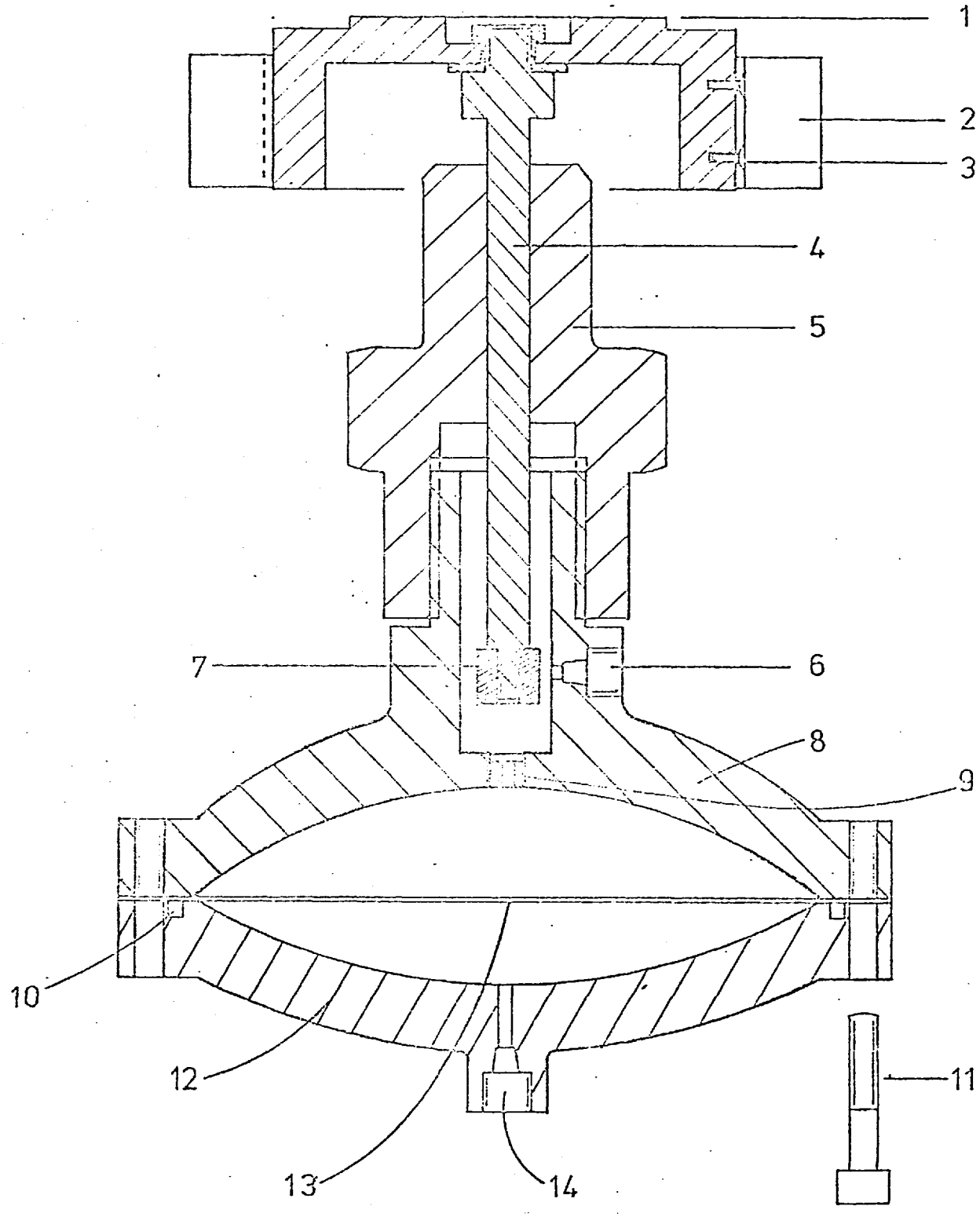


Figure A.1.xxi.

Appendix 1

Labels of constant pressure gas usage measuring equipment.

1. Weight carrier.
2. Blade for air rotation of weight carrier.
3. Securing screws of rotatory blades.
4. Plunger.
5. Sleeve body.
6. Oil inlet from pump to reset plunger position.
7. Nylock nut.
8. Pressure transfer unit upper plate.
9. Baffle plug.
10. 'O' fing groove for gas seal.
11. Cap screws (8x)
12. Pressure transfer unit lower plate.
13. P.T.F.E. diaphram.
14. Gas connection to reaction vessel.

ducer mounted vertically above the carriage. The position transducer used may be sensitive to less than 0.001 mms. change in position. This movement is equivalent to a volume change of about 10^{-5}mls. at the pressure of the reaction.

The carriage of the dead weight tester was to be fitted with rotatory blades to allow the plunger to be constantly and steadily turned by an air supply.

The upper, hydraulic, part of the arrangement was to be fitted with an oil inlet union to allow the plunger position to be adjusted, using a pump and resevoir. By this means resetting of the plunger and transducer after they move by their full travel is facilitated.

The mounting of the entire arrangement must be on adjustable points in order that vertical alignment of the moving plunger be possible.

A.1.5.iii. Fitting of the tantalum lined reaction vessel

The tantalum lined reaction vessel, and the gas usage monitoring device, has been designed to be used in conjunction with a Perkin-Elmer 356 Double beam / Double wavelength recording spectrophotometer.

This instrument has been chosen in order to facilitate the monitoring of the optical density changes in a solution even when the solution contains a solid phase in suspension which causes

turbidity. To allow turbidity independent optical density measurements to be made, the instrument was to be arranged so that two beams may pass through the same position in a single solution. One beam may be monochromated to a wavelength which is characteristic absorption peak for the species in which optical density measurements may be made; whilst the other beam may be of a wavelength where the species is non—absorbing or at least very nearly non—absorbing. It must then be assumed that turbid solutions absorb light by 'shuttering' or scattering without change of wavelength, and that no Rayleighian scattering occurs, so that turbidity may be assumed to be independent of incident wavelength.

By using the beam at the 'trough' wavelength as a reference beam, the output from the instrument would always be the solution absorbance, or optical density, only.

The existence of a double monochromator in the instrument also has the advantage that first derivative of the spectra may be easily determined by scanning across a required range with the two monochromators set at a small, by constant, wavelength apart. The arrangement may equally well be used for the accurate analyses of a species in solution where interference of another, possibly changing, component would otherwise effect the absorbance readings.

These advantages of the instrument could be made use of when the instrument is fitted with the tantalum lined reaction vessel, or if it is used with conventional spectrophotometer cells.

The Perkin-Elmer 356 is also arranged to be optically 'backed-off' so that optical densities of up to about 4.00 may be measured. That is a sensitivity to 0.01% transmission of incident light through the solution.

The tantalum lined reaction vessel was to be advantageous over the previously used cells for the optical measurements in solutions because of the rigidly mounted cell body in the spectrophotometer. As the windows of the pressure reaction vessel are designed to be in a fixed position relative to the optical paths of the instrument, the path of the beams through the solution may be identical during a number of reduction experiments. Due to the reproducibility of the optical path through the cell, direct comparison of optical density change determinations between different reactions may be made.

A.1.5.iv. Stirring of the solution within the tantalum lined reaction cell.

Stirring of the contents of the new cell has been arranged in a similar way to that described in Appendix A.1.1.iii. for the previously designed equipment. Stirring of the presently described

vessel design was to be by a magnetically coupled P.T.F.E. parallel stirrer rod. The coupling unit was to be driven at about 1500 r.p.m. by an electric motor mounted upon the spectrophotometer chassis.

To avoid straining and malaligning the upper end plate of the cell the 'Magne-Drive' coupling unit was to be rigidly supported by an overhead frame, at points above and below the outside magnets. Consequently side thrust due to the stirrer drive belt would not be an effect on the sealed end plate.

A.1.5.v. The temperature measurement and control of the cell

Temperature control of the body of the tantalum lined reaction vessel was to be made by the use of a thermocouple placed in the well for the purpose in the lower end plate. The control thermocouple was to be connected to a Model PID/SCR Eurotherm power controller. The controller was to supply to wire-wound, mica insulated heating mats, which were to surround the stainless steel body. Accurate temperature measurement was also to be made from a thermocouple in the well situated in the lower end plate.

A.1.5.vi. The arrangement to avoid overheating of the spectrophotometer

A 'Box sectioned' cooling plate, containing cooled circulating water was to surround the heating mats, so that sensitive parts of the spectrophotometer could not be effected by the heated cell block. The cooling plate was to be separated from the heating mates by an insulating layer of 'Triton' "Kaowool" kaolin fibre insulating material.

Drawings of the design of the cooling box are included in the design envelope at the back of this work.

A.1.5.vii Control of the gas supply to the reaction vessel

Arrangements for the fast induction of gaseous reagents and for pressure control in the reaction cell was to be similar to the equipment used on the vessels used during the present investigations. This arrangement may be seen in Figure A.1.iii.

Appendix 2

EVIDENCE OF THE EXISTENCE OF CUPRIC ACETATE DIMER IN AQUEOUS SOLUTIONS

The species present in a cupric acetate solution have been studied in less detail than those present in cupric sulphate in aqueous solution, as described in section 1.1.ii.

During the present work some evidence for the existence of a cupric acetate dimer was found, the structure of this dimer is probably of the form shown in Figure 1.1.ii.

The solid hydrated cupric acetate structure is a binuclear complex with acetate groups bridging between the copper sites on the four stronger co-ordinates. (1) The weak bonds at each end of the complex are occupied by hydration molecules, situated opposite the metal-metal bond.

In a non-ionised solution, benzene or dioxan for example, all the evidence indicates that a binuclear, bridged structure remains. (6 to 16) The similarity in the structure of the solid and the non-ionised solution, and the difference between these and the structure in aqueous solution may be shown by the distinct change in the magnetic properties. A few examples of the values of magnetic moments of the species in the solid, and in various solvents may be seen in Table A.2.T.i.

Appendix 2

Table A.2.T.i

Solvent	Magnetic Moment (B.M.)
None (solid)	$\mu s = 1.38$
Benzene	$\mu s = 1.40$
Dioxan	$\mu s = 1.31 \pm 0.06$
Water	$\mu s = 1.90 \pm 0.05$

It is possibly worth noting that from the magnetic moment measurements of Martin and Whitley [6], that the moment determined for cupric ions, in aqueous solution as the acetate, falls in the range 1.7 to 2.2 Bohr Magnetyon. A value in this range was to be expected for a 'free' copper (II) ion. The value shown is, moreover, not very different from the spin only magnetic moment of 1.73 B.M. thus indicating a significant quenching of the orbital contribution to the moment. This effect is to be expected in a complexed single nuclear form.

Similarly the lower value of μs for the solid and the non—ionising solution indicates a binuclear complex, since this form would partially eliminate the moment due to spin of the electrons which would be unpaired in the un-dimerised complex, but are quenched because of the proximity of another un-

paired state in the dimer.

A noticable change in colour between dilute aqueous solution and benzene solution also indicated a structural difference in the ionising and non-ionising solutions.

The wavelengths of maximum absorbance in the two solutions are:

Dilute aqueous solution : 765 $\pm$ 5.0n.m.

Benzene solution : 665n.m. and 370n.m.

Despite the evidence to support the existence of the monomeric cupric acetate complex in dilute solution the evidence of the absorbance spectra, determined during the present work, for cupric acetate solution at relatively high concentrations, and especially in large acetate concentrations, indicate a similarity in structure to that shown to exist in benzene and dioxan solutions.

During the present work a marked change in the wavelength of maximum absorption was observed in cupric acetate solutions as the acetate concentration approached 10 molar. This change may indicate the continued existence of the bridged dimer complex under these conditions.

The absorption spectra for various cupric acetate solutions may be seen in Figure A.1.xii and Figure A.1.xiii. and the absorption peaks are tabulated in Table A.2.T.ii.

Appendix 2

Table A.2.T.ii.

Solutions		Absorbance Peaks	
Copper conc'n (molar)	Acetate conc'n (molar)	1. n.m.	2. n.m.
0.053	2.8	760 to 770	none
0.053	11.1	720	362
0.053	13.9	686	363
$(Cu(Ac)_2)_2$ in benzene		665	370

The existence of a dimer in high acetate solution is proposed since the benzene solution has such a similar absorption spectra to the 13.9 molar acetate solution. This proposal is supported by the electronic configuration considerations described in section 1.1.iii. The structure proposed by a combination of these two considerations is:

$$(Cu_2(CH_3.COO.)_4.2CH_3COO)^{2-}$$

This complex should give an absorption spectra very similar to the hydrated dimeric version, since no major electronic configuration differs. The change

in the 'end of chain' groups would be the least effective since these co-ordination sites are the weakest and the furthest from the copper ion.

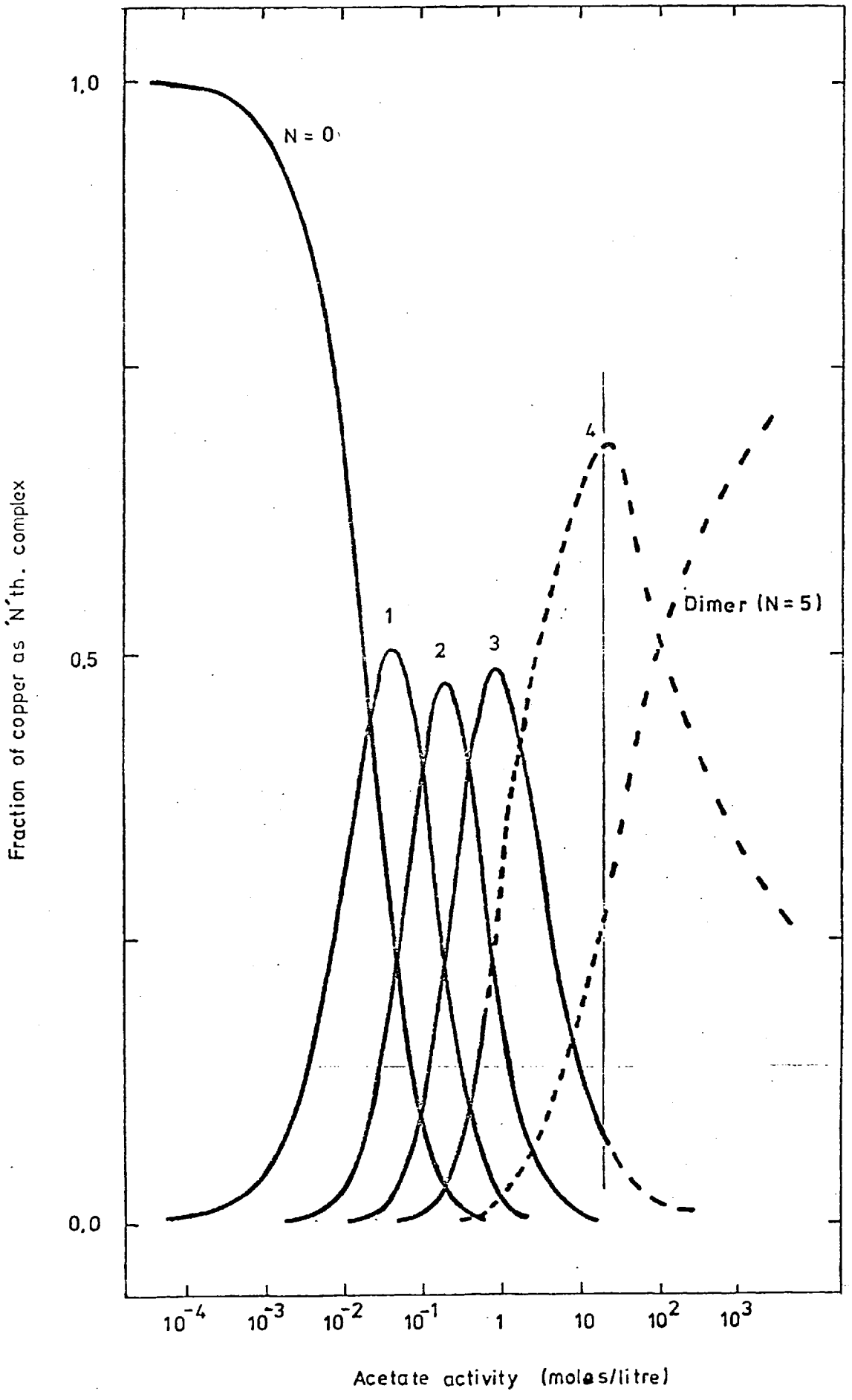
The comparative evidence put forward to propose the existence of a dimeric structure cannot be considered conclusive. This is because no evidence exists to indicate that the absorption characteristics observed in non-ionising solutions in the visible region of the spectra are caused by any effect of the existence of the dimer.

The proposed existence diagram to determine the predominant species to include the dimeric form of cupric acetate may be seen in figure A.2.ii.

This diagram was not quantitatively drawn since no information was available regarding the formation equilibrium of the fifth complex, the dimer.

The vertical line on the diagram indicates the point at which the solution being considered becomes hypothetical since above this acetate concentration the solution consists of more than 100% acetic acid

Figure A.2.ii.


1,0
0,5
0,0
N = 0
1
2
3
4
Dimer (N = 5)
Fraction of copper as 'N'th. complex
10^{-4}
10^{-3}
10^{-2}
10^{-1}
1
10
10^{2}
10^{3}
Acetate activity (moles/litre)

Appendix 3

SOLID ELECTROLYTE CELL TO ATTEMPT TO MEASURE ACTIVITY OF A SPECIES IN SOLUTION

A.3.1.i. General description of the electrolytic cell.

A solid electrolyte, electrode concentration cell was proposed as a possible device to measure the activity of an aqueous solution species. The species in the solution was to be allowed to come into contact with a similar ion in a solid crystalline electrode, which was one half of a solid cell, the other half being a similar material which was maintained in a standard state.

This method was an attempt to make measurements of the properties of a solution, by making potential measurements, whilst allowing no charge transfer to occur in the solution.

The solid electrolyte cell for measurements in chloride solutions is pictorially described in figure A.3.i. This cell consisted of a lead chloride electrolyte which was in contact with two electrodes of silver chloride. One of the electrodes was in close contact with metallic silver, and was thus kept under constant, standard conditions. The other electrode was allowed in contact with chloride ions in the aqueous solution. Thus the second electrode, when in equilibrium with the chloride ions in the solution no longer contained lattice chloride ions at the activity of those in the standard electrode.

Appendix 3

Because of the chloride activity difference across the solid electrolyte a chemical potential existed, this chemical potential should have been measurable as an electrical e.m.f.

The entire cell, including the leads, was encapsulated in high temperature Araldite AT.1. so that solution could not penetrate to the lead chloride electrolyte.

The materials for the manufacture of the cell were made in the following ways.

A.3.1.ii. Silver chloride pellets

About 4 grams of analytical reagent grade silver nitrate was dissolved in about 200 mls. of distilled water. The solution was warmed slightly and an addition of about 100 mls. of dilute hydrochloric acid was made, addition being continued until no further precipitation of silver chloride occured. It was found that a warmed silver nitrate solution caused some flocculation of the silver chloride product and hence settling of the solid was much quicker.

The precipitate was allowed to settle, and excess liquid was decanted off. The solid was then washed several times in distilled water before final decantation and drying slowly in an oven at about $60^{o}C$.

The silver chloride product was handled in

subdued light and stored in a dark cupboard to avoid any decomposition.

The pellets of silver chloride were made by melting the solid white precipitate into prepared flat bottomed silica tubes. Upon cracking the silica mould the pellet produced was uncoloured, translucent and non-porous. The as-cast pellets were carefully machined to shape using an ordinary steel machine tool.

To avoid any possibility of contamination of the pellets after casting in the silica tubes, the machine finished cylindrical pellets were washed in ammonia solution to remove the surface layer, and then dried before packing into the cell.

A.3.1.iii. Lead chloride solid electrolyte pellets

Lead chloride precipitate was produced similarly to the method used to produce silver chloride. The lead chloride was to be dried very thoroughly to ensure that ionic conduction alone occurs when the material was packed in the cell. Drying of the powder was performed in a silica boat in a tube furnace, having a stream of hydrogen chloride passing through the tube, which was heated to about 250°C.

Pelletising of the lead chloride was done by hydrostatic pressing in a P.T.F.E. sheathed 'Vynamould' silicone rubber mould. The pressure under which the pressing was performed was between 10 and 20 tons. inches^{-2}.

The pressed pellets were then mounted in a P.T.F.E. tube in a brass block to allow the end faces to be ground flat and parallel to one another on silicon carbide paper. Finished pellets were then redried by the method described above.

A.3.1.iv. Mounting of the pellets to make up the electrolyte cell

As shown in the diagram, Figure A.3.i., the pellets were packed between two stainless steel plates, 1.5 cms. diameter, together with insulating plates of P.T.F.E. and terminals of steel with a platinum contact. The cell pile also included a silver disc in contact with the 'standard' silver electrode.

The whole assembled cell pile was placed in a 1.5 cms. inside diameter cardboard tube and Araldite AT.1. cast into the space around the pellets. After curing of the resin filler, the cardboard case was machined off to form a resin encapsulated solid cell. Two 3 mm. slots were milled in the Araldite so that the silver chloride pellet which was not in contact with metallic silver was exposed.

A.3.1.v. The attempted use of the solid electrolyte cell

The finished arrangement was tested for sensitivity to chloride species in solution. A Vibron Model 33C-2 Electrometer was used to measure the potential between the electrodes. A complete lack

of reproducibility existed in the output from the cell. However the potential produced by the cell at one particular occasion appeared to be effected by the concentration of the sodium chloride or hydrochloric acid in the solution. Because of the lack of reproducibility in the measurement of the potentials the technique was abandoned.

A.3.1.vi. The proposed operation of the cell

It was proposed that the exposed silver chloride lattice chloride ions should be in equilibrium with aqueous solution chloride ions:

$$Cl^-_{lattice} \rightleftharpoons Cl^-_{Aq.solution}$$

Thus a change in chloride ion activity in the solution would have some effect upon the lattice chloride ion activity. Since the chloride ions in the other electrode, being in contact with metallic silver, must be at a constant activity at any one temperature, then a chloride chemical potential difference would be formed across the lead chloride solid electrolyte. Lead chloride in a pure state being an ionic conductor in chloride ions would allow a transfer of chloride ions, and thus a charge transfer, to attempt to occur across the electrolyte. This electrical potential should have been measurable by an external electrometer.

The measured potential 'E' should theoretically to have been given by:

Figure A. 4.i.

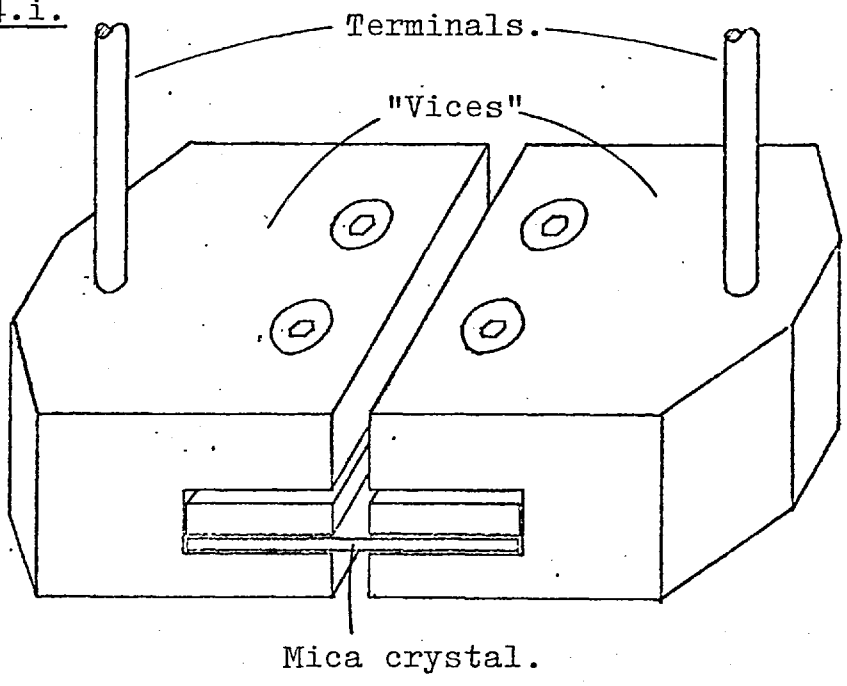
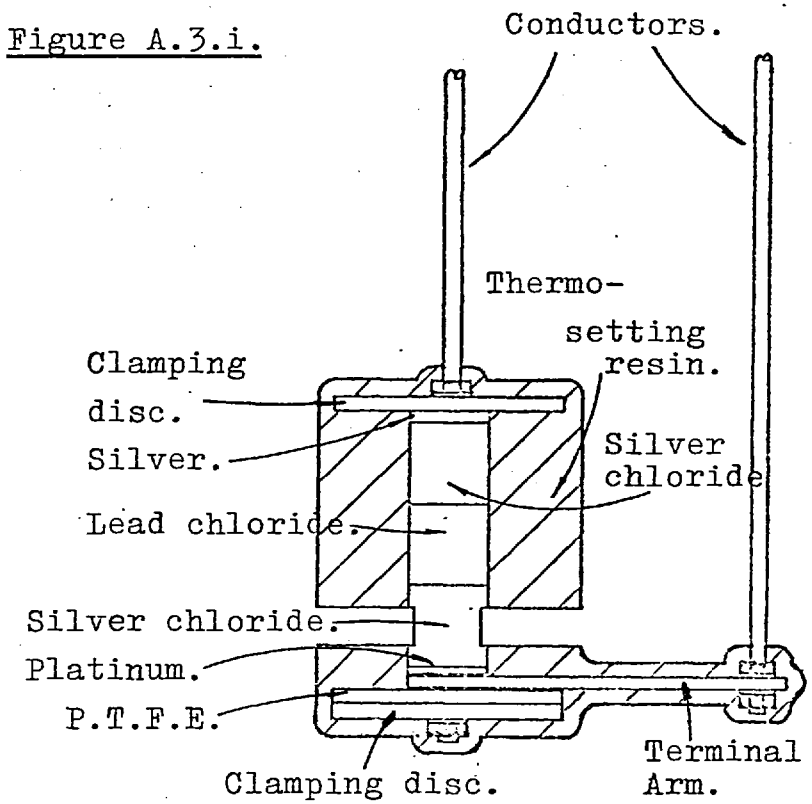


Figure A.3.i.



Appendix 3

$$E = \frac{RT}{F} \log_e \frac{[Cl^-_{lattice}]}{[Cl^-_{Aq.solution}]}$$

where the [ ] brackets indicate the activity of the species enclosed.

T is the absolute temperature (^oK)

R is the gas constant

F is the Faraday Number.

Appendix 4

THE USE OF THE CONDUCTIVITY OF MICA TO DETERMINE WATER VAPOUR ACTIVITY

A.4.i. The proposed method to determine thermodynamic information from mica conductivity data.

Metsik and Perevertaev [44] indicate that a relationship exists between the volume electrical conductivity and the water activity of the moisture absorbed in the surface of mica crystals. These authors had made use of this property to determine a correlation between the depth of the absorption layer, measured optically, and the surface and volume conductivity.

It was considered that this property of mica may be employed for the determination of the water vapour activity in the environment of a mica crystal, and that these measurements may be independent of other vapours present in the gaseous phase.

If the water vapour activity over a solution could be determined independently of and without any interference from any other constituents of the solution, further information could be obtained. Equipped with information relating to the thermodynamics of one component of a binary solution further information concerning the other component may be easily determined by application of conventional equations relating to solutions.

Appendix 4

A.4.ii. The design of the equipment used for mica conductivity determinations

To make measurements of the conductivity of mica in a pressure vessel the arrangement sketched in Figure A.4.i. was manufactured. This apparatus gave a minimum junction resistence between the steel conductor and the mica because a large force could be exerted across the junction by the vices built into the conductors. Fitting into a pressure vessel was made by the use of insulated terminal tubes.

Anti-microphonic cable was used to connect the terminal ends of the test rig to a Wayne-Kerr Auto-balancing conductivity/capacitance bridge. The auto-balancing bridge gave a milli-volt output suitable for monitoring using a potentiometric pen recorder.

The experiments which were carried out using this apparatus were performed in the same reactions vessels as have been described for the investigation of the auto-reduction phenomenon of cupric acetate. Section A.1.4. gives full details of the design of the pressure vessel.

A.4.iii. Measurement of the conductivity

To find the variation of conductivity of mica with temperature, when no water vapour was present, the conductivity cell described above was mounted in a chamber of the double pot autoclave block. The chamber was then flushed thoroughly with nitro-

gen and evacuated to as low a pressure as was attainable with a mechanical pump. The vessel was heated steadily and the equilibrium conductivity across the mica crystals at various temperatures was measured.

The variation of conductivity, measured in m $\mho$, was found to be dependent upon temperature according to the expression:

$$G = \exp(0.062T - 24.5335)$$

where:

G was the measured conductivity

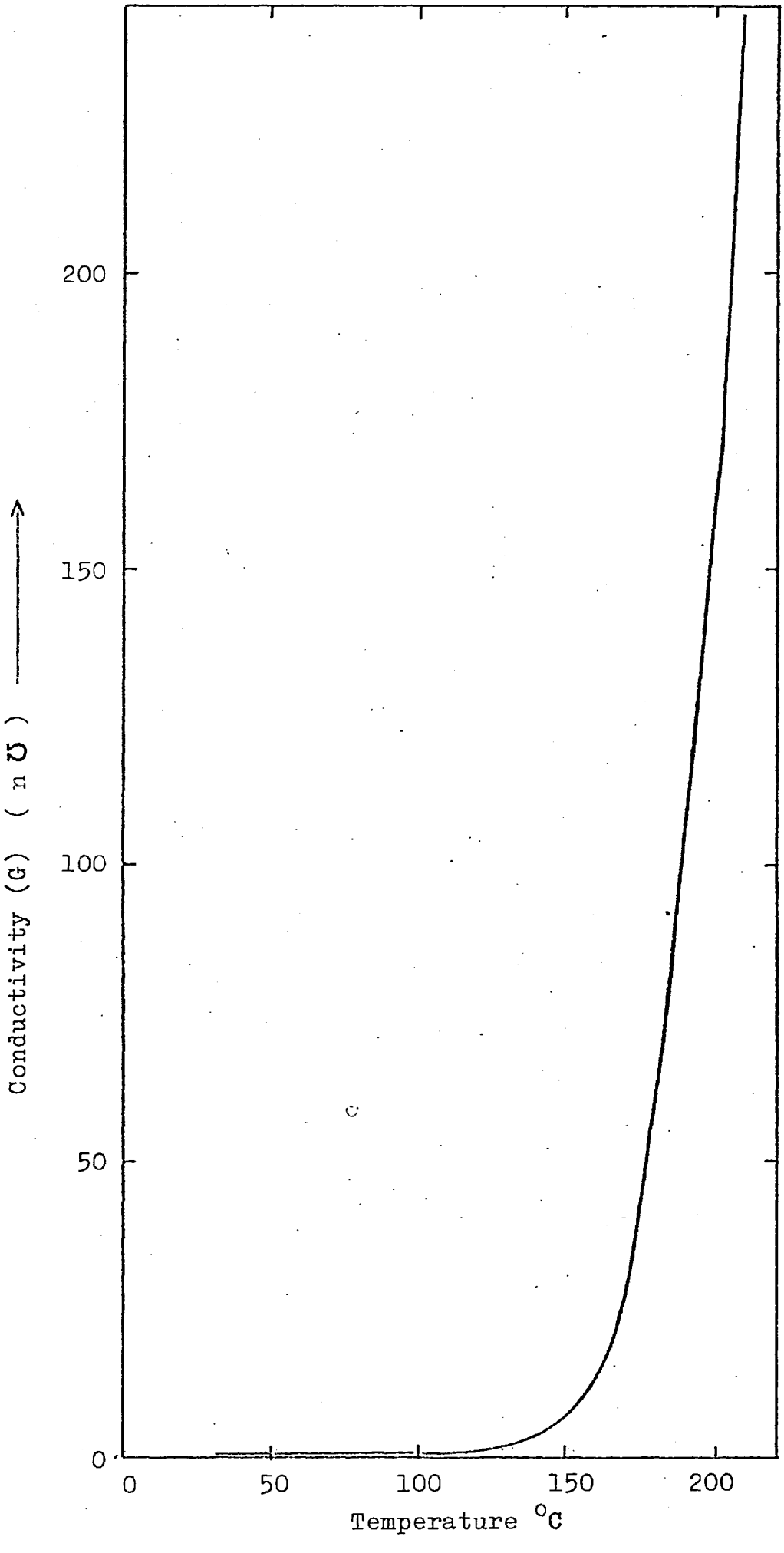
T was the temperature in ^{o}K

The graphs of the change of conductivity of dry mica with temperature may be seen in Figures A.4.ii. and A.4.iii.

Measuring the mica conductivity in water vapour was found to be more difficult using the simple apparatus described.

During investigations in the vessel with water present immediately temperature equilibrium was attained between the liquid and the mica crystal, condensation occured on the 'vices' of the terminals. When water droplets formed on the crystal and on the vices the conductivity measured was no longer that of the mica in contact with water vapour. Because of this problem, no results were obtainable regarding the change of the conductivity of mica with water activity, and therefore the technique to measure water activity had to be abandoned.

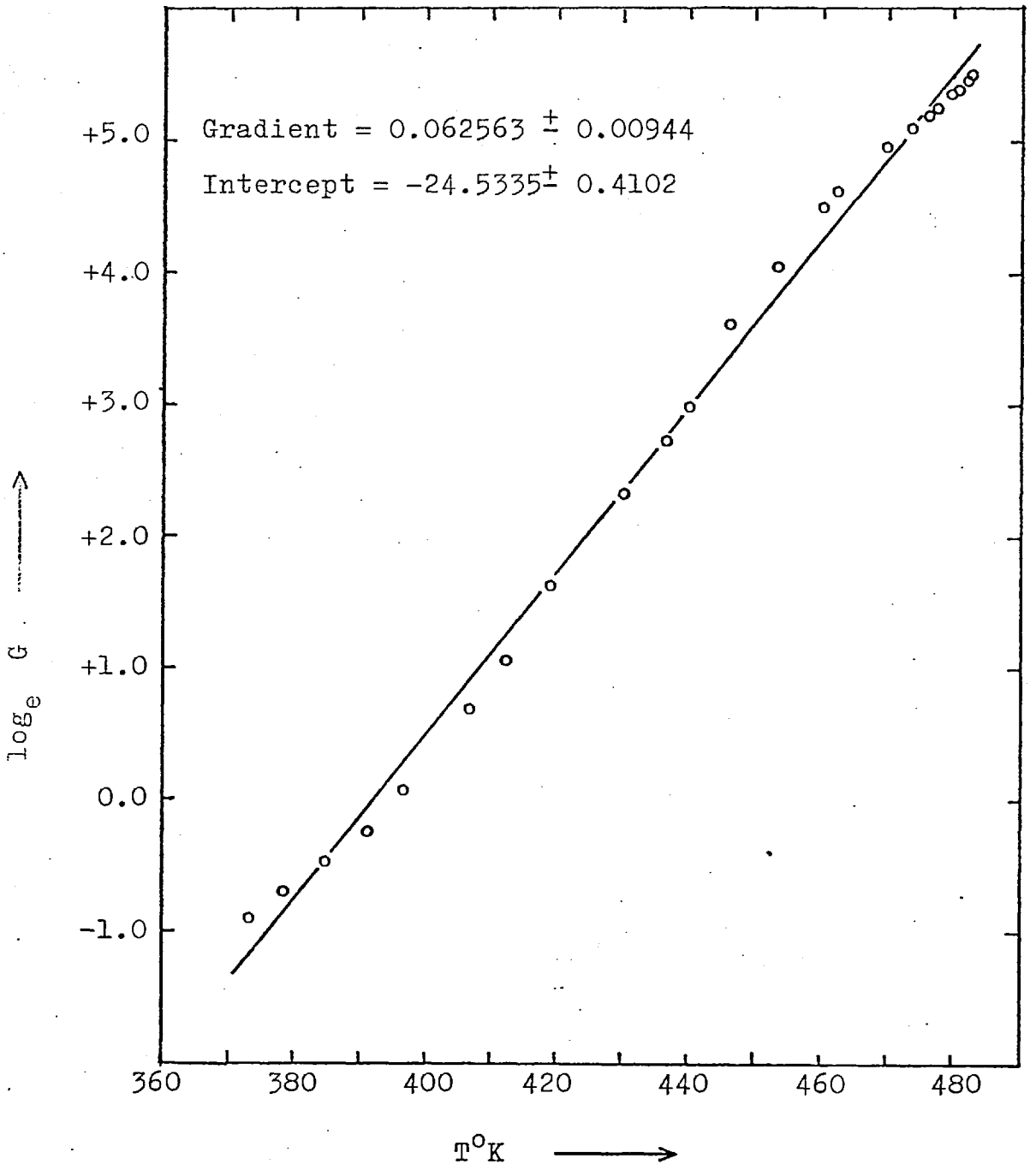
Figure A.4.ii.



Variation of mica conductivity with temperature

Figure A.4.iii.

The variation of the conductivity of dry mica with temperature.



$$G = \exp(0.062563T - 24.5335)$$

(G in n $\mho$)

Appendix 5

TABULATED RESULTS AND THE PROGRAM ALFRED

A.5.1.i. Cupric acetate reductions

Tables A.5.T.i. to A.5.T.xxvi.show the data used, obtained from optical density measurements during the cupric acetate reduction reactions.

The list at the top of each table shows the initial parameter used during the calculations. These values are:

The number of data points presented, this value corresponds to the number of optical density readings which are contained in the main table.

The 'cut in at -' and the 'cut out at point' values indicate the range of the data over which the two linear regressions were performed.

The time interval indicates the time difference between consecutive optical density values in the main table. These values are in minutes.

The initial cupric concentration shows the concentration before initiation of the reduction reaction. These are molar concentrations.

Appendix 5

The data in the main table starts with the initial optical density at the left hand end of the top line, subsequent values appear along the same line of print, and to the left hand end of next lower line after every eight values.

The list positioned at the bottom of each table shows some of the required output information which was determined by program Alfred.

These pieces of information are:

The rate constant for the decaying portion of the reaction. This value is in units of moles.litres^{-1}.minutes^{-1}. These values also include a statistical error value. The quoted errors are one standard deviation.

The concentration error correction indicated the amount of adjustment which was made by program Alfred to the input data before the rate constant value was determined. The units are moles.litres^{-1}.

The last value indicates the calibration constant for the spectrophotometer.

All the tables are ~~formatted~~ set out in the way described above.

A.5.1.ii. Hydrogen consumption data

Tables A.5.T.xxvii. to A.5.T.xxx. show the hydrogen pressure drop measurements which were used. The bracketed table numbers indicate to which optical density data table each set pertains. The readings which are tabulated are those of the transducer employed, and are thus in milli-volts.

A.5.1.iii. Cupric sulphate reductions

Tables A.5.T.xxxi. to A.5.T.xxxx. show the data used to determine the apparent rate constants for the decaying portion of the reduction reactions of a number of cupric sulphate solutions.

The format of the tables is identical to that which is described in section A.5.1.i.

A.5.2. Program Alfred

A listing of computer program Alfred may be seen on pages 307 to 311 . A flow chart upon which the program Alfred was built is to be seen in Figure A.5.2.i.

The purpose of the program was to perform the operations described in section 3.1.ii.

The main program was arranged to print the optical density data in the form seen in the tabulated results, and to co-ordinate the subroutines and single

operations.

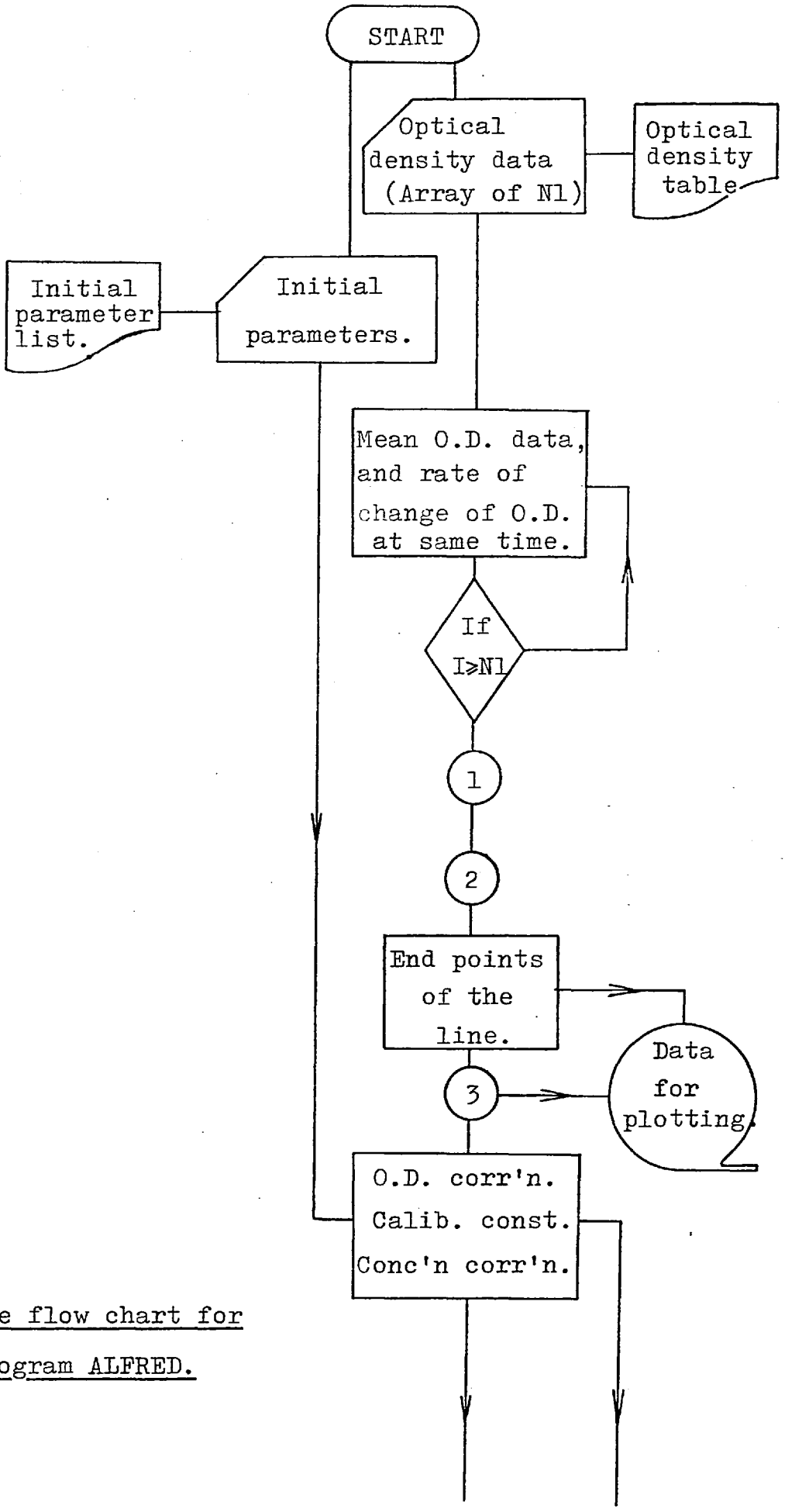
Mean optical density values and rates of change of optical density with time were determined between each consecutive pair of data points. A linear regression was performed on these arrays of points, in order that the correction could be made to the input optical density array. The regression was done using subroutine Lynne. The same data was automatically plotted by a Kingmatic plotter. Subroutine Snap was employed to arrange the data for plotting and to co-ordinate library routines involved in Kingmatic plotting. Each end of the regression line was also marked on the plot.

From the corrected optical array the true cupric concentration at each data point was calculated, together with an array of natural logarithm of the true concentration.

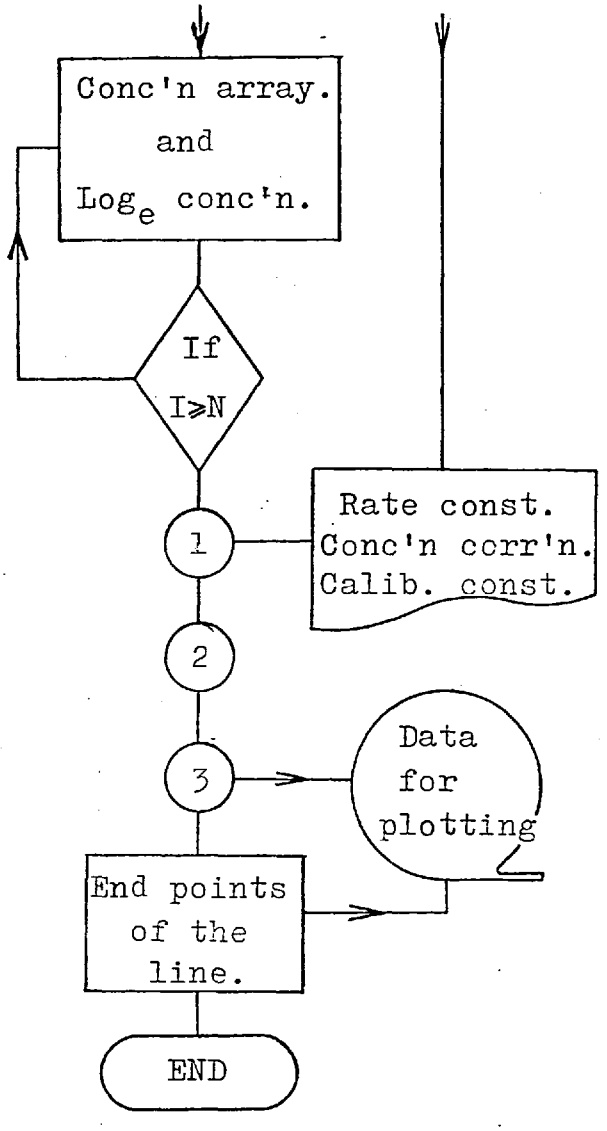
Using subroutine Lynne the linear regression was performed on the time and $\log_e$ concentration arrays.

Similarly to the plotting of the optical density data subroutine Snap was used to arrange the concentration data for plotting.

Figure A.5.2.i.



The flow chart for program ALFRED.



SUBROUTINES.

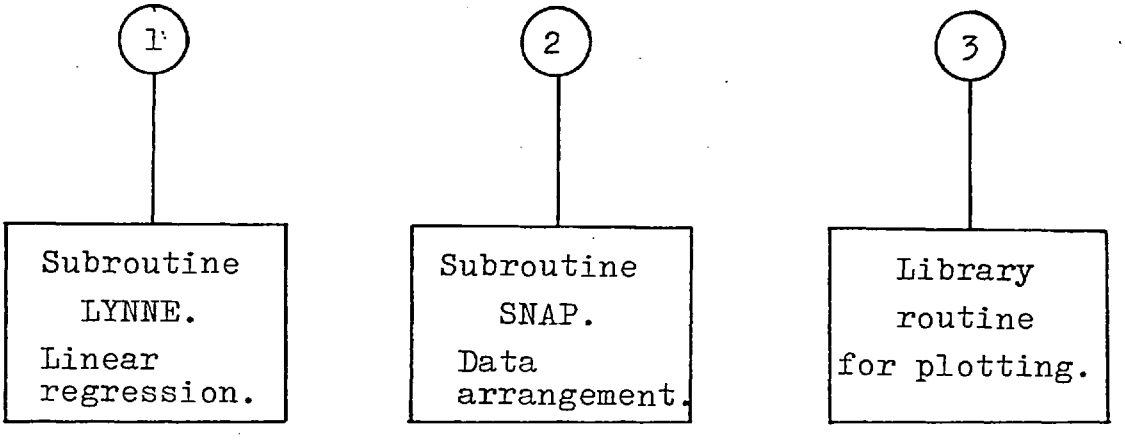


TABLE A.5.T.i.
(Figure 3.1.viii.)

NUMBER OF POINTS = 74

CUT IN AT POINT 34

CUT OUT AT POINT 53

TIME INTERVAL = 1.000

INITIAL CUPRIC CONCENTRATION = .015895000

OPTICAL DENSITY

0.299000	0.288990	0.288980	0.288970	0.286000	0.282500	0.277500	0.269500
0.266500	0.250300	0.238000	0.228600	0.220200	0.213500	0.208000	0.203500
0.198900	0.194300	0.189800	0.184000	0.180000	0.177000	0.173500	0.169500
0.167000	0.164200	0.160200	0.156800	0.152800	0.150500	0.147800	0.144200
0.142000	0.138500	0.135800	0.133500	0.130500	0.128800	0.127000	0.123800
0.121000	0.118000	0.115800	0.113500	0.111500	0.110500	0.108500	0.105800
0.104000	0.102000	0.100000	0.098000	0.096000	0.094000	0.091500	0.091000
0.087800	0.086500	0.084200	0.083500	0.081800	0.079700	0.078000	0.076200
0.075800	0.075000	0.073800	0.072000	0.071000	0.070000	0.069500	0.068100
0.067300	0.066500						

RATE CONSTANT = 0.022126019772 +/- 0.000168267589

CONCENTRATION ERROR CORRECTION = 0.011896869969

OPTICAL DENSITY TO CONCENTRATION CALIBRATION CONSTANT = 0.079642407

TABLE A.5.T.ii.
(Figure 3.1.ix.)

NUMBER OF POINTS = 91

CUT IN AT POINT 33

CUT OUT AT POINT 82

TIME INTERVAL = 1.000

INITIAL CUPRIC CONCENTRATION = .015895000

OPTICAL DENSITY

0.275800	0.275799	0.275798	0.275500	0.272800	0.269000	0.264500	0.259800
0.255500	0.248800	0.242200	0.234000	0.227000	0.220500	0.214500	0.209000
0.203500	0.198000	0.193500	0.188800	0.185500	0.180200	0.176800	0.173500
0.170000	0.166500	0.163500	0.159800	0.157200	0.154500	0.151800	0.149000
0.145500	0.143000	0.140200	0.138500	0.136000	0.133500	0.131000	0.129000
0.127000	0.125000	0.122500	0.120500	0.118000	0.115500	0.113500	0.111500
0.109500	0.107500	0.105500	0.104000	0.102500	0.100200	0.098500	0.096700
0.095000	0.093000	0.091800	0.089500	0.088000	0.086500	0.085000	0.084000
0.082200	0.080800	0.079600	0.078200	0.077000	0.076000	0.075000	0.073500
0.072500	0.071500	0.070000	0.068500	0.067800	0.067000	0.065500	0.064500
0.063500	0.062500	0.061800	0.061000	0.060000	0.059000	0.058200	0.057000
0.056000	0.055000	0.054200					

RATE CONSTANT = 0.0157283036[illegible] +/- 0.000080946844

CONCENTRATION ERROR CORRECTION = -0.000000671799

OPTICAL DENSITY TO CONCENTRATION CALIBRATION CONSTANT = 0.3559998122

TABLE A.5.T.iii.
(Figure 3.1.x.)

NUMBER OF POINTS = 63

CUT IN AT POINT 12

CUT OUT AT POINT 35

TIME INTERVAL = 1.000

INITIAL CUPRIC CONCENTRATION = .015899000

OPTICAL DENSITY

0.279000	0.278990	0.278500	0.273200	0.263200	0.248800	0.232300	0.214000
0.201500	0.190000	0.182000	0.173800	0.165000	0.157500	0.150000	0.142200
0.134200	0.128200	0.121200	0.116000	0.110000	0.105300	0.101500	0.097300
0.093200	0.089500	0.085000	0.081500	0.077800	0.075000	0.071500	0.066800
0.063200	0.060480	0.061500	0.059500	0.058000	0.055600	0.052500	0.051500
0.050000	0.048500	0.047000	0.045500	0.044200	0.043500	0.042200	0.041000
0.040000	0.039500	0.038000	0.037200	0.036500	0.036000	0.035400	0.034800
0.034400	0.033900	0.033300	0.032700	0.032000	0.031500	0.031000	

RATE CONSTANT = 0.030186700770 +/- 0.000611297157

CONCENTRATION ERROR CORRECTION = -0.001280864998

OPTICAL DENSITY TO CONCENTRATION CALIBRATION CONSTANT = 0.3523804122

TABLE A.5.T.iv.

(Figure 3.1.xi.)

NUMBER OF POINTS = 46

CUT IN AT POINT 18

CUT OUT AT POINT 33

TIME INTERVAL = 1.000

INITIAL CUPRIC CONCENTRATION = .015895000

OPTICAL DENSITY

0.326000	0.325990	0.324000	0.315500	0.292000	0.279000	0.248000	0.226000
0.208000	0.190000	0.176000	0.164000	0.154000	0.144000	0.135000	0.126500
0.120000	0.113500	0.106000	0.100500	0.096000	0.090500	0.086500	0.083000
0.080000	0.077500	0.075500	0.073000	0.071800	0.069200	0.068000	0.067000
0.065500	0.064000	0.062500	0.061000	0.060000	0.059500	0.058500	0.057800
0.057000	0.056200	0.055500	0.055000	0.054500	0.054000		

RATE CONSTANT = 0.021177344827 +/- 0.001226369064

CONCENTRATION ERROR CORRECTION = -0.002371043550

OPTICAL DENSITY TO CONCENTRATION CALIBRATION CONSTANT = 0.0414845290

TABLE A.5.T.v.

(Figure 3.1.xii.)

NUMBER OF POINTS = 33

CUT IN AT POINT 11

CUT OUT AT POINT 23

TIME INTERVAL = 1.000

INITIAL CUPRIC CONCENTRATION = .015095000

OPTICAL DENSITY

0.303000	0.302999	0.300500	0.292000	0.275800	0.250000	0 229000	0 205800
0.186000	0.175000	0.163500	0.154000	0.143500	0.134500	0 127500	0 120000
0.113200	0.107000	0.101500	0.096500	0.090500	0.087000	0 083500	0.079800
0.076500	0.073500	0.071000	0.069000	0.066500	0.064800	0 063800	0.062500
0.061000							

RATE CONSTANT = 0.042024674593 +/- 0.000960059410

CONCENTRATION ERROR CORRECTION = -0.001644187236

OPTICAL DENSITY TO CONCENTRATION CALIBRATION CONSTANT = 0.0463723194

TABLE A.5.T.vi.

(Figure 3.1.xiii.)

NUMBER OF POINTS = 18

CUT IN AT POINT 6

CUT OUT AT POINT 11

TIME INTERVAL = 1.000

INITIAL CUPRIC CONCENTRATION = .0015899000

OPTICAL DENSITY

0.265000	0.262500	0.262000	0.210000	0.188000	0.155500	0.124500	0.097500
0.080000	0.067000	0.056000	0.052000	0.047500	0.043500	0.040000	0.039000
0.037200	0.033800						

RATE CONSTANT = 0.1402749392[illegible] +/- 0.009165983721

CONCENTRATION ERROR CORRECTION = -0.001603602693

OPTICAL DENSITY TO CONCENTRATION CALIBRATION CONSTANT = 0.3501449730

TABLE A.5.T.vii.

(Figure 3.1.xiv.)

NUMBER OF POINTS = 13

CUT IN AT POINT 4

CUT OUT AT POINT 8

TIME INTERVAL = 1.000

INITIAL CUPRIC CONCENTRATION = .015000000

OPTICAL DENSITY

0.333000	0.313000	0.272000	0.240000	0.174000	0.122000	0.080000	0.06[illegible]
0.054000	0.050000	0.047500	0.046200	0.044200			

RATE CONSTANT = 0.308593952039 +/- 0.010564161615

CONCENTRATION ERROR CORRECTION = -0.000776021536

OPTICAL DENSITY TO CONCENTRATION CALIBRATION CONSTANT = 0.045402337?

TABLE A.5.T.viii.

(Figure 3.1.xv.)

NUMBER OF POINTS = 91

CUT IN AT POINT 42

CUT OUT AT POINT 75

TIME INTERVAL = 1.000

INITIAL CUPRIC CONCENTRATION = .015895000

OPTICAL DENSITY

0.296500	0.296499	0.296000	0.295800	0.294500	0.292000	0.289000	0.285000
0.282200	0.277000	0.271000	0.263500	0.256500	0.250000	0.241800	0.236000
0.230500	0.227000	0.221000	0.216500	0.212000	0.207000	0.204000	0.200000
0.196800	0.193500	0.189800	0.187000	0.183800	0.180000	0.177500	0.174500
0.172000	0.169800	0.167000	0.164200	0.162500	0.160200	0.158500	0.156800
0.155000	0.152500	0.149200	0.148000	0.145500	0.143500	0.141500	0.140000
0.138500	0.136800	0.135000	0.134000	0.132500	0.131000	0.129800	0.128800
0.127000	0.125500	0.124200	0.123000	0.120200	0.119500	0.118200	0.117000
0.115600	0.114000	0.112500	0.111800	0.111000	0.107500	0.106500	0.105000
0.104000	0.103000	0.102000	0.101500	0.099500	0.098500	0.097500	0.096500
0.095500	0.094800	0.093000	0.092800	0.092000	0.091000	0.090200	0.089500
0.088800	0.088000	0.087500					

RATE CONSTANT = 0.009746342457 +/- 0.000074617966

CONCENTRATION ERROR CORRECTION = -0.001732876413

OPTICAL DENSITY TO CONCENTRATION CALIBRATION CONSTANT = 0.049113401G

TABLE A.5.T.ix.
(Figure 3.1.xvi.)

NUMBER OF POINTS = 93

CUT IN AT POINT 25

CUT OUT AT POINT 85

TIME INTERVAL = 1.000

INITIAL CUPRIC CONCENTRATION = .015895000

OPTICAL DENSITY

0.312800	0.312799	0.312500	0.312000	0.310000	0.307500	0.304500	0.299800
0.295000	0.290000	0.284800	0.278200	0.272500	0.268000	0.262000	0.256200
0.252000	0.247000	0.240000	0.236000	0.232200	0.227500	0.223800	0.219800
0.216000	0.211500	0.207000	0.204000	0.200500	0.197500	0.194500	0.192000
0.189000	0.186500	0.183800	0.180200	0.177800	0.175000	0.172000	0.170000
0.167500	0.165500	0.163800	0.162800	0.161000	0.158000	0.155500	0.152800
0.151800	0.149800	0.148000	0.146000	0.144000	0.142500	0.141200	0.139500
0.137500	0.135800	0.134800	0.133800	0.131800	0.130000	0.129000	0.127400
0.126200	0.124000	0.122000	0.120800	0.119800	0.117500	0.116500	0.115200
0.113200	0.111800	0.110500	0.109400	0.108500	0.107500	0.106800	0.104800
0.103800	0.102800	0.100200	0.099500	0.098500	0.097800	0.096500	0.096000
0.095000	0.093500	0.092000	0.091000	0.090000			

RATE CONSTANT = 0.009077003183 +/- 0.000089276283

CONCENTRATION ERROR CORRECTION = -0.002419803376

OPTICAL DENSITY TO CONCENTRATION CALIBRATION CONSTANT = 0.0430792731

TABLE A.5.T.x.

(Figure 3.1.xvii.)

NUMBER OF POINTS = 61

CUT IN AT POINT 29

CUT OUT AT POINT 50

TIME INTERVAL = 1.000

INITIAL CUPRIC CONCENTRATION = .015695000

OPTICAL DENSITY

0.264000	0.263800	0.261500	0.257200	0.252000	0.243500	0.233800	0.221500
0.208500	0.196000	0.186000	0.178500	0.172200	0.165500	0.159500	0.153500
0.147000	0.141500	0.136000	0.130500	0.124500	0.120000	0.115000	0.110500
0.104500	0.100500	0.096000	0.092000	0.087500	0.084000	0.080200	0.077000
0.072500	0.069500	0.066500	0.064000	0.061500	0.058800	0.056000	0.054500
0.052200	0.050500	0.048500	0.046500	0.044500	0.042800	0.040900	0.039200
0.037200	0.035500	0.033500	0.032200	0.031000	0.030000	0.029000	0.028000
0.027000	0.025800	0.024500	0.023500	0.022500			

RATE CONSTANT = 0.041875242037 +/- 0.000302576482

CONCENTRATION ERROR CORRECTION = -0.000010708220

OPTICAL DENSITY TO CONCENTRATION CALIBRATION CONSTANT = 0.0501677719

TABLE A.5.T.xi.

(Figure 3.1.xviii.)

NUMBER OF POINTS = 25

CUT IN AT POINT 9

CUT OUT AT POINT 18

TIME INTERVAL = 5.000

INITIAL CUPRIC CONCENTRATION = .015695000

OPTICAL DENSITY

0.292000	0.287500	0.267000	0.236500	0.217000	0.200000	0.183000	0.172000
0.161500	0.151000	0.143000	0.135000	0.128000	0.121500	0.115500	0.108000
0.102500	0.096000	0.088500	0.087500	0.084000	0.081500	0.077500	0.074000
0.070000							

RATE CONSTANT = 0.016767049935 +/- 0.000308338141

CONCENTRATION ERROR CORRECTION = 0.002522642986

OPTICAL DENSITY TO CONCENTRATION CALIBRATION CONSTANT = 0.0530741198

TABLE A.5.T.xii.

(Figure 3.1.xix.)

NUMBER OF POINTS = 41

CUT IN AT POINT 25

CUT OUT AT POINT 39

TIME INTERVAL = 1.000

INITIAL CUPRIC CONCENTRATION = .015895000

OPTICAL DENSITY

0.304000	0.303800	0.303000	0.298800	0.294500	0.287500	0.277000	0.266000
0.255000	0.244500	0.235000	0.227200	0.218000	0.209000	0.203000	0.196500
0.190000	0.184500	0.179000	0.174500	0.169200	0.164500	0.160500	0.156800
0.152800	0.149000	0.145000	0.141200	0.137500	0.134200	0.131500	0.128500
0.125500	0.122800	0.119200	0.116200	0.113500	0.110200	0.107500	0.104500
0.101500							

RATE CONSTANT = 0.028473548007 +/- 0.000236206402

CONCENTRATION ERROR CORRECTION = 0.000924738756

OPTICAL DENSITY TO CONCENTRATION CALIBRATION CONSTANT = 0.0553280880

TABLE A.5.T.xiii.

(Figure 3.1.xx.)

NUMBER OF POINTS = 51

CUT IN AT POINT 18

CUT OUT AT POINT 43

TIME INTERVAL = 1.000

INITIAL CUPRIC CONCENTRATION = .015895000

OPTICAL DENSITY

0.314000	0.313500	0.312000	0.309000	0.304500	0.300000	0.293000	0.283000
0.268500	0.256000	0.244500	0.235000	0.224000	0.213000	0.205300	0.199200
0.192500	0.185800	0.180000	0.175000	0.169500	0.164500	0.160000	0.155800
0.150000	0.146500	0.142000	0.138000	0.134000	0.130800	0.127000	0.123500
0.120000	0.116500	0.113200	0.110500	0.108000	0.104800	0.102500	0.099000
0.096000	0.093500	0.091500	0.089000	0.088500	0.086000	0.084000	0.082000
0.080000	0.078500	0.077000					

RATE CONSTANT = 0.024182485041 +/- 0.000169093401

CONCENTRATION ERROR CORRECTION = -0.001036545535

OPTICAL DENSITY TO CONCENTRATION CALIBRATION CONSTANT = 0.0473199187

TABLE A.5.T.xiv.

(Figure 3.1.xxi.)

NUMBER OF POINTS = 46

CUT IN AT POINT 18

CUT OUT AT POINT 33

TIME INTERVAL = 1.000

INITIAL CUPRIC CONCENTRATION = .015695000

OPTICAL DENSITY

0.299000	0.298500	0.296000	0.289000	0.273500	0.253500	0.232000	0.213500
0.199000	0.184000	0.173500	0.164000	0.155000	0.146500	0.137500	0.129500
0.123000	0.117500	0.111200	0.106200	0.101000	0.096000	0.092000	0.088000
0.084000	0.080000	0.077000	0.073500	0.070800	0.067500	0.064000	0.062000
0.060000	0.058200	0.056500	0.055500	0.054500	0.053800	0.053000	0.052500
0.052000	0.051500	0.051000	0.050500	0.049800	0.049200		

RATE CONSTANT = 0.033629230340 +/- 0.000515034488

CONCENTRATION ERROR CORRECTION = -0.001353671225

OPTICAL DENSITY TO CONCENTRATION CALIBRATION CONSTANT = 0.0486332066

TABLE A.5.T.xv.

(Figure 3.1.xxii.)

NUMBER OF POINTS = 40

CUT IN AT POINT 13

CUT OUT AT POINT 23

TIME INTERVAL = 1.000

INITIAL CUPRIC CONCENTRATION = .015695000

OPTICAL DENSITY

0.323001	0.323000	0.322800	0.321800	0.318500	0.311200	0.297800	0.282000
0.263500	0.251800	0.239500	0.231000	0.219000	0.205500	0.193500	0.180800
0.169200	0.159800	0.149800	0.141500	0.133500	0.126800	0.120800	0.114800
0.108500	0.103000	0.099000	0.095000	0.091000	0.087200	0.084000	0.080800
0.078000	0.076500	0.074500	0.072000	0.070000	0.068500	0.069000	0.065500

RATE CONSTANT = 0.047046869466 +/- 0.000903195047

CONCENTRATION ERROR CORRECTION = -0.001952604787

OPTICAL DENSITY TO CONCENTRATION CALIBRATION CONSTANT = 0.0431651766

TABLE A.5.T.xvi.

(Figure 3.1.xxiii.)

NUMBER OF POINTS = 30

CUT IN AT POINT 23

CUT OUT AT POINT 27

TIME INTERVAL = 0.250

INITIAL CUPRIC CONCENTRATION = .011110000

OPTICAL DENSITY

0.283200	0.283200	0.282800	0.281500	0.280000	0.277000	0.274900	0.269000
0.265500	0.260500	0.255500	0.249500	0.240800	0.233000	0.225200	0.216500
0.208000	0.196200	0.185500	0.174900	0.165000	0.153000	0.137700	0.125000
0.110000	0.097500	0.088000	0.080000	0.075100	0.072000		

RATE CONSTANT = 0.421877964101 +/- 0.010785207170

CONCENTRATION ERROR CORRECTION = -0.000351957441

OPTICAL DENSITY TO CONCENTRATION CALIBRATION CONSTANT = 0.0379874384

TABLE A.5.T.xvii.

(Figure 3.1.xxiv.)

NUMBER OF POINTS = 23

CUT IN AT POINT 18

CUT OUT AT POINT 22

TIME INTERVAL = 0.250

INITIAL CUPRIC CONCENTRATION = .013376000

OPTICAL DENSITY

0.240000	0.239999	0.238900	0.238000	0.236000	0.233100	0.230700	0.226700
0.221000	0.215500	0.210000	0.201800	0.193800	0.182000	0.173500	0.161100
0.144000	0.133000	0.116000	0.102100	0.085100	0.065500	0.049000	

RATE CONSTANT = 0.083532963718 +/- 0.003238675945

CONCENTRATION ERROR CORRECTION = -0.009943810531

OPTICAL DENSITY TO CONCENTRATION CALIBRATION CONSTANT = 0.0143007895

TABLE A.5.T.xviii.

(Figure 3.1.xxv.)

NUMBER OF POINTS = 25

CUT IN AT POINT 20

CUT OUT AT POINT 24

TIME INTERVAL = 0.200

INITIAL CUPRIC CONCENTRATION = .010700900

OPTICAL DENSITY

0.284100	0.283400	0.282500	0.280200	0.277800	0.274700	0.272000	0.265000
0.258200	0.252000	0.245800	0.236000	0.225500	0.212800	0.199000	0.183500
0.164000	0.145000	0.124000	0.110800	0.086000	0.060000	0.042200	0.030000
0.026000							

RATE CONSTANT = 1.723247742732 +/- 0.060721876076

CONCENTRATION ERROR CORRECTION = 0.000072929256

OPTICAL DENSITY TO CONCENTRATION CALIBRATION CONSTANT = 0.0379226655

TABLE A.5.T.xix.
(Figure 3.1.xxvi.)

NUMBER OF POINTS = 33

CUT IN AT POINT 23

CUT OUT AT POINT 32

TIME INTERVAL = 0.167

INITIAL CUPRIC CONCENTRATION = .016051300

OPTICAL DENSITY

0.237200	0.237200	0.236800	0.235200	0.232500	0.228500	0.224000	0.218200
0.211800	0.204000	0.196000	0.184100	0.175600	0.160200	0.150000	0.136800
0.123200	0.115500	0.100000	0.084000	0.068500	0.055500	0.043000	0.032100
0.022200	0.014800	0.010500	0.008000	0.005400	0.004000	0.003000	0.002200
0.002000							

RATE CONSTANT = 2.062155151398 +/- 0.024990906301.

CONCENTRATION ERROR CORRECTION = 0.000013241285

OPTICAL DENSITY TO CONCENTRATION CALIBRATION CONSTANT = 0.0677256936

TABLE A.5.T.xx.

(Figure 3.1.xxvii.)

NUMBER OF POINTS = 24

CUT IN AT POINT 19

CUT OUT AT POINT 23

TIME INTERVAL = 0.167

INITIAL CUPRIC CONCENTRATION = .016051400

OPTICAL DENSITY

0.270200	0.270100	0.269200	0.266800	0.264000	0.261500	0.256000	0.252100
0.244700	0.237000	0.228800	0.219800	0.204000	0.196000	0.177700	0.162200
0.148100	0.128500	0.111400	0.091000	0.071200	0.055000	0.041100	0.037000

RATE CONSTANT = 1.476538409698 +/- 0.053808053657

CONCENTRATION ERROR CORRECTION = -0.000057708404

OPTICAL DENSITY TO CONCENTRATION CALIBRATION CONSTANT = 0.0591920488

TABLE A.5.T.xxi.

(Figure 3.1.xxviii.)

NUMBER OF POINTS = 32

CUT IN AT POINT 25

CUT OUT AT POINT 31

TIME INTERVAL = 0.167

INITIAL CUPRIC CONCENTRATION = .015287000

OPTICAL DENSITY

0.248100	0.248100	0.248000	0.247900	0.247500	0.246800	0.244200	0.241500
0.238200	0.235500	0.231000	0.227700	0.220800	0.215800	0.208600	0.201700
0.195100	0.184100	0.174400	0.164200	0.152200	0.140500	0.132600	0.119900
0.110000	0.096000	0.081000	0.067000	0.056100	0.046500	0.040200	0.039600

RATE CONSTANT = 0.946052846220 +/- 0.017182525065

CONCENTRATION ERROR CORRECTION = -0.000371871355

OPTICAL DENSITY TO CONCENTRATION CALIBRATION CONSTANT = 0.0601174069

TABLE A.5.T.xxii.

(Figure 3.1.xxix.)

NUMBER OF POINTS = 28

CUT IN AT POINT 22

CUT OUT AT POINT 27

TIME INTERVAL = 0.250

INITIAL CUPRIC CONCENTRATION = .015287000

OPTICAL DENSITY

0.229800	0.229700	0.229200	0.228500	0.227800	0.224800	0.222000	0.217500
0.213800	0.208500	0.203800	0.199100	0.190800	0.182700	0.174000	0.166300
0.156000	0.146500	0.135900	0.126500	0.116200	0.104200	0.092500	0.077000
0.064000	0.051700	0.045800	0.041500				

RATE CONSTANT = 0.700803359115 +/- 0.027933418002

CONCENTRATION ERROR CORRECTION = 0.000067459669

OPTICAL DENSITY TO CONCENTRATION CALIBRATION CONSTANT = 0.0568166217

TABLE A.5.T.xxiii.

(Figure 3.1.xxx.)

NUMBER OF POINTS = 35

CUT IN AT POINT 14

CUT OUT AT POINT 28

TIME INTERVAL = 0.250

INITIAL CUPRIC CONCENTRATION = .049046000

OPTICAL DENSITY

1.297500	1.296000	1.291000	1.277500	1.250000	1.226000	1.189000	1.149000
1.084000	1.027500	0.979000	0.930000	0.855000	0.786000	0.700001	0.620000
0.542500	0.471000	0.406000	0.350000	0.298500	0.260000	0.227500	0.202500
0.187500	0.175000	0.165000	0.157500	0.151000	0.144000	0.139000	0.133500
0.130000	0.129000	0.126000					

RATE CONSTANT = 0.422123608570 +/- 0.017430649098 .

CONCENTRATION ERROR CORRECTION = -0.001924379048

OPTICAL DENSITY TO CONCENTRATION CALIBRATION CONSTANT = 0.0363172416

TABLE A.5.T.xxiv.

(Figure 3.1.xxxi.)

NUMBER OF POINTS = 36

CUT IN AT POINT 16

CUT OUT AT POINT 24

TIME INTERVAL = 0.250

INITIAL CUPRIC CONCENTRATION = .049046000

OPTICAL DENSITY

1.259000	1.254000	1.236000	1.213000	1.195000	1.172000	1.139500	1.106000
1.059500	1.012000	0.951500	0.874000	0.809000	0.719500	0.638000	0.558000
0.482000	0.400000	0.332000	0.279500	0.221500	0.184500	0.160000	0.140000
0.127000	0.115000	0.108000	0.102000	0.097000	0.092000	0.089000	0.086000
0.083000	0.080000	0.078000	0.077000				

RATE CONSTANT = 0.697961670757 +/- 0.015261830416.

CONCENTRATION ERROR CORRECTION = -0.000312484766

OPTICAL DENSITY TO CONCENTRATION CALIBRATION CONSTANT = 0.0387081139

TABLE A.5.T.xxv.

(Figure 3.1.xxxii.)

NUMBER OF POINTS = 25

CUT IN AT POINT 12

CUT OUT AT POINT 20

TIME INTERVAL = 0.500

INITIAL CUPRIC CONCENTRATION = .049046000

OPTICAL DENSITY

1.212000	1.200000	1.174000	1.136000	1.086000	1.038000	0.977000	0.900000
0.820000	0.729000	0.615000	0.516000	0.420000	0.320000	0.242000	0.185000
0.152000	0.130000	0.116000	0.105000	0.100000	0.095000	0.092000	0.091000
0.090000							

RATE CONSTANT = 0.332507311422 +/- 0.024744762338

CONCENTRATION ERROR CORRECTION = -0.002080869650

OPTICAL DENSITY TO CONCENTRATION CALIBRATION CONSTANT = 0.0387500910

TABLE A.5.T.xxvi.

(Figure 3.1.xxxiii.)

NUMBER OF POINTS = 35

CUT IN AT POINT 23

CUT OUT AT POINT 30

TIME INTERVAL = 0.500

INITIAL CUPRIC CONCENTRATION = .049046000

OPTICAL DENSITY

1.262000	1.260000	1.256000	1.244000	1.228000	1.210000	1.184000	1.156000
1.125000	1.095000	1.055000	1.022000	0.978000	0.935000	0.890000	0.832000
0.779000	0.719000	0.654000	0.599000	0.530000	0.469000	0.400000	0.346000
0.290000	0.236000	0.196000	0.172000	0.156000	0.141000	0.138000	0.125000
0.122000	0.121000	0.121000					

RATE CONSTANT = 0.230679978076 +/- 0.014124738779

CONCENTRATION ERROR CORRECTION = -0.002903035914

OPTICAL DENSITY TO CONCENTRATION CALIBRATION CONSTANT = 0.0365633630

TABLE A.5.T.xxvii.

The millivolt output at specified times after the start of the reduction reaction at 150°C and 400p.s.i. of hydrogen. (Figures 3.1.i. and 3.1.v.)

Time. (Mins.)	Transducer output. (mV.)
0.0	940.2
0.25	934.0
0.50	928.4
0.75	923.0
1.00	918.2
1.25	913.2
1.50	908.5
1.75	903.5
2.00	899.4
2.25	895.4
2.50	890.8
2.75	887.1
3.00	883.5
3.25	880.5
3.50	877.2
3.75	874.5
4.00	870.0
4.25	866.6
4.50	863.6
4.75	861.2

Time. (Mins.)	Transducer output. (mV.)
5.00	858.5
5.50	855.5
6.00	852.8
6.50	850.8
7.00	849.4
7.50	848.3
8.00	847.5
8.50	846.8
9.00	846.4
9.50	846.0
10.0	845.5
10.5	845.4
11.0	845.3
11.5	845.1
12.0	845.0
13.0	844.8
14.0	844.5
15.0	844.2
20.0	843.5

The leakage rate was equivalent to 0.085 $mV.min^{-1}$.

Appendix 5.

TABLE A.5.T.xxviii.

The millivolt output at specified times after the start of the reduction reaction at 140°C and 400p.s.i. of hydrogen. (Figures 3.1.ii. and 3.1.vi.)

Time. (Mins.)	Transducer output. (mV.)	Time. (Mins.)	Transducer output. (mV.)
0.00	1020.0	6.00	946.1
0.25	1014.5	6.50	942.2
0.50	1007.2	7.00	938.4
0.75	1002.2	7.50	934.7
1.00	997.4	8.00	931.6
1.25	993.4	8.50	928.8
1.50	989.4	9.00	926.1
1.75	985.8	9.50	924.1
2.00	982.3	10.0	922.1
2.25	979.2	10.5	920.5
2.50	976.2	11.0	919.0
2.75	973.6	11.5	917.9
3.00	971.1	12.0	917.0
3.25	968.8	13.0	915.6
3.50	966.5	14.0	914.8
3.75	964.1	15.0	914.4
4.00	961.8	16.0	914.2
4.50	957.7	17.0	913.9
5.00	953.6	The leakage rate was equivalent to 0.2942 $mV.min^{-1}$.	
5.50	949.8		

Appendix 5.

TABLE A.5.T.xxix.

The millivolt output from the transducer at specified times after the start of the reduction reaction at 130°C and 400 p.s.i. of hydrogen. (Figures 3.1.iii. and 3.1.viii.)

Time. (Mins.)	Transducer output. (mV.)	Time. (Mins.)	Transducer output. (mV.)
0.0	990.8	10.0	910.0
0.5	980.4	11.0	905.5
1.0	970.9	12.0	901.0
1.5	963.2	13.0	896.7
2.0	957.0	14.0	893.6
2.5	951.6	15.0	891.0
3.0	947.0	16.0	889.2
3.5	943.0	17.0	887.9
4.0	939.4	18.0	887.1
4.5	936.2	19.0	886.2
5.0	933.3	20.0	885.0
5.5	930.5	22.0	883.4
6.0	928.0	24.0	881.8
6.5	925.5	26.0	880.1
7.0	923.1	28.0	878.2
7.5	920.8	30.0	876.8
8.0	918.6	35.0	872.8
8.5	916.4	40.0	869.3
9.0	914.2	The leakage rate was equivalent to 0.360 $mV.min^{-1}$.	
9.5	912.2		

Appendix 5.

TABLE A.5.T.xxx.

The millivolt output from the transducer at specified times after the start of the reduction reaction at 130°C and 400 p.s.i. of hydrogen. (Figure. 3.1.iv.)

Time. (Mins.)	Transducer output. (mV.)
0.0	1001.5
0.5	990.8
1.0	981.4
1.5	975.5
2.0	970.1
2.5	965.0
3.0	960.5
3.5	956.4
4.0	951.9
4.5	949.3
5.0	946.4
5.5	943.4
6.0	940.6
6.5	938.0
7.0	935.6
7.5	933.0
8.0	930.5
8.5	928.2
9.0	925.5
9.5	923.2
10.0	920.5

Time. (Mins.)	Transducer output. (mV.)
11.0	915.4
12.0	911.0
13.0	907.8
14.0	904.9
15.0	902.6
16.0	900.7
17.0	899.0
18.0	897.7
19.0	896.5
20.0	895.3
21.0	894.2
22.0	893.3
23.0	892.3
24.0	891.6
26.0	890.0
28.0	888.5
30.0	886.9
35.0	883.2
40.0	880.8

The leakage rate was equivalent to 0.450 $mV.min^{-1}$.

TABLE A.5.T.xxxi.

(Figure 3.2.ii.)

NUMBER OF POINTS = 38

CUT IN AT POINT 16

CUT OUT AT POINT 19

TIME INTERVAL = 0.500

INITIAL CUPRIC CONCENTRATION = .078683000

OPTICAL DENSITY

1.565000	1.564000	1.555000	1.542000	1.520000	1.504000	1.475000	1.450000
1.428000	1.387000	1.323000	1.260000	1.193000	1.116000	1.016000	0.924000
0.813000	0.715000	0.626000	0.549000	0.680000	0.682000	0.635000	0.582000
0.550000	0.525000	0.512000	0.500000	0.486000	0.482000	0.470000	0.454000
0.443000	0.431000	0.420000	0.410000	0.400000	0.389000		

RATE CONSTANT = 0.285610234137 +/- 0.002992970964

CONCENTRATION ERROR CORRECTION = 0.003660931902

OPTICAL DENSITY TO CONCENTRATION CALIBRATION CONSTANT = 0.0526156670

TABLE A.5.T.xxxii.

(Figure 3.2.iii.)

NUMBER OF POINTS = 50

CUT IN AT POINT . 20

CUT OUT AT POINT 25

TIME INTERVAL = 0.500

INITIAL CUPRIC CONCENTRATION = .078683000

OPTICAL DENSITY

1.608000	1.605000	1.600000	1.593000	1.581000	1.562000	1.542000	1.521000
1.485000	1.450000	1.406000	1.352000	1.288000	1.230000	1.170000	1.102000
1.039000	0.962000	0.900000	0.820000	0.746000	0.680000	0.614000	0.570000
0.560000	0.557000	0.573000	0.595000	0.612000	0.619000	0.623000	0.621000
0.614000	0.601000	0.591000	0.581000	0.570000	0.559000	0.548000	0.535000
0.523000	0.510000	0.499000	0.490000	0.480000	0.471000	0.461000	0.452000
0.443000	0.438000						

RATE CONSTANT = 0.092460486493 +/- 0.008641626020

CONCENTRATION ERROR CORRECTION = -0.018521456932

OPTICAL DENSITY TO CONCENTRATION CALIBRATION CONSTANT = 0.0374138949

TABLE A.5.T.xxxiii.

(Figure 3.2.iv.)

NUMBER OF POINTS = 61

CUT IN AT POINT 19

CUT OUT AT POINT 26

TIME INTERVAL = 0.500

INITIAL CUPRIC CONCENTRATION = .078683000

OPTICAL DENSITY

1.663000	1.663000	1.662000	1.660000	1.658000	1.649000	1.640000	1.623000
1.613000	1.592000	1.565000	1.540000	1.489000	1.435000	1.390000	1.340000
1.266000	1.230000	1.180000	1.090000	1.000000	0.923000	0.842000	0.779000
0.719000	0.681000	0.672000	0.682000	0.721000	0.776000	0.810000	0.818000
0.815000	0.800000	0.785000	0.770000	0.756000	0.742000	0.729000	0.714000
0.700000	0.683000	0.667000	0.654000	0.642000	0.631000	0.621000	0.613000
0.600000	0.590000	0.581000	0.570000	0.560000	0.552000	0.544000	0.537000
0.530000	0.521000	0.513000	0.506000	0.498000			

RATE CONSTANT = 0.100880013811 +/- 0.002683506393

CONCENTRATION ERROR CORRECTION = -0.015095157729

OPTICAL DENSITY TO CONCENTRATION CALIBRATION CONSTANT = 0.0382368264

TABLE A.5.T.xxxiv.

(Figure 3.2.v.)

NUMBER OF POINTS = 43

CUT IN AT POINT 19

CUT OUT AT POINT 22

TIME INTERVAL = 0.500

INITIAL CUPRIC CONCENTRATION = .078683000

OPTICAL DENSITY

1.609000	1.609000	1.602000	1.580000	1.562000	1.545000	1.532000	1.505000
1.470000	1.432000	1.383000	1.337000	1.280000	1.220000	1.160000	1.084000
1.022000	0.952000	0.880000	0.800000	0.715000	0.638000	0.600000	0.600000
0.603000	0.610000	0.620000	0.632000	0.642000	0.650000	0.650000	0.635000
0.620000	0.604000	0.588000	0.574000	0.560000	0.548000	0.532000	0.521000
0.510000	0.497000	0.476000					

RATE CONSTANT = 0.152710220081 +/- 0.003167169007

CONCENTRATION ERROR CORRECTION = -0.012623550871

OPTICAL DENSITY TO CONCENTRATION CALIBRATION CONSTANT = 0.0410562095

TABLE A.5.T.xxxv.

(Figure 3.2.vi.)

NUMBER OF POINTS = 22

CUT IN AT POINT 16

CUT OUT AT POINT 20

TIME INTERVAL = 0.500

INITIAL CUPRIC CONCENTRATION = .03934160

OPTICAL DENSITY

1.241000	1.240000	1.235000	1.227000	1.212000	1.205000	1.197000	1.180000
1.148000	1.402000	1.065000	1.026000	0.970000	0.912000	0.843000	0.770000
0.671000	0.583000	0.503000	0.430000	0.395000	0.410000		

RATE CONSTANT = 0.237410232681 +/- 0.001517100058

CONCENTRATION ERROR CORRECTION = -0.003688040980

OPTICAL DENSITY TO CONCENTRATION CALIBRATION CONSTANT = 0.0287296946

TABLE A.5.T.xxxvi.

(Figure 3.2.vii.)

NUMBER OF POINTS = 42

CUT IN AT POINT 16

CUT OUT AT POINT 19

TIME INTERVAL = 0.500

INITIAL CUPRIC CONCENTRATION = .039341600

OPTICAL DENSITY

1.211000	1.211000	1.208000	1.201000	1.192000	1.175000	1.156000	1.135000
1.115000	1.080000	1.035000	0.986000	0.932000	0.862000	0.782000	0.700000
0.601000	0.520000	0.440000	0.375000	0.405000	0.440000	0.422000	0.398000
0.375000	0.360000	0.348000	0.338000	0.329000	0.320000	0.315000	0.310000
0.303000	0.298000	0.293000	0.288000	0.284000	0.279000	0.275000	0.270000
0.267000	0.264000						

RATE CONSTANT = 0.387400019560 +/- 0.012231543003

CONCENTRATION ERROR CORRECTION = 0.004051502592

OPTICAL DENSITY TO CONCENTRATION CALIBRATION CONSTANT = 0.0358324547

TABLE A.5.T.xxxvii.

(Figure 3.2.viii.)

NUMBER OF POINTS = 61

CUT IN AT POINT 16

CUT OUT AT POINT 22

TIME INTERVAL = 0.500

INITIAL CUPRIC CONCENTRATION = .039341600

OPTICAL DENSITY

1.252000	1.252000	1.252000	1.250000	1.240000	1.229000	1.212.00	1.195000
1.162000	1.123000	1.108000	1.031000	0.978000	0.917000	0 842000	0 780000
0.710000	0.632000	0.559000	0.495000	0.428000	0.382000	0 360000	0.360000
0.390000	0.410000	0.421000	0.422000	0.420000	0.413000	0.408000	0 400000
0.392000	0.381000	0.376000	0.369000	0.361000	0.356000	0 348000	0 343000
0.338000	0.336000	0.334000	0.330000	0.327000	0.323000	0 320000	0 317500
0.315000	0.311000	0.307000	0.303000	0.300000	0.297500	0 295000	0 291000
0.287000	0.284000	0.281000	0.278000	0.276000			

RATE CONSTANT = 0.242612309206 +/- 0.005471256837

CONCENTRATION ERROR CORRECTION = -0.000008294511

OPTICAL DENSITY TO CONCENTRATION CALIBRATION CONSTANT = 0.0314163782

TABLE A.5.T.xxxviii.

(Figure 3.2.ix.)

NUMBER OF POINTS = 22

CUT IN AT POINT 9

CUT OUT AT POINT 17

TIME INTERVAL = 1.000

INITIAL CUPRIC CONCENTRATION = .031473000

OPTICAL DENSITY

0.308000	0.306000	0.301000	0.292000	0.280000	0.270000	0.253000	0.231000
0.205000	0.180000	0.159000	0.140000	0.121000	0.102000	0 088000	0.074000
0.062000	0.054000	0.075000	0.064000	0.060000	0.058000		

RATE CONSTANT = 0.246709461247 +/- 0.016572850581

CONCENTRATION ERROR CORRECTION = 0.004803289039

OPTICAL DENSITY TO CONCENTRATION CALIBRATION CONSTANT = 0.1177801592

TABLE A.5.T. xxxix.

(Figure 3.2.x.)

NUMBER OF POINTS = 23

CUT IN AT POINT 11

CUT OUT AT POINT 17

TIME INTERVAL = 1.000

INITIAL CUPRIC CONCENTRATION = .031473000

OPTICAL DENSITY

0.282000	0.281000	0.273000	0.259000	0.245000	0.230000	0.211000	0.191000
0.172000	0.158000	0.140000	0.124000	0.107000	0.093000	0.078000	0.066000
0.057000	0.050000	0.057000	0.059000	0.055000	0.053000	0.052000	

RATE CONSTANT = 0.206130583021 +/- 0.008007479154

CONCENTRATION ERROR CORRECTION = 0.002701071190

OPTICAL DENSITY TO CONCENTRATION CALIBRATION CONSTANT = 0.1211846496

TABLE A.5.T.xxxx.

(Figure 3.2.xi.)

NUMBER OF POINTS = 23

CUT IN AT POINT 14

CUT OUT AT POINT 22

TIME INTERVAL = 0.500

INITIAL CUPRIC CONCENTRATION = .078683000

OPTICAL DENSITY

1.760000	1.758000	1.742000	1.730000	1.718000	1.698000	1.670000	1.620000
1.575000	1.536000	1.460000	1.380000	1.295000	1.221000	1.133000	1.042000
0.960000	0.875000	0.792000	0.710000	0.665000	0.650000	0.640000	

RATE CONSTANT = 0.120164133327 +/- 0.004781898158

CONCENTRATION ERROR CORRECTION = -0.013344791441

OPTICAL DENSITY TO CONCENTRATION CALIBRATION CONSTANT = 0.0371239821

```
      PROGRAM ALFRED(INPUT,OUTPUT,TAPE62,TAPE5=INPUT,TAPE6=OUTPUT)
      DIMENSION OD(150), CU(152), XARRAY(152), YARRAY(152)
    1 READ(5,1000) N, CUO, TIME, KUTS, KUTF
      IF(N.EQ.0) STOP
 1000 FORMAT(I3, 2X, F9.6, 2X, F5.2, 2X, I3, 2X, I3)
      WRITE(6,5000) N, KUTS, KUTF, TIME, CUO
 5000 FORMAT(1H1, ////////////////, * NUMBER OF POINTS = *, I3, //,
     +* CUT IN AT POINT    *, I3, //,* CUT OUT AT POINT    *, I3, //,
     +* TIME INTERVAL    = *, F6.3, //,
     +* INITIAL CUPRIC CONCENTRATION = *,F10.9,///)
      CALL START(2)
      READ(5,2000) (OD(I), I=1,N)
 2000 FORMAT(4F10.6)
      WRITE(6,6000)
 6000 FORMAT (53X, * OPTICAL DENSITY *,//)
      WRITE(6,3000) (OD(I), I=1,N)
 3000 FORMAT(8(4X,F10.6), /)
      N1 = N-1
      DO 10 I=1, N1
      XARRAY(I) = (OD(I) + OD(I+1))/2.0
   10 YARRAY(I) = (OD(I+1) - OD(I))/TIME
```

Input initial parameters.

Output of initial parameters in tabular form.

Input optical density data.

Output of optical density data in tabular form.

Determination of mean optical density and rate of change of optical density

```
      CALL LYNNE(XARRAY, YARRAY, KUTS, KUTF, SLOPE, ES, YC, EYC)
      CALL SNAP(XARRAY, YARRAY, N1, 1)
COMMENT          PLOT REGRESSION LINE
      FIRSTV = XARRAY(N)
      DELTAV = XARRAY(N1 + 2)
      X = FIRSTV
      X1 = (X - FIRSTV) / DELTAV
      Y = ((SLOPE * X + YC) - YARRAY(N))/YARRAY(N1+2)
      CALL SYMBOL (X1, Y, 0.07, 4, 0.0, -1 )
      X = (X + ( DELTAV * 4.0 ))
      X1 = (X - FIRSTV) / DELTAV
      Y = ((SLOPE * X + YC) - YARRAY(N))/YARRAY(N1+2)
      CALL SYMBOL (X1, Y, 0.07, 4, 0.0, -1 )
      ODC = YC/SLOPE
      DENS = CUO/(OD(1) - ODC)
      CUC = ODC * DENS
      DO 20 I = 1, N
      CU(I) = (OD(I) - ODC) * DENS
      YARRAY(I) = ALOG(CU(I))
   20 XARRAY(I) = FLOAT(I - 1) * TIME
      CALL SNAP(XARRAY, CU, N, 2)
      CALL SNAP(XARRAY, YARRAY, N, 3)
```

Linear regression routine.

Plotting routine.

Fixing and marking of each end of the best line through the optical density vs. change of optical density curve.

Determination of:

Optical density correction.

Calibration constant.

Concentration correction.

Concentration array.

Log_e concentration array.

Time from initiation array.

Plotting routine.

```
      CALL LYNNE(XARRAY, YARRAY, KUTS, KUTF, SLOPE, ES, YC, EYC)
C COMMENT        PLOT REGRESSION LINE
      FIRSTV = XARRAY(N+1)
      DELTAV = XARRAY(N +2)
      X = FIRSTV
      X1 = (X - FIRSTV) / DELTAV
      Y = ((SLOPE * X + YC) - YARRAY(N+1))/YARRAY(N+2)
      CALL SYMBOL (X1, Y, 0.07, 4, 0.0, -1 )
      X = (X + ( DELTAV * 2.0 ))
      X1 = (X - FIRSTV) / DELTAV
      Y = ((SLOPE * X + YC) - YARRAY(N+1))/YARRAY(N+2)
      CALL SYMBOL (X1, Y, 0.07, 4, 0.0, -1 )
      SLOPE = -SLOPE
      WRITE(6,4000) SLOPE, ES, CUC, DENS
 4000 FORMAT(1X, ///, * RATE CONSTANT = *, F16.12, *  +/-  *, F16.12, ///
     +, * CONCENTRATION ERROR CORRECTION = *, F16.12, //,
     +* OPTICAL DENSITY TO CONCENTRATION CALIBRATION CONSTANT = *,
     +F12.10, //)
      CALL ENPLOT
      GO TO 1
      END
```

Linear regression routine.

Fixing and marking of each end of the best line through the $\log_e$ optical density vs time curve.

Output of determined information.

```
      SUBROUTINE SNAP(X, Y, N, IPOS)
      DIMENSION X(100), Y(100)
      CALL SCALE (X, 5.0, N, 1)
      CALL SCALE (Y, 4.0, N, 1)
      GO TO(1, 2, 3),IPOS
1      CALL PLOT (0.7, 5.45, -3)
      CALL SYMBOL (1.9   , -0.5, 0.07,
     + 17H OPTICAL DENSITY , 0.0, +17)
      CALL SYMBOL(-0.5, 0.8, 0.07,
     +34H RATE OF CHANGE OF OPTICAL DENSITY , 90.0, +34)
      GOTO 5
2     CALL PLOT (7.3, 0.00, -3)
      CALL SYMBOL (1.975, -0.5, 0.070, 15HTIME  (MINUTES), 0.0, +15)
      CALL SYMBOL(-0.5, 0.450, 0.07,
     +37H CUPRIC CONCENTRATION  (MOLES/LITRE) ,90.0, +37)
      GOTO 5
3     CALL PLOT (0.0, -5.45, -3)
      CALL SYMBOL(1.975, -0.5, 0.07,
     X         15HTIME  (MINUTES), 0.0, +15)
      CALL SYMBOL(-0.5, 0.950, 0.07,
     X         28HLN TRUE CUPRIC CONCENTRATION, 90.0, +28)
      GO TO  5
5     CALL AXIS(0.0, 0.0, 1H ,-1, 5.0, 0.0, X(N+1), X(N+2))
      CALL AXIS(0.0, 0.0, 1H , 1, 4.0, 90.0, Y(N+1), Y(N+2))
      CALL LINE(X, Y, N, 1, -1, 2)
      RETURN
      END
```

```
      SUBROUTINE LYNNE(X, Y, N1, N2, SLOPE, ESLOPE, YCEPT, EYCEPT)
      DIMENSION X(100), Y(100)
      SUMY = 0.0
      SUMX = 0.0
      SUMXY =0.0
      SUMXSQ = 0.0
      SUMRSQ = 0.0
      DO 10 J=N1, N2
      SUMX = SUMX + X(J)
      SUMY = SUMY + Y(J)
      SUMXY = SUMXY + X(J) * Y(J)
   10 SUMXSQ = SUMXSQ + X(J) * X(J)
      N = N2 - N1 + 1
      DENOM = FLOAT(N) * SUMXSQ - SUMX * SUMX
      SLOPE = (FLOAT(N) * SUMXY - SUMX * SUMY)/DENOM
      YCEPT = (SUMY * SUMXSQ - SUMX * SUMXY)/DENOM
      DO 20 J=N1, N2
      RESID = Y(J) - SLOPE * X(J) - YCEPT
   20 SUMRSQ = SUMRSQ + RESID * RESID
      ALPHA = SUMRSQ / (N-2)
      ESLOPE =SQRT (( FLOAT (N) * ALPHA) / DENOM )
      EYCEPT = SQRT(( SUMXSQ * ALPHA) / DENOM )
      RETURN
      END
```

Appendix 6.

Appendix 6.

UNITS USED.

The following table shows the units which have been used in the text of this thesis and which are not units of the 'Systeme International d'Unit'.

Together with the units employed the convertion factors both to and from the S.I. units are included in the table.

S.I. units were not universally used in the thesis since it was considered that most prospective readers would more readily understand the descriptions in the units used.

Dimension	Unit Used	To S.I.	From S.I.	S.I. Units.
Length	Inch (In.)	25.40	0.0394	m. Metre (mm.)
Force	Pound force (lbf.)	4.4482	0.2248	Newton (N.)
Pressure Stress	$lbf.In^{-2}$. (p.s.i.)	6.8948	0.1450	k.Newton $metre^{-2}$. ($kN.m^{-2}$.)
Time	Minute (Min.)	60.0	0.0167	Second (Sec.)
Angular velocity	Revolution $minute^{-1}$. (r.p.m.)	9.5511	0.1047	Radians $second^{-1}$. ($Rad.sec^{-1}$.)
Conductance.	Conductance (Mho, $\mho$) = Resistence^{-1}. (Ohm, Ω)			
Temperature	Degrees Celcius ($^{o}C.$) = Degree Kelvin - 273.15 ($^{o}K.$)			

REFERENCES.

1. Cotton F.A. and Wilkinson G. Advanced inorganic chemistry. Second edition. Interscience Publications, John Wiley and Sons. 1966.

2. Bjerrum J. Metal amine formation in aqueous solution. P.Hasse and Sons, Copenhagen. 1957.

3. Rosenblatt F.
Z. Anorg. Chem. (1932), pp. 204-341.

4. Bales W.D., Davies E.W. and Monk C.B.
Trans. Faraday Society, (1956), 52, 816.

5. Brown P.G.M. and Prue J.E.
Proc. Royal Society, (1955), 232A, 320.

6. Martin R.L. and Whitley A.
J. Chem. Soc., (1958), Part II, pp.1313-2636, 1394.

7. Reiman C.W., Kokasyka G. and Gordon G.
Inorg. Chem., (1965), 4, 1082.

8. Von Nickenk J.N. and Schoening F.R.L.
Acta. Cryst. (1953), 6, 227-232.

9. Dubicki L. and Martin R.L.
Inorg. Chem. (1966), 5, 2203-2209.

10. Tsushida R. and Yamada S.
Nature, (1955), 176, 1171.

11. Ross R.G.
Trans. Faraday Society, (1959), 55, 1057-1063.

References.

12. Dubicki L., Harris C.H., Rokat E. and Martin R.L.
Inorg. Chem. (1966), 5, 93.

13. Graddon D.P.
J. Inorg. Nuclear Chem. (1961), 17, 222.

14. Forster L.S. and Ballhausen C.J.
Acta. Chem. Scand. (1962), 16, 1385.

15. Kando M. and Kubo M.
J. Phys. & Coll. Chem. (1958), 62, 468-469.

16. Figgis B.N. and Martin R.L.
J. Chem. Society, (1956)(Oct.), Part III, 3837-3846.

17. Fronaeus S.
Acta. Chem. Scand. (1951), 5, 859.

18. Fronaeus S.
Doct. Diss. Lund. (1948).

19. Tanaka and Kato.
Bull. Chem. Soc. Japan, (1960), 23, 1067.

20. Lloyd, Wycherley and Monk.
J. Chem. Society, (1951), Part II, 1786.

21. Tanaka and Kato.
Bull. Chem. Soc. Japan, (1960), 33, 417, 1412.

22. Stability Constants of Metal Ion Complexes.
Published by The Chemical Society of London.
London. 1964.

23. Latimer Oxidation Potentials.,
Prentice Hall Inc., New York. 1952.

References.

24. Truter and Rutherford
J. Chem. Society, (1962), Part II, 1748-1756.

25. Bjerrum J.
Mat. Fys. Medd. Det. Kgl. Dansk. Videnskab. Selskab, (1932-34), XII, N° 15.

26. Van Hahn E.A. and Peters E.
J. Phys. Chem., (1965), 69, N° 2, 547-552.

27. Dunning W.J. and Potter P.E.
Proc. Chem. Society, (1960), 244.

28. Dakers R.G. and Halpern J.
Canadian J. Chem., (1954), 32, 969-978.

29. Byerley J.J. and Peters E.
Unit Processes in Hydrometallurgy, p 183. Metal. Society Conferences, Volume 24. Gordon and Breach, N.Y. & London, 1963.

30. Unit processes in Hydrometallurgy. Metallurgical Society Conferences, Volume 24. Gordon and Breach, N.Y. & London, 1963.

31. Burkin A.R., The Chemistry of Hydrometallurgical Processes. Spon. London, 1966.

32. Derry R., Mineral Processing information note N° 7.. Pressure Hydrometallurgy, A Bibliographic review. Warren Spring Laboratory. 1972.

33. Pantony D.A. A Chemist's introduction to Statistics, Theory of Errors and Design of Experiment. Royal Institute of Chemistry. 1961.

References.

34. Clark I., Royal School of Mines, London.
Personal communication.

35. Ugarte F.J.G., Ph.D. Thesis, 1971. University of London. Imperial College.

36. Handbook of Chemistry and Physics. 48th. Edition. The Chemical Rubber Company. 1968.

37. Needes C., Ph.D. Thesis, 1969, University of London. Imperial College.

38. Bruhn G., Gerlach J. and Pawlech F.
Z. Anorg. Allg. Chem., (1965)(April), 337, 1/2, 68-79.

39. Stephen E.B., Hatfield N.S., Peoples R.S. and Pray H.A.
Battelle Memorial Institute report N° B.M.I. 1067.

40. Schweichert C.E., Minnich B.H. and Pray H.A., Ind. Eng. Chem., (1952), 44, 1146.

41. Publicity literature from Murex Refractory Metals. (June 1972)

42. Tweedale J.G., Practical Mechanical Design. Iliffe, London. 1963.

43. Alumina as a Ceramic Material, Edited by Gitzen W.H. American Ceramic Society, Special Publication N° 4. 1970.

44. Metsik M.S. and Perevertev V.D.
Koll. Zh., (1966), 28, N° 1, 99-104.

ACKNOWLEDGMENTS.

The author wishes, at the end of this work, to express his gratitude to Dr. A.R.Burkin, Reader in Hydrometallurgy at the Royal School of Mines. Dr. Burkin supplied advice, encouragement and supervision during the research work involved and during production of this thesis.

The author also wishes to thank the numerous students and staff within The Royal School of Mines who offered advice and assistance during the experimental work. Special thanks must go to fellow members of the Hydrometallurgy research group, in particular Mr. J.E.A.Burgess for his advice upon the use of pressure equipment and for his manual assistance.

Others whom the author wishes to thank are; Messrs. P.Huckle, B.Holt, and W.Harman of the Mining department, Messrs. G.Green and L.Russell of the Metallurgy Department workshop and Mr.C.Morecombe and his technicians in the chemical metallurgy teaching laboratory.

The author also wishes to extend his thanks to Miss J.B. Gilmour for her invaluable assistance in typing, proofing and checking of the written work, and also for arranging for the copying of the finished thesis.

Finally the author wishes to express his

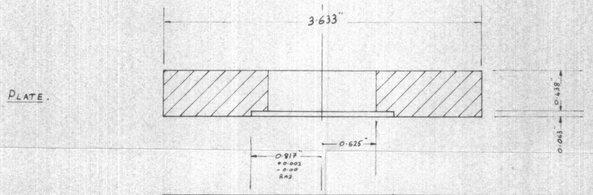
Acknowledgements.

appreciation to the Science Research Council for financial assistance for the duration of the experimental work.

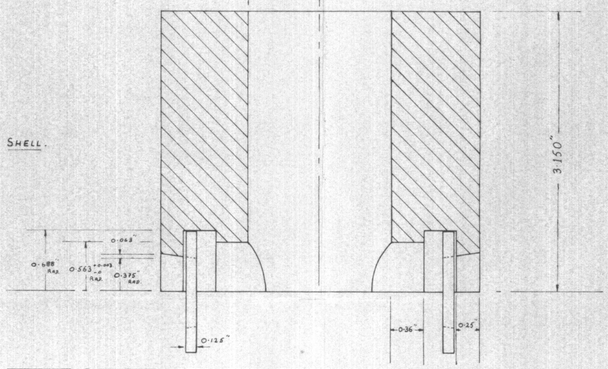
T.F.Mason.

June 1973.

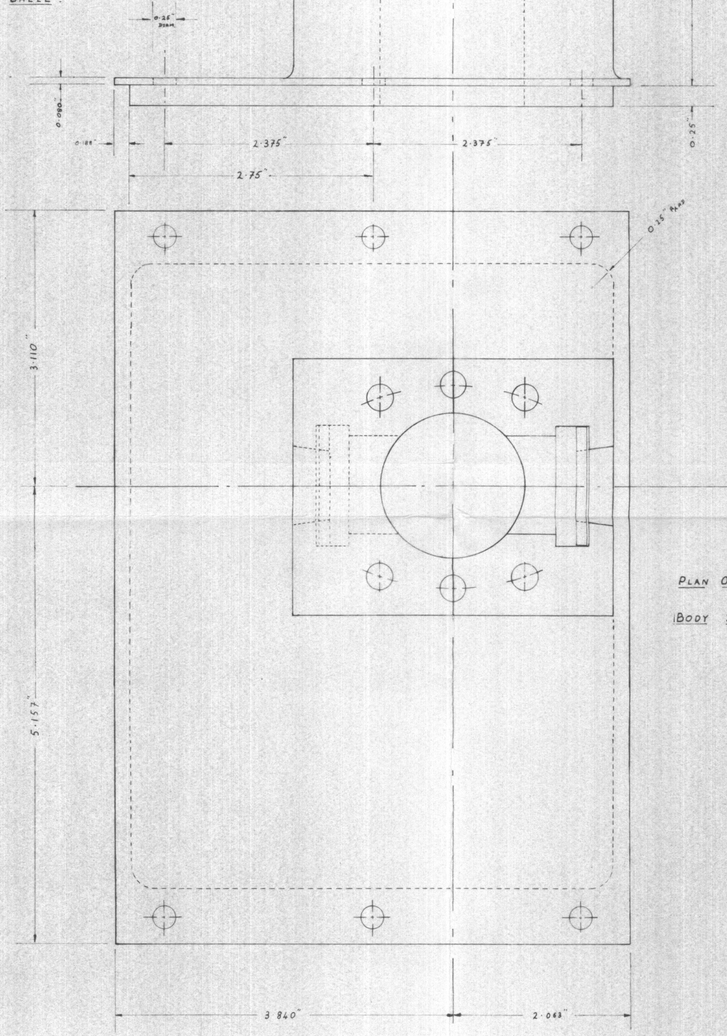
SECTION A-A OF RETAINING PLATE.



SECTION B-B OF UPPER BODY SHELL.



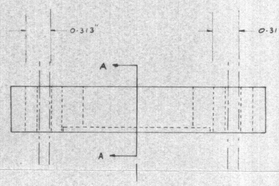
ELEVATION OF LOWER BODY SHELL.



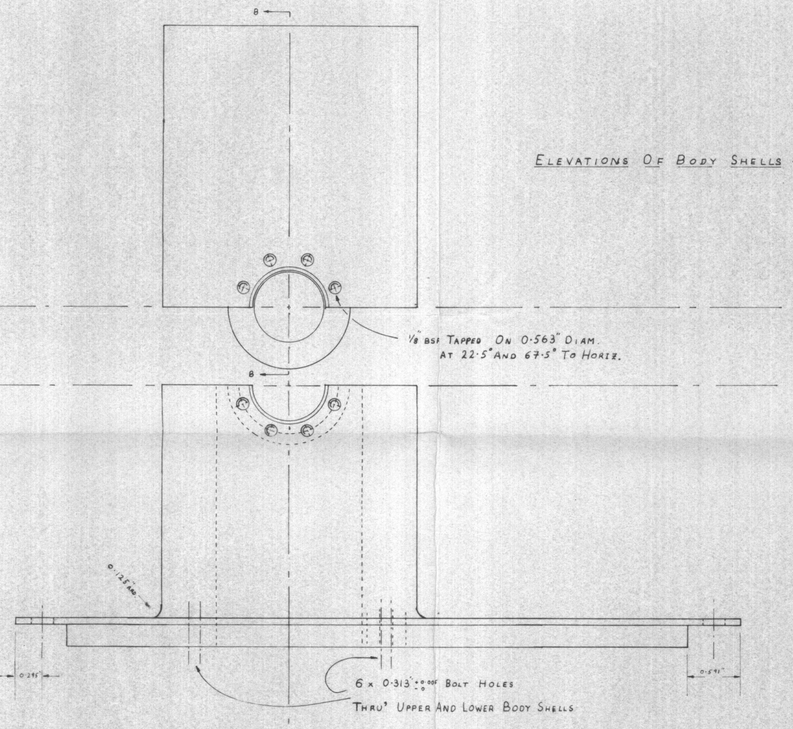
PLAN OF BODY SHELL.

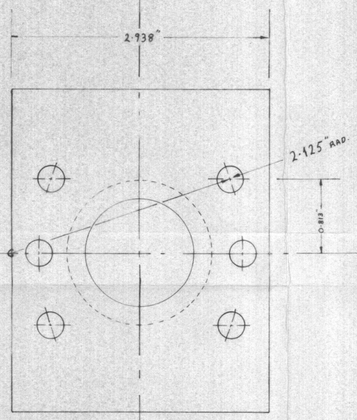
PLAN OF LOWER BODY SHELL

ELEVATION OF RETAINING PLATE



ELEVATIONS OF BODY SHELLS - BOLT HOLES NOT DETAILED.





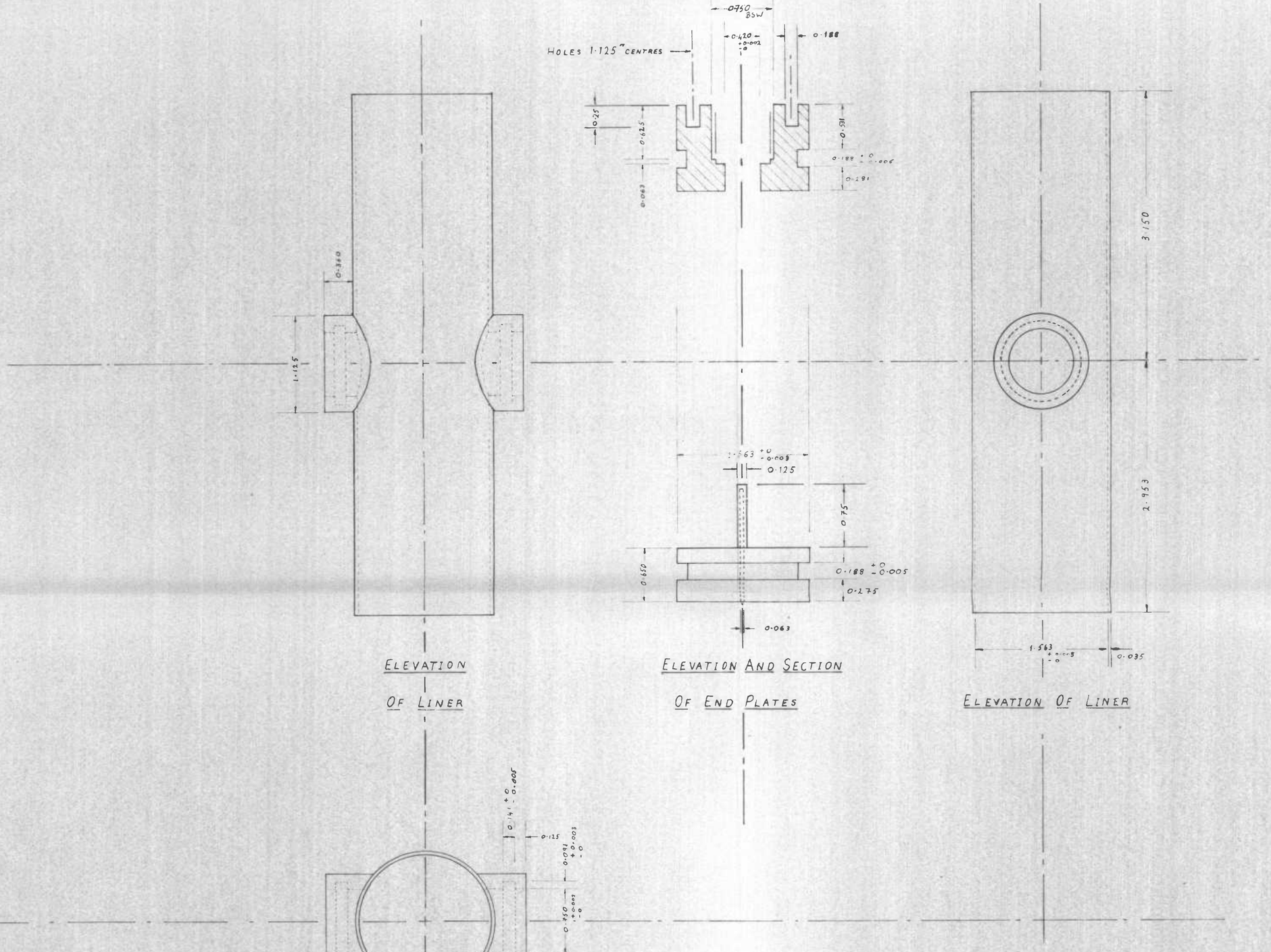
PLAN OF RETAINING PLATE

PRESSURE / REACTION CELL BODY SHELL.

T. F. MASON. 2:11:72

SCALE - FULL SIZE

MATERIAL - EN 58



ELEVATION OF LINER

ELEVATION AND SECTION OF END PLATES

ELEVATION OF LINER

PLAN.

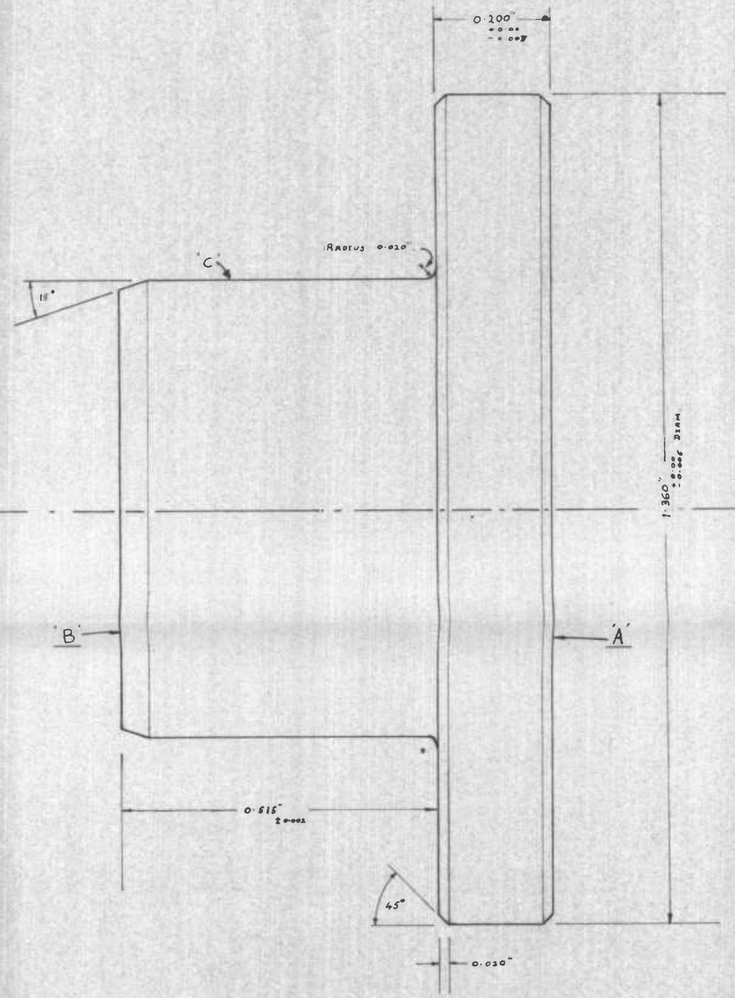
LINER FOR PRESSURE/REACTION VESSEL WITH WINDOW HOLES

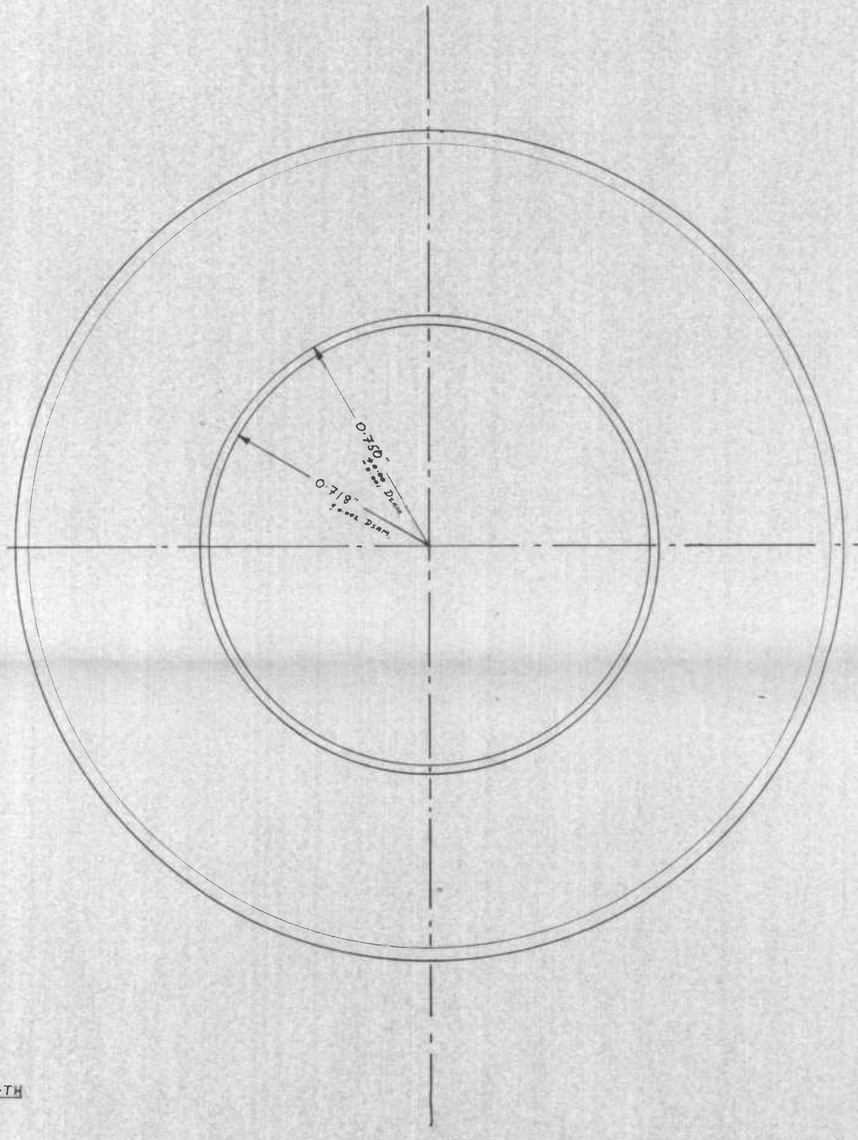
DIMENSIONS IN INCHES

T. F. MASON OCTOBER '72

SCALE : FULL SIZE

MATERIAL : TANTALUM

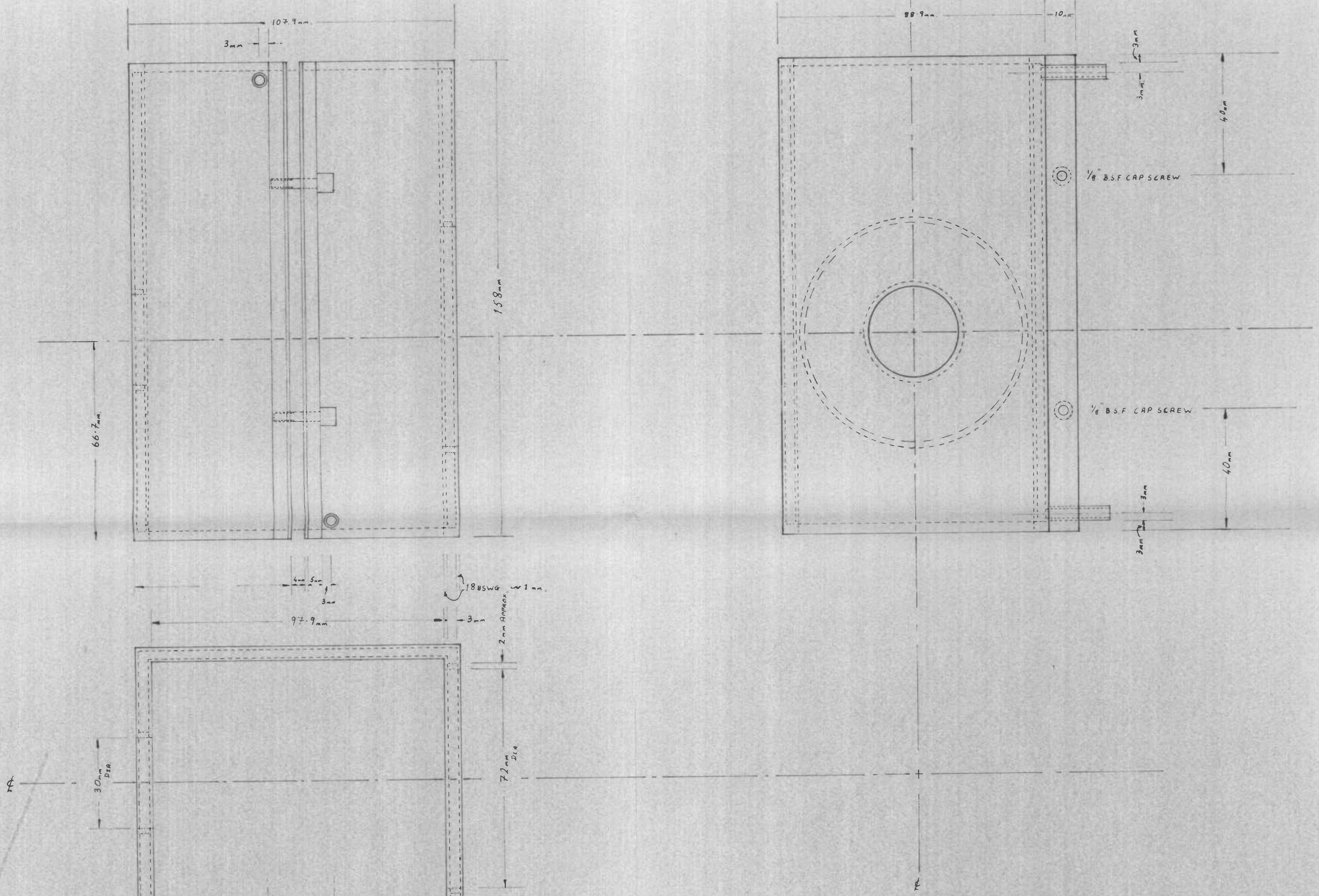




FACES 'A' AND 'B' POLISHED AND PARALLEL TO 0·25 WAVELENGTH / 8-9 SECONDS OF ARC.

SURFACE 'C' POLISHED TO 0·25-0·5 WAVELENGTH TO GIVE REFLECTING FINISH.

QUARTZ OR SAPPHIRE WINDOW FOR REACTION VESSEL.	SCALE : 5 x FULL SIZE
T.F. MASON. 6:11:72	MATERIAL : QUARTZ OR SAPPHIRE.



COOLING PLATE FOR SPECTROPHOTOMETER CELL.	MATERIAL : COPPER, STEEL SCREWS.
	SCALE : FULL SIZE
T.F. MASON. FEB. 1973	GENERAL TOLERANCE : ± 0·05mm.